BLDSC no ÷ DX218621

BADMINTON PRESS
18 THE HALFCROFT
SYSTON
LEICESTER. LE7 8LD
ENGLAND
TEL: 0533 602917
FAX: 0533 696636

A STUDY OF CHEMICALLY MODIFIED POLY (VINYL BUTYRAL)

BY

DAVID CUNLIFFE

A Doctoral Thesis submitted in partial fulfilment of the requirements for the award of Doctor of Philosophy of Loughborough University of Technology.

1993

Acknowledgements

I would like to thank my supervisor, Professor J V Dawkins, for his valued support, good humour and patience throughout the period of this work.

My gratitude must also go to Coates Lorilleux International Limited for initiating this research and their generous financial assistance. In particular, to Dr G C Battersby for his keen interest and input throughout.

I would also like to thank Dr E Meehan and S O'Donahue of Polymer Laboratories (Church Stretton, Shropshire) for help with SEC analysis, and Dr D K Thomas of the University of Durham Industrial Research Laboratories for the solid state NMR measurements. Also, to my colleagues in the polymer research group, and Mr D Wilson, the polymer technician and Mr J C Kershaw for recording the NMR spectra.

Finally, to the staff of I and S Advertising and Business Services Limited, Loughborough, for typing this thesis, many thanks.

Originality

The work presented in this thesis has been carried out by the author, except where otherwise acknowledged, and has not been previously submitted to this, or any other University or Institution, for the award of a higher degree.

Abstract

Poly (vinyl butyral) (PVB) is prepared by the acetalisation of poly (vinyl alcohol) with butanal. Due to the random nature of the reaction, some of the hydoxyl groups are left unreacted. The residual hydroxyl groups greatly influence its solution behaviour leading to aggregate formation in many solvents.

A number of modified samples of PVB were prepared by esterification of the hydroxyl groups with butanoic anhydride, benzoic anhydride, trifluroacetic anhydride, phthalic anhydride and succinic anhydride. These modified samples were examined by size exclusion chromatography (SEC) and dilute solution viscometry. The degree of modification was determined by chemical determination of the residual hydroxyl groups, by nuclear magnetic resonance spectroscopy (NMR) or Fourrier transform infrared spectroscopy (FTIR).

Viscosity measurements showed that modification with non-polar ester groups diminished the degree of aggregate formation in THF while modification with the cyclic anhydrides showed an increased tendency towards aggregation in THF while the aggregates were efficiently disrupted by methanol.

The miscibility of the modified PVB with a polyester, a polyurethane, polyethylenimine and poly (vinyl pyrrolidone) was investigated by dynamic mechanical thermal analysis (DMTA). It was found that samples modified with non-polar ester groups showed reduced miscibility with these polymers, while samples modified with cyclic anhydrides showed improved miscibility with these polymers and formed macromolecular complexes with polythylenimine and poly (vinyl pyrrolidone).

It was concluded that intermolecular hydrogen bonding affected the viscosity behaviour of PVB in various solevents and was the main thermodynamic reason for promoting miscibility with the polymers studied.

Contents

1. INTRODUCTION

Synthetic polymers are prepared with the intention of producing materials with particular properties. The desired properties may depend, at least in part, on the presence of specific functional groups either in the polymer backbone, or substituents in pendent groups linked to the main chain. This functionality may be incorporated in two ways, either a suitably substituted monomer is polymerized, or the substituents are introduced at a later stage by chemical modification of a preformed polymer. The first method leads to a fully substituted product of known overall structure, the second method gives a product which is rarely fully functionalized, and where the precise positions of functional groups along the polymer chain are not known. Often, a random distribution of substituents is assumed.

The ease of modification depends upon the chemical and physical nature of the starting material, particularly on whether it is linear or cross-linked. For insoluble polymers chemical modification might only occur on the outer surface.

It would seem, at least superficially, that a functionalized reactive polymer might be best prepared from a suitably substituted monomer. However, this is not always possible. The monomers may be very expensive, or difficult to synthesis, or the desired substituent may inhibit polymerization. In addition, if the functional groups of a modified polymer are themselves to be utilized in the product a large proportion may be in an inaccessible part of an insoluble bead.

In general, the reasons for carrying out modification of polymers are:

1. Changing the physical properties to improve the biocompatibility, fire retardancy, adhesion, or ability to blend with other polymers. Sometimes changes are made to the outer surface in order to alter properties such as solvent repellancy or friction.
2. Preparing polymer supported reagents. It is sometimes advantageous to use reagents in polymeric form the desired products, and reagent recovery and recycling are facilitated. This is particularly important for expensive reagents and

catalysts. A wide range of such substituents have been prepared.[1-8]

3. Controlling the release of drugs and pesticides can be achieved by attaching the pharmacologically active unit to a polymer [9].

4. Studying the mechanism of reactions, where the linking of the reacting groups to polymers facilitate mechanistic interpretation.[10]

The aim of this work was to prepare a number of samples of chemically modified poly (vinyl butyral), with the objective of reducing the solution viscosity and improving the miscibility of poly (vinyl butyral) with other polymers. The residual hydroxyl groups lend themselves to the type of chemistry used in carbohydrate chemistry by etherification or esterification. We chose to modify poly (vinyl butyral) by esterification of the hydroxyl group, to produce side groups of low polarity and high polarity. The esters chosen were butanoate, benzoate, triflouroethanoate, phthalate and succinate. The effect of degree of modification upon solution and miscibility was to be studied.

2. THEORY

2.1 Reactions of Functional Polymers

2.1.1 General Considerations

Chemical modification of polymers probably began in 1781[11] with the isomerization of natural rubber in the presence of acids. The mid-nineteenth century saw the first successful attempts to modify polymers in a useful way; nitration of cellulose[12] was reported in 1833 and the Goodyear vulcanization process was patented in 1844 [13]. Until 1845 reactions were carried out on natural polymers only and their first application to totally synthetic polymers is very probably the nitration of polystyrene[14]. An important step forward was the development by Staudinger of the concept of polymer analogous reactions which consisted in the transformation of a polymer into a derivative of equivalent molecular mass. He obtained evidence for this concept by hydrogenating rubber [15] and polystyrene[16] with almost no chain degradation.

Any reaction of classical organic chemistry can be applied to polymers; however, the mechanism and kinetics of the reaction may be different according to whether reaction is carried out on a small molecule or on a polymer. Over the last thirty years, several interesting and well documented reviews on macromolecular chemistry have been published[17-43] proposing general theories of macromolecular reactions.

The reactivity of a functional group in a polymer depends upon (i) the nature of the neighbouring groups, (ii) the nature, length and conformation of the chain (iii) the morphology of the polymer and its history, and (iv) the experimental conditions, which have a greater influence with polymers than with small molecules. The neighbouring group effect is probably the most important determining factor of the reactivity of a functional group in a polymer. The significant factors are :-

i. Steric factors - which inhibit the approach of the reagents.
ii. Polar and electrostatic effects - these may hinder or enhance the approach of charged reagents.

iii. Concentration - local concentration of functional groups in polymer solutions can be considerably higher than could be obtained if each of the groups belonged to a small molecule.

iv. Stabilization of intermolecular complexes. When part M of a compound MN reacts with a group A in a polymer it may happen that the intermediary complex is stabilized by interaction of part N with another group A⁻.

v. Hydrophobic interactions - the existence of attractive interactions between the polymer and the reagent is well known particularly in aqueous media [44-48]

vi. Specific interactions between neighbouring groups - these may lead to cyclisations involving adjacent monomer units or may lead to anchimeric assistance. This is illustrated by the hydrolysis of poly (4 - nitro - phenyl methacrylate - co - acrylic acid) in basic media, as shown is scheme 1. The efficiency of the interaction depends upon the distance and relative positions of the groups.

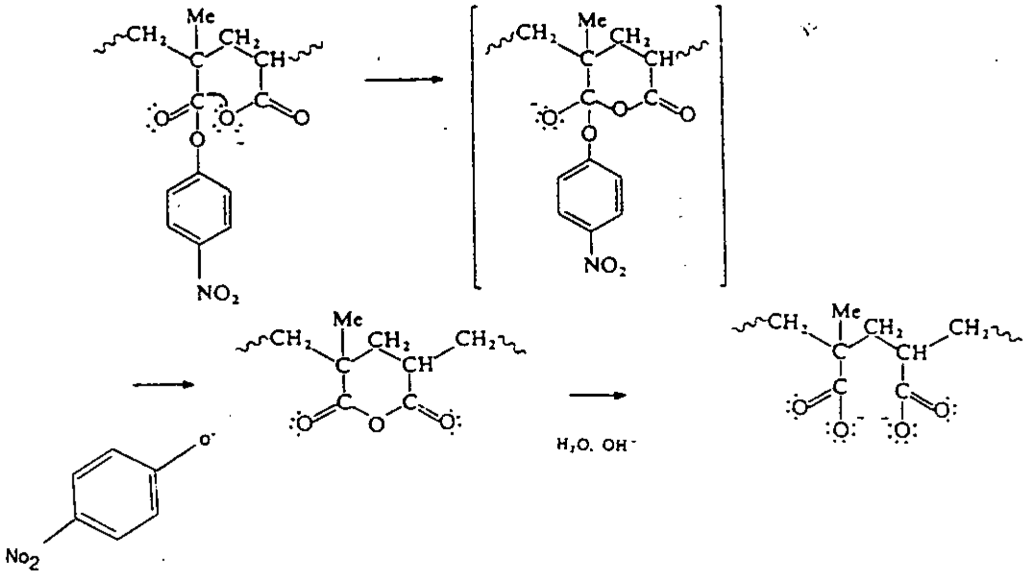

Scheme 1

Thus, for the two polymers isotactic polymethacrylate (IMA) (1) and syndiotactic (SMA) (2), the rate of hydrolysis of (IMA) is approximately ten times that of (SMA). As the formation of a cyclic intermediate is favoured by the (IMA) structure.

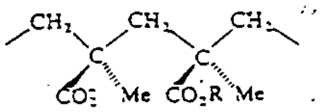

(1) (IMA)

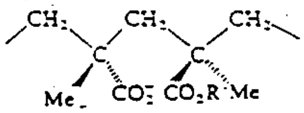

(2) (SMA)

This is confirmed by the study of (3) for which the hydrolysis rate is about 200 times that of mono succinate; in this case the two interacting functions are rigidly maintained in an immediate neighbourhood.

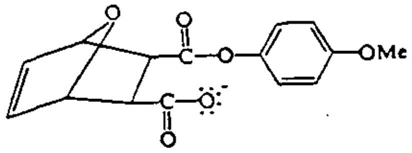

(3)

The acetalyzation of poly(vinyl alcohol) (PVA) is another example of the specific effect of a neighbouring group; the reaction of an aldehyde with PVA results in the formation of intramolecular acetals rather than the formation of intermolecular compounds. This is due to the mechanism of the acetalyzation reaction (Scheme 2).

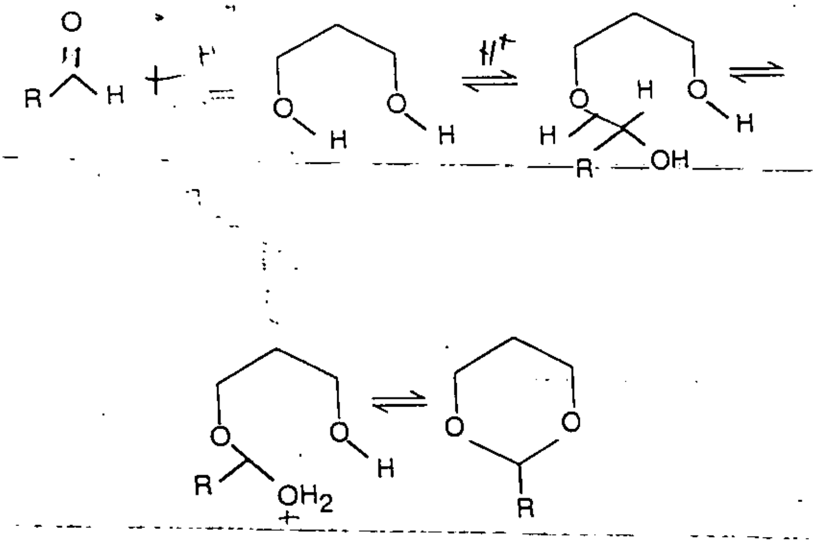

Scheme 2

The influence of tacticity, conformation and their evaluation during reaction has been reviewed by several authors[26,28,31] and summarized by Millan[49] and Galin[50]. The relationship between stereotypes of poly(vinyl alcohol) and acetalyzation has been studied[51,53]. The isotactic portion of poly(vinyl alcohol) might give the cis-m-dioxane(4) while the syndiotactic portion might give the trans-m-dioxane(5).

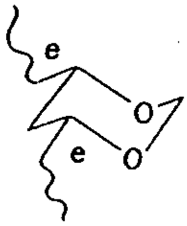

(4)

cis derivative
isotactic

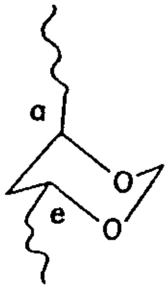

(5)

trans derivative
syndiotactic

The di-equatorial conformation is more stable than the axial-equatorial conformation.

2.1.2 Kinetics

If we consider triads of monomer units, the rate contants can be defined for the reaction of a function A to yield a group B. They are generally called k_o for $A\dot{A}A$ triads, k_1 for $A\overset{x}{A}B$ or $B\dot{A}A$ triads and k_2 for $B\overset{x}{A}B$ triads, where $\dot{A}$ is the reacting species. In many cases, appreciable influence is exerted on the reactivity of a $\dot{A}$ function by the neighbouring units[54,55]. A good theoretical framework emphasizing the major role of the ratios of the three kinetic constants $k_0:k_1:k_2$, has been elaborated. It allows a quantitative description of the reactions on polymers from these related points of view; (i) kinetic analysis and limiting yields, (ii) compositional heterogeneity, and (iii) unit distribution. These points are illustrated in table 1. If $k_0=k_1=k_2$ all reaction probabilities are the same leading to a random distribution of reacted groups. If $k_0<k_1<k_2$ then the probability of reaction adjacent to a reacted site becomes greater, leading to a blocky distribution of reacted sites. If $k_0>k_1>k_2$ then the probability of reaction decreases leading to a distribution of isolated reacted sites between blocks of unreacted sites.

Boucher[26], proposed scheme 3 where ● and O are respectively reacted and unreacted groups at time t in a linear array of m. sites. The possible situations are reported in table 2.

Scheme 3

The reaction probabilities of different sites during time dt are k_0dt, k_1dt and k_2dt respectively. A neighbouring group effect is considered as a localised phenomenon operating on a few atoms in the vicinity of each neighbouring group. Boucher[26,56] established the kinetic expressions relative to chemical modification.

Table 1: Overview of cooperative effects on macromolecular chain reactivity

Neighbouring Group Effects	one single rate constant	three different rate constants	
	$k_0=k_1=k_2$	$k_0<k_1<k_2$	$k_0>k_1>k_2$
kinetics	pure random processes	autoacceleration	autoretardation
Conversion	may be quantitative	may be quantitative	may be limited $K_2=O-DS_M=0.666$ $k_1=k_2=0$ - DSm=0.432
Compositional heterogeneity	moderate $\overline{\sigma}^2 = DP_n^{-1}(DS_m - DS_m^2)$	may be quite high	may be very low
Distribution of A and B units	Bernouilli statistics	Markov statistics - formation of B_n blocks	Markov statistics isolated B units between A_n blocks

$\bar{D}\bar{S}_m$ = Substitution degree in mole or molar fraction of B units in the copolymer

$\overline{\sigma}^2$ = Mean square standard deviation to the average composition

Table 2

Description of the Possible Situations in Reactions of Polymers

Model representation	*Remarks*
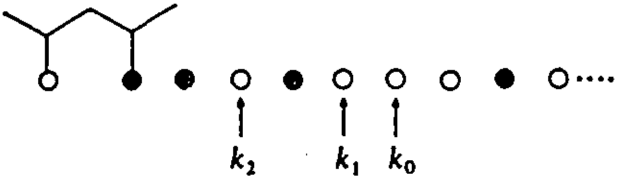	Singleton reaction with neighboring group effect
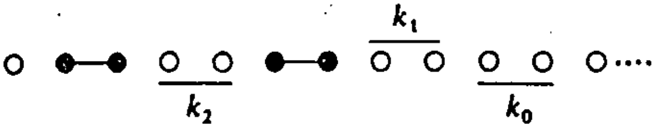	Basic pairing with neighboring group effect
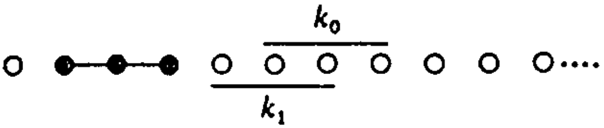	General '*n*-on-*m*' model, *e.g.* $n = 3$, with neighboring group effect
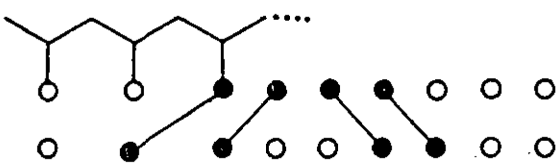	Complex pairing or random ladder formation, *e.g.* upper row CO and lower row Me
	Zip reaction. Initiation at sites followed by rapid propagation (many variations)
	Continuum models where discrete groups are ignored

Reactions can be considered as either, pairing or non-pairing. An example of non-pairing is the quaternization of poly(vinyl pyridine) as in scheme 4.

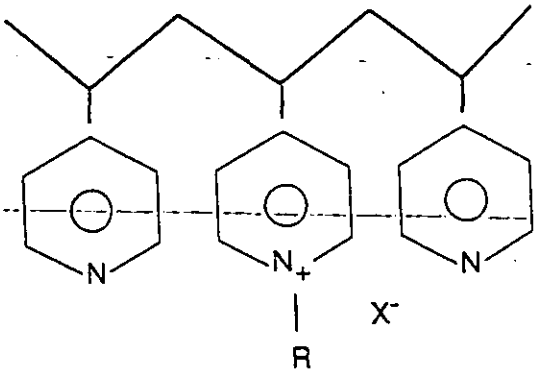

Scheme 4

The intial stage of reaction follows second-order kinetics; however, later stages show retardation. Fuoss[57,58] et al attributed retardation due to a build up of charge during the reaction. Bourquignon[59] reported that in the quaternization of poly(4-vinyl pyridine) with butyl bromide in sulphalone, retardation requires both neighbouring groups to have reacted and that the decrease in rate is due to an electric field effect. However, Frere and Gramain[60] have shown that with voluminous reagents the steric effect induces the greater limiting factor.

Pairing reactions show a statistical feature which in principle can be recognised at any extent of reaction including the $t \rightarrow \infty$ limit, as well as departure from overall first or second-order kinetic behaviour. Consequently, the comparison of experimental data with the model should give a way of testing a proposed reaction scheme, whether or not there is a neighbouring group effect. Non-reversible reactions of pairs of adjacent substituents in linear polymers have been treated fairly exhaustively[61-65]. In the simple cases, each substituent X of the chain is capable of reacting with only one of its neighbouring substituents X, the pair of groups may react directly with one another or jointly with a monomeric reactant. This is demonstrated in Scheme 5.

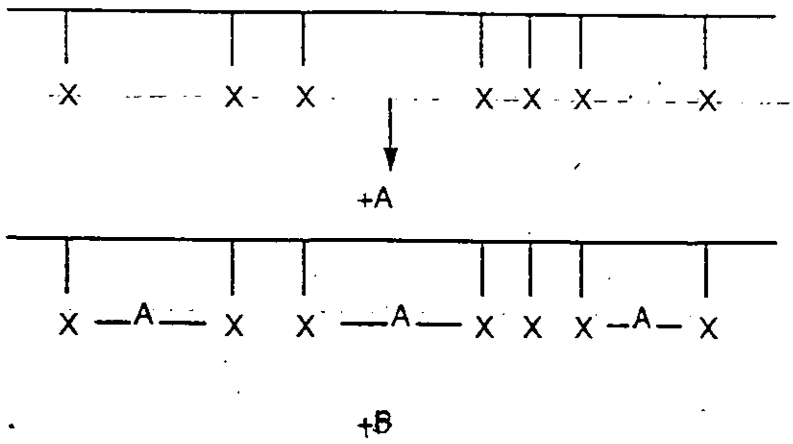

Scheme 5

Where X-A-X represents the condensation product between 2X and A, and B is the byproduct of that reaction. For a tandem irreversible reaction of a high molecular mass polymer compound of -CH_2-CHX- units, when the units are arranged head to tail along the chain, 13.53%[61] of them are prevented from reaction due to isolation between reacted pairs. Analogous condesation in polymers which have their subsitituents orientated at random where reaction between 1,4- pairs of substituents does not occur, 18.40% of the substituents of a random polymer remain isolated after the possibilities for 1,2- and 1,3- reactions have been exhausted. A treatment of vinyl copolymers of the type in Scheme 6 in which X may condense with Y has been presented[66].

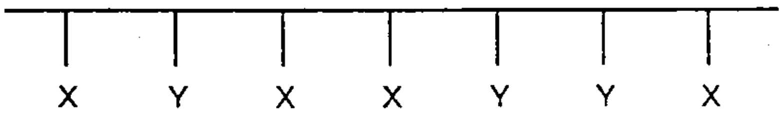

Scheme 6

Most of the known reactions involving neighbouring pairs of substituents in chains are easily reversible and subject to interchange. Examples include the formation of poly(vinyl acetal) from poly(vinyl alcohol) and aldehydes and include formation of imides on heating polyacrylamide, as exemplified in scheme 7.

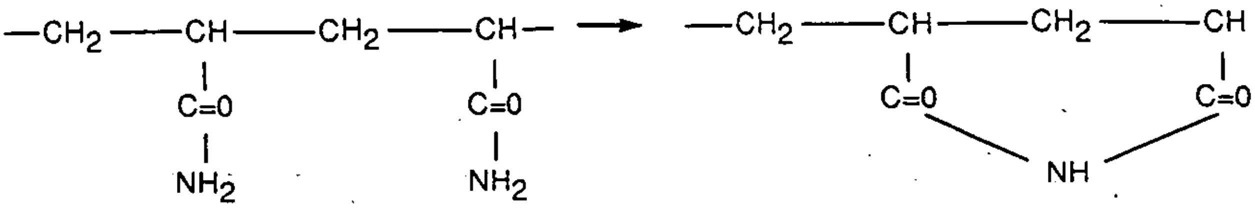

Scheme 7

If under the conditions during the intramolecular reaction between pairs of subsituents the reverse process may also take place, a reacted pair which is adjacent to an isolated subsituent may dissociate and the other pair of sequences of these substances may then react as illustrated in Scheme 8.

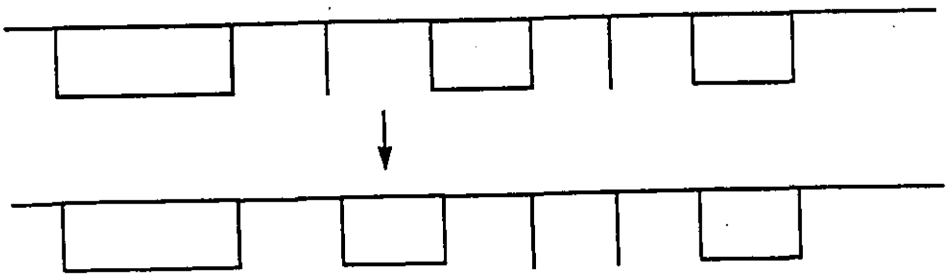

Scheme 8

Experimental evidence demonstrating the feasibility of carrying out such a reaction exceeding the 86% limit for non-reversible random reactions is found in the literature on poly(vinyl acetal) where conversions exceeding 90% have been reported[67]. Hence, assuming a reversible reaction Flory[68] extended the upper limit of acetalisation to 100%. Though such conversions would be possible if the acetalisation were reversible, there is no positive evidence in the literature to suggest reversibility and experimental studies[52,69] have concluded that the reverse reaction is insignificant. It has been recently shown[70] that by considering the rate constants for the types of -OH groups in Scheme 9 that high conversion can be achieved.

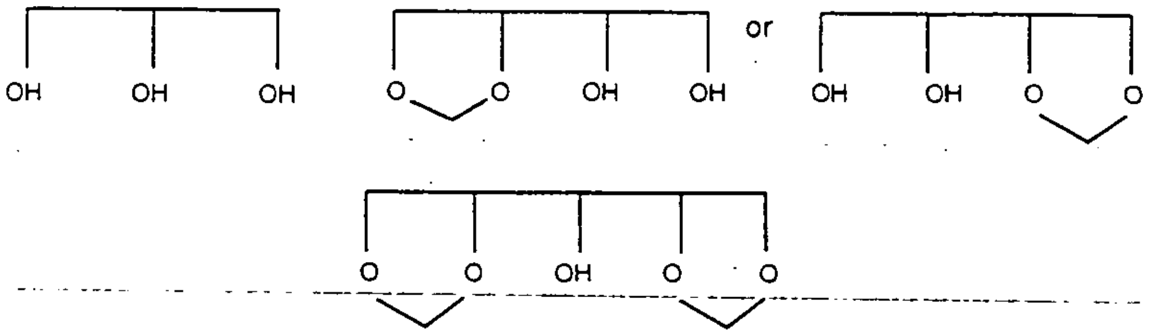

Scheme 9

The results of the kinetic model are given in Table 3.

Maximum attainable conversion for various k_0/k_1

k_0/k_1	Conversion %
0.05	96.64
0.1	93.13
0.2	91.45
0.5	89.19
1.1	87.66
2.0	86.46
4.0	85.64

Table 3

Most kinetic studies have been carried out on dilute solutions. When the raction is carried out in the melt, diffusion may control the kinetics. De Gennes[71,72] studied the kinetics of diffusion - controlled processes in dense polymer systems in the case of non-entangled and entangled regions. When the degree of polymerization N is smaller than a critical value N_c, then entanglement effects are not important. If $N >> N_c$, then entanglement becomes dominant and dynamics are severely modified. The study of the reaction between groups A and B attached to a long flexible chain in melts or in concentrated solutions leads to the following fundamental types of behaviour.

i) Non-compact exploration, which is obtained in the classical case when A and B belong to small molecules and where simple diffusion prevails. The space volumes where A and B may overlap significantly without any reaction taking place, and this regime leads to a second order rate constant k, where k is independent of time.

ii) Compact exploration, when as soon as the space volume explored by A and B overlap the reaction takes place and the rate constant is time dependent.

2.2 Viscosities of Polymer Solutions

The viscosities of even very dilute solutions of high polymers are always significantly greater than those of solvents. This is a consequence of the very large size of the polymer molecules, relative to those of solvents and the extension of a chain molecule in space. Parameters derived from measurements of dilute solution viscosity can be related to molecular mass and chain dimensions of the polymer and to interactions between polymer and solvent. They may also be used in studies of chain stiffness, chain branching, polydispersity and association of polymers in solution.

The viscosity of a dilute polymer solution is often expressed relative to the viscosity of the solvent in which the polymer is dissolved. This is determined by measuring the time for a fixed amount of liquid to flow through a capillary of uniform diameter under the weight of solution. Hence, the relative viscosity η_r is defined in (2.1)

$$\eta_r = t/t_o \qquad (2.1)$$

where t is the efflux time of the polymer solution and t_o is the efflux time of the solvent. The specific viscosity η_{sp} which is given by (2.2)

$$\eta_{sp} = \eta_r - 1 = \frac{t - t_o}{t_o} \qquad (2.2)$$

expresses the incremental viscosity attributable to the polymer solute. The ratio η_{sp}/c is a measure of the specific capacity of the polymer to increase the viscosity.

The limiting value of this ratio at infinite dilution is called the intrinsic viscosity. (2.3)

$$\frac{\eta_r - 1}{C \lim c \to o} = \frac{\eta_{sp}}{C \lim c \to o} = [\eta] (2.3)$$

The most general relationship between intrinsic viscosity and dilute soluton viscosity takes the form of a polynominal (2.4).

$$\frac{\eta_{sp}}{c} = [\eta] + k_1[\eta]^2 c + k_2[\eta]^3 c^2 + k_3[\eta]^4 c^3 \ldots (2.4)$$

where k_1, k_2, k_3 etc. are dimensionless constants. Huggin's theoretical analysis of the hydrodynamics of both flexible and rigid polymer molecules[73-75] produces the following equation (2.5)

$$\frac{\eta_{sp}}{c} = \frac{[\eta]}{1 - k'[\eta]c} \quad (2.5)$$

where k is a dimensionless constant introduced to correct for certain deficiencies in the analysis and is commonly referred to as the Huggin's constant, which related to the size and shape of polymer segments and hydrodynamic interactions between different segments of the same polymer molecule. Series expansion of (2.5) is permissible provided that $o<k'[\eta]c<1$ and gives a convergent series which is equivalent to equation (2.4) with $k_n = k'^n$ for $n = 1,2,3$, etc. Thus, k, corresponds to the Huggin's constant. The Huggin's constant typically has values which fall in the range 0.3 (for good polymer-solvent pairs) to 0.5 (for poor-solvent pairs). Experimental data for which $k_1>0.5$ should be treated with caution since this indicates aggregation of polymer molecules[76]. A large number of equations have been recommended for the evaluation of $[n]$ by extrapolation of experimental data. The most commonly encountered are listed below.

Huggin's[75] $$\frac{\eta_{sp}}{c} = [\eta]_H + k_H[\eta]_H^2 c \quad (2.6)$$

Kraemer[77] $$\frac{ln\,\eta_r}{c} = [\eta]_k - k_k[\eta]^2_k c \quad (2.7)$$

Schulz-Blaschke[78] $$\frac{\eta_{sp}}{c} = [\eta]_{SB} + k_{SB}[\eta]_{SB}\eta_{sp} \quad (2.8)$$

Martin[84] $$\ln\left(\frac{\eta_{sp}}{c}\right) = \ln[\eta]_m + k_m[\eta]_m c \quad (2.9)$$

The Huggin's equation is simply a truncation of the series expansion (2.4); and strictly, is only applicable when $[\eta]$ C<<1. At higher concentration, experimental data shows upward curvature when plotted according to this equation. The Kraemer equation is an approximation of the Huggin's equation, from which it may be derived assuming that $[\eta]$sp<<1. Theory predicts that $k_H + k_k$) = 0.5 when the approximation is satisfactory. The Schulz-Blaschke equation was deduced empirically and is identical to (2.5) with $[\eta] = [\eta]_{SB}$ and $k = k_{SB}$. Experimental data plotted according to this equation shows decreased curvature as the concentration increases, though such plots are usually linear to higher concentrations than for application of the Huggins equation. Similar observations have been made with regard to the Martin equation, which was also deduced empirically. Series expansion of the equation gives an expression which is equivalent to equation (2.4), with $[\eta] = [\eta]_M$ and $k_n = k_m^n/n!$, for n= 1, 2, 3 etc. Assuming the solutions were sufficiently dilute to ensure that each of the equations (2.6 - 2.9) is valid, it is easy to show that:

$$[\eta]_H = [\eta]_k = [\eta]_{SB} = [\eta]_M = [\eta] \qquad (2.10)$$

and

$$k_H = k_{SB} = k_M = k' = k_1 \qquad (2.11)$$

Thus each equation is capable of giving a good estimate of $[\eta]$. Solution concentrations should be chosen such that $\eta_{sp}<1$, the lower limit depending upon both the precision with which η_{sp} is measured and the magnitude of adsorption effects. Plots of experimental data must then be carefully inspected for signs of curvature before selecting the data points to be fitted to a straight line. In particular, data points corresponding to $[\eta]\ c>1$ should be viewed with caution, especially for the plots according to the Huggins and Kraemer equations. If straight lines are fitted to data which show curvature when plotted according to equation (2.6-2.9) then extrapolations are predicted[80] to yield different estimates of $[\eta]$ and k_1.

$$[\eta]_{SB} > [\eta]_m > [\eta] > [\eta]_H = [\eta]_K \qquad (2.12)$$

and

$$k_{SB} < k_M < k_1 < k_H \qquad (2.13)$$

These trends are often observed[81-85] and highlight the possible undrestimation of $[\eta]$ when employing the most common method for its evaluation, which involves fitting of the data to both Huggin's and

Kraemer equations. Sakai[80] has suggested that $[\eta]$ and k_l are best estimated by taking arithmetic means of values obtained from application of the Huggins equation and either the Martin equation for good polymer -solvent pairs, or the Schulz-Blaschke equation for poor polymer-solvent pairs. The inconvenience of extrapolation methods for routine analysis has given rise to considerable interest in estimation of $[\eta]$ from a single specific viscosity measurement, particulaly when $[\eta]$ need only be evaluated approximately, and these have recently been reviewed[76,86].

When completely, or partially, neutralized polyelectrolytes are studied, a massive increase in specific viscosity is observed in the region of low concentration as shown in figure 2.1[87,88].

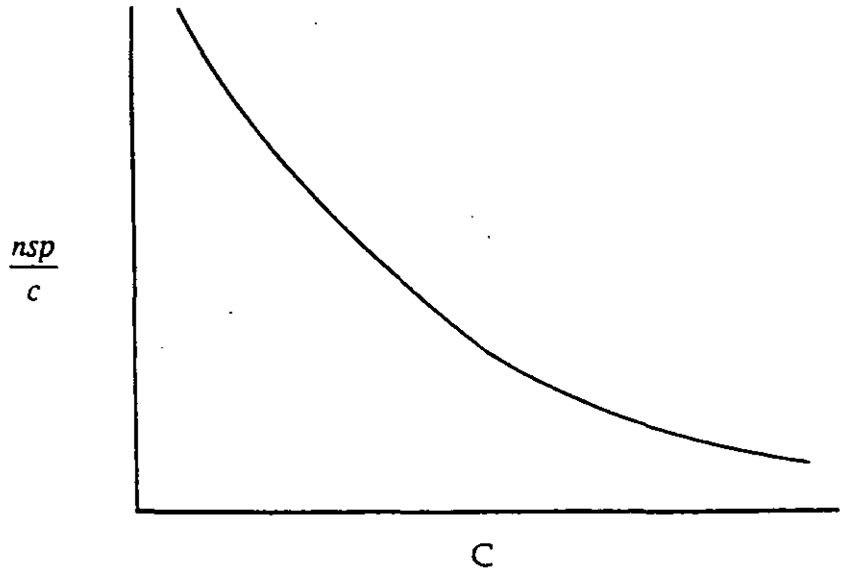

Figure 2.1

Variation of reduced viscosity with polymer concentration for a polyelectrolyte

This arises from variation in the degree of dissociation of the ionizable groups. Fuoss and Strauss[87,88] found that the reduced viscosity (η_{sp}/C) and concentration of a charged polyelectrolyte follow the relation (2.14)

$$\frac{\eta_{sp}}{c} = \frac{A}{1+B\sqrt{c}} + D \qquad (2.14)$$

The quantity (A+D) is the limit approached at zero concentration in the analogue of intrinsic viscosity. Equation 2.14 is usually arranged in the form (2.15).

$$\left(\frac{\eta_{sp}}{c}\right)^{-1} = [\eta] + \gamma C^{-1/2} \qquad (2.15)$$

where γ is a constant. The values so obtained correspond to a rod like shape and are sensitive to the shear rate. A more acceptible procedure for evaluation of $[\eta]$ involves the suppression of the effect of ionization by the use of an inert low molecular mass electrolyte as co-solute[89,90].

As has been previously mentioned, viscosity data which gives $k_1 > 0.5$ indicate aggregate behaviour of the polymer. Association behaviour can often be seen in plots of reduced viscosity against concentration (Figure 2.2)[91,92]

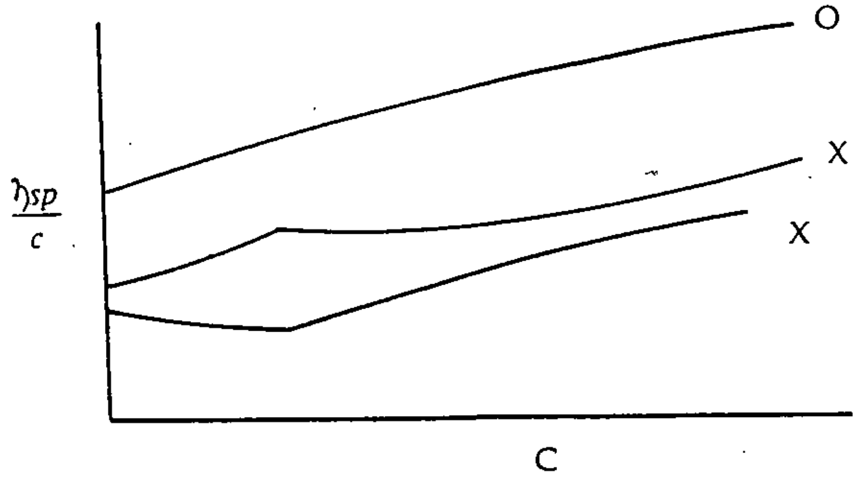

Figure 2.2

O= open association ,x = closed association.
Effect of association upon the variation of reduced viscosity with concentration.

Figure 2.2

The thermodynamics of aggregation have been recently reviewed by Higgins[93] et al. Viscosity data can be used to assess thermo-reversible gelation of many polymers in different solvents. The aggregation behaviour of poly(vinyl butyral)[94-101] in many solvents has been observed by size exclusion chromatography, solution viscosity and low angle laser light scattering.

2.3 Polymer Miscibility

2.3.1 Introduction

At equilibrium, a system of two amorphous polymers may exist as a simple phase of intimately mixed segments of the two macromolecular components or separate into two distinct phases consisting primarily of the individual components. Which of these occurs is dictated by the same thermodynamic principles governing the phase behaviour of low molar mass liquids, with some quantitative differences arising from the higher molar mass in the case of polymers.

The most widely used definition of a miscible polymer blend is one which exhibits a single glass transition temperature. Miscibility therefore implies by this definition, a level of homogeneity within the mixture, such that any separate domains present are smaller than the segmental size responsible for the glass transition. Miscibility in this sense does not imply ideal molecular mixing, but suggests a level of mixing adequate to yield the macroscopic properties expected of a single phase material. Therefore, a technique used for studying miscibility on the basis of glass transition may lead to the conclusion of a single phase, whilst a more sensitive technique may be capable of differentiating between small domains, leading to a conclusion of immiscility. The use of solid state N.M.R.[103-110] has recently been used to determine the domain size of polymer blends. It has been suggested that the segmental size associated with the glass transition is of the order of 15nm[111] while NMR techniques are capable of measuring domain sizes down to 3nm. In practice, many polymer blends are neither completely miscible nor completely inmiscible, but exhibit a degree of partial miscibility. In this situation, two glass transitions may occur at temperatures intermediate between the transitions, which would occur in an immiscible blend of the two polymers. This suggests that there is limited solubility of the two polymers in each other, but insufficient to yield a single glass transition. A partially miscible system may however show a single broad transition which might span over the range between the transitions of the blend components. Clearly, when studying the miscibility of a blend using a single glass transition criterion, problems will arise if the two polymers have transitions at similar temperatures. In this situation it is very difficult to determine whether one or two transitions are present, making conclusions about miscibility almost impossible. There has been considerable interest in the area of polymer blending in recent years[112-119].

2.3.2 Phase Behaviour

The equilibrium phase behaviour of mixtures in general is given by the free energy of mixing as defined in equation 2.16.

$$\Delta G_m = \Delta H_m - T\Delta S_m \qquad (2.16)$$

A plot of ΔG_m against blend compositions ($\varnothing_2$, volume fraction of component 2) as in Figure 2.3, shows three possible types of mixing behaviour for a binary system. The three curves represent the miscible (A), partially miscible (B) and completely immiscible (C) situations.

The necessary conditions for a binary system to be miscible at a particular composition are:

$$\Delta G_m < 0 \qquad (2.17)$$

$$\left(\frac{\partial^2 \Delta G}{\partial \varnothing_2^2}\right)_{T,P} > 0 \qquad (2.18)$$

Clearly to determine the nature of the miscibility of a given binary system, information quantifying ΔH_m and ΔS_m are required in order to know the sign and magnitude of ΔG_m at a given composition. The various thermodynamic therories, therefore, attempt to relate ΔH_m and ΔS_m to physical parameters of the two components of the blend which can be easily obtained experimentally or otherwise.

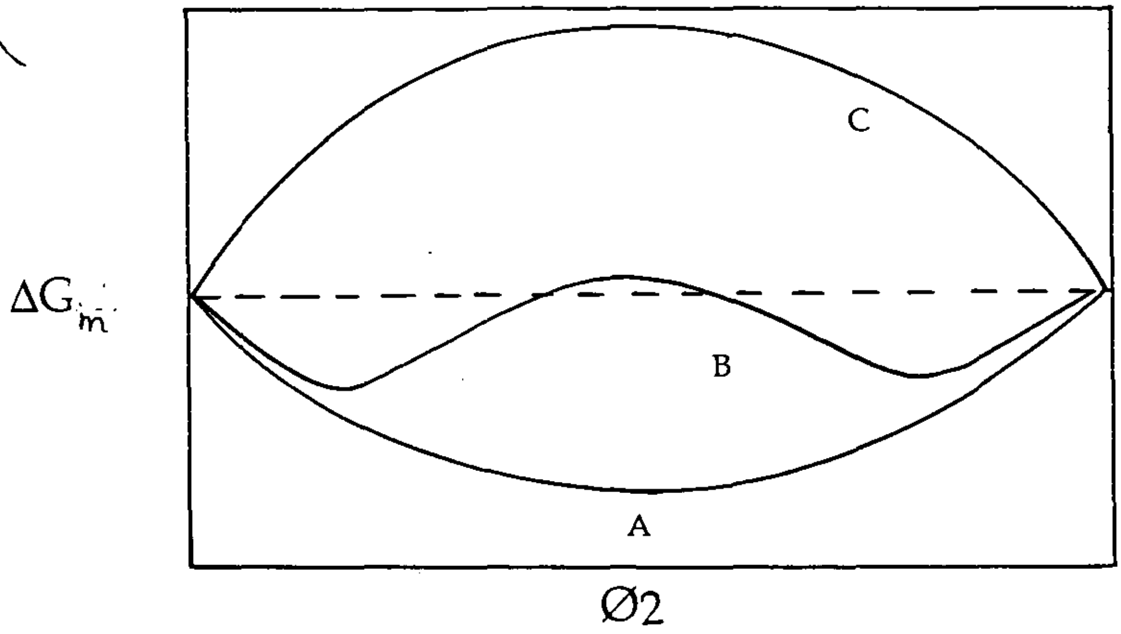

Figure 2.3
ΔGm vs. Composition for a Binary System

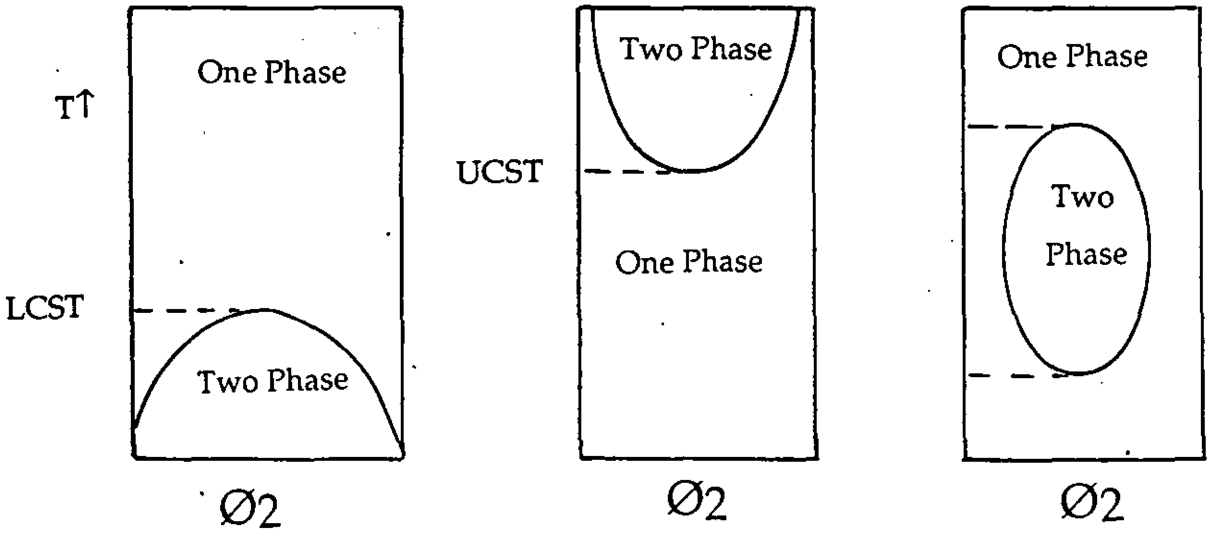

Figure 2.4
Phase Separation Behaviour in Binary System

It is rare that enough information is available from either experiment or theory to be able to predict the miscibility of a given system. It is more common to first observe the phase behaviour which is then explained by the combination of theoretical and experimental knowledge.

Phase diagrams for binary polymer systems are shown in figure 2.4, illustrating upper and lower critical solution temperatures (UCST and LCST). It is assumed that the polymers are in their liquid state and the presence of a glass transition is neglected. It is well established that lower critical solution temperature (LCST) behaviour is the predominant mode of phase separation in a polymer-polymer mixture and has been observed for many systems[20-123]. It can be seen from Figure 2.3 that the shape of the curve for the free energy of mixing ΔG_m plotted against composition ($\varnothing_2$) can indicate the state of miscibility of a binary system.

Since the entropy change (ΔS_m) on mixing two polymers is very small, it follows from equation 2.16 that a small positive ΔH_m can lead to positive ΔG_m and hence phase separation. At constant temperature and pressure, for a binary mixture to be homogenous at all compositions, the equilibrium condition of free energy requires a free energy composition curve that is curved upwards over the whole composition range from its maximum point. Figure 2.5 shows free energy-composition curves for a completely mircible system (a) and a partially miscible system (b), which is characterised by a curve having a portion of negative curvature. In this two phase system, a double tangent can be drawn which touches the curve at two points, representing the composition of the two coexisting phases $\varnothing_2'$ and $\varnothing_2''$ The double tangent intercepts the free-energy axis at points representing the chemical potential of the two components. The chemical potential of species *i* in solution (μ_i)relative to its chemical potential is the pure state (μ_i^*)is defined as the first derivative of ΔG_m with respect to concentration (μ_i) of *i*

$$\mu_i - \mu_i^* = \left(\frac{\partial \Delta G}{\partial M_i}\right)_{T,P,i} = \Delta\mu_i \qquad (2.19)$$

Figure 2.5

ΔG - Composition Curves

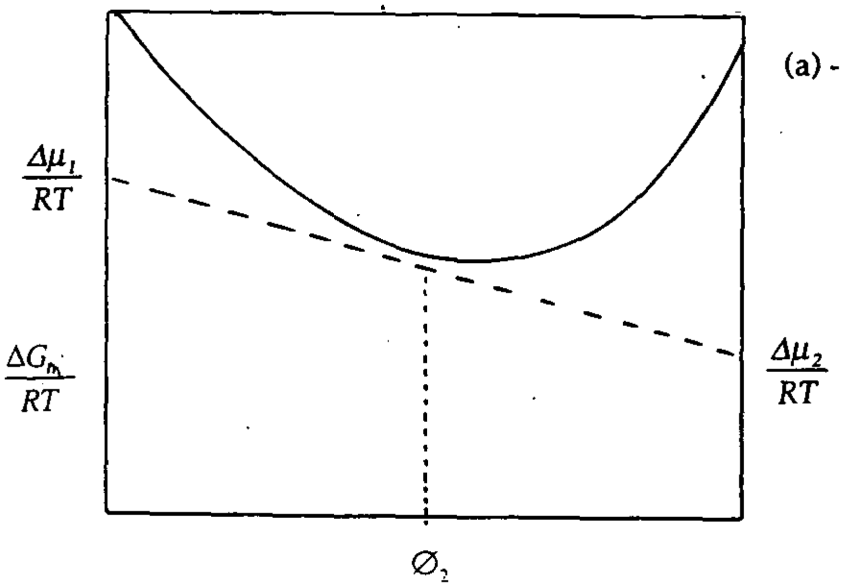

(a) - Completely Miscible System

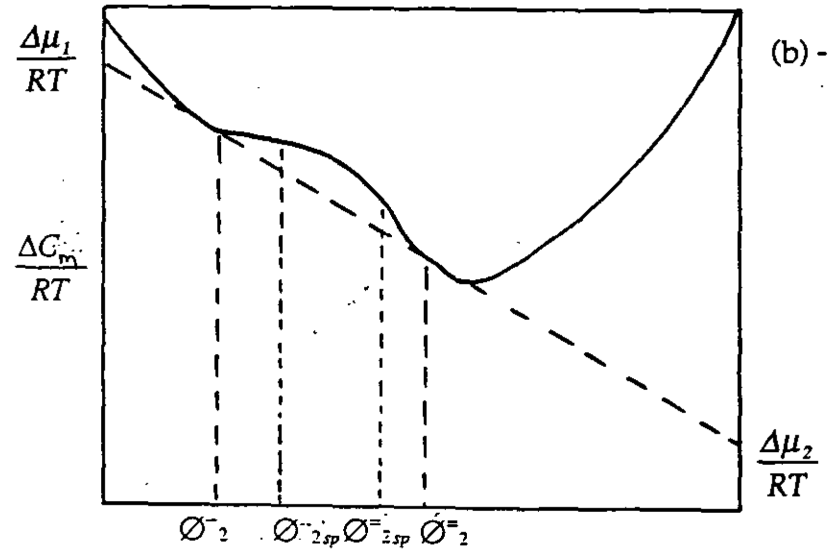

(b) - Partially Miscible System

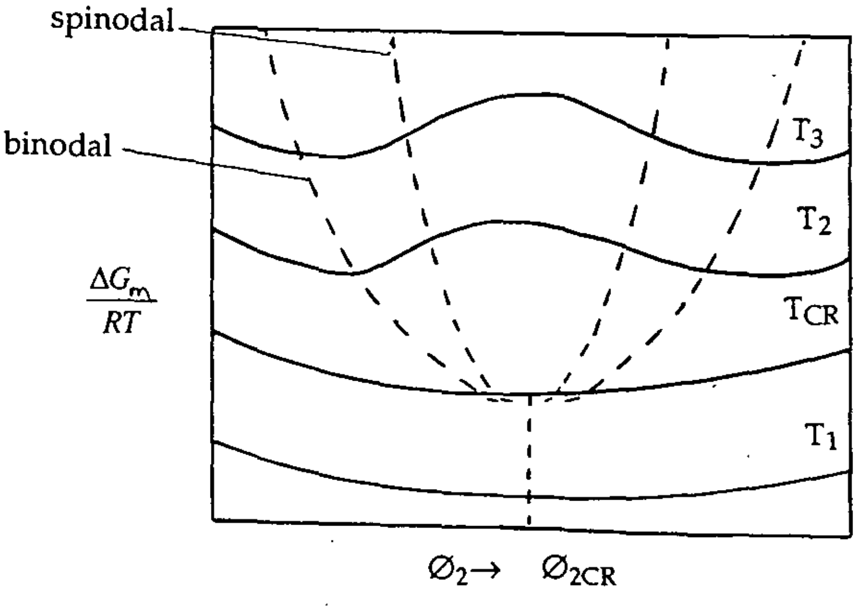

(c) - Temperature Dependence of

$\Delta G_m'$

$T_1 < T_{CR} < T_2 < T_3$

The two inflexion points on this curve separate the positively and negatively curved parts of ΔG_m. Any system within this region is unstable and will phase separate, because the slightest change in concentration will

lead to a decrease in the free energy of the system and cause further separation, until the stable situation of free energy for the two phase system has been reached, (ie a point on the double tangent). This process is known as spinodal phase separation[124]. At the inflexion points

$$\left(\frac{\partial^2 \Delta G_m}{\partial \phi_2^2}\right)_{T,p} = 0 \qquad (2.20)$$

The range of concentrations between the point of inflexion and tangent point are called metastable, since the system can resist small concentration fluctuations on account of the positive curvature.

Increasing the temperature in a two phase system, serves to bring together the two sets of tangents and inflexion points until they form a critical point (Figure 2.5c) at which

$$\left(\frac{\partial^3 \Delta G_m}{\partial \phi_2^3}\right)_{T,p} = 0 \qquad (2.21)$$

Plotting the locus of tangent and inflexion points as a function of temperature yields the phase diagrams showing the coexistence curve (binodal) and locus of inflexion points (spinodal) (Figure 2.6). These two curves have a common horizontal tangent at the critical point parallel to the lines which connect the composition of the coexisting phases.

It is likely that (Figure 2.6) represents only the simplest case and many polymer systems will be characterised by the curves having more complicated shapes. It should also be noted that the critical point may be affected by polydispersity, chain length, temperature and composition.

Figure 2.6

Binary phase diagram for a liquid mixture

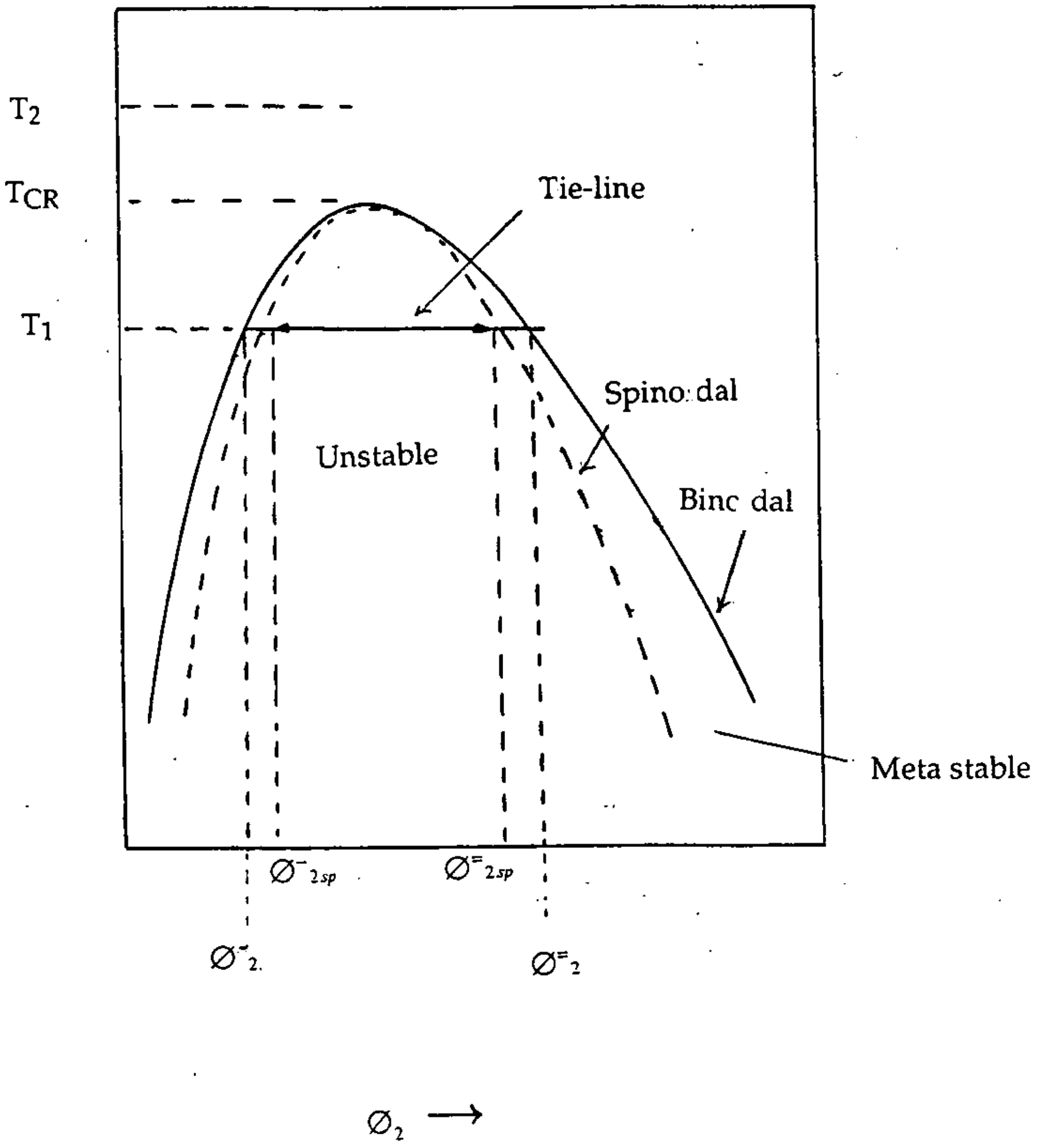

The thermodynamic treatment of phase behaviour for mixtures becomes more useful when specific models for the enthalpic and entropic terms are used. The simplest such model, is that developed by Flory[125] and Huggins[126] originally for the treatment of polymer solutions. Each suggests a lattice model in order to derive expressions for the enthalpy and entropy of mixing.

When a polymer chain is placed in an imaginary two-dimensional lattice, each polymer segment occupies a site on the lattice in an overall random way. A second polymer can then be placed randomly in the remaining lattice sites. It is assumed that the same lattice sites can be used to describe the configuration of both components and that the geometry of the two species is identical. This makes no allowance for specific inter-molecular interactions. The Flory-Huggins theory gives the entropy as

$$\Delta S_m = -R(N_1 \ln \varnothing_1 + N_2 \ln \varnothing_2) \qquad (2.22)$$

Where N_i is the number of moles of i and $\varnothing_i$ is the volume fraction of i. The enthalpy of mixing is given by

$$\Delta H_m = RT\chi_{12} N_1 \varnothing_2 \qquad (2.23)$$

$$\chi_{12} = \frac{z\Delta w_{12} N_A}{RT} \qquad (2.24)$$

N_A is Avagadros' number, z the co-ordination number of the lattice and w_{12} is the energy for the formation of an unlike contact pair which can be expressed as

$$\Delta w_{12} = w_{12} - \tfrac{1}{2}(w_{11} + w_{22}) \qquad (2.25)$$

where W_{12}, W_{11} and W_{22} are the energies of the respective pair interactions. Substituting (2.22) and (2.23) into (2.16) gives the free energy of mixing.

$$\Delta G_m = RT(\chi_{12} N_1 \varnothing_2 + N_1 \ln \varnothing_1 + N_2 \ln \varnothing_2) \qquad (2.26)$$

As real polymers are generally polydisperse this gives

$$\Delta G_m = RT\left[\sum_i N_{1,i}\ln\phi_{1,i} + \sum_i N_{2,i}\ln\phi_{2,i} + \chi_{12}N_1\phi_2\right] \quad (2.27)$$

assuming that interaction parameters are independant of molecular mass.

As previously mentioned, one major assumption is that the same lattice is applicable for describing the configuration of components, and this cannot be justified if the two polymer chains have different spatial requirements. This may lead to a difference between the observed behaviour and that predicted by theory.

It is believed that the entropy contribution to the free energy of mixing, is made up of both a combinatorial entropy term ($\Delta S_m(C)$) and an excess entropy term ($\Delta S_m(e)$). The free energy of mixing becomes

$$\Delta G_m = \Delta H_m - T\left(\Delta S_m(c) + \Delta S_m(e)\right) \quad (2.28)$$

The Flory-Huggins lattice theory takes into account only the combinatorial entropy. However, if specific interactions occur between chain segments, then there will be deviation from random mixing and this may result in a volume change on mixing. Attractive interactions between chains might be expected to lead to a reduction in volume compared to that predicted. The combinatorial entropy term alone takes no account of such volume changes, but equation of state theories attempt to allow for this.

The lattice and equation of state theories attempt to explain or model experimentally observed miscibility behaviour, but they cannot easily predict such behaviour given only information about the physical properties of the pure unmixed components. The interaction parameter χ has been related to the solubility parameters of the polymers.

$$\frac{\Delta Hm}{V} = \frac{RT\chi}{V} = (\delta_1 - \delta_2)^2 \quad (2.29)$$

The use of solubility parameters in predicting miscibility behaviour has been critically reviewed recently[127,128]. Inverse gas chromatography and small angle neutron scattering have also been used to determine χ

The simple Flory-Huggins theory for the thermodynamics of mixing of polymers predicts negligibly small combinatorial entropy and positive enthalpy terms. To obtain miscible homopolymer blends, it is usually necessary to have some sort of attractive force beteween unlike segments. Hydrogen bonding interactions lead to true association of polymer segments, and above the Tg there is a dynamic equilibrium distribution of hydrogen bonds. When polymer segments are associated by hydrogen bonding, the rotational and vibrational degrees of freedom become seriously modified, which can be observed in the infrared spectrum. Painter et al[124,132] have developed an association model for a binary polymer blend in which one polymer self-associates, whilst the second does not, but is capable of hydrogen bonding with the first. This theory depends upon the following assumptions.

a The hydrogen bonded species that can form are unaffected by the covalent linkage of interacting units in the polymer chain.

b The equilibrium constants are independent of the length of hydrogen bonded chains

c The equilibrium constants can be defined in terms of a chemical repeat unit.

2.4 Glass Transition

When a high molecular mass amorphous polymer in its liquid or rubbery phase is cooled, at some temperature called the glass transition (Tg), the physical and mechanical behaviour of the polymer will be transformed to that of a rigid glassy material. At this temperature there is a marked change in the temperature dependence of volume (V), and enthalpy (H) as shown in figure 2.7. There is also a discontinuity in the temperature dependence of heat capacity and expansion coefficient at Tg.

There is debate as to whether the glass transaction is a true thermodynamic phenomenon. Although the glass transition displays second order behaviour, its position depends upon the rate of cooling, and so the kinetics of the process are also important. On heating Tg is usually interpreted as the point at which there is sufficient thermal energy to initiate the onset of molecular motion and conformational change, due to rotation about the bonds along the main backbone of the polymer chain. Below the Tg (α transition) such movement is severely limited, although for many polymers β-transitions (secondary relaxations) have been observed, which are believed to be due to movement in side chains or groups.

Figure 2.7

Volume and Enthalpy versus Temperature

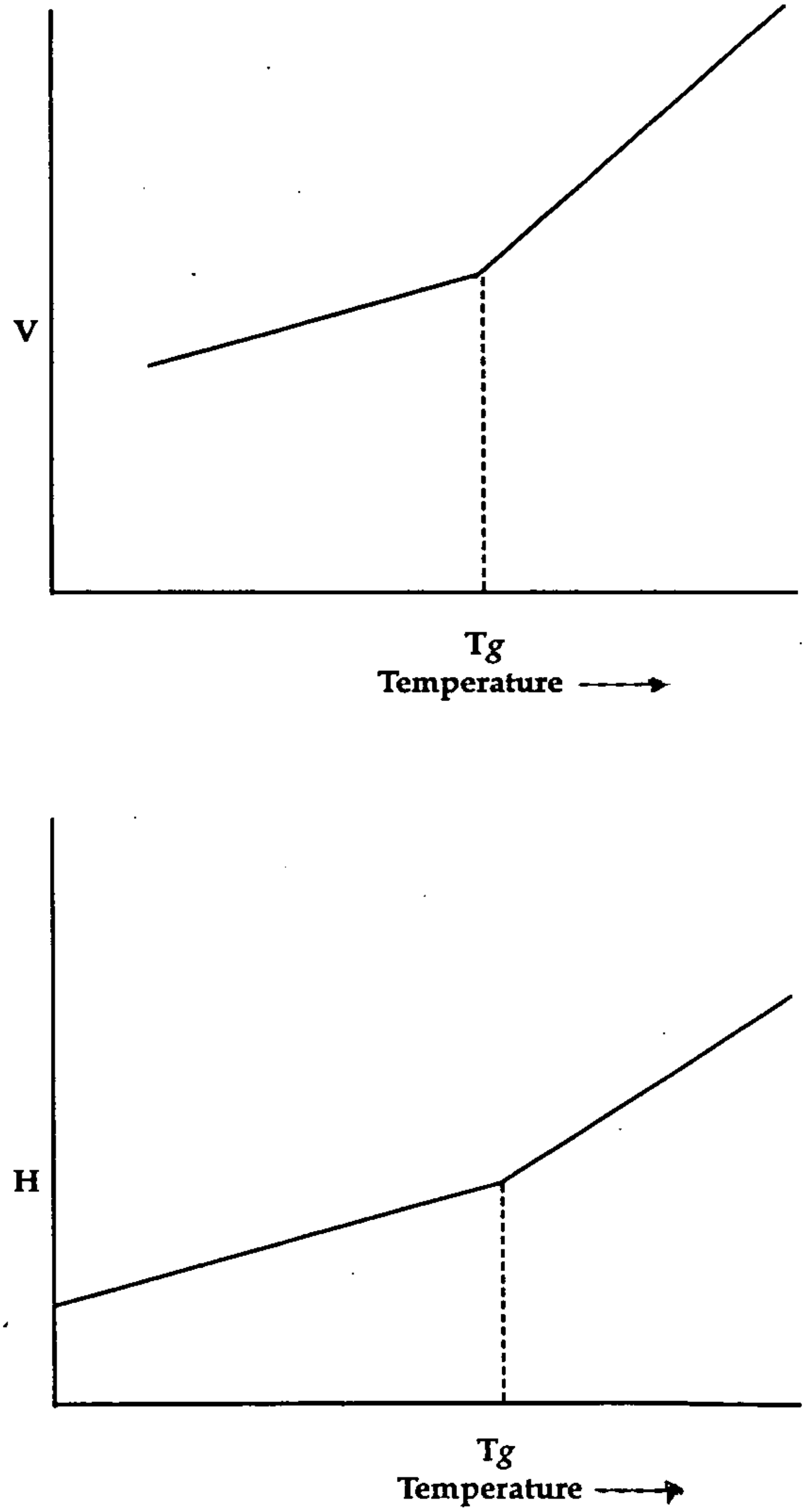

2.4.1 Kinetic Theory

The most widely used theory quantifying the behaviour observed in the region of the glass transition is the kinetic theory of Flory and Fox[133,134]. They proposed that a material may be considered to have a volume made up of two contributions, that which is occupied by molecules and that which consists of vacancies or holes, making up a free volume. Conformational changes are, therefore, movements of chain segments into free volume. The greater the free volume, the greater the extent of molecular motion possible. The glass transitions temperature is the point below which there is insufficient free volume for significant molecular motion to be possible, and so below this temperature the conformational structure of the chains is "frozen in".

Below T_g, the only temperature-induced volume changes are due to molecular expansion or contraction, as the free volume is considered to be constant. The total volume at T_g (V_g) is given by

$$V_g = V_o + Vf \left(\frac{dv}{dt}\right)_g Tg \qquad (2.30)$$

Where V_o is the molecular volume of the material at absolute zero, V_f represents the free volume within the glassy region and $(dV/dt)g$ is the expansivity of the molecular or occupied volume in the glass. At a temperature T, above Tg, the total volume, V_R is given by

$$V_R = V_g + \left(\frac{dv}{dt}\right)_R (T - T_g) \qquad (2.31)$$

$(dV/dT)_R$ represents the expansivity of the total volume above Tg. Doolittle[135,136] derived an expression relating viscosity and volume, incorporating the concept of free volume.

$$\ln\left(\frac{\eta}{\eta_g}\right) = \frac{B}{f_g}\left(\frac{T - Tg}{f/\Delta\alpha + (T - T_g)}\right) \qquad (2.32)$$

Where $\Delta\alpha$ is the difference in thermal expansion coefficients for the rubbery and glassy state and fg is the fraction of free vlume at T_g. This is of the same form on the Williams, Landel, Ferry (WLF) equation[137]

$$\lg\left(\frac{\eta}{\eta_g}\right) = \left(\frac{-C_1(T-T_g)}{C_2+(T-T_g)}\right) = \lg a_T \qquad (2.33)$$

Where C_1 and C_2 are constants and a_T is the ratio of relaxation time at T to the relaxation time at T_g

2.4.2 Thermodynamic Theories

As already mentioned, on cooling the melt of an amorphous polymer, at some point it will undergo a transition to a glassy state. The nature of the glass and the extent of disorder frozen in will depend on the rate at which the transition is approached, as will the temperature at which the transition occurs. Thermodynamic theories propose that there is a true thermodynamic glass transition, at some temperature below the experimentally observed T_g, which could be attained if the melt was cooled at an infinitely slow rate.

The most well known thermodynamic theory of the glass transition is that due to Gibbs and DiMarzio[138]. This attempts to explain the glass transition from a more molecular point of view, with allowances made for the choice stiffness and variations of volume with temperature. Using a lattice model, each segment of the polymer chain is allowed several different orientations, with different energies. The lattice has a number of vacant sites into which chain segments can move. As the temperature is decreased, the system tends towards minimum free energy, that is having a smaller number of holes and a larger percentage of bonds existing in the low flex-energy orientation. The entropy decreases until, at a temperature T_2, the number of allowed states available to the system is reduced to one or a very small number. In this state no conformational changes are possible, and below this temperature T_2, the entropy of the system remains constant, that is zero conformational entropy. Thus T_2, is the equilibrium glass transition temperature, to which the experimentally observed glass transition converges in the case of an infinitely slow time scale.

Adams and Gibbs[134], extended the Gibbs-DiMarzio approach to allow for non-equilibrium conditions. The temperature of relaxation behaviour is explained in terms of the variation in size of a co-operatively rearranging system, defined as the smallest unit that can undergo a transition without a simultaneous change on or outside its boundary. An equation similar to the WLF equation is derived

$$-\lg a_T = \frac{a_1(T - T_s)}{a_2 + (T - T_s)} \qquad (2.34)$$

where T_s is a reference temperature.

2.4.3 Factors Affecting Glass Transition Temperature

a) Chemical Structure

There are several structural factors which influence Tg of a polymer, one of the most important being the flexibility of the backbone. Clearly, a polymer having a structure which allows easy rotation around main chain bonds will have a lower Tg than one where such rotations, and hence conformational changes are hindered.

b) Crosslinking

Crosslinking has been observed to increase the Tg of a polymer to an extent depending on the degree of network formation.

c) Molecular Mass

For high molecular mass polymers, Tg is effectively independent of molecular mass. However, Tg of shorter chain polymers decreases with chain length. Lower molecular mass polymers have a higher proportion of chain ends and hence, free volume. An expression which relates to the effect of molecular mass on the glass transition temperature is

$$T_g = T_{g\infty} - \frac{K}{M} \qquad (2.35)$$

where Tg_∞ is the glass transition temperature at infinite molecular mass and M is the molecular mass of the polymer.

d) Effect of Diluents

Adding a lower molecular mass species to a polymer causes plasticisation. Again, the decrease in the Tg observed on addition of diluents can be explained in terms of an increase in free volume.

e) Blending

A special case of diluent additon is the incorporation of another polymer. The effect this has on the Tg depends upon the miscibility of the two polymers. A miscible polymer blend will exhibit a single Tg, at some point in between the Tg values of the two unmixed components, the exact position depending on the blend composition. An immiscible blend exhibits two glass transitions which correspond closely to the Tg values of the two components. A partially miscible blend will usually show two glass transitions at positions determined by the nature of the phases present in the mixture.

Several equations have been proposed to describe the composition dependence of miscible blends. Gordon and Taylor[140] derived an expression of the form

$$\mathrm{Tg} = \mathrm{Tg}_A + \frac{(K\mathrm{Tg}_B - \mathrm{Tg}_A)W_B}{1+(1-K)W_B} \qquad (2.36)$$

The Fox[141] equation is a special case of the Gordon-Taylor equation, where K is equal to the ratio of the equivalent homopolymer glass transitions (Tg_A/Tg_B)

$$\frac{1}{Tg} = \frac{W_A}{Tg_A} + \frac{W_B}{Tg_B} \qquad (2.37)$$

Couchman[142] has proposed a classical thermodynamic treatment of the effect of compositon on glass transition temperature. Di Marzio[143] has recently critically reviewed the equations used to predict the glass transitions of polymer blends.

2.4.4 Dynamic mechanical Properties of Polymers

Materials under the influence of an applied strain are characterised depending on the nature of their response. Perfectly elastic materials obey Hooke's Law, the applied stress being proportional to the strain Perfectly viscous liquids obey Newton's Law of viscosity, the applied stress being directly proportional to the strain rate. Polymeric materials are neither completely elastic or viscous, but can exhibit both types of behaviour and are so termed viscoelastic.

One of the most important techniques for studying the mechanical behaviour of polymers is dynamic mechanical analysis, which usually entails the application of a sinusoidal load leading to a sinusoidal deformation (Figure 2.8). The resulting strain is neither in phase with the stress (as in perfectly elastic materials) nor 90° out of phase (as in perfectly viscous liquids), instead there is a phase lag δ (phase angle).

Dynamic mechanical analysis is usually carried out in association with a heating program as in dynamic mechanical thermal analysis (DMTA). It is possible to carry out the experiment at constant frequency whilst varying the temperature or vice versa. The stress (σ) resulting from the applied strain (γ) is measured and the time dependency of stress and strain can be written

$$\gamma = \gamma_o \sin \omega t \qquad (2.38)$$

$$\sigma = \sigma_0 \sin(\omega t + \delta) \qquad (2.39)$$

ω is the cyclic frequency γ_o and δ_0 are the strain and stress amptitude. Equation 2.39 can be expanded to

$$\sigma = \sigma_0 \sin \omega t \cos \delta + \sigma_0 \cos \omega t \sin \delta \qquad (2.40)$$

So it can be seen that stress is made up of the two components, one which is in phase with strain (of magnitude $\sigma_0 \cos \delta$ and one which is out of phase with strain (of magnitude $\sigma_o \sin \delta$)

Figure 2.8

Relationship Between Stress and Strain in Dynamic Mechanical Analysis

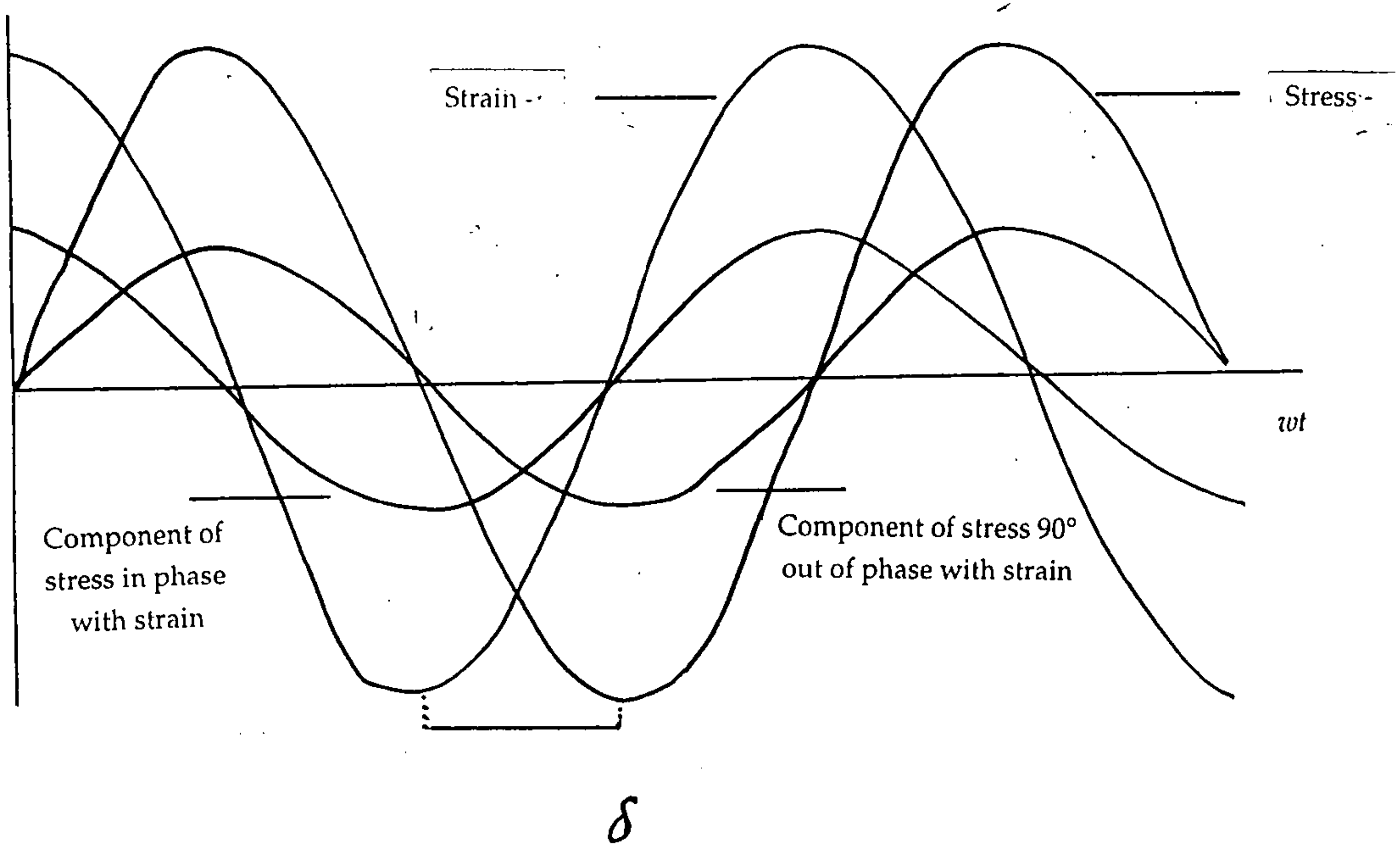

The stress-strain relationship, therefore is as follows:

$$\sigma = \gamma_o E' \sin \omega t + \gamma_o E'' \cos \omega t \qquad (2.41)$$

Where the storage modulus E' is equal to $(\sigma_o / \gamma_o)\cos\delta$, that is the component of stress in-phase with strain divided by the strain amplitude, and where loss modulus E'' is equal to $(\sigma_o / \gamma_o)\sin\delta$, the component of stress out of phase with strain divided by the strain amptitude.

Dividing the loss modulus by the storage modulus leads to the loss tangent

$$\frac{E''}{E'} = \frac{(\sigma_o / \gamma_o)\sin\delta}{(\sigma_o / \gamma_o)\cos\delta} = \tan\delta \qquad (2.42)$$

This effectively means that tan δ is the ratio of energy stored to the energy lost per cycle. A complex modulus can be derived such that

$$E^* = \sqrt{(E'')^2 + (E')^2} \qquad (2.43)$$

This can be represented by an Argand diagram as in Figure 2.9. Figure 2.10 shows the variation of E' and tan δ against frequency and temperature for a typical homopolymer in the region of its glass transition. At high frequencies and low temperature the storage modulus E''_g is characteristic of a glassy material. On decreasing the frequency or increasing the temperature, the storage modulus becomes characteristic of a rubbery material, the loss modulus in both cases having passed through its peak. The peak in $\tan\delta$ corresponds to the maximum in the hysteresis or damping and is interpreted as occuring at the glass transition of the polymer.

2.4.5. Factors Affecting Dynamic Mechanical Behaviour

Random or statistical copolymers are generally characterized by a single Tg and hence a single $\tan\delta$ peak at a temperature determined by copolymer composition. A broadening of the peak may be observed if

Figure 2.9

Argánd Diagram Relating E', E'' and δ

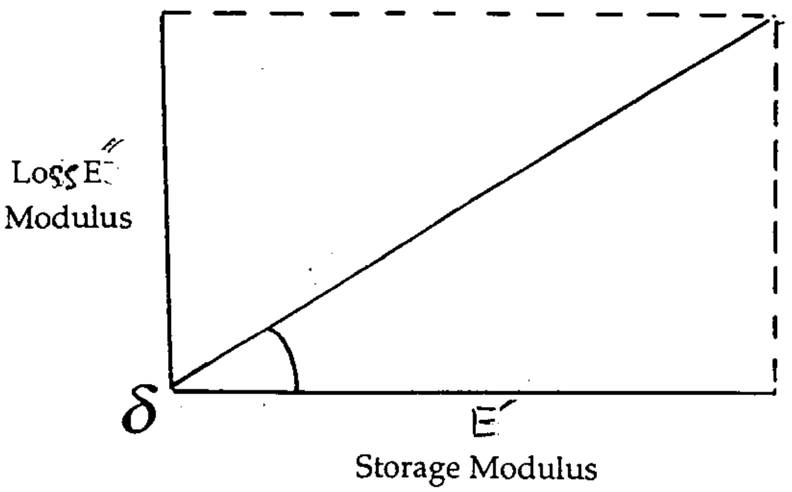

$$E^* = \sqrt{(E')^2 + (E'')^2}$$

= Complex modulus

Figure 2.10

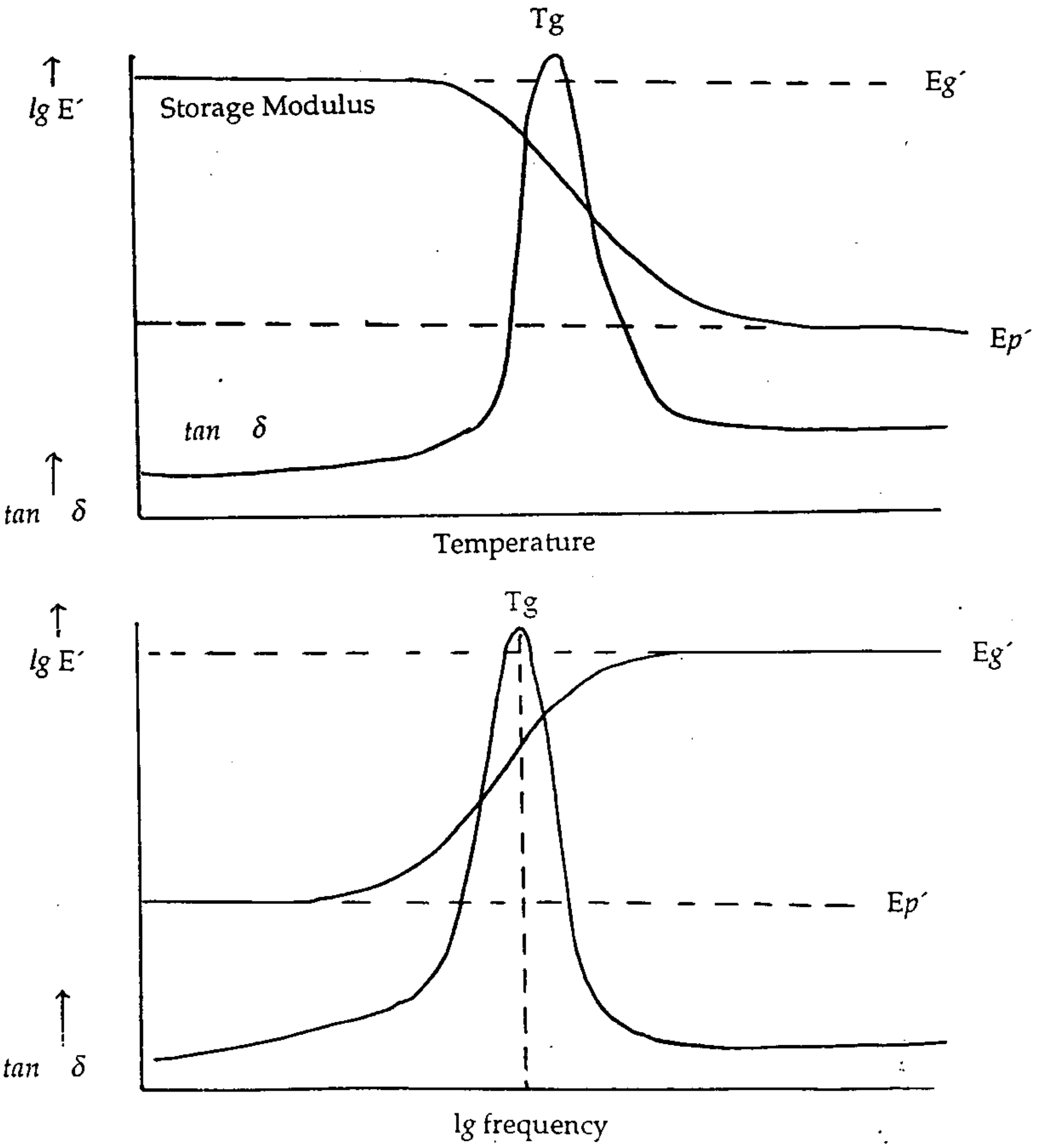

there are long sequences of a given comonomer unit, especially if these units experience poor mixing with other comonomer segments.

The miscibility of two or more component polymers within a blend can have a marked effect on the appearance of both the loss modulus and loss tangent curves. Figure 2.11 shows the loss modulus and tan δ curves characteristic of miscible, partially miscible and immiscible binary mixtures. Completely miscible blends are characterised by a single tan δ peak at some point between the points expected for the Tg values of the unmixed components, due to a single glass transition for the single phase present. The breadth of the tan δ peak should, for completely miscible blends, be no wider than the tan δ peaks of the blend components. A broadening of the peak may result if there is incomplete miscibility.

Totally immiscible blends are indicated by two tan δ peak at the same temperature close to the peaks for the unmixed components. A shift of peaks towards each other relative to the two components suggests some degree of partial mixing.

A broad loss peak covering the temperature range between the peak positions of the blend components is a special case of partial miscibility termed micro-heterogeneity. This effect is due to the presence of a large number of phases of varying compositions. The dynamic mechanical behaviour of polymers has been extensively reviewed.[144,145]

Figure 2.11

Tan δ and Log Modulus Curves Illustrating Different Types of Mixing Behaviours

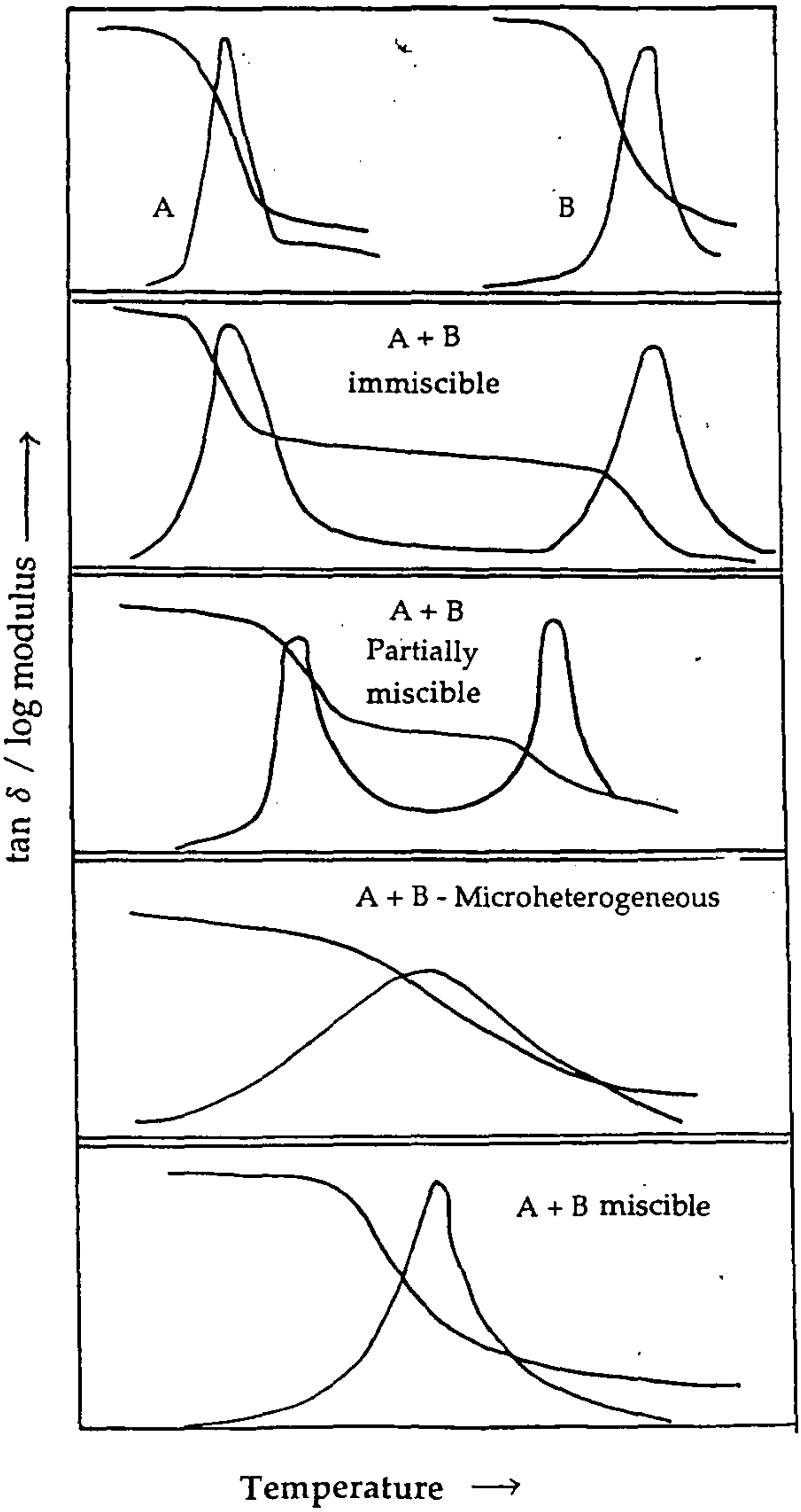

3. EXPERIMENTAL

3.1 Reagents and Materials

The poly (vinyl butyral) samples were B20H and B30H mowitals supplied by Hoechst with 75 - 77 wt % acetal units, 3 wt % acetate units and 18-21% alcohol units. Tetrahydrofuran (THF), was unstablised HPLC grade supplied by Fisons. Dioxane (99% ACS reagent) was distilled from sodium before use. Pyridine (99% Gold Label) was stored over sodium hydroxide before use. Benzoic anhydride (99%) was recrystalised from benzene/petrol before use. Phthalic anhydride (99%) and succinic anhydride (97%) were recrystalised from ethanoic anhydride before use. Ethanoic anhydride (98% ACS reagent) and butanoic anhydride (98%) were distilled from phosphorous pentoxide before use. Trifluoracetic anhydride (99%) was used as supplied. Triethylamine (99%) was distilled from sodium before use. All these were supplied by the Aldrich Chemical Company. Polyethylenimine was Polymin P supplied by BDH as a solution in water, the water was removed by heating in a vacuum oven at 60°c for 24 hours. Poly (vinyl pyrrolidone) (~10,000) was supplied by the Aldrich Chemical Company, this was dried by heating under vacuum at 180° for 24 hours and stored in a desiccator before use. The polyester Diorex and the polyurethane TMXD1/NPG were supplied by Coates Lorrilleux International Limited, as solutions in ethyl acetate/industrial alcohol. Solvent was removed by heating in an oven at 40°C for 24 hours followed by heating at 40°C under vacuum for 24 hours. All other solvents were supplied by Careless Solvents Limited. Unless otherwise stated these were used as supplied.

3.2 Instrumentation

Infrared spectra of polymer films cast on to sodium chloride discs from a solution in THF or chloroform were recorded on a Nicolet 20DX Fourier transform spectrometer. Nuclear magnetic resonance spectra (NMR 250 MHz) were recorded on a Bruker AC 250 spectrometer of samples in deuterated dimethyl sulphoxide (d_6-DMS0, 99%) supplied by the Aldrich Chemical Company, with chemical shifts (δ_H ppM) expressed relative to tetramethyl silane (TMS) used as an internal standard. Size exclusion chromatography (SEC) was performed using a Polymer Laboratories mixed gel column with a particle size of $10 \mu m$ using THF as eluent with toluene as an internal standard. Solutions were approximately 0.15% w/v loaded into a six port injection valve containing a 200 μl loop. Elution was with a Knauer High Pressure Liquid Chromatography Pump 64 at a flow rate of 1.0 ml min^{-1}. Detection was accomplished using a Knauer 98 differential refractometer connected to a J J chart recorder, set with a chart speed of 200 mm min^{-1}. The column was calibrated with polystyrene standards supplied by Polymer Laboratories. Values of average molecular masses were obtained using a computer programme, from values of peak heights over a range of elution times.

Mechanical thermal analysis was carried out with a Polymer Laboratories Mark II Dynamic Mechanical Thermal Analyzer (DMTA) in the dual cantilever mode. Most of the polymers were too soft to prepare bar samples, so they were imbedded into an inert support material[146]. These samples were pressed into filter paper or bleached cotton cloth between the jaws of a press heated to 20 - 50°C above the expected Tg and held at six tons for thirty seconds then cooled rapidly to room temperature. A comparison of cast polystyrene and supported polystyrene is given in Appendix 1.

3.3 Intrinsic Viscosities

Approximately 0.25g of poly (vinyl butyral) was dissolved in 15ml of THF by refluxing and stirring for one hour. After cooling this was transferred to a 25ml volumetric flask and diluted to the mark. The viscosity of the solutions was determined relative to the THF at 25°C using a Schott-Gerate AVS 310 automatic viscometer with a Schott-Gerate 531 01 Ubbelohde capillary viscometer tube. All solutions and solvents were filtered through Whatman glass microfilters before placing in the viscometer tube. The solution was allowed to reach thermal equilibrium for 15 minutes before measurements were taken. Dilution was carried out internally with rapid mixing. Relative viscosities were determined for at least five different concentrations maintaining $1.2 \leq \eta_r \leq 2$. The viscosities of acid derivatised poly (vinyl butyral) were determined in distilled methanol and distilled water using a Schott-Gerate 531 03 Ubbelohde capillary viscometer tube.

3.4 Determination of hydroxyl content of samples of poly (vinyl butyral)[147,148,149]

This involves the conversion of the hydroxyl groups to acetate groups using ethanoic anhydride followed by titrimetric determination of the remaining acetylating agent. Approximately 0.1 g of poly (vinyl butyral) dried at 40°c under vacuum for 24 hr. was dissolved in acetylating agent (10:1 pyridine/ethanoic anydride) and left in a stoppered flask at room temperature overnight. To this 30ml of chloroform and 20ml of water were added. This was then titrated with approximately 0.2M aqueous sodium hydroxide with vigarous stirring using phenolphthalein as indicator. Blank solutions of acetylating agent were treated in the same way.

Ethanoic anhydride provides 2 moles of ethanoic acid per mole of anhydride. One mole of acid attaches to the polymer chain, the other being complexed with pyridine. For every mole of hydroxyl groups in the polymer, one mole of ethanoic acid is produced and one mole of sodium hydroxide is required in the titration. The blank solution will require two moles of sodium hydroxide per mole of ethanoic anhydride.

Let x = moles of ethanoic acid in blank
Let y = moles of ethanoic anhydride required for acetylation

This requires $2(x-y)$ moles of sodium hydroxide in the titration. Since y moles of ethanoic anhydride gives y moles of ethanoic acid during acetylation, the total amount of ethanoic acid produced is $2(x-y) + y = 2x - y$ moles which require $2x - y$ moles of sodium hydroxide. The amount of hydroxyl groups due to polymer is:

$$y = 2x - (2x-y) \text{ or}$$

$$\frac{(\text{Blank Titre - Sample Titre}) \times [\text{Na OH}] \times 10^{-3}}{\text{Mass of Polymer}} \text{ per gramme}$$

3.5 Modification of Poly (Vinyl Butyral)

3.5.1. Butyration

Approximately 10g of poly (vinyl butyral) was dried overnight in a vacuum oven at 100°c. This was then dissolved in 50ml of dioxane with 20ml of triethylamine by refluxing under an atmosphere of nitrogen. Butanoic anhydride was added via a pressure equilibrating dropping funnel at room temperature over a period of 30 minutes, and the resulting mixture left at room temperature for 24 hours. The polymer was then precipitated into water. The precipitate was filtered, washed with water, redissolved in a mixture of acetone and methanol and reprecipitated into water. This was repeated twice more and the final product dried in a vacuum oven at 60°C for 24 hours. The degree of modification can be varied by changing the amount of anhydride used.

3.5.2 Trifluoroacetylation

A solution of poly (vinyl butyral) in dioxane and triethylamine was prepared as in section 3.5.1. This was then cooled to 0°C with an ice water bath. Trifluoroacetic anhydride was added dropwise over a period of 30 minutes under an atmosphere of nitrogen. When addition was complete, the reaction mixture was allowed to warm to room temperature and left for 24 hours. The product was obtained and purified as in section 3.5.1. The degree of modification can be varied by changing the amount of anhydride used.

3.5.3 Benzoation

A solution of poly (vinyl butyral) in dioxane and triethylamine was prepared as in section 3.5.1., and a solution of benzoic anhydride in dioxane. The benzoic anhydride solution was added dropwise over 30 minutes under a nitrogen atmosphere and then left for 24 hours at room temperature. The product was obtained and purified as in section 3.5.1. The degree of modification can be varied by changing the amount of anhydride used.

3.5.4. Reaction with succinic and phthalic anhydride[150,151,152]

A solution of poly (vinyl butyral) in dioxane and triethylamine was prepared as in Section 3.5.1. The anhydride was dissolved in sodium dried benzene. The solution was added slowly under an atmosphere of nitrogen and brought to reflux and left for 24 hours. After cooling, the mixture was concentrated under reduced pressure. The residue was dissolved in a little methanol and poured into a litre of water containing 15g of sodium chloride. The aqueous mixture was usually at a pH of 10-11 with the polymer completely dissolved. The pH was lowered by slowly adding hydrochloric acid. Precipitation began at a pH of 8.5 and should be complete at pH 5-6. The particles could be coagulated by adding a small amount of acetone. This was then filtered and the precipitate washed with a large amount of water. This was then dried in a vacuum oven at 100°c for 24 hours. The degree of modification can be changed by varying the amount of anhydride used.

3.6 Determination of acid groups in phthalated and succinated poly (vinyl butyral)

Approximately 1% solutions of derivised poly (vinyl butyral) was made in freshly distilled methanol and titrated with 0.009M potassium hydroxide solution in distilled methanol using phenophthalein as indicator

3.7 Solubilities

Approximately 0.1g of polymer was mixed with 4ml of solvent. The solvents were methanol, methanol/ethyl acetate (1:1), ethyl acetate, acetone, THF, benzene, toluene, hexane, cyclohexane and chloroform. These were shaken for 30 minutes at room temperature and observed for signs of swelling or dissolution.

3.8 Blend Preparation

Blends with Diorex

Samples of poly (vinyl butyral) and diorex were dissolved separately in a 3:1 mixture of ethyl acetate and industrial alcohol. When the polymers were dissolved the solutions were mixed and poured into crystalisation dishes and left in a fume cupboard for 24 hours to allow the solvent to evaporate. The blends were further dried in a vacuum oven at 100°C for a further 24 hours. The blend compositions were 2:1 poly (vinyl butyral)/diorex, 1:1 poly (vinyl butyral)/diorex and 1:2 poly (vinyl butyral)/diorex with a total mass of polymer mass of about 0.4g. The transparency of the films were observed and the blends analysed by DMTA

Blends with TMXDI/NPG

Samples of poly (vinyl butyral) and TMXDI/NPG were dissolved separately in a 3:1 mixture of ethyl acetate and industrial alcohol. When the polymers were dissolved the solutions were mixed and poured into crystalisation dishes and left in a fume cupboard for 24 hours to allow the solvent to evaporate. The blends were then further dried in a vacuum oven at 100°C for 24 hours. The blend compositions were 2:1 poly (vinyl butyral)/TMXDI/NPG, 1:1 poly (vinyl butyral)/TMXDI/NPG and 1:2 poly (vinyl butyral)/TMXDI/NPG, with a total mass of polymer of about 0.4g. The transparency of the films was observed, and the blends analysed by DMTA.

Blends with polyethylenimine

Samples of poly (vinyl butyral) and polyethylenimine were dissolved separately in a 3:1 mixture of ethyl acetate and industrial alcohol. When the polymers were dissolved the solutions were poured into crystalisation dishes and left in a fume cupboard for 24 hours to allow the solvent to evaporate. The blends were further dried in a vacuum oven at 100°C for a further 24 hours. The blend compositions are 2:1 poly (vinyl butyral)/polythylenimine, 1:1 poly (vinyl butyral)/ polythylenimine, and 1:2 poly (vinyl butyral)/polyethylenimine, with a total mass of polymer of about 0.4g. The transparency of the films was observed, and the blends analysed by DMTA.

Blends with poly (vinyl pyrrolidone)

Samples of poly (vinyl butyral) and poly (vinyl pyrrolidone) were dissolved separately in a 3:1 mixture of ethyl acetate and industrial alcohol. When the polymers were dissolved, the solutions were poured into crystalisation dishes and left in a fume cupboard for 24 hours to allow the solvent to evaporate. The blends were further dried in a vacuum oven at 100°c for 24 hours. The blend compositions were 2:1 poly (vinyl butyral)/poly (vinyl pyrrolidone), 1:1 poly (vinyl butyral)/ poly (vinyl pyrrolidone) and 1:2 poly (vinyl butyral)/ poly (vinyl pyrrolidone), with a total mass of polymer of about 0.4g. The transparency of the films was observed. Once the samples for analysis by DMTA were prepared, they were further dried in a vacuum oven at 120°C for 24 hours and stored in a desiccator before analysis wich was carried out under an atmosphere of dry nitrogen. This is to prevent the uptake of water from the atmosphere by the poly (vinyl pyrrolidone) which causes microphase separation in the blend.

Errors

The error in determining the intrinsic viscosity (η) and slope constant k, are 2% and 5% respectively based upon 95% confidence limits. The error in determining the chemical composition can be as high as 80%.

4. RESULTS AND DISCUSSION

4.1 Unmodified Poly (Vinyl Butyral) PVB

The intrinsic viscosities of the mowitals B20H and B30H in THF were determined using the Huggins-Kraemer[74,77] (equations 2.6 and 2.7), Schulz-Blaschke[78] (equation 2.8) and Martin[79] (equation 2.9) methods. The results are given in table 4.1. The higher value of the slope constant for B30H is an indication of aggregation, both samples of PVB show non ideal behaviour; as has been previously mentioned a theoretical value of the slope constant is approximately 0.3. This behaviour is also illustrated by the size exclusion chromatography (SEC) data in table 4.2, by the higher polydispersity of B30H, and the shoulder on the high molecular mass region of the chromatogram of B30H in figure 4.1. This has also been observed by Cotts et al.[96-100] and Remson[101] indicating that the shoulder is due to aggregation. The aggregates are difficult to detect with a refractive index detector but are easily seen with the use of a low angle laser light scattering (LALLS) detector. Solubility was investigated in a number of solvents as indicated in table 4.3.

There have been few reports of miscibility studies of poly (vinyl butyral) or poly (vinyl acetal) with other polymers in the literature[153-155]. Guo[156] has
studied the miscibility of poly (vinyl formal) with poly (vinyl pyrrolidone) (PVP) and found the polymers to be miscible in all proportions. Eguiazabal[157] found that blends of poly (vinyl butyral) with poly (vinyl pyrrolidone) gave a single Tg when they contain less than 50 wt% of PVP.

Blends of PVB with PVP, polyethylenimine (PEI) an aliphatic polyester (diorex) and a poluyrethane (TMXDI/NPG) were prepared by solution casting and examined by DMTA.

Figure 4.1

SEC of B30H in THF

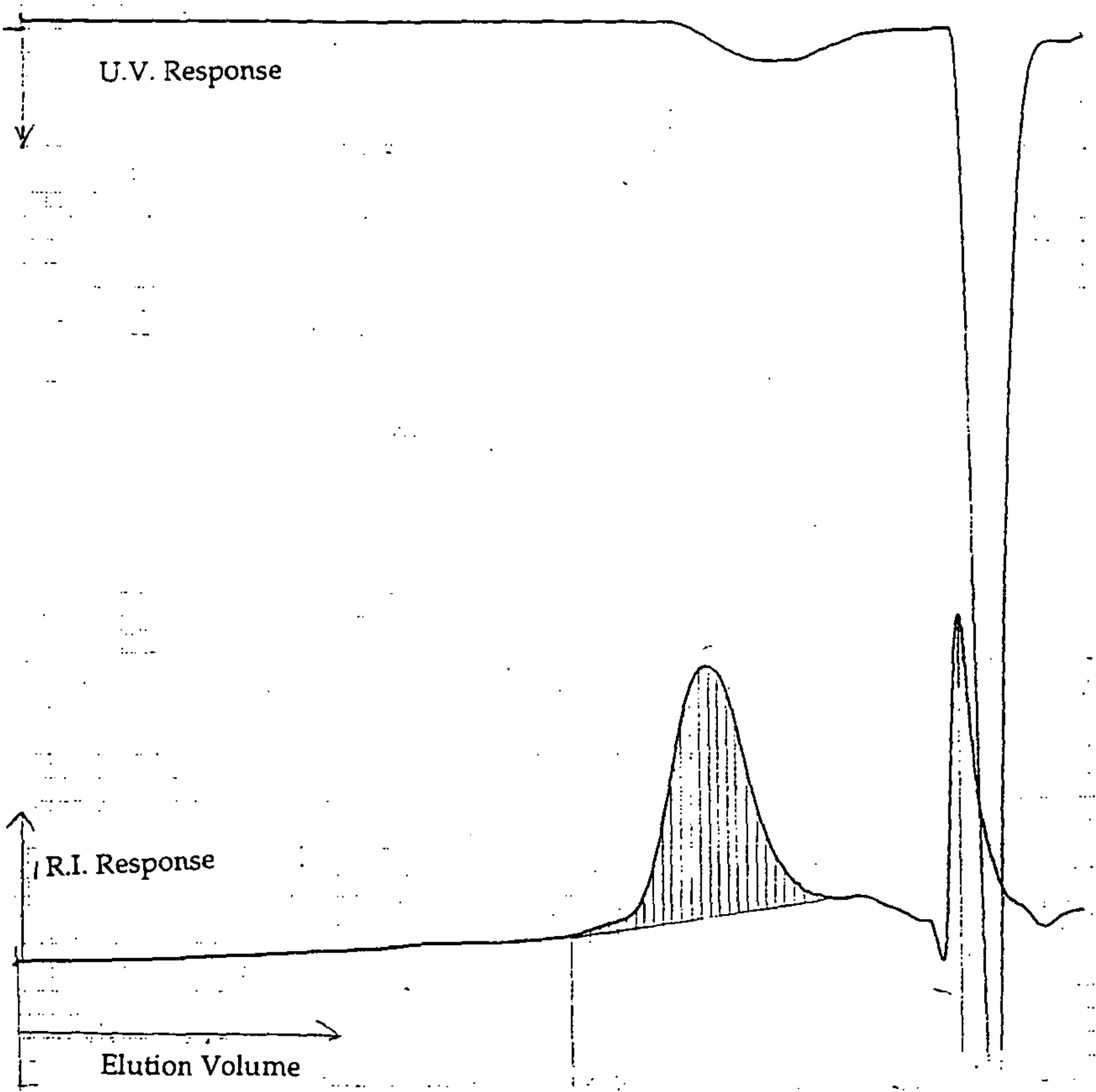

Table 4.1
Intrinsic Viscosity Data of PVB in THF

polymer	$[\eta]_H / g^{-1}dl$	$[\eta]_K / g^{-1}dl$	$[\eta]_{SB} / g^{-1}dl$	$[\eta]_M / g^{-1}dl$	k_H	k_k	k_{SB}	k_M
B30H	0.5948	0.6103	0.6144	0.6065	0.815	0.0728	0.5115	0.6282
B20H	0.3382	0.3464	0.3436	0.3411	0.4737	0.0845	0.3592	0.4099

Table 4.2
Molecular Mass, Hydroxyl and Transition Data of Homopolymers

Polymer	$\bar{M}n$	$\bar{M}w$	$\bar{M}p$	$\bar{M}wd$	[OH]/mmol g^{-1}	Tg/°c
B30H	16000	58000	31000	3.55	4.00	70
B20H	9000	23000	14000	2.56	4.00	71
Diorex	2100	4900	3200	2.33	-	-35
TMXDI/NPG	5300	10000	7300	1-9	-	98.5
PEI	-	-	-	-	-	-26.5
PVP	10000	-	-	-	-	171

Table 4.3

Solubility Characteristics of PVB

polymer	Methanol	Acetone	Ethyl Acetate	Ethyl Acetate/ Methanol 1:1	THF	Benzene	Toluene	Hexane	Cyclohexane	Chloroform
B30H	✓	✓	✓	✓	✓	swell	swell	X	X	✓
B20H	✓	✓	✓	✓	✓	swell	swell	X	X	✓

The transition data of the homopolymers are given in table 4.2 and the results of blending are given in table 4.4. It was found that atmospheric moisture greatly influences the miscibility of PVB with PVP illustrated by a broad tan δ peak at the glass transition temperature in figure 4.2. Under an atmosphere of dry nitrogen, a single Tg was observed with a PVB/PVP ratio of 2:1, which is in close agreement with that predicted by the Fox equation[141] (equation 2.37) and that predicted by the rule of mixtures[158] (equation 4.1)

$$Tg = W_1 Tg_1 + W_2 Tg_2 \qquad 4.1$$

Where W_1 is the weight fraction of component 1. This indicates miscibility of the two polymers with a single phase morphology. With a PVB/PVP ratio of 1:1 and 1:2 two values of Tg are observed. With a ratio of 1:1 the lower Tg is narrow and the higher one is broad. This indicates the presence of two phases, one a mixture of PVB with PVP the other a phase very rich in PVP with some partial miscibility with PVB. With a ratio of 1:2, the values of Tg are narrow; one phase is a mixture of PVB with PVP the other is unmixed PVP. This is in agreement with the results reported by Eguizabal[157] and illustrated in figure 4.3. Blends of PVB with PEI show a single narrow Tg with a PBV/PEI ratio of 2:1, which is 10°C lower than that of unmixed PVB but does not correlate with the predictions of the Fox equation or rule of mixtures. This indicates that there is partial miscibility of PVB with PEI giving a phase which is rich in PVB. With a PVB/PEI ratio of 1:1 two broad values of Tg are observed in between those of the umixed polymers, indicating partial miscibility with some microphaseheterogeneity. With a PVB/PEI ratio of 1:2 the tan δ peak is very broad covering the region between the values of the Tg of the unmixed polymers, indicating microphaseheterogeneity as illustrated in figure 4.4.

Blends of PVB with diorex show a narrowTg with a PVB/diorex ratio of 2:1 which does not correlate with that predicted by the Fox equation or the rule of mixtures but is 10°C lower than that of unmixed PVB. This indicates some miscibility of PVB with diorex. With a PVB/diorex ratio of 1:1 a single broad Tg is observed 19°C lower than that of unmixed PVB indicating partial miscibility with some microheterogeneity. With a

PVB/diorex rato of 1:2, a narrow T*g* is observed corresponding to umixed diorex and a very broad $\tan\delta$ curve giving a T*g* at 45.8°C corresponding to a microhetergeneous blend of PVB/diorex, as indicated in figure 4.5. Blends of PVB with TMXDI/NPG show a single narrow T*g* with a PVP/TMXDI/NPG ratio of 2:1 which correlates with that predicted by the Fox equation and rule of mixtures indicating single phase morphology. However there may be some error in this conclusion as the values of T*g* of the unmixed polymers are quite close and only just resolved by DMTA. With a PVB/TMXDI/NPG ratio of 1:1, two poorly resolved T*g* values are observed in between those of the unmixed polymers. With a PVB/TMXDI/NPG ratio of 1:2, two broad and poorly resolved T*g*'s are observed which are close to those of the unmixed polymers. This indicates partial miscibility with some microphaseheterogeneity as illustrated in figure 4.6.

The chemistry that can be used to modify PVB is similar to that used in polysaccharide chemistry, by esterification or etherification of the hydroxyl groups as shown in scheme 10.

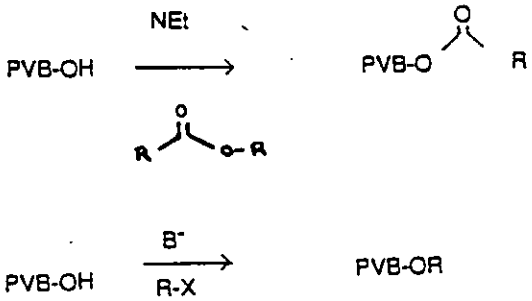

Scheme 10

Danhelka[95] has acetylated PVB to aid characterisation by SEC. Harris[159] has prepared acrylate and methacrylate esters of poly (vinyl formal). When a cyclic anhydride is used at least two equivalents of triethylamine must be used to avoid cross-linking. It has been reported[160] that some care must be taken with the reaction conditions to avoid degradation of the polymer chain. Other chemical modifications of PVB which have been reported are metalation with aluminium alcoholates[161-163] and recently Velichkova[164] has grafted poly (ethylene oxide) and poly (dimethyl siloxane) onto the free hydroxyl groups of PVB.

4.2 Butyrated PVB

A number of butyrated samples of B20H and B30H were prepared. The intrinsic viscosities of the modified PVB samples were determined and the results given in table 4.5. The molecular mass, hydroxyl content, transition data and ratio of butyrate plus butyral groups to acetate groups are given in table 4.6. Determination of hydroxyl content by acetylation and titrating the excess reagent can introduce large errors, possibly due to incomplete acetylation[149] and absorption of acetylating agent in precipitated polymer. The accuracy of analysis by NMR depends upon the signal from the substitutents being well resolved from other signals. In the case of butyrated samples of PVB, the easiest to use is from the methyl protons on the butyrate ester with those of the butyral groups. An NMR spectrum of modified PVB is given in figure 4.7.

Table 4.4
Blends of B20H

With poly (vinyl pyrrolidone) (PVP) in air

Blend	wt fraction PVB	wt fraction PVP	Film Appearance	DMTA Tg/°C	Fox Eqn Tg/°C	Rule of Mixtures Tg/°C
	1	0		71		
158(a)	2/3	1/3	clear	96.1,167	98.92	104.33
158(b)	1/2	1/2	clear	182	114.66	121
158(c)	1/3	2/3	clear	184	131.71	137.61
	0	1		171		

With PVP under dry nitrogen

Blend	wt fraction PVB	wt fraction PVP	Film Appearance	DMTA Tg/°C	Fox Eqn Tg/°C	Rule of Mixtures Tg/°C
	1	0		71		
186(a)	2/3	1/3	clear	106	98.92	104.33
186(b)	1/2	1/2	clear	105,166	114.66	121
187(c)	1/3	2/3	clear	119,170	131.71	137.61
	0	1		171		

With polyethylenemine (PEI) in air

Blend	wt fraction PVB	wt fraction PEI	Film Appearance	DMTA Tg/°C	Fox Eqn Tg/°C	Rule of Mixtures Tg/°C
	1	0		71		
159(a)	2/3	1/3	clear	60	30.93	38.5
159(b)	1/2	1/2	clear	-0.1,54.3	14.20	22.25
159(c)	1/3	2/3	clear	-3.4,65.6	-0.78	6
	0	1		-26.5		

Table 4.4
Blends of B20H

With Diorex in air

Blend	wt fraction PVB	wt fraction Diorex	Film Appearance	DMTA Tg/°C	Fox Eqn Tg/°C	Rule of Mixtures Tg/°C
	1	0		71		
161(a)	2/3	1/3	clear	60.8	26.54	35.67
161(b)	1/2	1/2	clear	52.2	8.35	18
161(c)	1/3	2/3	clear	-35.5,45.8	-7.75	0.33
	0	1		-35		

With TMXDI/NPG in air

Blend	wt fraction PVB	wt fraction TMXDI/NPG	Film Appearance	DMTA Tg/°C	Fox Eqn Tg/°C	Rule of Mixtures Tg/°C
	1	0		71		
171(a)	2/3	1/3	clear	77.3	79.71	80.17
171(b)	1/2	1/2	clear	76.4,91.3	84.23	84.76
171(c)	1/3	2/3	clear	74.6,94.7	88.87	89.35
	0	1		98.5		

Figure 4.2

DMTA
Head: Standard 300°C

TITLE : PVB
SUBTITLE: B20H
FILENAME: B20H
OPERATOR: D.Cunliffe

DATE RUN: May/29/1991
FREQ : 1
STRAIN : 4
DIM: 2.00, 11.955, .275

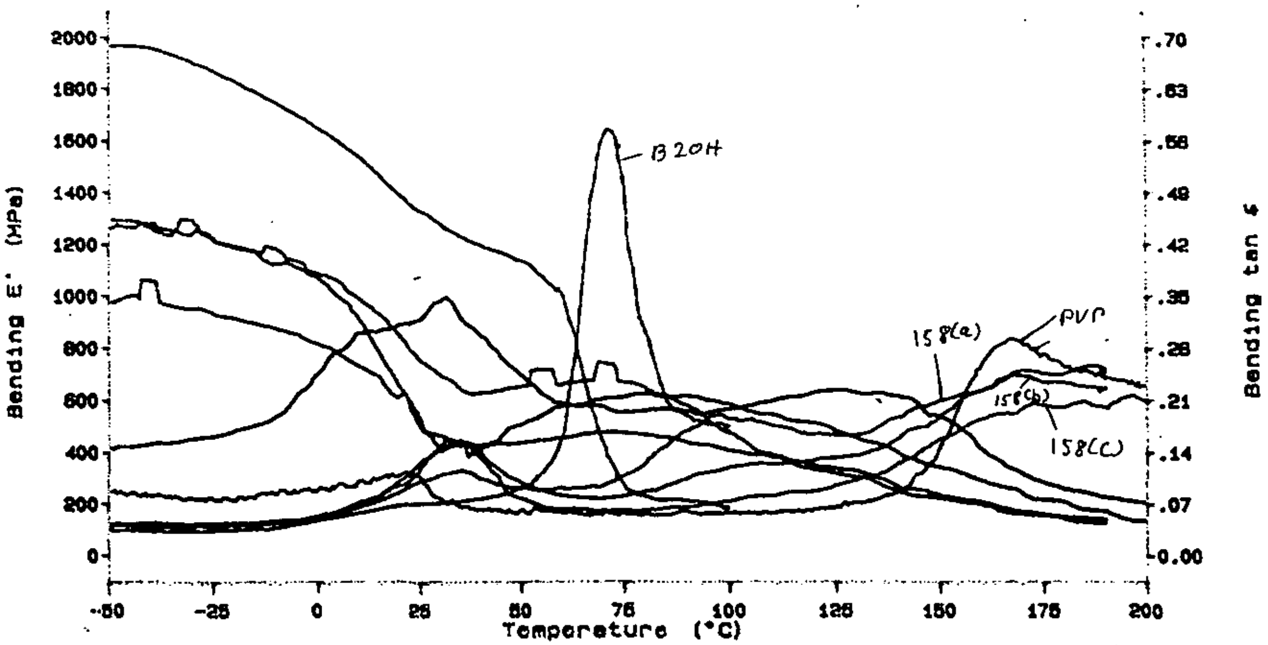

Blends of PVB with PVP in air

VERSION: V5.20

Figure 4.3

DMTA
Head: Standard 300°C

TITLE : PVP
SUBTITLE: Pressed film
FILENAME: Nitrogen
OPERATOR: D.Cunliffe

DATE RUN: May/14/1992
FREQ : 1
STRAIN : 1
DIM: 1.00, 14.107, .348

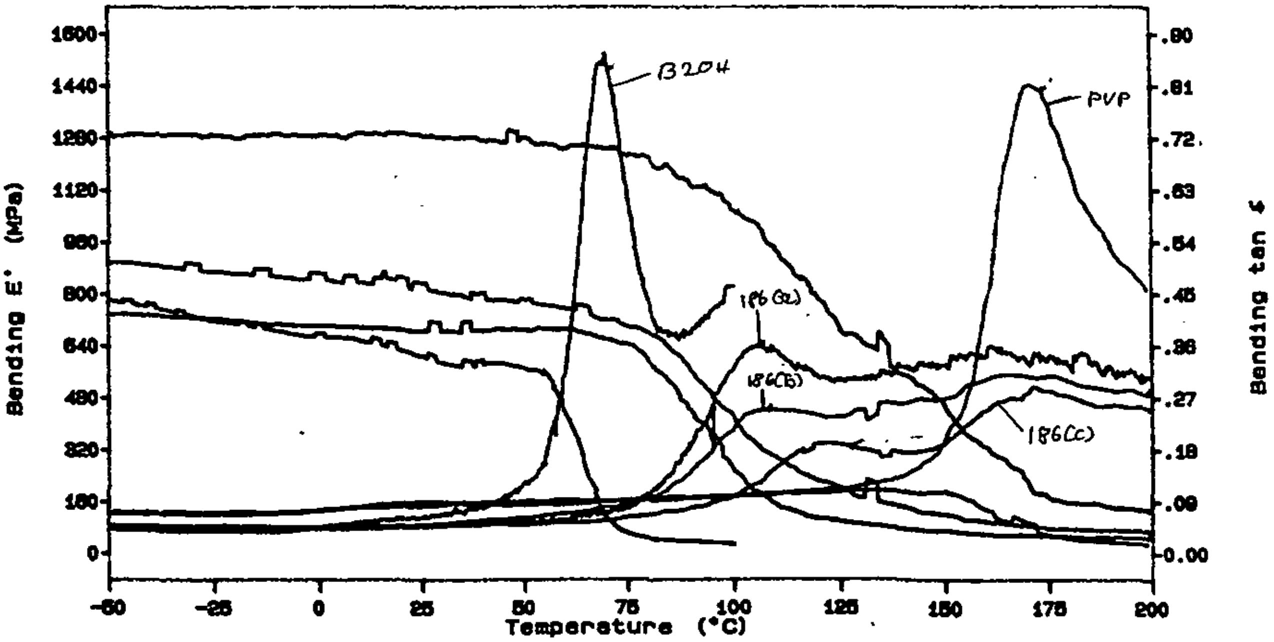

Blends of PVB with PVP under nitrogen

VERSION: V5.20

Figure 4.4

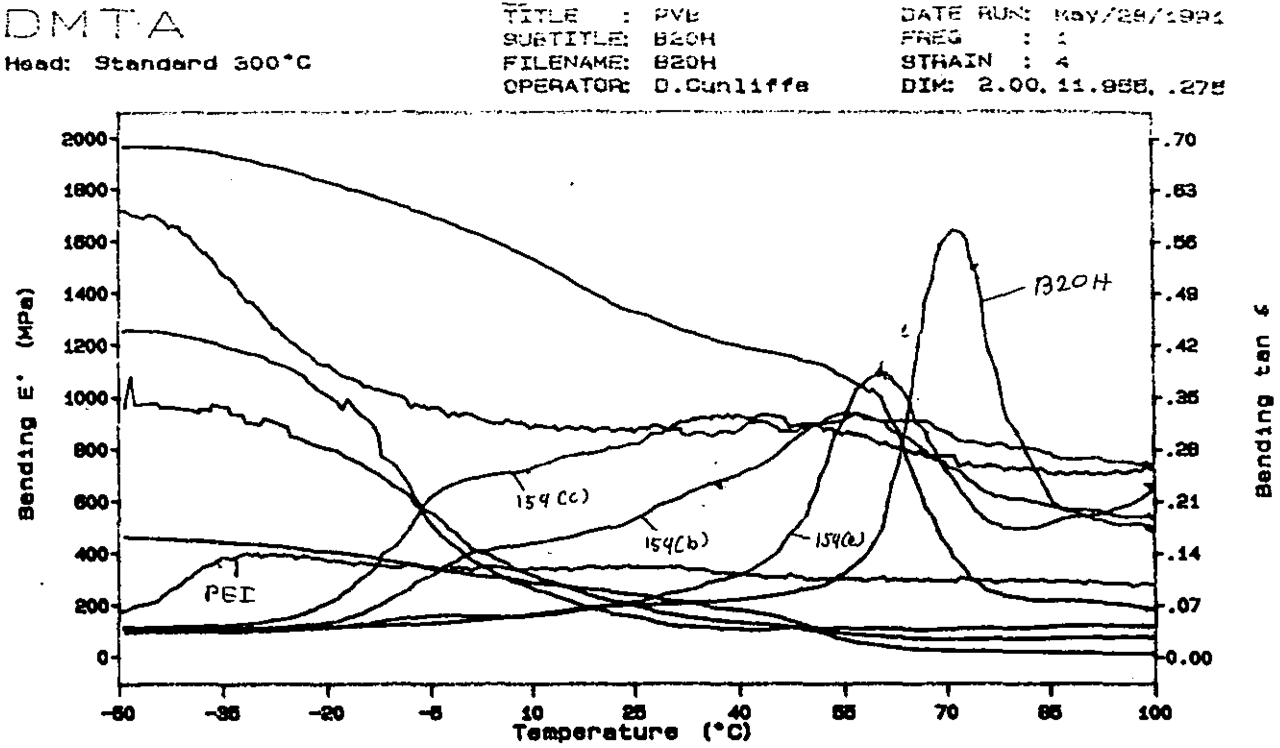

Blends of PVB with PEI in air

VERSION: V5.20

Figure 4.5

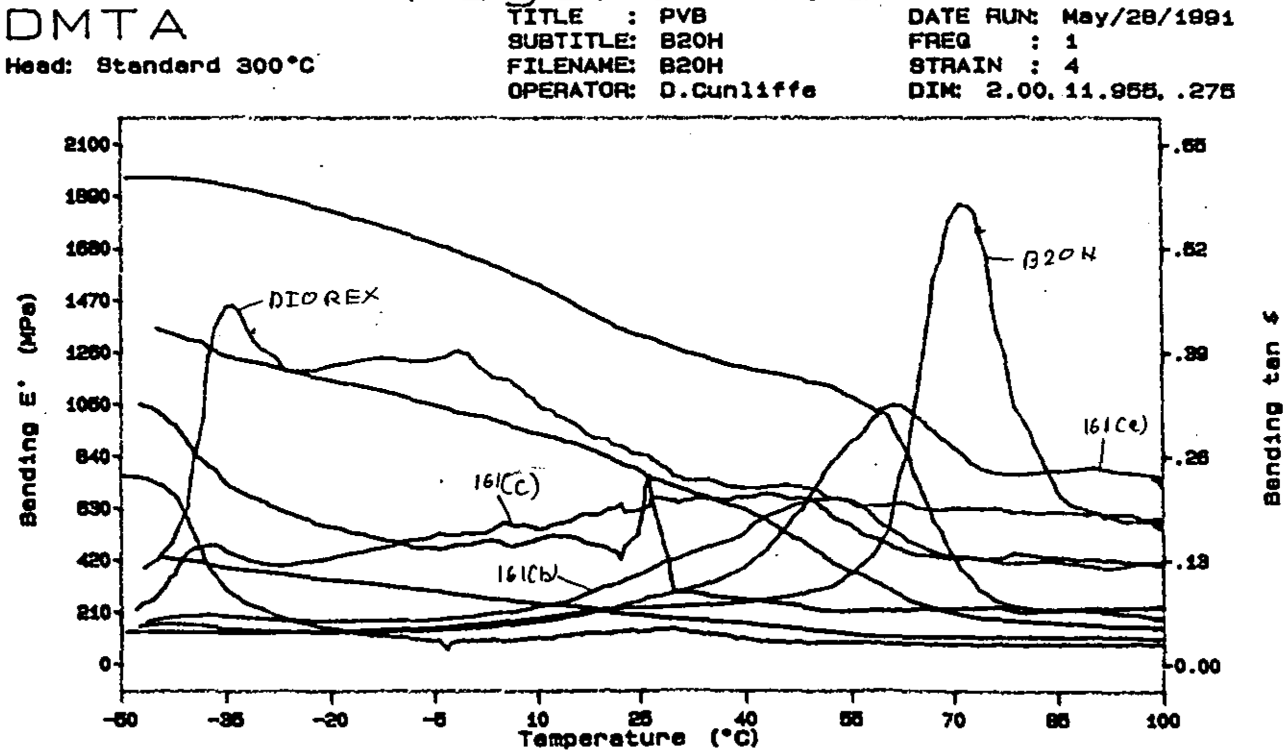

Blends of PVB with Diorex in air

VERSION: V5.20

Figure 4.6

DMTA
Head: Standard 300°C

TITLE : PVB
SUBTITLE: B20H
FILENAME: B20H
OPERATOR: D.Cunliffe

DATE RUN: May/28/1991
FREQ : 1
STRAIN : 4
DIM: 2.00, 11.955, .278

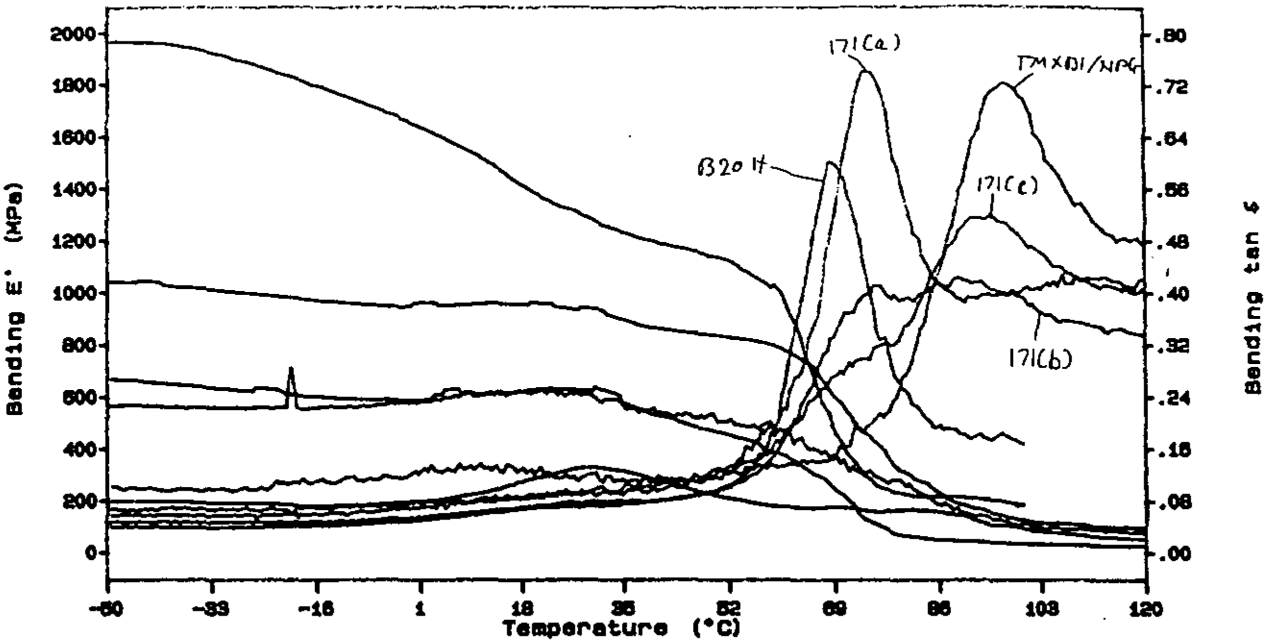

Blends of PVB with TMXD1/NPG in air

VERSION: V5.20

Figure 4.7

H. NMR Spectrum of Butyrated B20H

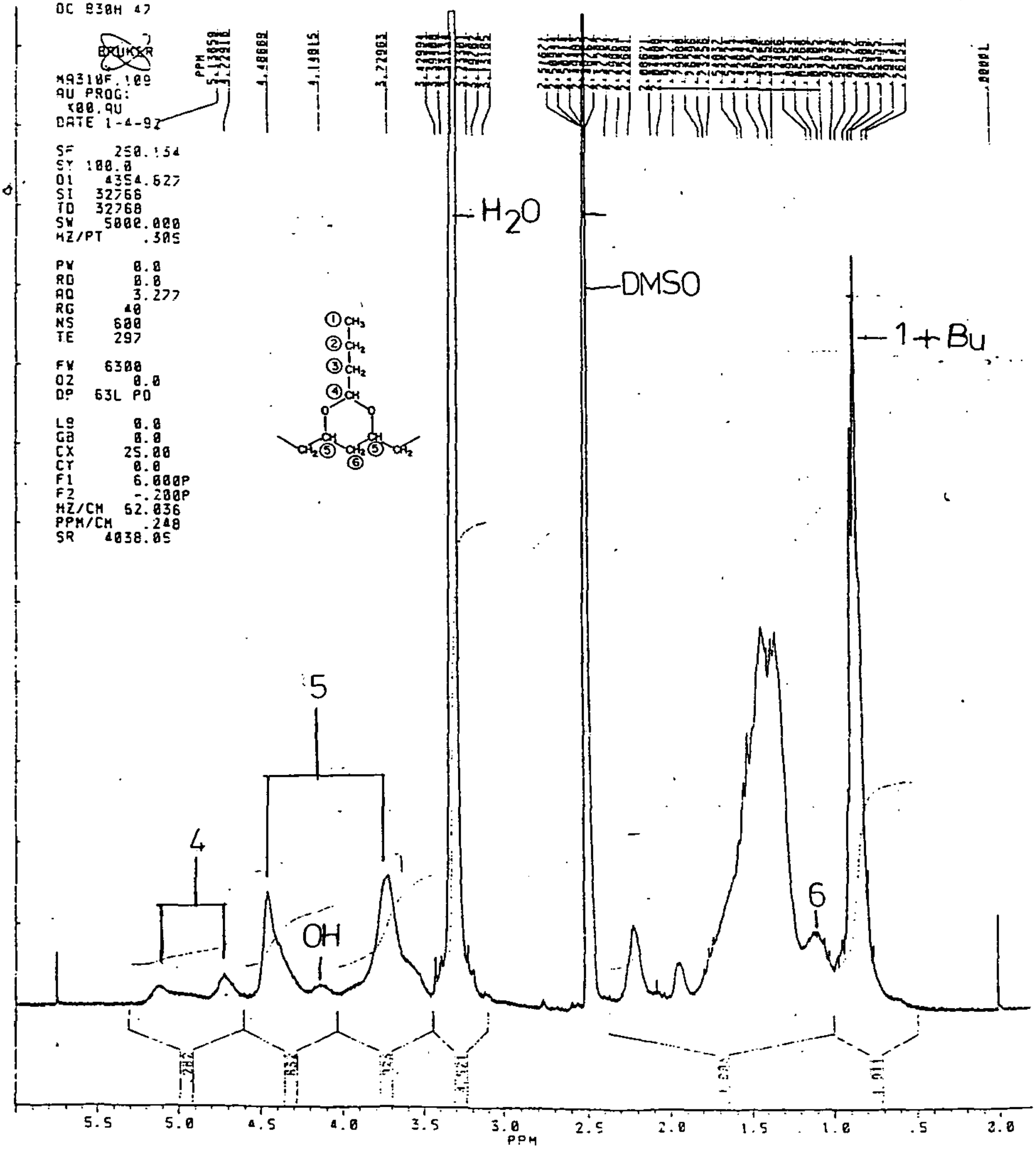

Table 4.5
Viscosity data for Butyrated PVB samples in THF

polymer	$[\eta]_H / g^{-1}dl$	$[\eta]_k / g^{-1}dl$	$[\eta]_{SB} / g^{-1}dl$	$[\eta]_M / g^{-1}dl$	k_H	k_k	k_{SB}	k_M
B30H	0.5948	0.6103	0.6144	0.6065	0.815	0.153	0.512	0.628
B30H-46	0.3901	0.3963	0.4013	0.3963	0.679	0.0331	0.467	0.554
B30H-47	0.4950	0.5137	0.5204	0.5093	0.712	0.0136	0.425	0.534
B30H-50	0.5258	0.5324	0.5433	0.5331	0.553	0.478	0.373	0.456
B20H	0.3382	0.3464	0.3436	0.3411	0.474	0.0816	0.359	0.410
B20H-52	0.3189	0.3202	0.3229	0.3211	0.418	0.115	0.327	0.366
B20H-54	0.3366	0.3372	0.3387	0.3377	0.382	0.135	0.322	0.349
B20H-58	0.3496	0.3514	0.3537	0.3517	0.447	0.0960	0.354	0.396
B20H-66	0.3596	0.3612	0.3642	0.3620	0.436	0.103	0.341	0.384
B20H-69	0.3521	0.3532	0.3559	0.3542	0.414	0.114	0.333	0.365
B20H-86	0.3011	0.3012	0.3030	0.3020	0.363	0.144	0.306	0.332
B20H-92	0.334	0.333	0.336	0.335	0.313	0.176	0.268	0.290

Table 4.6

Molecular Mass, Hydroxyl and Transition Data of Butyrated samples of PVB

Polymer	$\bar{M}_n$	$\bar{M}_w$	M*p*	M*wd*	[OH]/*mmol* g^{-1}	Tg/°C	Bu/OAc
B30H	16000	58000	31000	3.55	4.0	70	6.8
B30H-46	19000	68000	36000	3.5	3.60	57.5	9.4
B30H-47	17000	50000	29000	2.85	2.90	57.5	11.3
B30H-50	10000	32000	18000	3.17	4.10	70.7	12.8
B20H	9000	23000	14000	2.56	4.0	71	8.9
B20H-52	15000	32000	22000	2.12	2.8	57.4	-
B20H-54	4100	9100	6100	2.23	4.7	66.3	11.3
B20H-58	7100	23000	13000	3.19	3.8	63.6	11.2
B20H-66	10000	24000	16000	2.36	3.7	66.5	12.3
B20H-69	9400	26000	16000	2.74	3.5	68.5	12.0
B20H-86	9600	24000	15000	2.45	2.3	70.1	10.6
B20H-92	9400	21000	14000	2.18	0.5	65.8	12.7

It has been reported[83] that the Schulz-Blaschke[78] equation provides the best estimate of intrinsic viscosity and slope constant for polymers in poor solvents and this has been used by Cotts et al[96-99] in their studies of PVB. This is the method used to investigate the effect of modification upon solution viscosity and slope constant, though the Huggins[75] and Martin[79] equations produce similar trends. The variation of intrinsic viscosity against hydroxyl content and the ratio of butyrate plus butyral groups to acetate groups are given in figures 4.8 and 4.9. These show little variation of intrinsic viscosity with degree of modification. The variation of k_{SB} with hydroxyl content and ratio of butyrate plus butyral groups to acetate groups are shown in figures 4.10 and 4.11. These show a much greater dependence of the slope constant upon the degree of modification.

Blends of butyrated samples of PVB with diorex, TMXDI/NPG and PEI were prepared by solution casting and examined by DMTA. The results of blending with diorex are given in table 4.7. With B20H-52 PVB/diorex ratios of 2:1, 1:1 and 1:2, two broad transitions are observed which are situated between those of the unmixed polymers. The transitions became broader and move closer together as the diorex content is increased. This indicates partial miscibility with microphaseheterogeneity as the diorex content is increased as illustrated in Figure 4.12. blends with B20H-54 shows a single narrow Tg with a PVB/diorex ratio of 2:1 which does not correlate with the Fox equation or rule of mixtures, indicating partial miscibility of those polymers giving a phase rich in PVB. With PVB/diorex ratios of 1:1 and 1:2 two broad Tg values are observed, one quite close to that of pure diorex the other 20°C below that of PVB indicating partial miscibility with microphaseheterogeneity as shown in figure 4.13. Blends of B20H-58 with PVB/Diorex ratios of 2:1, 1:1 and 1:2, show two broad values of Tg are observed which become broader and move closer together as the diorex content is increased indicating partial miscibility with microphase-heterogeneity as shown in Figure 4.14. Blends of B20H-66, with a PVB/diorex ratio of 2:1 a single broad Tg is observed which does not correlate with those predicted by the Fox equation or rule of mixtures indicating partial miscibility. With PVB/diorex ratios of 1:1 and 1:2 show two broad values of Tg between those of the unmixed

Figure 4.8

$[\eta]_{SB}$ against $[OH]$ for butyrated $B2OH$

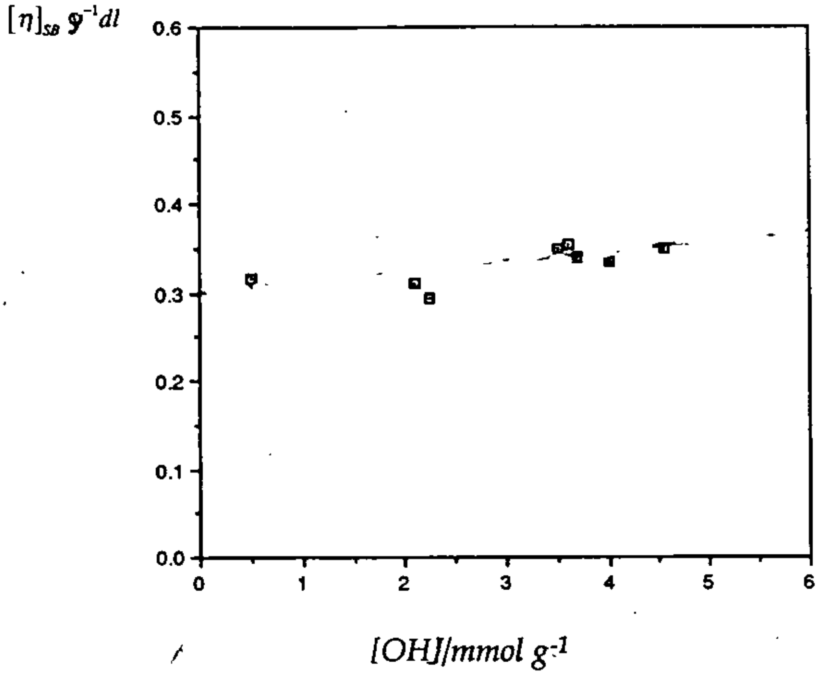

Figure 4.9

$[\eta]_{SB}$ against molar ratio $Bu/0.Ac$ for butyrated $B2OH$

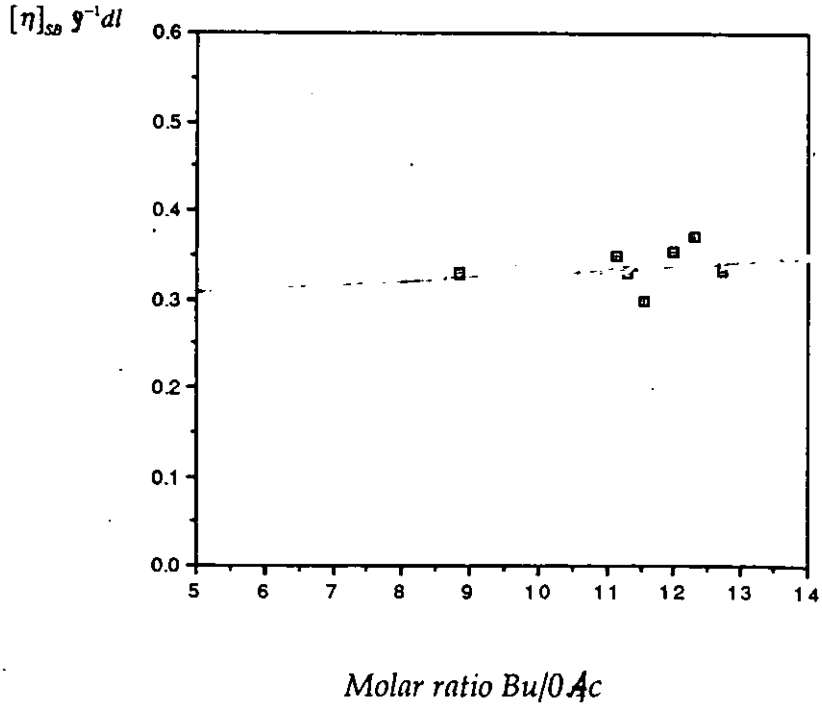

Figure 4.10

k_{SB} against $[OH]$ for butyrated $B2OH$

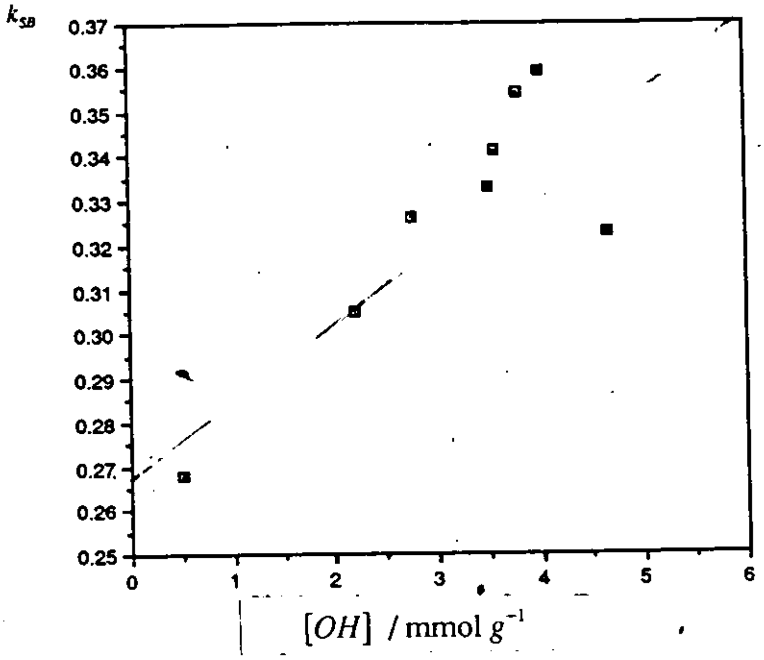

Figure 4.11

k_{SB} against molar ratio Bu / OAc for butyrated $B2OH$

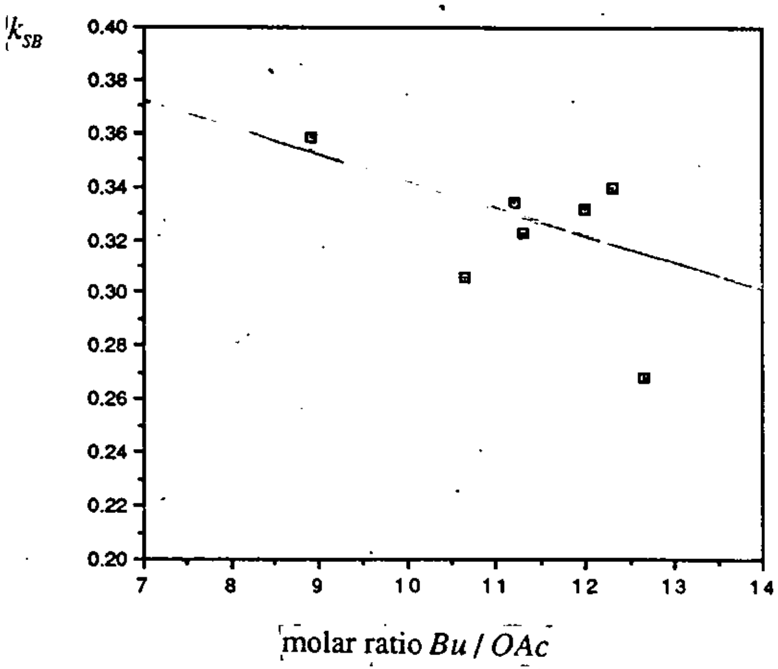

polymers are observed, these broaden as the diorex content is increased, indicating microphaseheterogeneity this is illustrated in Figure 4.15.

Blends of B20H-69 with a PVB/diorex ratio of 2:1 a single broad Tg is observed which does not correlate with the predictions of the Fox equation or rule of mixtures indicating partial miscibility of these polymers. With PVB/diorex ratios of 1:1 and 1:2 two broad transitions are observed inbetween those of the umixed polymers which broaden as the diorex content is increased indicating partial miscibility with microphaseheterogeneity as illustrated in figure 4.16. Blends of B20H-86 with a PVB/diorex ratio of 2:1 a single broad Tg is observed which does not correlate with those predicted by the Fox equation or the rule of mixtures indicating partial miscibility of these polymers. With PVB/diorex ratios of 1:1 and 1:2, two broad transitions are observed. One is very close to that of umixed diorex the other 23.4°C lower than that of PVB. These transition broaden as the direox content is increased, indicating partial miscibility with some microphaseheterogeneity. This

Table 4.7
Blends of Butyrated B20H with Diorex

B20H-52

Blend	wt fraction PVB	wt fraction Diorex	Film Appearance	DMTA Tg/°C	Fox Eqn Tg/°C	Rule of Mixtures Tg/°C
	1	0		57.4		
164(a)	2/3	1/3	clear	-36,45.1	19.39	26.4
164(b)	1/2	1/2	clear	-31.1,30.9	3.59	11.05
164(c)	1/3	2/3	clear	-30.1,31.2	-10.59	-4.3
	0	1		-35		

B20H-54

Blend	wt fraction PVB	wt fraction Diorex	Film Appearance	DMTA Tg/°C	Fox Eqn Tg/°C	Rule of Mixtures Tg/°C
	1	0		66.3		
164(d)	2/3	1/3	clear	56.3	24.15	32.53
164(e)	1/2	1/2	clear	-33.6,51.1	6.77	15.65
164(f)	1/3	2/3	clear	-35.4,48.3	-8.69	-1.23
	0	1		-35		

B20H-58

Blend	wt fraction PVB	wt fraction Diorex	Film Appearance	DMTA Tg/°C	Fox Eqn Tg/°C	Rule of Mixtures Tg/°C
	1	0		63.6		
164(g)	2/3	1/3	clear	-34,49.5	22.76	30.73
164(h)	1/2	1/2	clear	-32.1,47.5	5.84	14.3
164(i)	1/3	2/3	clear	-34.9,47.3	-9.24	-2.3
	0	1		-35		

Table 4.7

Blends of Butyrated B20H with Diorex

B20H-66

Blend	wt fraction PVB	wt fraction Diorex	Film Appearance	DMTA Tg/°C	Fox Eqn Tg/°C	Rule of Mixtures Tg/°C
	1	0		66.5		
164(j)	2/3	1/3	clear	56.5	24.25	32.66
164(k)	1/2	1/2	clear	-28.7,51.8	6.83	15.75
164(l)	1/3	2/3	clear	-34.2,49.1	-8.65	-1.12
	0	1		-35		

B20H-69

Blend	wt fraction PVB	wt fraction Diorex	Film Appearance	DMTA Tg/°C	Fox Eqn Tg/°C	Rule of Mixtures Tg/°C
	1	0		68.5		
164(m)	2/3	1/3	clear	56.7	25.27	34
164(n)	1/2	1/2	clear	-37.8,53.4	7.51	16.75
164(o)	1/3	2/3	clear	-34.5,52.3	-8.25	-0.5
	0	1		-35		

B20H-86

Blend	wt fraction PVB	wt fraction Diorex	Film Appearance	DMTA Tg/°C	Fox Eqn Tg/°C	Rule of Mixtures Tg/°C
	1	0		70.1		
164(p)	2/3	1/3	clear	52.2	26.08	35.07
164(q)	1/2	1/2	clear	-36.7,49	8.05	17.55
164(r)	1/3	2/3	clear	-36.6,46.7	-7.93	0.03
	0	1		-35		

Figure 4.12

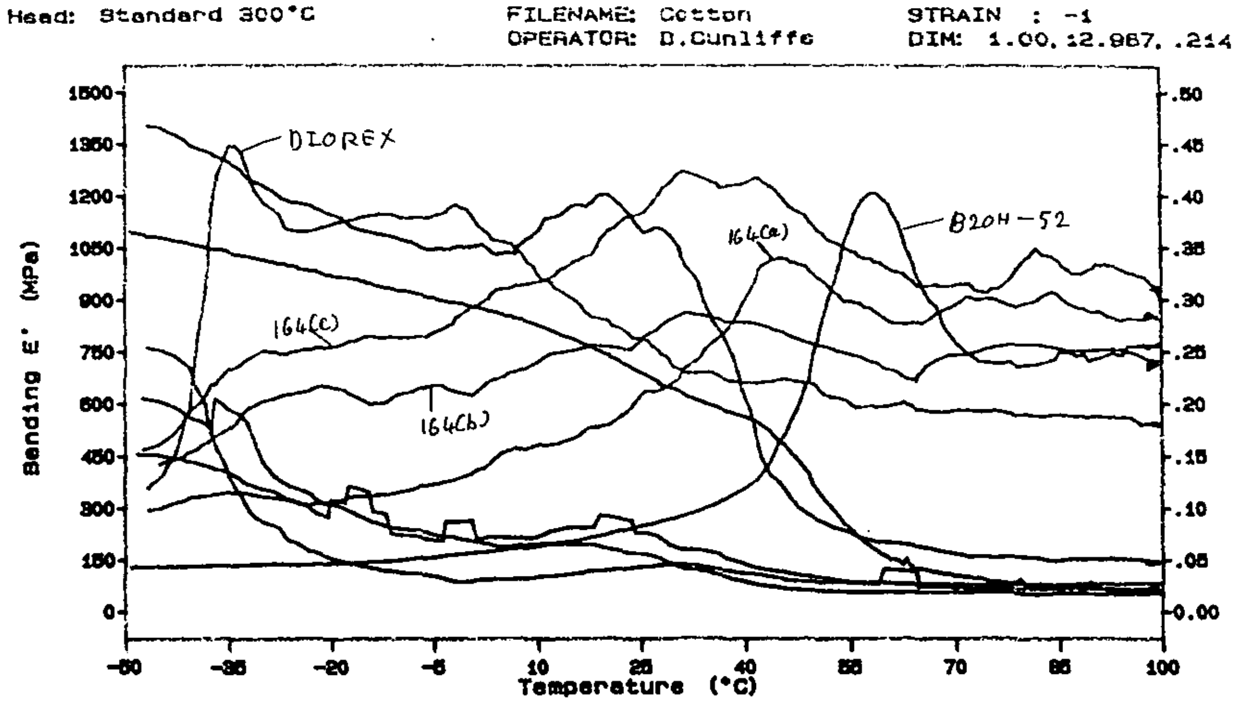

Blends B20H-52 with Diorex in air

VERSION: V5.20

Figure 4.13

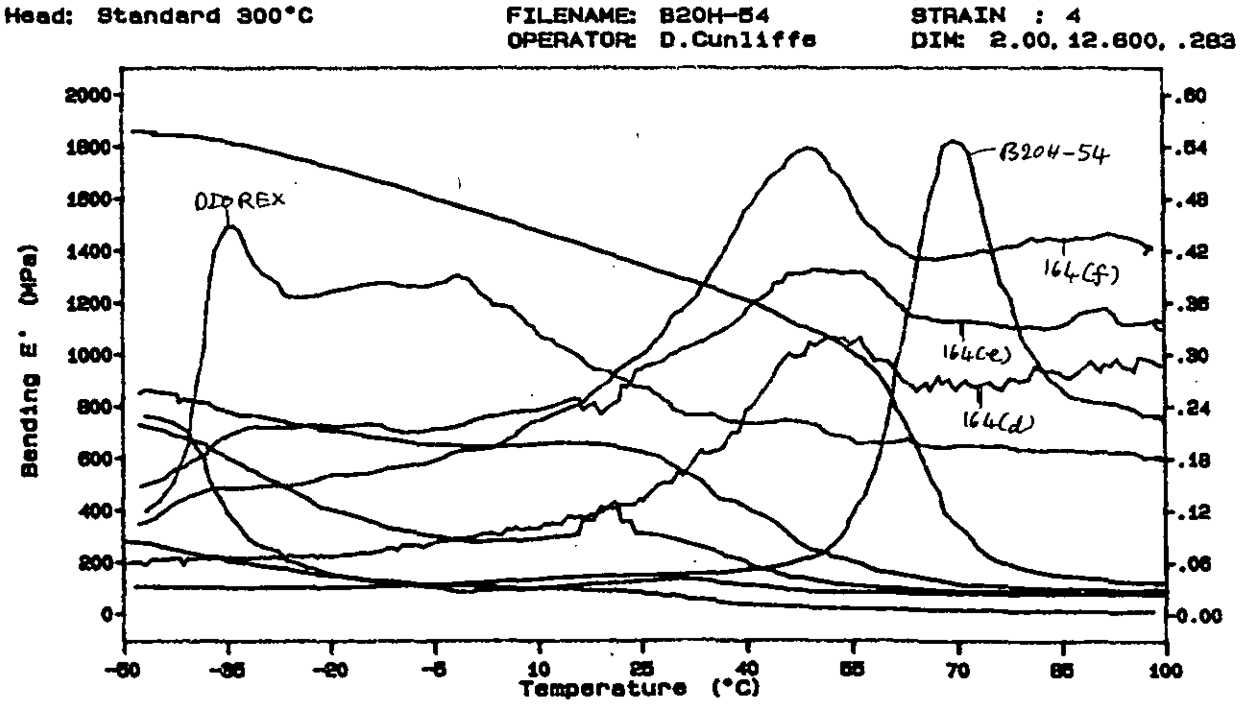

Blends of B20H-54 with Diorex in air

VERSION: V5.20

Figure 4.14

DMTA
Head: Standard 300°C

TITLE : PVB
SUBTITLE: B20H-58
FILENAME: B20H-58
OPERATOR: D.Cunliffe

DATE RUN: Jun/06/1991
FREQ : 1
STRAIN : 4
DIM: 2.00, 12.808, .310

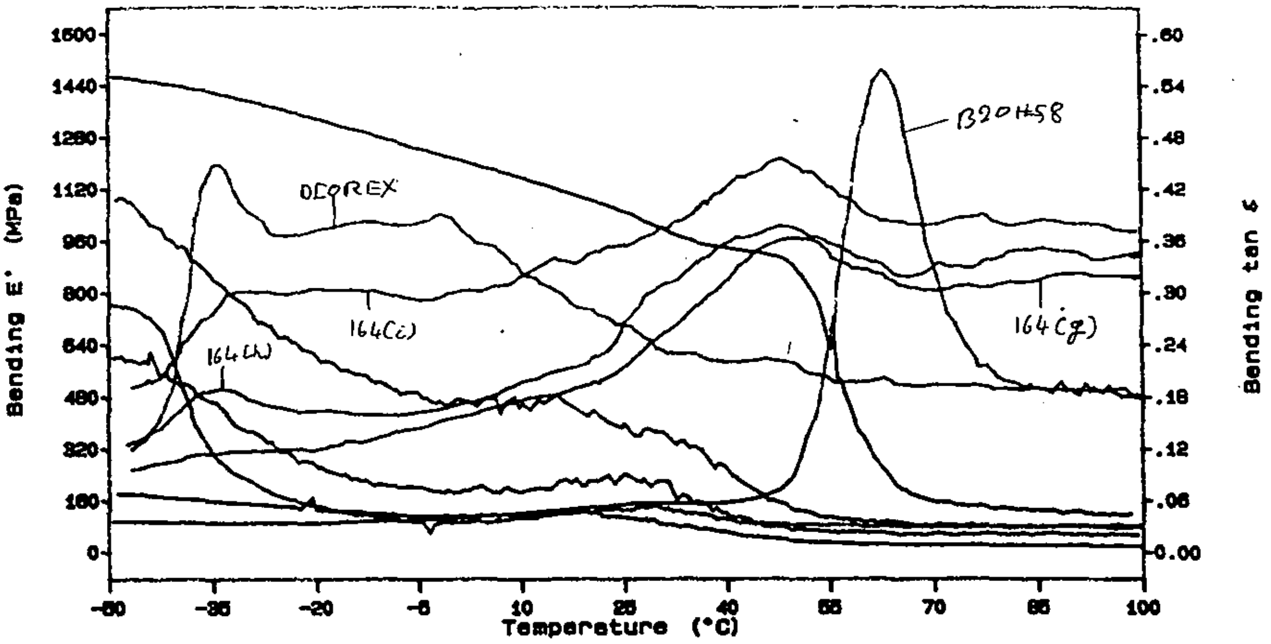

Blends of B20H-58 with Diorex in air

VERSION: V5.20

Figure 4.15

DMTA
Head: Standard 300°C

TITLE : PVB
SUBTITLE: B20H-66
FILENAME: B20H-66
OPERATOR: D.Cunliffe

DATE RUN: Jun/07/1991
FREQ : 1
STRAIN : 4
DIM: 2.00, 12.960, .307

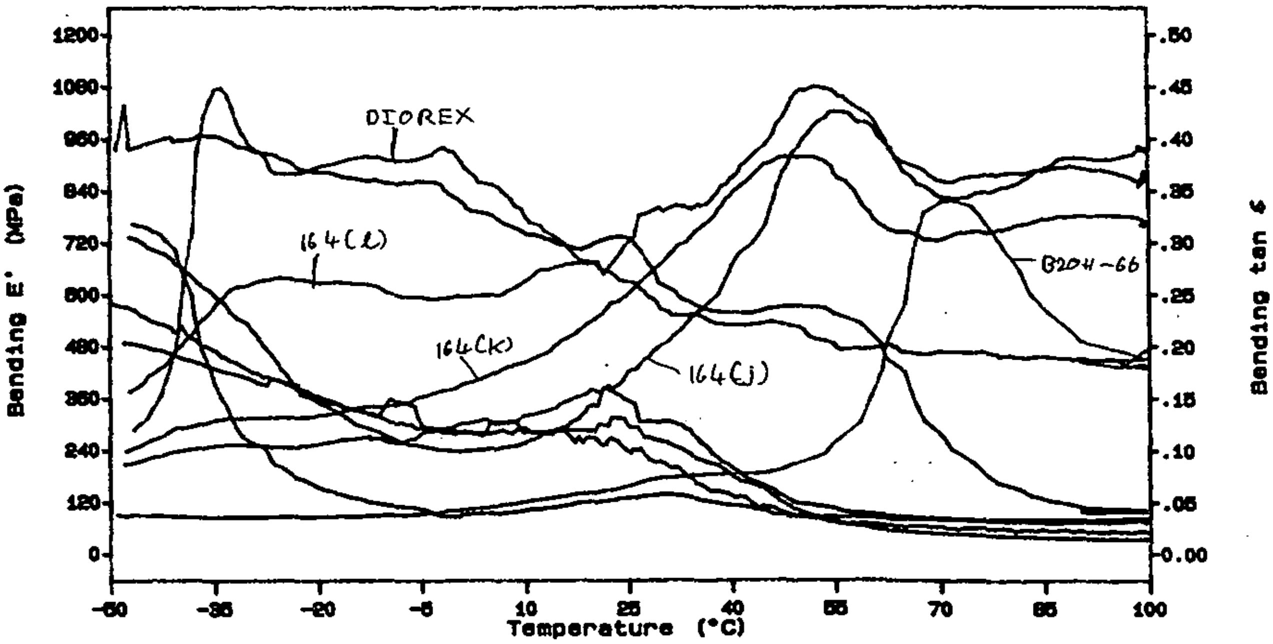

Blends of B20H-66 with Diorex in air

VERSION: V5.20

Figure 4.16

DMTA
Head: Standard 300°C

TITLE : Diorex
SUBTITLE: Pressed Film
FILENAME: Cotton
OPERATOR: D.Cunliffe

DATE RUN: Feb/25/1992
FREQ : 1
STRAIN : -1
DIM: 1.00, 12.867, .214

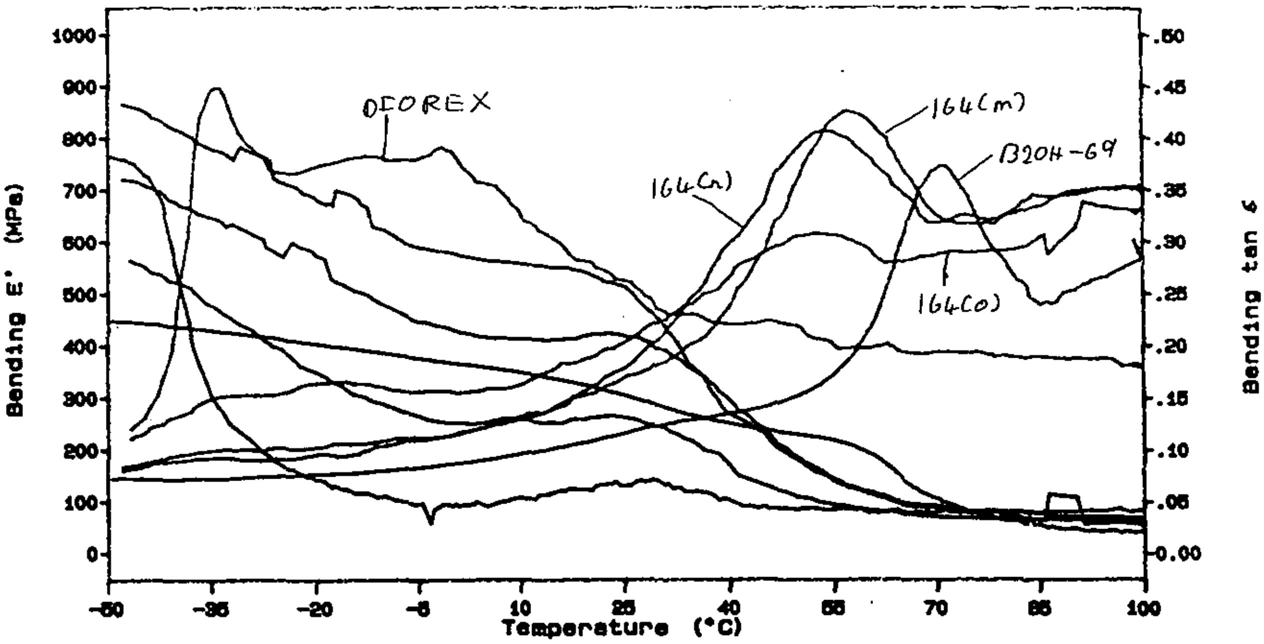

Blends of B20-69 with Diorex in air

VERSION: V5.20

Figure 4.17

DMTA
Head: Standard 300°C

TITLE : PVB
SUBTITLE: B20H-86
FILENAME: B20H-86
OPERATOR: D.Cunliffe

DATE RUN: Jun/11/1991
FREQ : 1
STRAIN : 4
DIM: 2.00, 12.693, .318

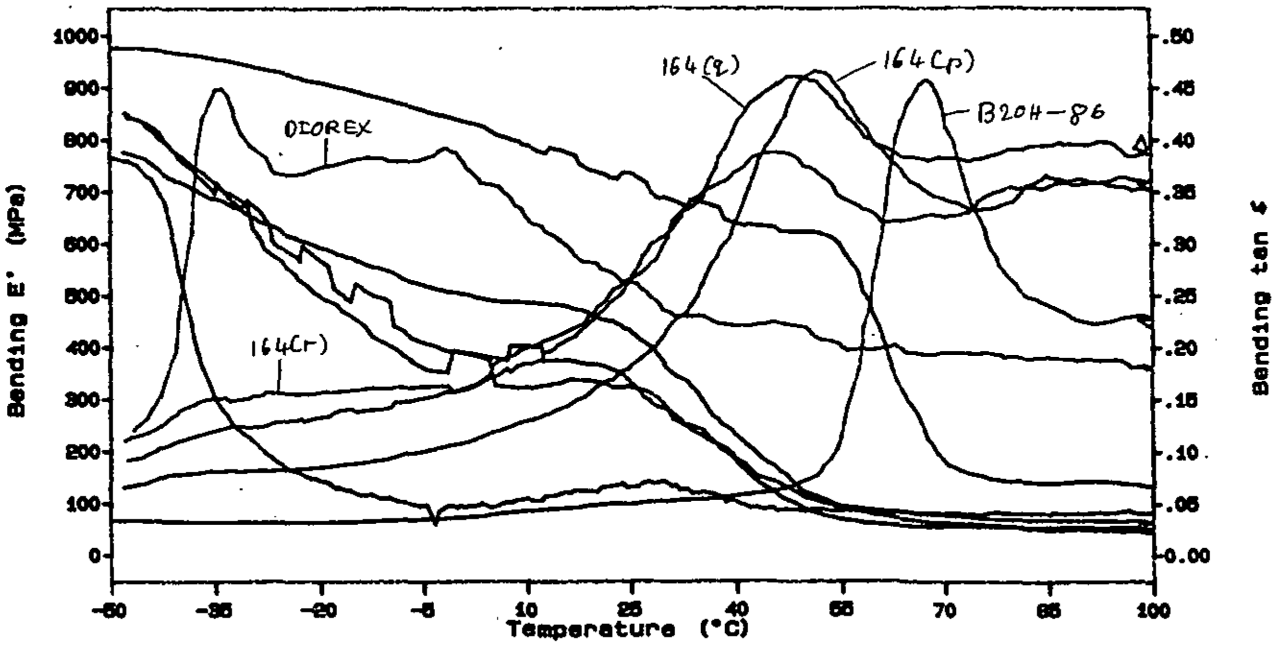

Blends of B20H-86 with Diorex in air

VERSION: V5.20

Figure 4.18

DMTA
Head: Standard 300°C

TITLE : PVB
SUBTITLE: B20H-92
FILENAME: B20H-92
OPERATOR: D.Cunliffe

DATE RUN: Jun/11/1991
FREQ : 1
STRAIN : 4
DIM: 2.00, 14.230, .317

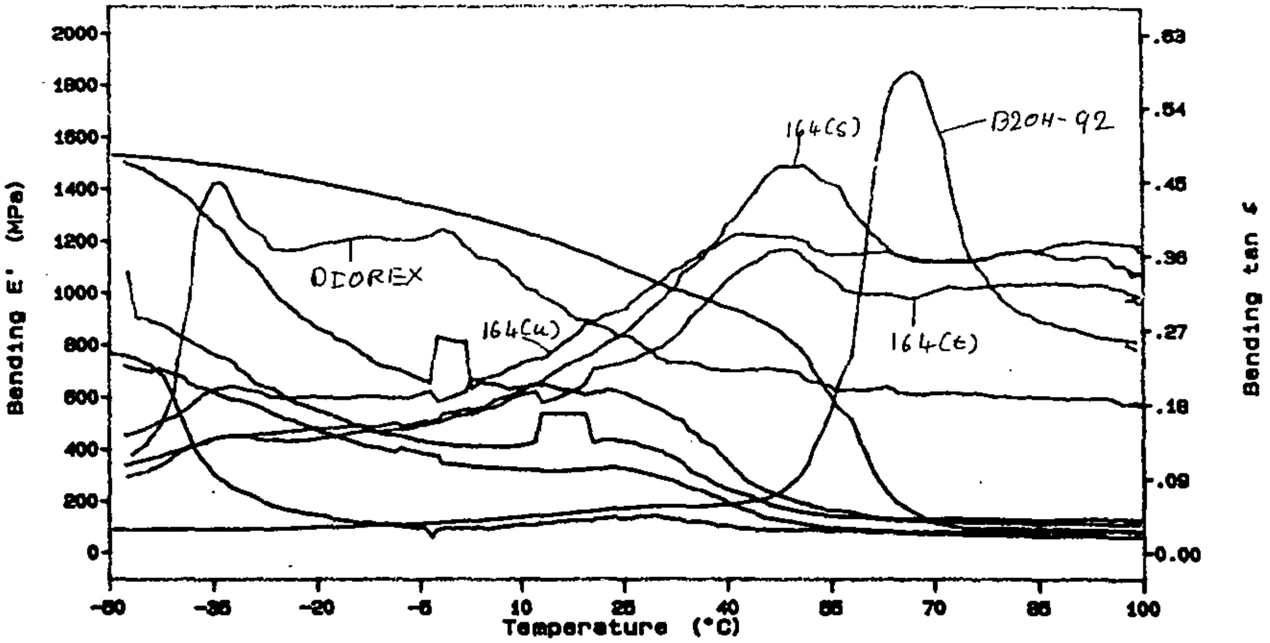

Blends of B20H-92 with Diorex in air

VERSION: V5.20

Table 4.7

Blends of Butyrated B20H with Diorex

B20H-92

Blend	wt fraction PVB	wt fraction Diorex	Film Appearance	DMTA Tg/°C	Fox Eqn Tg/°C	Rule of Mixtures Tg/°C
	1	0		65.8		
164(s)	2/3	1/3	clear	49.3	20.20	29.87
164(t)	1/2	1/2	clear	-34.5,48.8	1.71	11.9
164(u)	1/3	2/3	clear	-33.5,43.7	-14.6	-6.07
	0	1		-35		

is shown in figure 4.17. Blends of B20H-92 with a PVB/diorex ratio of 2:1 show a single broad Tg which does not correlate with the predictions of the Fox equation or rule of mixtures. With PVB/diorex ratios of 1:1 and 1:2 two broad transition are observed, the lower is very close to that of diorex, the higher about 20°Clower than PVB. These transitions broaden as the diorex content is increased, indicating partial miscibility with some microphaseheterogeneity. This is shown in figure 4.18.

The results of blending with TMXDI/NPG are given in table 4.8. Blends of B20H-54 with a PVB/TMXDI/NPG ratio of 2:1 a single narrow Tg is observed which correlates with the predictions of the Fox equation and the rule of mixtures indicating miscibility of the polymers with single phase morphology. With PVB/TMXDI/NPG ratios of 1:1 and 1:2 two Tg values are observed, one in between those of the unmixed polymers, the other quite close to that of TMXDI/NPG indicating the presence of two phases one a mixture of PVB/TMXDI/NPG the other unmixed polyurethane. This is shown in figure 4.19. Blends of B20H-58 with a PVB/TMXDI/NPG ratio of 2:1 a single narrow Tg is observed, correlating with the predictions of the Fox equation and rule of mixtures, indicating single phase morphology. With PVB/TMXDI/NPG ratios of 1:1 and 1:2 two Tg values are observed one in between those of the unmixed polymers, the other corresponding to TMXDI/NPG. This indicates the presence of two phases one a mixture of PVB with

TMXDI/NPG the other unmixed polyurethane as illustrated in figure 4.20. Blends of B20H-66 with a PVB/TMXDI/NPG ratio of 2:1,a single narrow Tg is observed which correlates with the predictions of the Fox equation and rule of mixtures indicating single phase morphology. With PVB/TMXDI/NPG ratios of 1:1 and 1:2, two broad Tg values are observed:one in between those of the unmixed polymers and one corresponding to TMXDI/NPG. This indicates the presence of two phases, one a mixture of PVB/TMXDI/NPG the other unmixed polyurethane. This is illustrated in figure 4.21.

The results of blending with PEI are given in table 4.9 with PVB/PEI ratios of 2:1, 1:1, and 1:2 single broad Tg values are observed which do not correlate with the predictions of the Fox equation or rule of mixtures. The transitions broaden as the PEI content is increased, indicating partial miscibility with microphaseheterogeneity. This is illustrated in figure 4.22. In general, butyration decreases the miscibility of B20H with diorex and PEI as the tan δ peaks are broadened and multiphase morphology is readily observed. No definite conclusion concerning the miscibility of butyrated B20H with TMXDI/NPG can be made, as the transitions of the unmixed polymers are quite close and not easily resolved by DMTA.

The solubility of butyrated samples of PVB were investigated in a number of solvents and the results given in table 4.10. This has shown no change in solubility characteristics upon butyration.

Table 4.8
Blends of Butyrated B20H with TMXDI/NPG

B20H-54

Blend	wt fraction PVB	wt fraction TMXDI/ NPG	Film Appearance	DMTA Tg/°C	Fox Eqn Tg/°C	Rule of Mixtures Tg/°C
	1	0		66.3		
173(a)	2/3	1/3	clear	76.1	76.39	77.03
173(b)	1/2	1/2	opaque	69.5,95.2	81.67	82.4
173(c)	1/3	2/3	opaque	75.4,98.6	87.11	87.77
	0	1		98.5		

B20H-58

Blend	wt fraction PVB	wt fraction TMXDI/ NPG	Film Appearance	DMTA Tg/°C	Fox Eqn Tg/°C	Rule of Mixtures Tg/°C
	1	0		63.6		
173(d)	2/3	1/3	clear	71.8	74.48	75.23
173(e)	1/2	1/2	opaque	71.7,94.7	80.19	81.05
1739f)	1/3	2/3	opaque	77.9,98.4	86.09	86.82
	0	1		98.5		

B20H-66

Blend	wt fraction PVB	wt fraction TMXDI/ NPG	Film Appearance	DMTA Tg/°C	Fox Eqn Tg/°C	Rule of Mixtures Tg/°C
	1	0		66.5		
173(g)	2/3	1/3	clear	75.6	76.54	77.17
173(h)	1/2	1/2	opaque	79.9,91.4	81.78	82.5
173(i)	1/3	2/3	opaque	70.2,40.2	87.18	87.83
	0	1		98.5		

Table 4.9

Blends of Butyrated B20H with PEI

B20H-54

Blend	wt fraction PVB	wt fraction PEI	Film Appearance	DMTA Tg/°C	Fox Eqn Tg/°C	Rule of Mixtures Tg/°C
	1	0		66.3		
177(a)	2/3	1/3	clear	47.3	28.47	35.37
177(b)	1/2	1/2	clear	39.5	12.55	19.9
177(c)	1/3	2/3	clear	23.5	-1.77	4.43
	0	1		-26.5		

Figure 4.19

DMTA
Head: Standard 300°C

TITLE : PVB
SUBTITLE: B20H-54
FILENAME: B20H-54
OPERATOR: D.Cunliffe

DATE RUN: Jun/03/1991
FREQ : 1
STRAIN : 4
DIM: 2.00, 12.600, .283

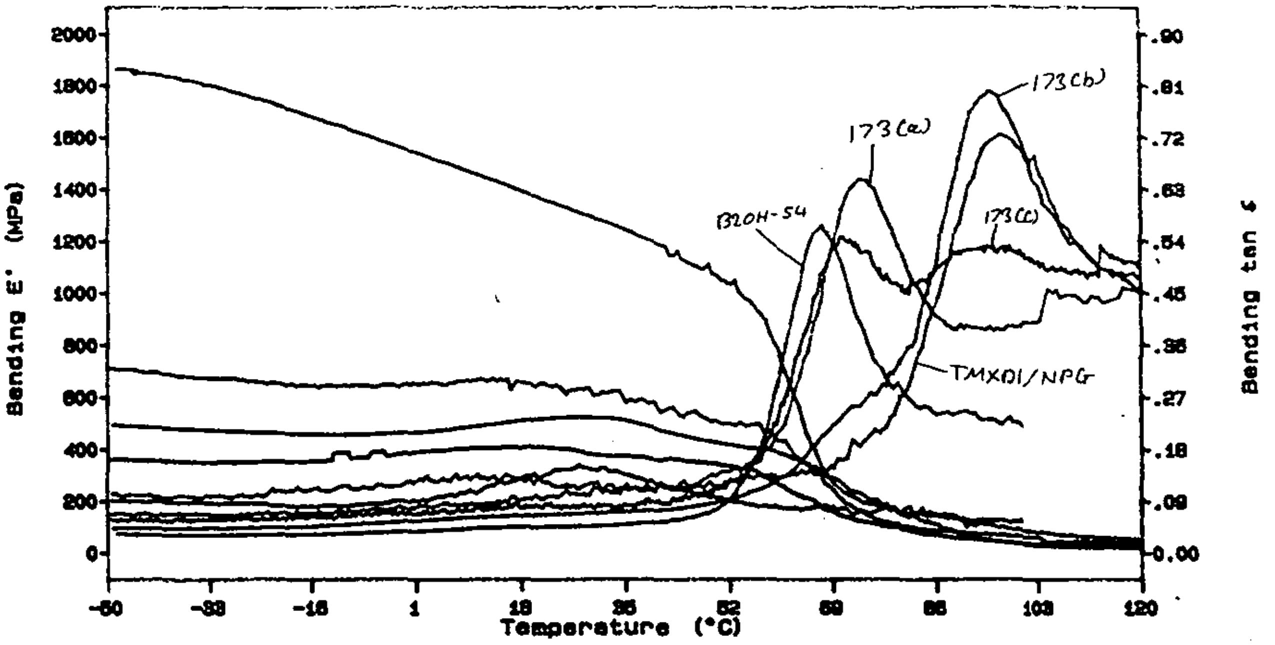

Blends of B20H-54 with TMXDi/NPG in air

VERSION: V5.20

Figure 4.20

DMTA
Head: Standard 300°C

TITLE : PVB
SUBTITLE: B20H-58
FILENAME: B20H-58
OPERATOR: D.Cunliffe

DATE RUN: Jun/05/1991
FREQ : 1
STRAIN : 4
DIM: 2.00, 12.808, .310

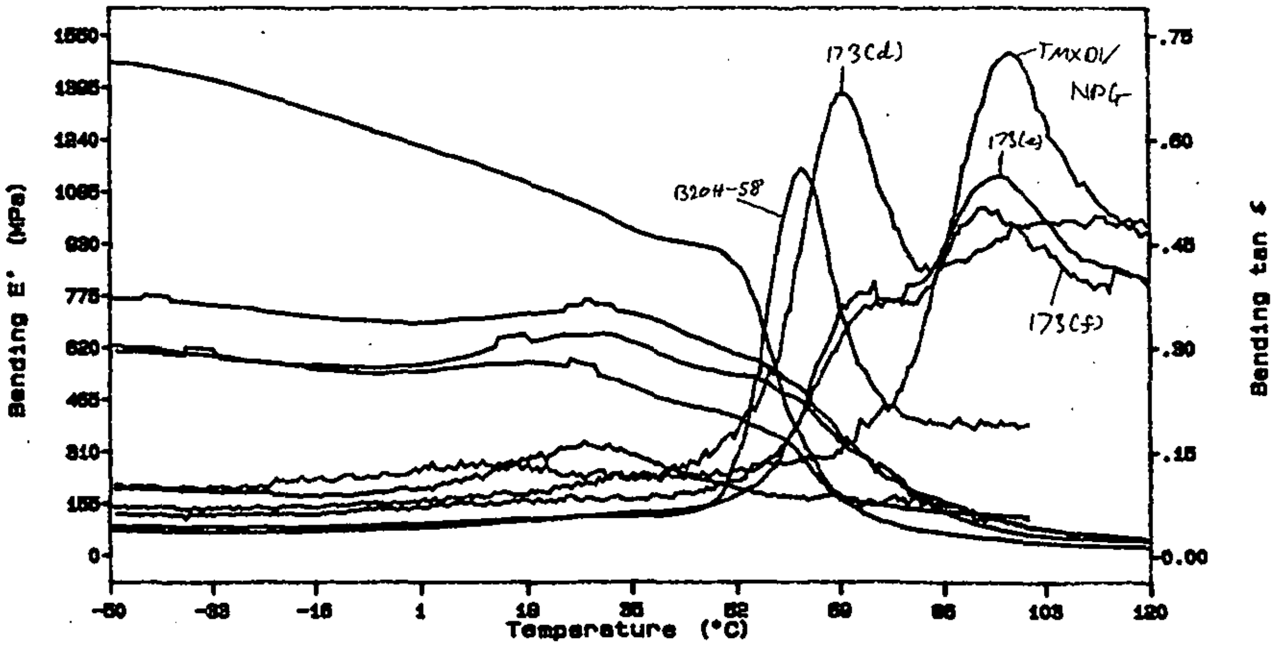

Blends of B20H-58 with TMXDi/NPG in air

VERSION: V5.20

Figure 4.21

DMTA
Head: Standard 300°C

TITLE : PVB
SUBTITLE: B20H-66
FILENAME: B20H-66
OPERATOR: D.Cunliffe

DATE RUN: Jun/07/1991
FREQ : 1
STRAIN : 4
DIM: 2.00, 12.960, .307

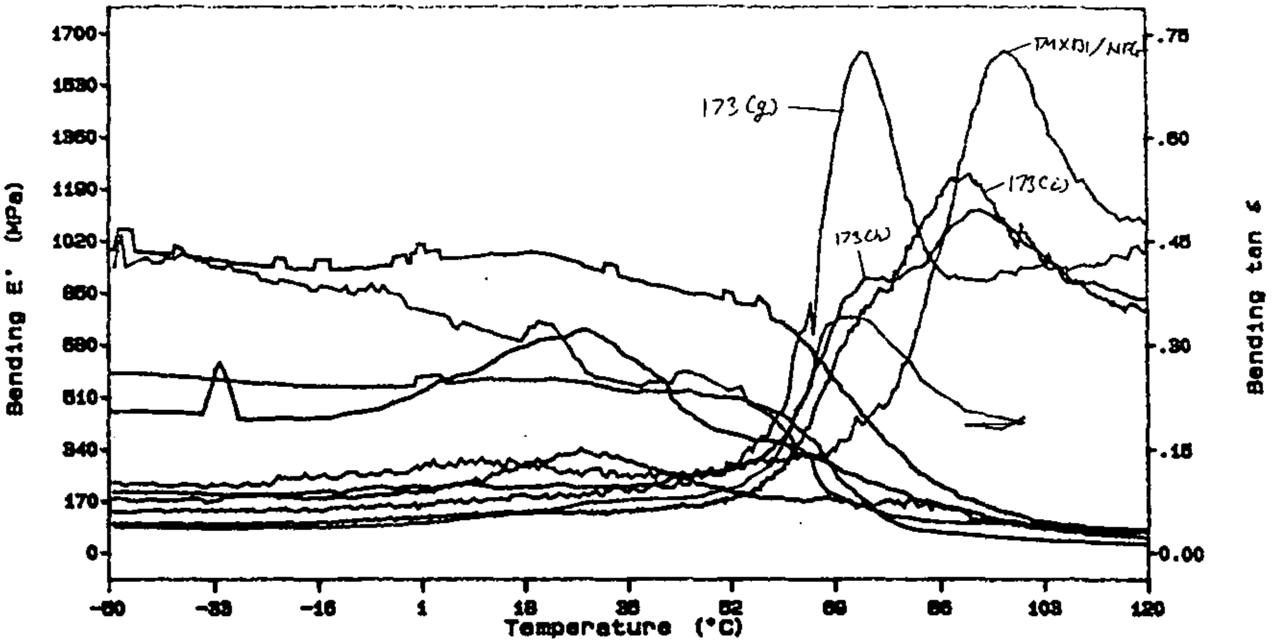

Blends of B20H-66 with TMXDi/NPG in air

VERSION: V5.20

Figure 4.22

DMTA
Head: Standard 300°C

TITLE : PVB
SUBTITLE: B20H-54
FILENAME: B20H-54
OPERATOR: D.Cunliffe

DATE RUN: Jun/03/1991
FREQ : 1
STRAIN : 4
DIM: 2.00, 12.600, .283

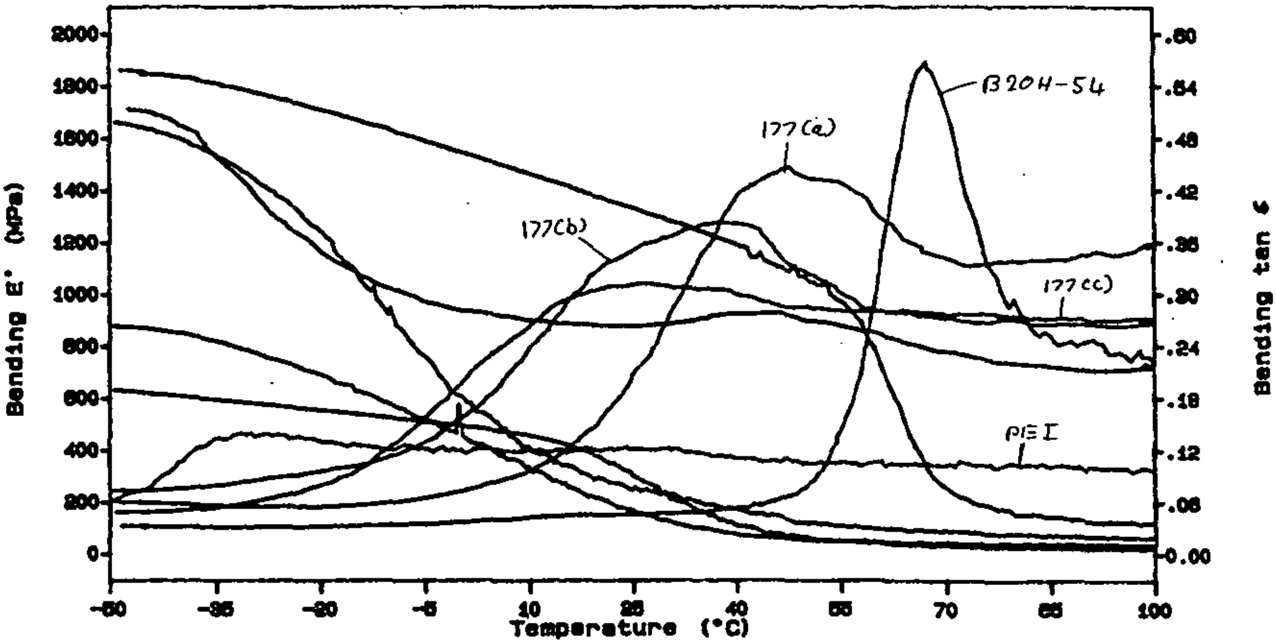

Blends of B20H-54 with PEI in air

VERSION: V5.20

Table 4.10

Solubility Characteristics of Butyrated samples of PVB

Polymer	Methanol	Acetone	Ethyl Acetate	Ethyl Acetate/ Methanol 1:1	THF	Benzene	Toluene	Hexane	Cyclohexane	Chloroform
B30H	✓	✓	✓	✓	✓	swell	swell	X	X	✓
B30H-46	✓	✓	✓	✓	✓	swell	swell	X	X	✓
B30H-47	✓	✓	✓	✓	✓	swell	swell	X	X	✓
B30H-50	✓	✓	✓	✓	✓	swell	swell	X	X	✓
B20H	✓	✓	✓	✓	✓	swell	swell	X	X	✓
B20H-52	✓	✓	✓	✓	✓	swell	swell	X	X	✓
B20H-54	✓	✓	✓	✓	✓	swell	swell	X	X	✓
B20H-58	✓	✓	✓	✓	✓	swell	swell	X	X	✓
B20H-66	✓	✓	✓	✓	✓	swell	swell	X	X	✓
B20H-69	✓	✓	✓	✓	✓	swell	swell	X	X	✓
B20H-86	✓	✓	✓	✓	✓	swell	swell	X	X	✓
B20H-96	✓	✓	✓	✓	✓	swell	swell	X	X	✓

4.3 Benzoated PVB

A number of benzoated samples of B20H were prepared. The intrinsic viscosities of the modified PVB samples were determined and the results given in table 4.11. The molecular mass, hydroxyl content, transition data and ratio of benzoate groups to butyral groups are given in table 4.12. An NMR spectrum of benzoated PVB is given in figure 4.23. The variation of $[\eta]_{SB}$ with hydroxyl content and ratio of benzoate groups to butyral groups are given in figures 4.24 and 4.25 and the variation of k_{SB} with hydroxyl content and ratio of benzoate groups to butyral groups are given is figures 4.26 and 4.27. These show that the effect upon slope constant with degree of modification is [illegible] greater than the effect of modification upon intrinsic viscosity as seen in the case of butyrated PVB.

Blends of benzoated samples of B20H were prepared by solution casting with TMXDI/NPG, diorex, PEI and PVP. The results of blending with TMXDI/NPG are given in table 4.13. Blends of B20H-94 with PVB/TMXDI/NPG ratios of 2:1, 1:1 and 1:2 show single broad Tg values about 10°C higher than those predicted by the Fox equation, the films are also opaque in appearance. In this case, it is possible that crosslinking has taken place between unreacted hydroxyl groups and free isocyanate groups in the polyurethane as indicated in figure 4.28. Blends of B20H-99 with PVB/TMXDI/NPG ratios of 2:1, 1:1 and 1:2 show two broad values of Tg which are quite close to those of the unmixed polymers indicating a decrease in miscibility of these polymers upon benzoation of PVB, as illustrated in figure 4.29. Blends of B20H-109 with PVB/TMXDI/NPG ratios of 2:1, 1:1 and 1:2 show single broad Tg values which are 10-14°C above those predicted by the Fox equation or rule of mixtures, as illustrated in figure 4.30.

Table 4.11

Intrinsic Viscosity Data of Benzoated B20H in THF

polymer	$[\eta]_H / g^{-1}dl$	$[\eta]_k / g^{-1}dl$	$[\eta]_{SB} / g^{-1}dl$	$[\eta]_M / g^{-1}dl$	k_H	k_k	k_{SB}	k_M
B20H	0.3382	0.3464	0.3436	0.3411	0.474	0.0816	0.359	0.410
B20H-94	0.3328	0.3319	0.3386	0.3365	0.469	0.0643	0.348	0.393
B20H.95	0.3086	0.31102	0.3132	0.3121	0.396	0.138	0.307	0.336
B20H-99	0.3165	0.3172	0.3189	0.3177	0.389	0.130	0.322	0.353
B20H-106	0.3368	0.3343	0.3369	0.3366	0.211	0.240	0.192	0.201
B20H-109	0.2669	0.2664	0.2726	0.2673	0.351	0.140	0.181	0.332

Table 4.12

Molecular Mass, Hydroxyl and Transition Data of Benzoated PVB Samples

Polymer	$\bar{M}$n	$\bar{M}$w	Mp	M*wd*	[OH]/mmol g^{-1}	Tg/°c	Moler Ratio benzoate/butyral
B20H	9000	23000	14000	2.56	4.0	71	0.00
B20H-94	8600	22000	14000	2.54	4.2	68.7	0.017
B20H-95	16000	33000	23000	2.05	8.0	76.3	0.015
B20H-99	14000	32000	21000	2.22	2.3	74.2	0.029
B20H-106	1200	2100	16000	1.77	7.6	70.1	0.040
B20H-109	19000	31000	24000	1.6	15.1	72.2	0.088

Figure 4.23
^1H - N.M.R. Spectrum of Benzoated B2OH

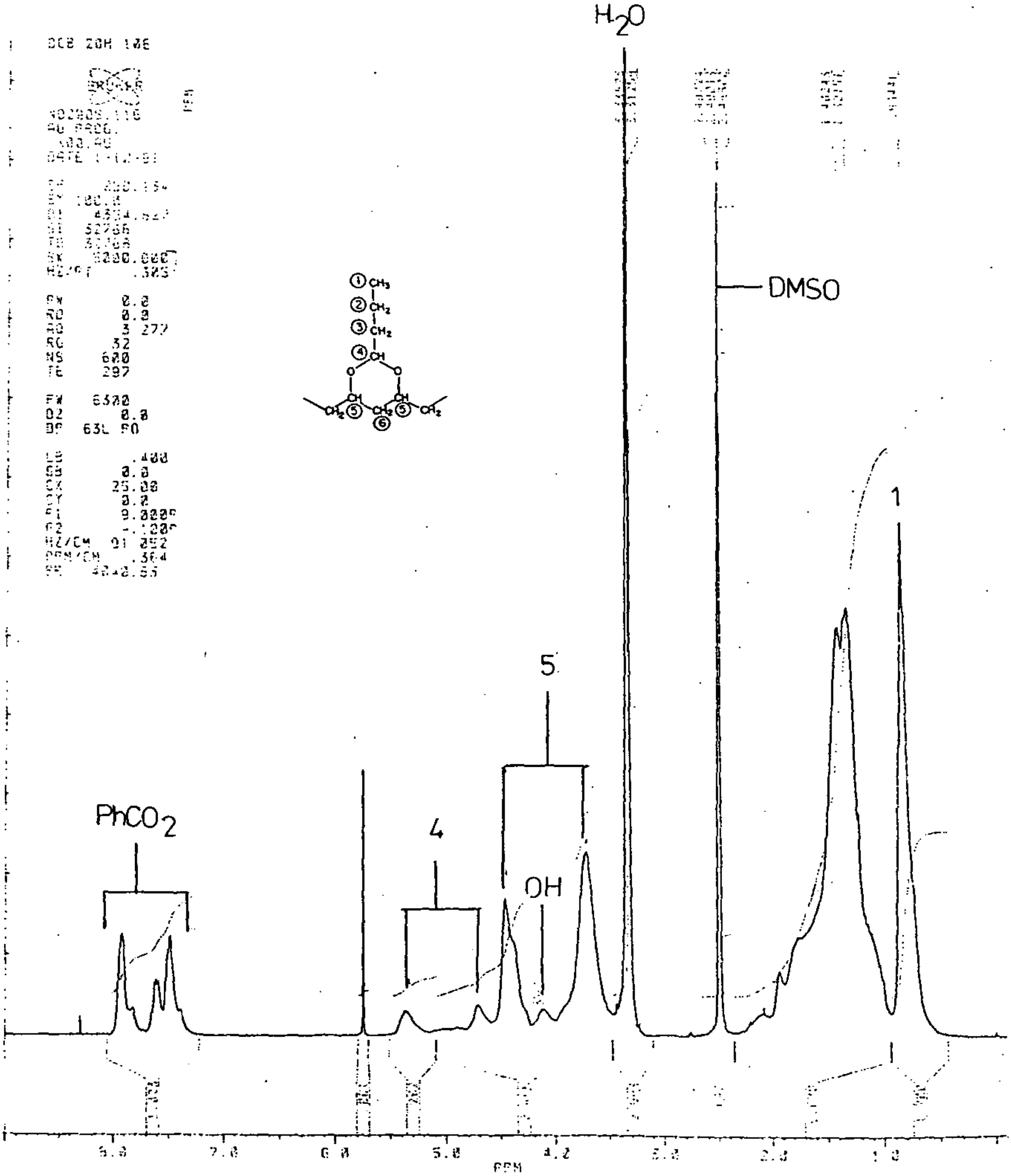

Figure 4.24

Plot of $[\eta]_{SB}$ against $[OH]$ for Benzoated $B2OH$ in THF

$y = 0.352 -$ [illegible] $\times 10^{-3}x$, $r = -0.32$

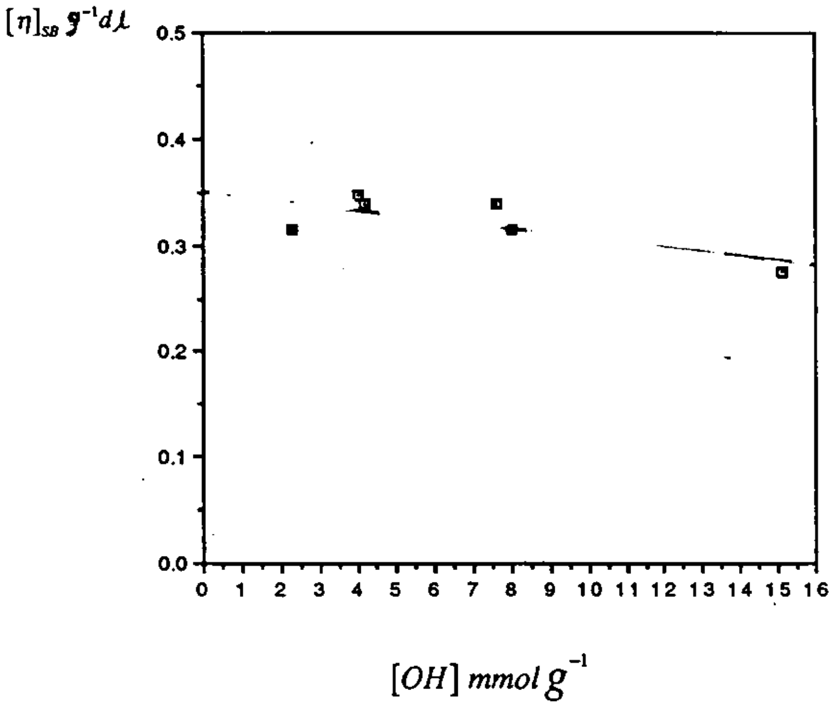

Figure 4.25

$[\eta]_{SB}$ against ratio Benzoate / Butyral for Benzoated $B2OH$ in THF

[illegible]

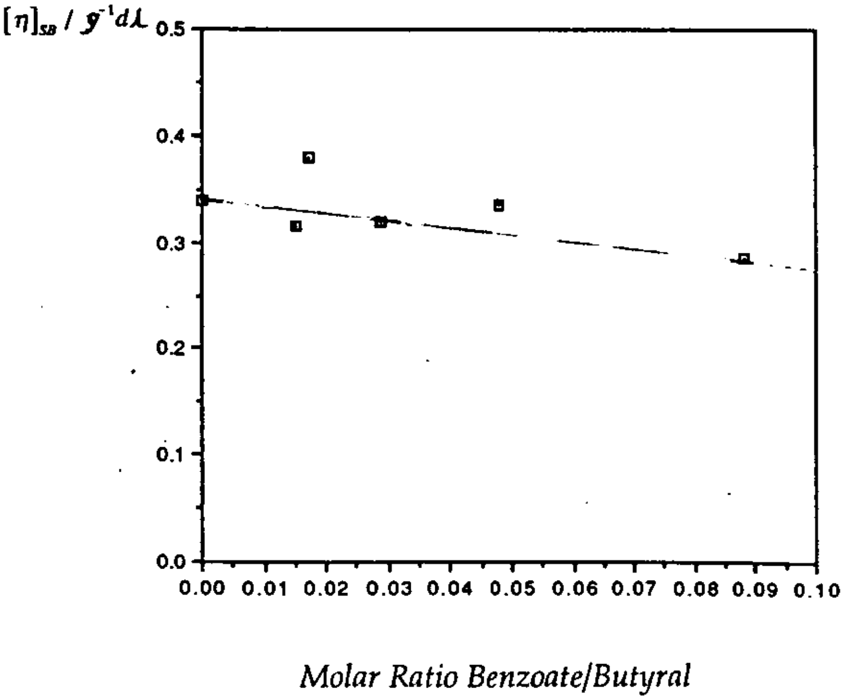

Figure 4.26

k_{SB} against $[OH]$ for Benzoated *B2OH* in *THF*

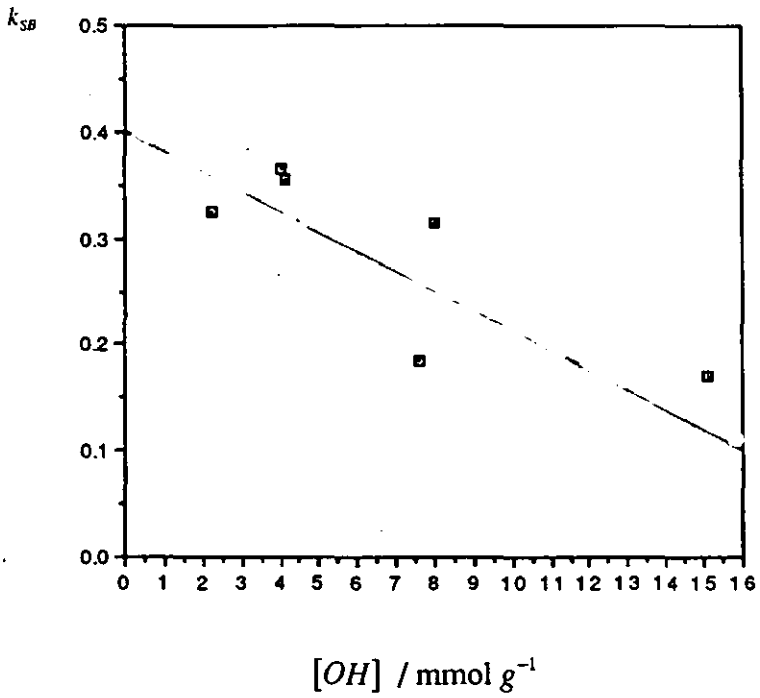

Figure 4.27

k_{SB} against ratio of Benzoate / Butyral for Benzoated *B2OH* in *THF*

$y = 0.35 - 2.2x$, $r = -0.85$

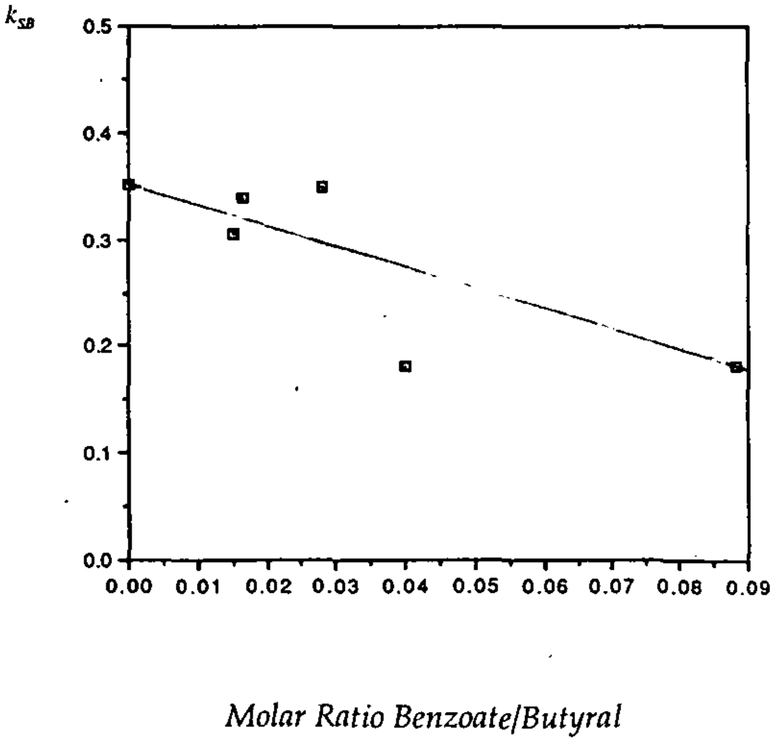

Table 4.13

Blends of Benzoated B20H with TMXDI/NPG

B20H-94

Blend	wt fraction PVB	wt fraction TMXDI/ NPG	Film Appearance	DMTA Tg/°C	Fox Eqn Tg/°C	Rule of Mixtures Tg/°C
	1	0		68.7		
189(a)	2/3	1/3	opaque	88.5	78.09	78.63
189(b)	1/2	1/2	opaque	94.4	83.0	83.6
189(c)	1/3	2/3	opaque	96.9	88.0	88.57
	0	1		98.5		

B20H-99

Blend	wt fraction PVB	wt fraction TMXDI/ NPG	Film Appearance	DMTA Tg/°C	Fox Eqn Tg/°C	Rule of Mixtures Tg/°C
	1	0		74.2		
175(a)	2/3	1/3	clear	74.7,95.2	81.94	82.3
175(b)	1/2	1/2	clear	75.7,96.9	85.94	86.35
175(c)	1/3	2/3	opaque	66.5,94	90.03	90.4
	0	1		98.5		

B20H-109

Blend	wt fraction PVB	wt fraction TMXDI/ NPG	Film Appearance	DMTA Tg/°C	Fox Eqn Tg/°C	Rule of Mixtures Tg/°C
	1	0		72.2		
189(d)	2/3	1/3	opaque	94	80.54	81.0
189(e)	1/2	1/2	opaque	93.2	84.87	85.35
189(f)	1/3	2/3	opaque	101	89.73	89.73
	0	1		98.5		

Table 4.14
Blends of Benzoated B20H with Diorex

B20H-99

Blend	wt fraction PVB	wt fraction Diorex	Film Appearance	DMTA Tg/°C	Fox Eqn Tg/°C	Rule of Mixtures Tg/°C
	1	0		74.2		
166(a)	2/3	1/3	clear	46.3	28.15	37.8
166(b)	1/2	1/2	clear	-34,36.2	9.42	19.6
166(c)	1/3	2/3	clear	-30.5,26.3	-7.12	1.4
	0	1		-35		

Table 4.15
Blends of Benzoated B20H with PEI

B20H-94

Blend	wt fraction PVB	wt fraction PEI	Film Appearance	DMTA Tg/°C	Fox Eqn Tg/°C	Rule of Mixtures Tg/°C
	1	0		68.7		
190(a)	2/3	1/3	clear	45.1	29.73	37.0
190(b)	1/2	1/2	clear	-24.6,38.2	13.40	21.1
190(c)	1/3	2/3	clear	-26,14.3	-1.26	5.23
	0	1		-26.5		

Table 4.16
Blends of Benzoated B20H with PVP

B20H-94 under dry nitrogen

Blend	wt fraction PVB	wt fraction PVP	Film Appearance	DMTA Tg/°C	Fox Eqn Tg/°C	Rule of Mixtures Tg/°C
	1	0		68.7		
191(a)	2/3	1/3	clear	107,167	97.13	102.8
191(b)	1/2	1/2	clear	123,172	131.65	119.85
191(c)	1/3	2/3	clear	130,166	144	146.9
	0	1		171		

Figure 4.28

DMTA
Head: Standard 300°C

TITLE : 189 (a)
SUBTITLE: B20H-94/TMXD1
FILENAME: Pressed Film
OPERATOR: D.Cunliffe

DATE RUN: Jun/01/1992
FREQ : 1
STRAIN : 1
DIM: 1.00, 9.510, .387

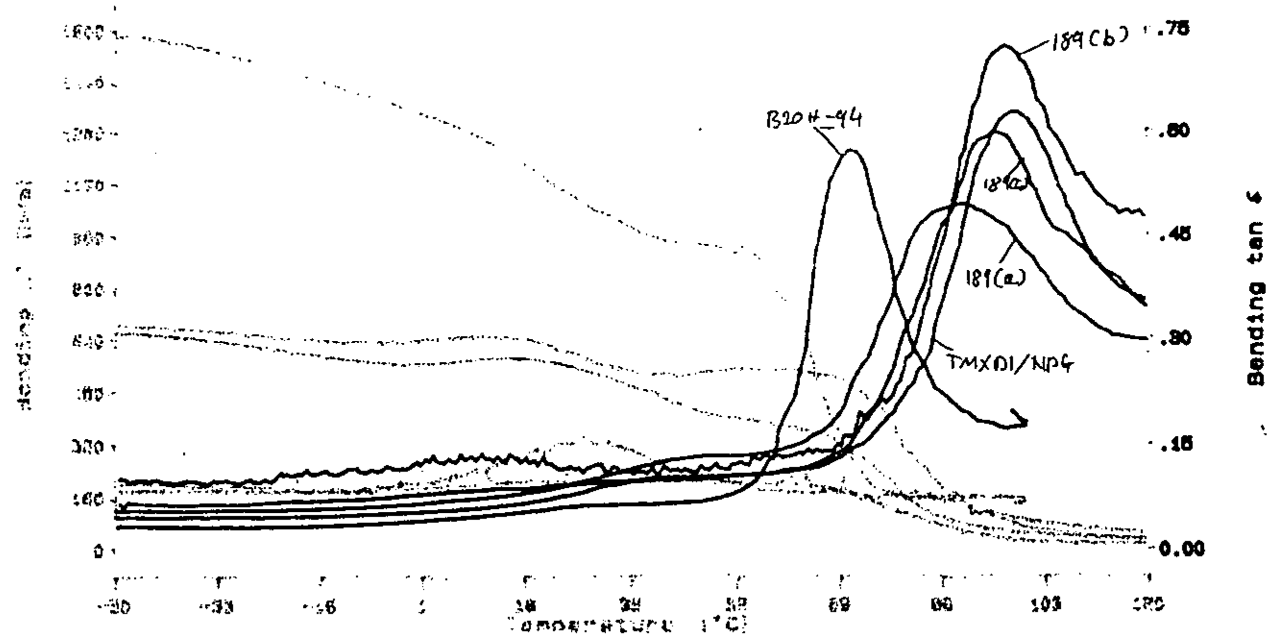

Blends of B20H-94 with TMXD1/NPG in air

VERSION: V5.20

Figure 4.29

DMTA
Head: Standard 300°C

TITLE : PVB
SUBTITLE: B20H-99
FILENAME: B20H-99
OPERATOR: D.Cunliffe

DATE RUN: Jun/13/1991
FREQ : 1
STRAIN : 4
DIM: 2.00, 11.605, .273

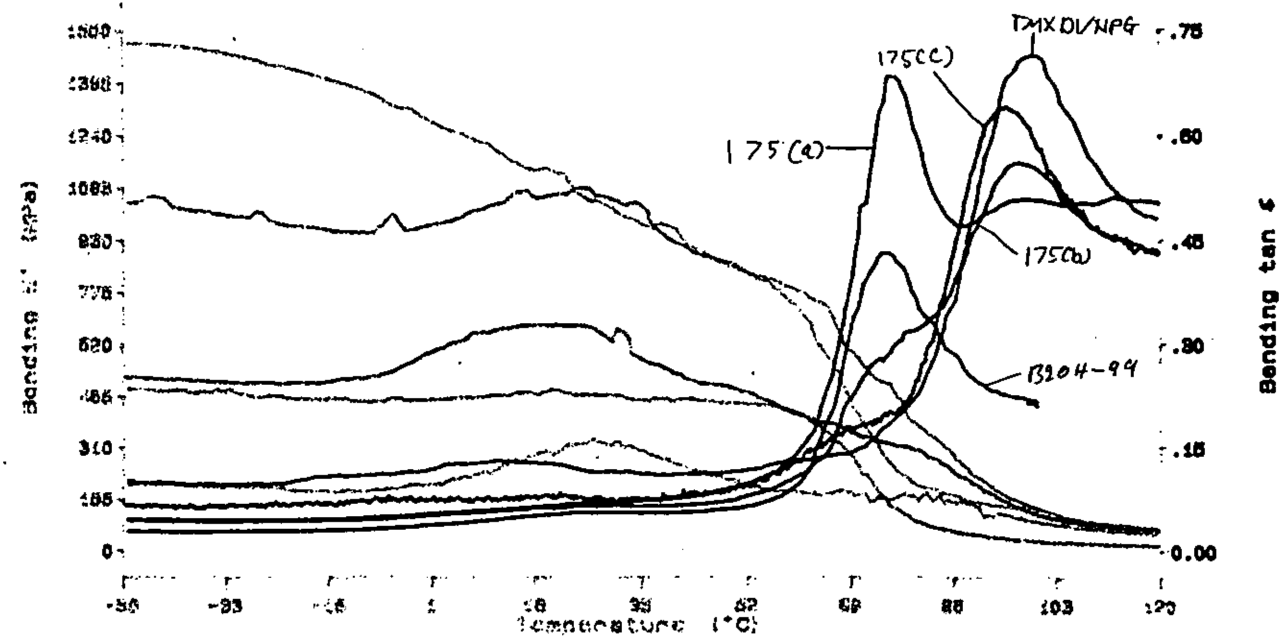

Blends of B20H-99 with TMXD1/NPG in air

VERSION: V5.20

Figure 4.30

DMTA
Head: Standard 300°C

TITLE : 189 (f)
SUBTITLE: B20H-109/TMXD1
FILENAME: Pressed Film
OPERATOR: D.Cunliffe

DATE RUN: Jun/02/1992
FREQ : 1
STRAIN : 1
DIM: 1.00, 11.150, .300

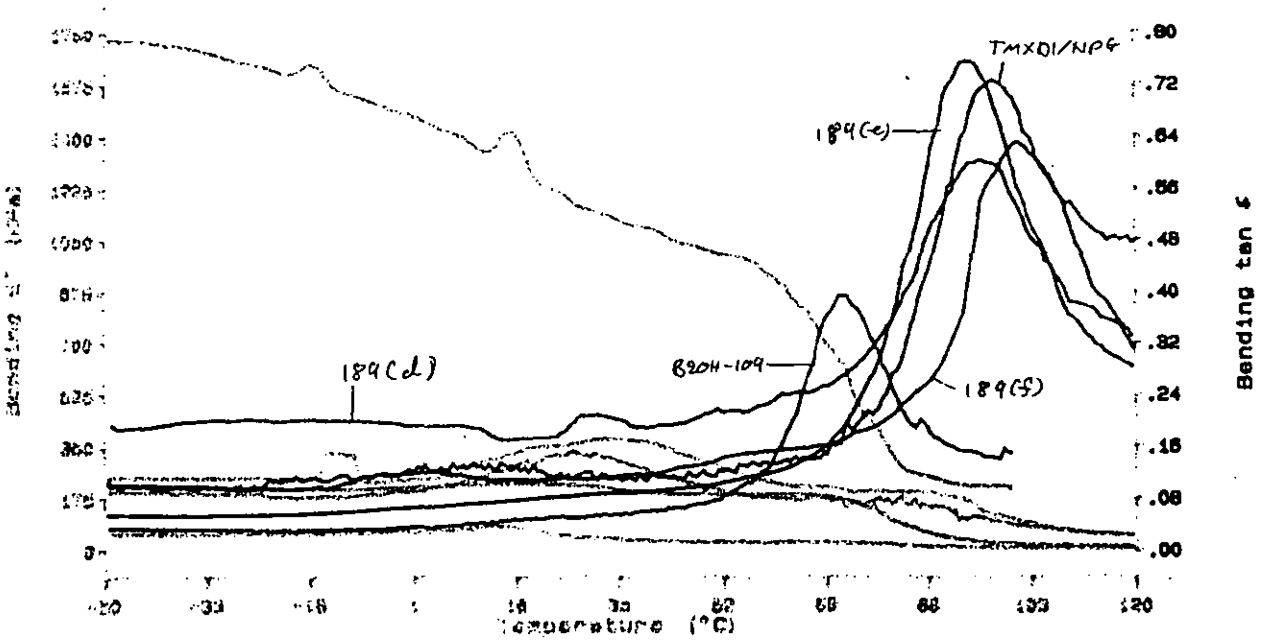

Blends of B20H-109 with TMXD1/NPG in air

VERSION: V5.20

Figure 4.31

DMTA
Head: Standard 300°C

TITLE : PVB
SUBTITLE: B20H-99
FILENAME: B20H-99
OPERATOR: D.Cunliffe

DATE RUN: Jun/13/1991
FREQ : 1
STRAIN : 4
DIM: 2.00, 11.605, .273

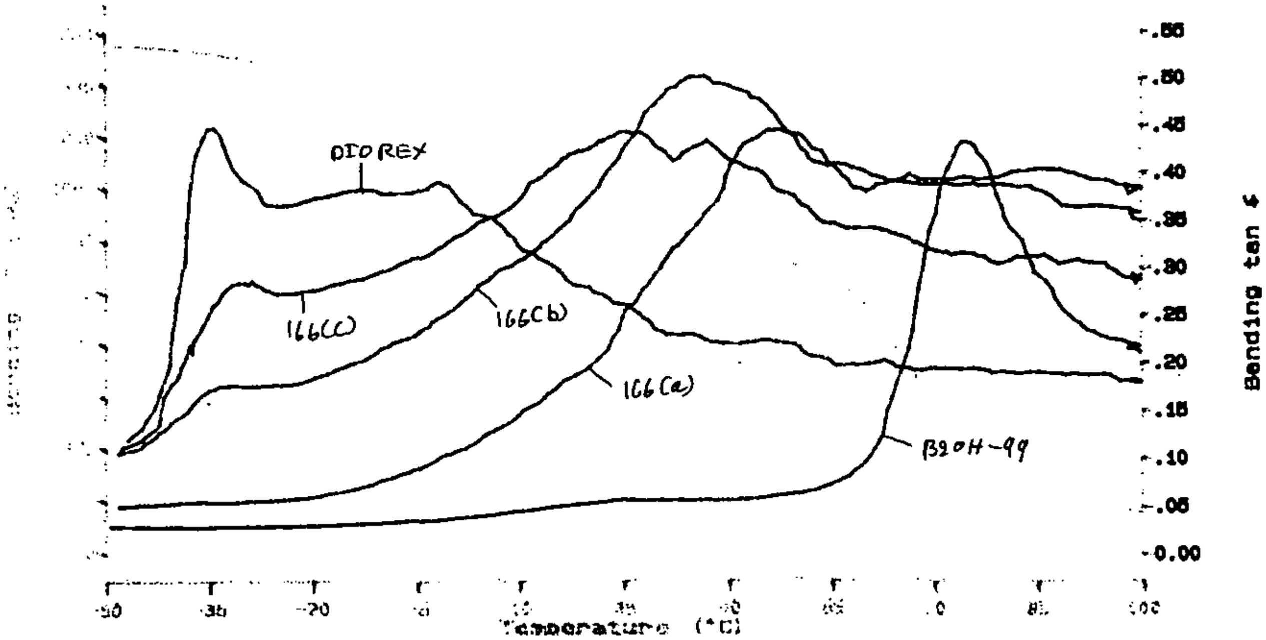

Blends of B20H-99 with Diorex in air

VERSION: V5.20

Figure 4.32

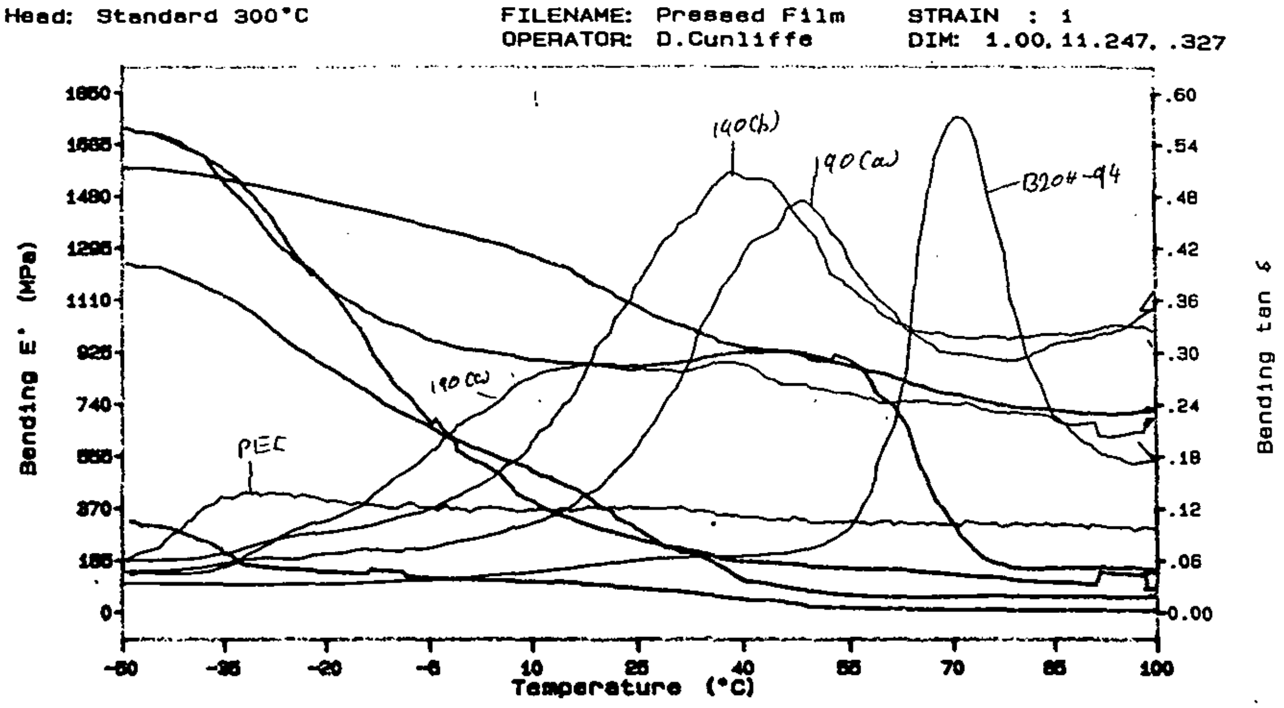

DMTA

Head: Standard 300°C

TITLE : 190 (a)
SUBTITLE: B20H-94/PEI
FILENAME: Pressed Film
OPERATOR: D.Cunliffe

DATE RUN: Jun/09/1992
FREQ : 1
STRAIN : 1
DIM: 1.00, 11.247, .327

Blends of B20H-94 with PEI in air

VERSION: V5.20

Figure 4.33

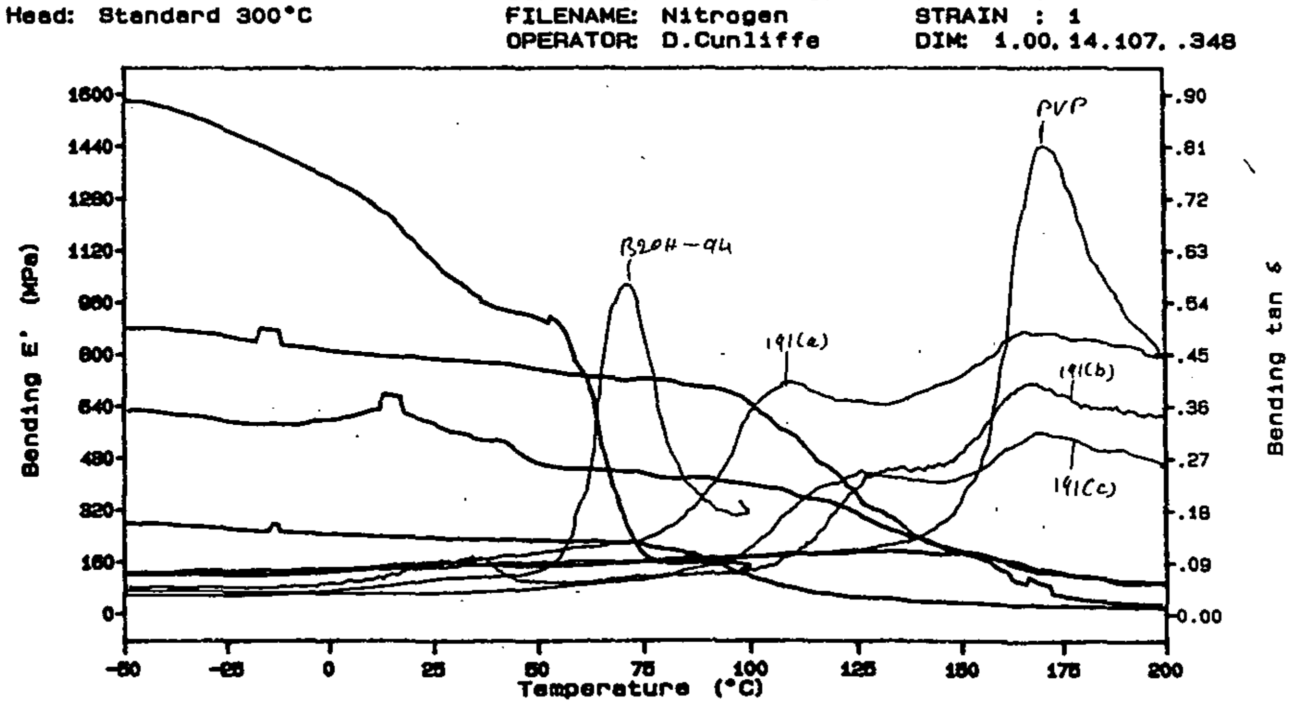

DMTA

Head: Standard 300°C

TITLE : PVP
SUBTITLE: Pressed film
FILENAME: Nitrogen
OPERATOR: D.Cunliffe

DATE RUN: May/14/1992
FREQ : 1
STRAIN : 1
DIM: 1.00, 14.107, .348

Blends of B20H-94 with PVP under dry nitrogen

VERSION: V5.20

These blends are opaque in appearance and like those of B20H-94 are insoluble, indicating that cross linking has taken place between the free hydroxyl groups of PVB and free isocynate groups of the polyurethane.

The results of blending with diorex are given in table 4.14. Blends of B20H-99 with a PVB/diorex ratio of 2:1 a single broad Tg is observed which does not correlate with that predicted by the Fox equation or the ruleof mixtures, indicating partial miscibility with some microphaseheterogeneity. With PVB/diorex ratios of 1:1 and 1:2 two broad Tg values are observed the lower corresponds to that of unmixed diorex while the higher transitions broadens and shifts to a lower temperature as the diorex content is increased. This is illustrated in figure 4.31.

The results of blending with PEI are given in table 4.15. Blends of B20H-94 with a PVB/PEI ratio of 2:1 a single broad Tg is observed which does not correlate with that predicted by the Fox equation or rule of mixtures, indicating partial miscibility with some microphaseheterogeneity. With PVB/PEI ratios of 1:1 and 1:2, two broad Tg values are observed. The low temperature transition corresponds to thatof unmixed PEI. The high temperature Tg broadens and moves to a lower value as the PEI content is increased. This is illustrated in figure 4.32.

The results of blending with PVP are given in table 4.16. With PVB/PVP ratios of 2:1, 1:1 and 1:2 two broad values of Tg are observed. The lower temperature transition is in between the values of the unmixed polymers and its value increases as the PVP content is increased. The higher temperature transition does not vary as the PVP content changes and corresponds to that of unmixed PVP. This is illustrated in figure 4.33. In general benzoation of PVB decreases its miscibility with the other polymers. Similar to the case of butyration. The solubility characteristics of benzoated samples of B20H were studied and the results given in table 4.17. This shows an increased solubility of PVB in non-polar hydrocarbon solvents and a decrease in highly polar solvents, as the degree of benzoation is increased.

Table 4.17

Solubility Characteristics of Benzoated B20H

Polymer	Methanol	Acetone	Ethyl Acetate	Ethyl Acetate/ Methanol 1:1	THF	Benzene	Toluene	Hexane	Cyclohexane	Chloroform
B20H	✓	✓	✓	✓	✓	swell	swell	X	X	✓
B20H-94	✓	✓	✓	✓	✓	swell	swell	X	swell	✓
B20H-95	✓	✓	✓	✓	✓	swell	swell	X	swell	✓
B20H-99	✓(a)	✓	✓	✓	✓	✓	✓	swell	swell	✓
B20H-106	✓(a)	✓	✓	✓	✓	✓	✓	X	swell	✓
B20H-109	✓	✓(a)	X	✓(a)	✓(a)	swell	swell	X	swell	✓(a)

(a) slightly soluble

4.4 Trifluoroacetylated PVB

A number of trifluoroacetylated samples of B20H were prepared and their intrinsic viscosities in THF were determined and the results are given in table 4.18. Molecular mass, hydroxyl content, transition data and ratio of trifluoroacetate groups plus acetate groups to hydroxyl groups are given in table 4.19. The ratio of acetate groups to alcohol groups was determined by FTIR. As the films are thin enough to obey Beer Lamberts law, the heights of the peaks are proportional to the number of groups present hence a ratio of peak heights is proportional to the ratio of groups percent. An infrared spectrum of a trifluoracetylated sample of B2OH is given in figure 4.34.

It was found that incomplete modification of PVB does not prevent aggregation in THF. This shown by the chromatogram[165] in figure 4.35 which compares the response from a RI detector with the response from a LALLS detector. Aggregation is indicated by a shoulder in the high molecular mass region in the LALLS response which is not observed by the RI detector. The molecular mass of the trifluoroacetylated B20H was also determined by light scattering in THF and acetic acid[165]. Figure 4.36 shows a Zimm plot for B20H-79 in THF, the curvature of the plot is due to aggregate formation in THF and gives a value for MWof 608000. Figure 4.37 shows a Zimm plot for B20H-79 in acetic acid, this is a better solvent for PVB and gives a linear Zimm plot indicating the lack of aggregate formation and gives a value for Mw of 28000 which is similar to the value obtained at Loughborough by SEC in THF.

The variation of $[\eta]_{SB}$ and k_{SB} with hydroxyl content and ratio of acetate groups to hydroxyl groups are given in figures 4.38 - 4.41. These show that the variation of $[\eta]_{SB}$ and k_{SB} with the degree of modificaton are of the same order [illegible] whereas with benzoation and butyration there is a[illegible] difference in the variation of $[\eta]_{SB}$and k_{SB} with the degree of modification.

Table 4.18

Viscosity Data for Trifluoroacetylated B20H in THF

polymer	$[\eta]_H / g^{-1}dl$	$[\eta]_k / g^{-1}dl$	$[\eta]_{SB} / g^{-1}dl$	$[\eta]_M / g^{-1}dl$	k_H	k_k	k_{SB}	k_M
B20H	0.3382	0.3464	0.3436	0.3411	0.474	0.0816	0.359	*0.41*
B20H-74	0.3303	0.332	0.3326	0.3326	0.478	0.0768	0.375	0.420
B20H-76	0.3162	0.3162	0.3175	0.3175	0.389	0.125	0.328	0.354
B20H-78	0.2828	0.2985	0.2979	0.2979	0.172	0.599	0.293	0.352
B20H-79	0.3279	0.3283	0.3293	0.3295	0.368	0.142	0.364	0.333
B20H-84	0.3011	0.3012	0.3021	0.3021	0.363	0.144	0.306	0.332
B20H-103	0.2763	0.2765	0.2812	0.2812	0.377	0.136	0.268	0.296

Table 4.19

Molecular Mass, Hydroxyl and Transition Data of Trifluoroacetylated PVB Samples

Polymer	$\bar{M}$n	$\bar{M}$w	Mp	M*wd*	[OH]/mmol g^{-1}	Tg/°c	$\frac{\text{Trifluroacetate plus Acetate}}{\text{Hydroxyl}}$
B20H	9000	23000	14000	2.56	4.0	71	0.84
B20H-74	7900	17000	12000	2.18	3.75	66.5	0.97
B20H-76	6900	22000	12000	3.1	2.81	63.5	0.41
B20H-78	5500	24000	12000	4.5	2.15	65.1	10.9
B20H-79	10000	26000	16000	2.7	2.30	69.6	3.0
B20H-84	11000	32000	19000	2.8	1.55	64.4	3.1
B20H-103	8300	14000	11000	1.7	6.4	59.9	14.3

Figure 4.34 Infrared Spectrum of Trifluoroacetylated B20H

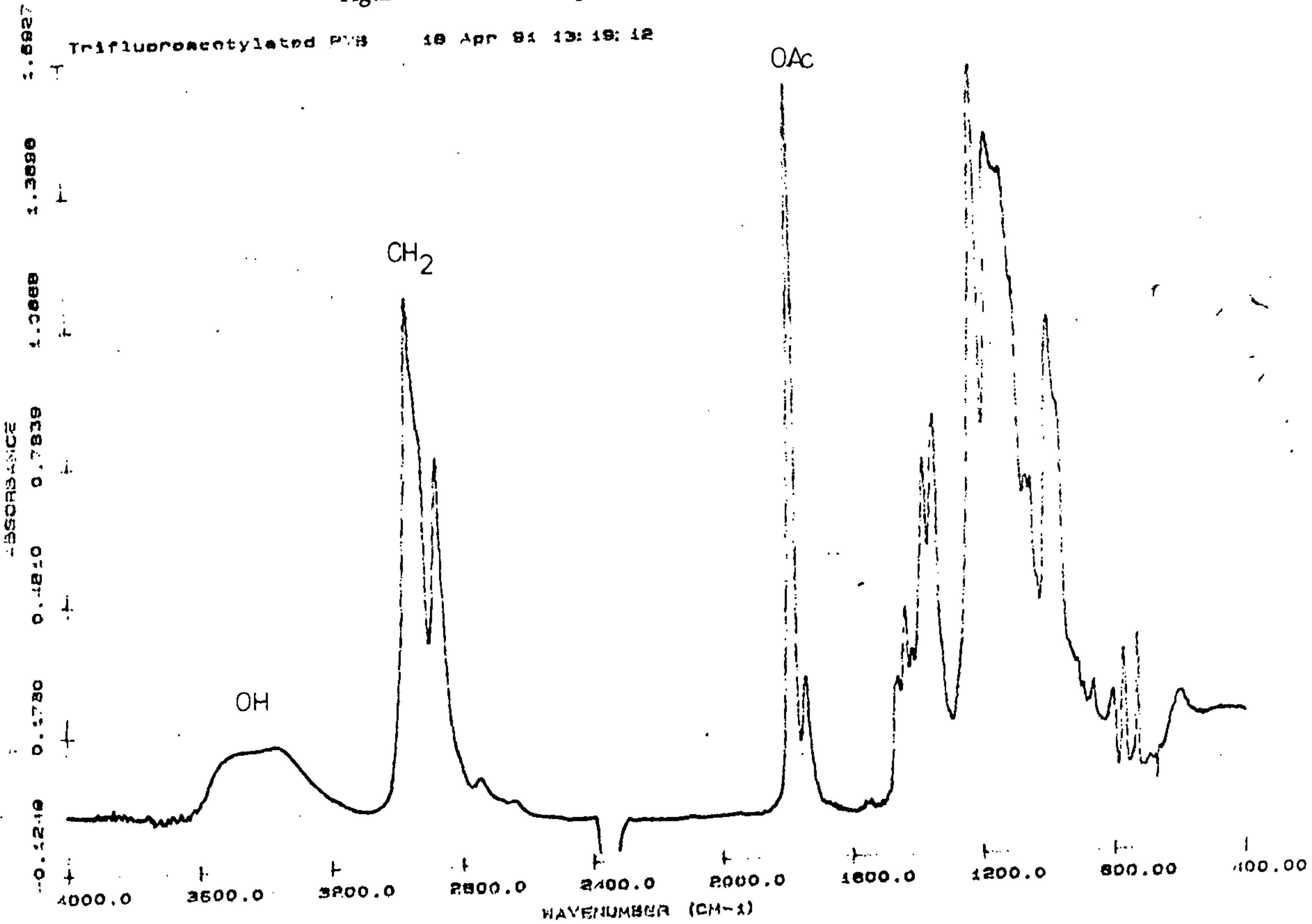

Figure 4.35

Size Exclusion Chromatogram of Trifluoroacetylated B20H

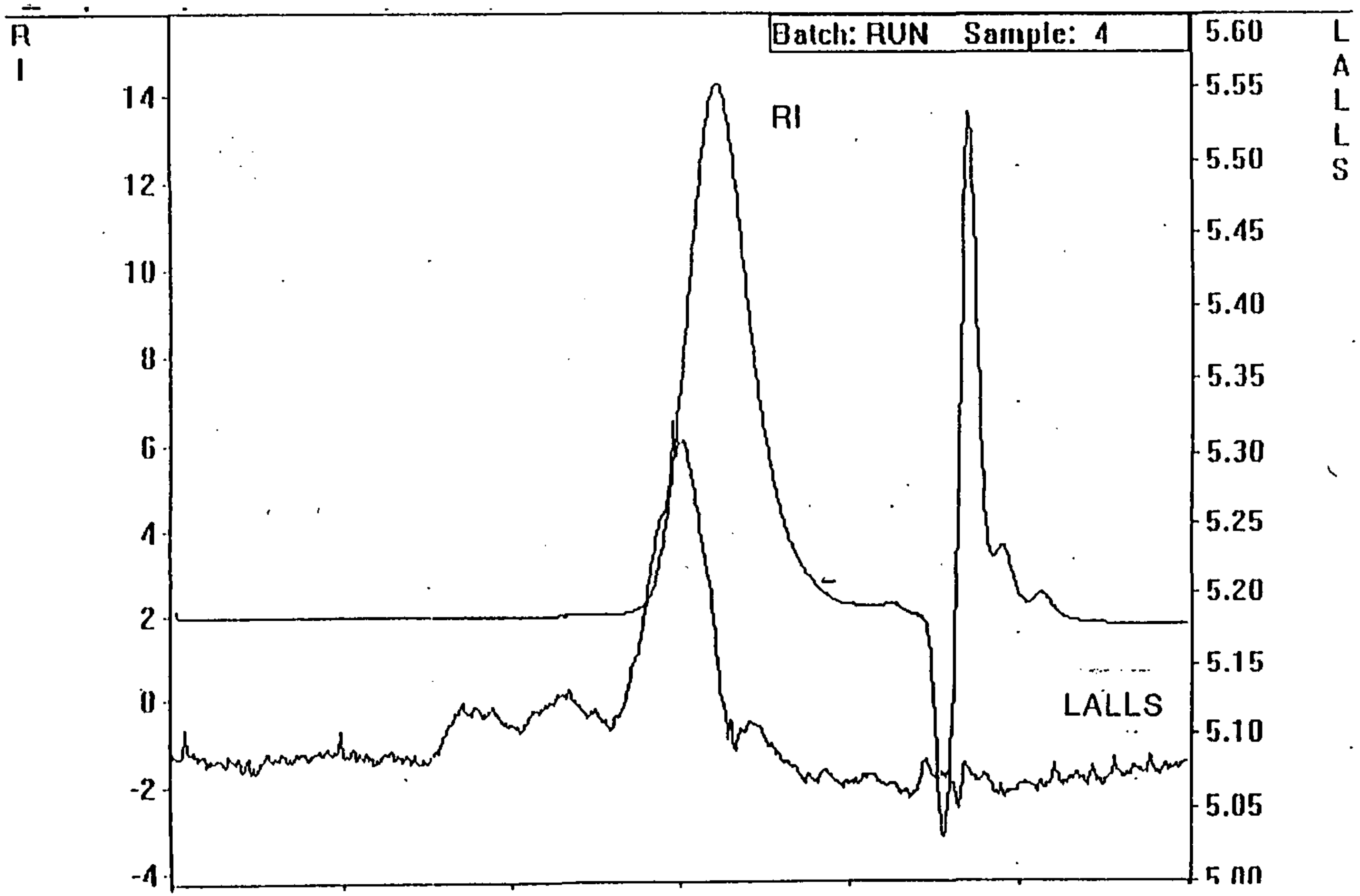

Figure 4.36

Zimm plot of trifluoroacetylated B20H in THF

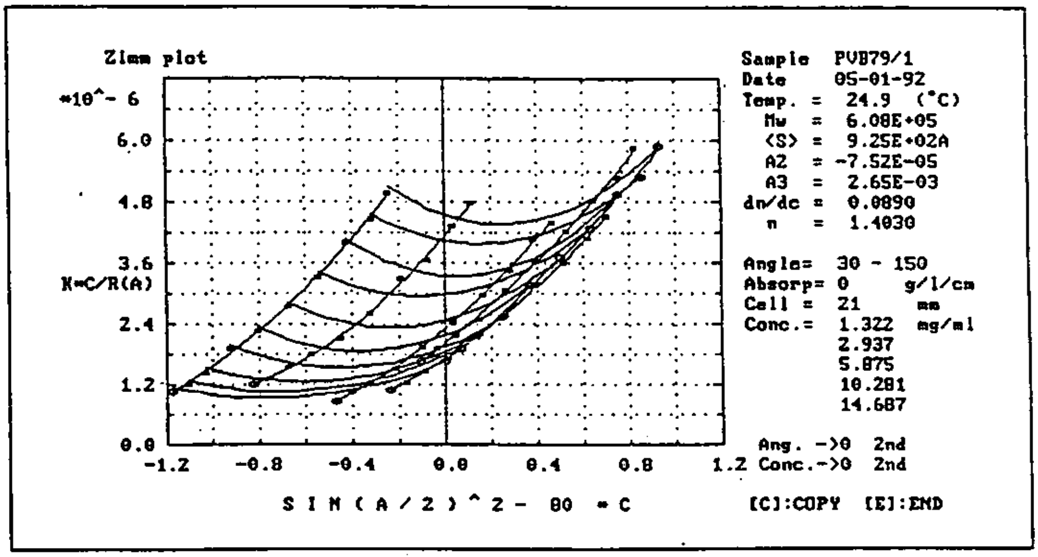

```
Sample  PVB79/1
Date    05-01-92
Temp. =  24.9  (°C)
  Mw  =  6.08E+05
  <S> =  9.25E+02A
  A2  = -7.52E-05
  A3  =  2.65E-03
dn/dc =  0.0890
  n   =  1.4030

Angle=  30 - 150
Absorp= 0      g/l/cm
Cell =  21      mm
Conc.=  1.322  mg/ml
        2.937
        5.875
        10.281
        14.687

 Ang. ->0  2nd
 Conc.->0  2nd

[C]:COPY  [E]:END
```

Figure 4.37

Zimm plot of trifluoroacetylated B20H in acetic acid

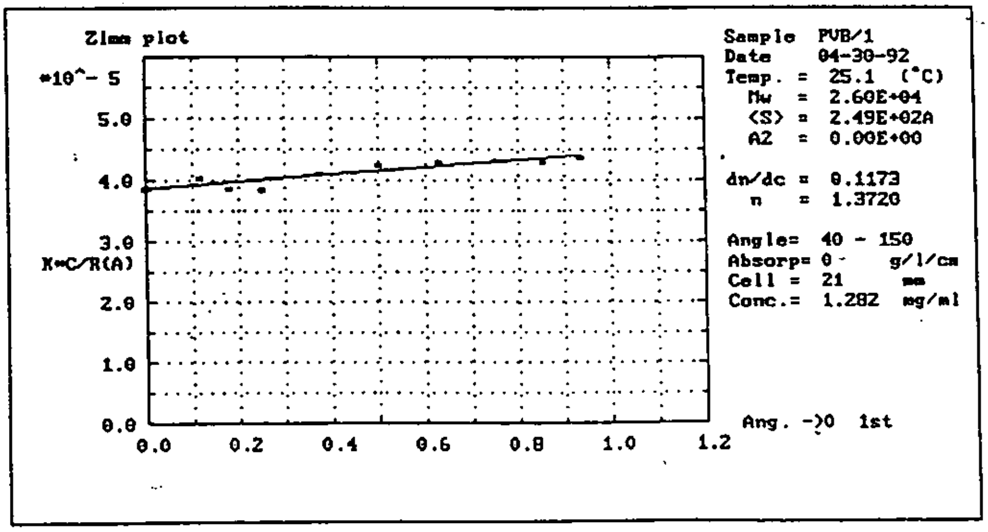

```
Sample  PVB/1
Date    04-30-92
Temp. =  25.1  (°C)
  Mw  =  2.60E+04
  <S> =  2.49E+02A
  A2  =  0.00E+00

dn/dc =  0.1173
  n   =  1.3720

Angle=  40 - 150
Absorp= 0      g/l/cm
Cell =  21      mm
Conc.=  1.282  mg/ml

 Ang. ->0  1st
```

Figure 4.38

$[\eta]_{SB}$ against $[OH]$ for trifluorracetylated $B2OH$ in THF

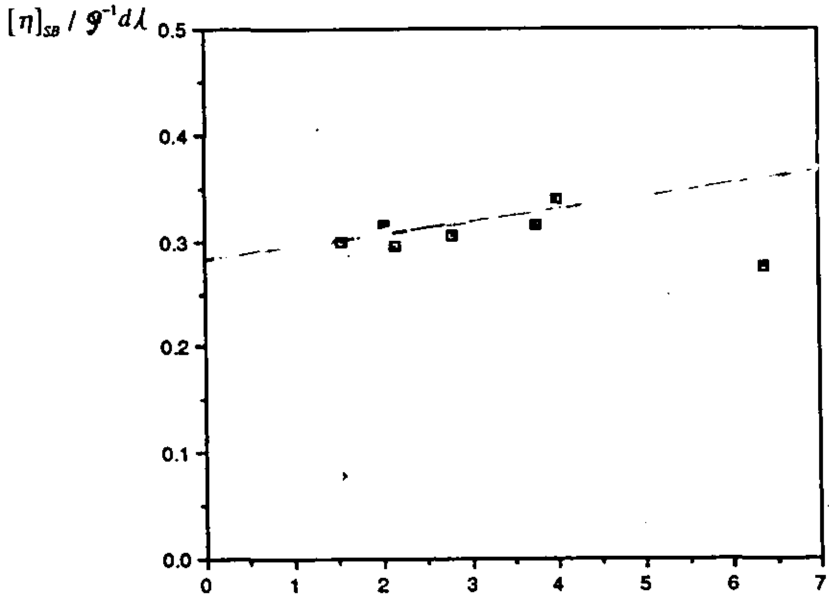

[OH]/mmol g^{-1}

Figure 4.39

k_{SB} against $[OH]$ for trifluorracetylated $B2OH$ in THF

$y = 0.27 + 0.025x$ $r = 0.725$

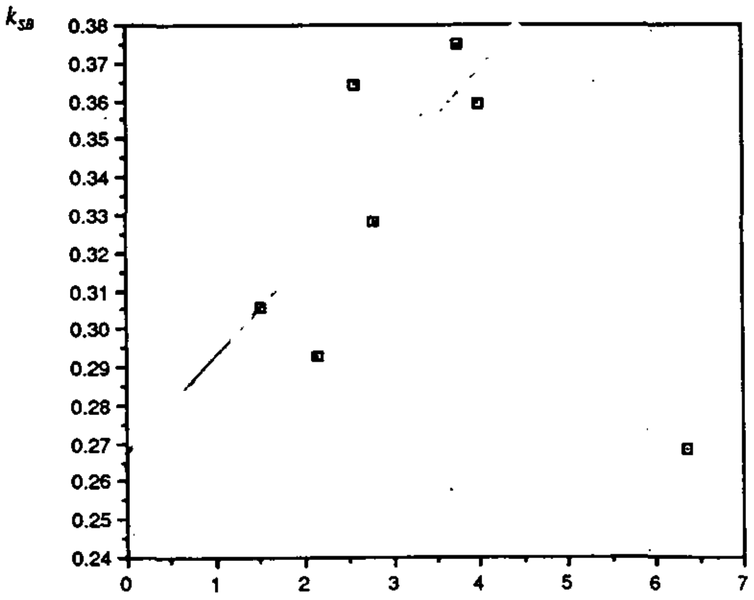

[OH]/mmol g^{-1}

Figure 4.40

$[\eta]_{SB}$ against ratio acetate / hydroxyl for trifluoracetylated *B2OH* in *THF*

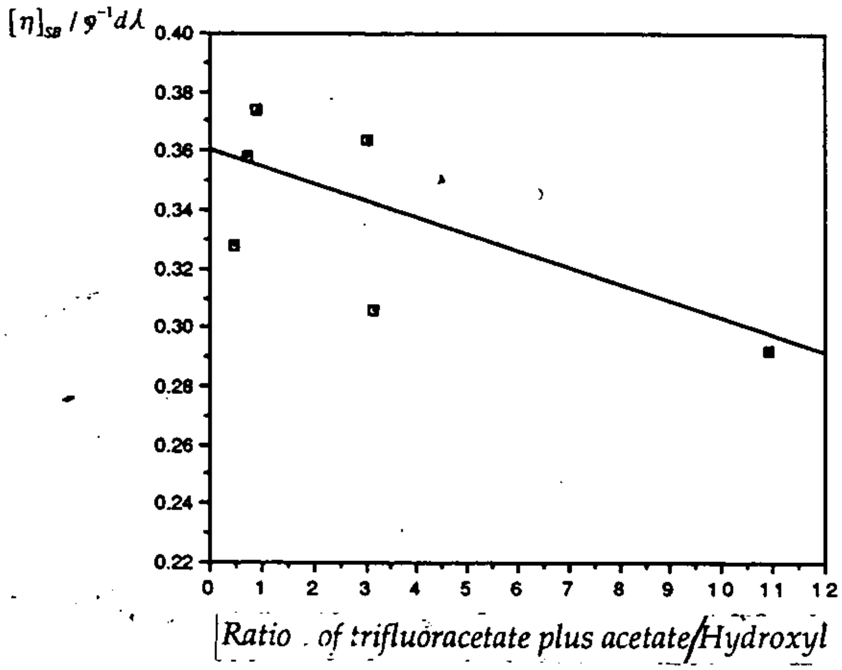

Figure 4.41

k_{SB} against ratio of trifluoracetate plus acetate groups for trifluoracetylated *B2OH* in *THF*

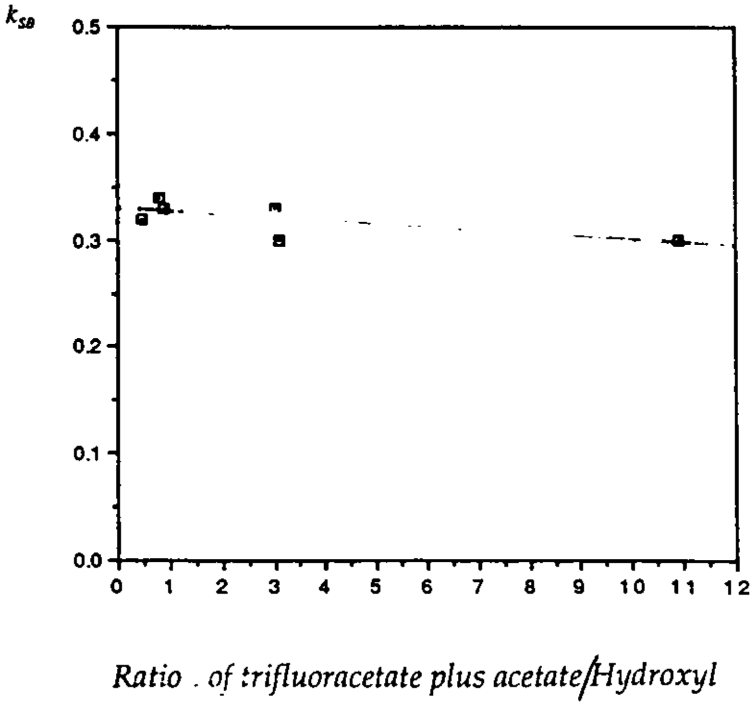

Blends of trifluoroacetylated B20H were prepared with PEI, diorex and TMXDI/NPG by solution casting and examined by DMTA. The results of blending with PEI are given in table 4.20. Blends of B20H-74 with PVB/PEI ratios of 2:1, 1:1 and 1:2, two broad Tg glass transitions are observed with values in between those of the unmixed polymers. As the PEI content is increased the low value Tg shifts towards that of PVB and the high value Tg shifts to a lower temperature and the tan δ peak is broadened, as illustrated in figure 4.42. This indicates that the polymers are partially miscible with microphaseheterogeneity. Blends of B20H-76 with PVB/PEI ratios of 2:1, 1:1 and 1:2 give two broad values. With a ratio of 2:1 the high temperature transition is 4°C lower than that of PVB and the lower transition is 20°C above that of PEI. As the PEI content is increased the low temperature transition shifts towards that of PEI, the other also shifts to a lower temperature and broadens as shown in figure 4.43. This indicates partial miscibility between the two polymers with microphaseheterogeneity. Blends of B20H-78 with a PVB/PEI ratio of 2:1 two Tg values are observed the higher transition corresponding with that of unmixed PVB, the lower transition is 20°C higher than that of PEI. As the PEI content is increased the lower temperature transition shifts towards that of PEI and the higher temperature transition shifts to the lower temperature the tan δ peak broadening, as illustrated in figure 4.44. This indicates partial miscibility of the two polymers with microphaseheterogeneity. Blends of B20H-79 with PVB/PEI ratios of 2:1, 1:1 and 1:2 two broad transitions, in between those of the unmixed polymers are observed. As the PEI content is increased the low temperature transition shifts towards that of PEI and the higher value Tg moves towards a lower temperature and broadens with increasing PEI content, as illustrated in figure 4.45. This indicates partial miscibility of the two polymers with microphaseheterogeneity. Blends of B20H-84 with a PVB/PEI ratio of 2:1, two glass transition are observed, the higher temperature transition corresponds to that of unmixed PVB, the lower transition is 20°C above that PEI. As the PEI content is increased the low temperature transition shifts towards that of PEI and the high temperature transition decreases and broadens as illustrated in figure 4.46. This indicates partial miscibility of these polymers with microphaseheterogeneity.

Table 4.20

Blends of Trifluoroacetylated B20H with PEI

B20H-74

Blend	wt fraction PVB	wt fraction PEI	Film Appearance	DMTA Tg/° C	Fox Eqn Tg/° C	Rule of Mixtures Tg/° C
	1	0		66.5		
183(a)	2/3	1/3	clear	-28,62.3	28.6	35.5
183(b)	1/2	1/2	clear	-19.5,48.8	12.6	20
183(c)	1/3	2/3	clear	-23.2,37.4	-1.7	4.5
	0	1		-26.5		

B20H-76

Blend	wt fraction PVB	wt fraction PEI	Film Appearance	DMTA Tg/° C	Fox Eqn Tg/° C	Rule of Mixtures Tg/° C
	1	0		63.5		
183(d)	2/3	1/3	clear	-5.4,67.9	27	35.5
183(e)	1/2	1/2	clear	-19.6,51.2	11.6	18.5
183(f)	1/3	2/3	clear	-25,41.9	-2.4	3.5
	0	1		-26.5		

B20H-78

Blend	wt fraction PVB	wt fraction PEI	Film Appearance	DMTA Tg/° C	Fox Eqn Tg/° C	Rule of Mixtures Tg/° C
	1	0		65.1		
184(a)	2/3	1/3	clear	-7.6,67.3	27	33.5
184(b)	1/2	1/2	opaque	-6.7,58.4	11.6	18.5
184(c)	1/3	2/3	opaque	-16.7,53.8	-2.4	3.5
	0	1		-26.5		

Table 4.20

Blends of Trifluoroacetylated B20H with PEI

B20H-79

Blend	wt fraction PVB	wt fraction PEI	Film Appearance	DMTA Tg/°C	Fox Eqn Tg/°C	Rule of Mixtures Tg/°C
	1	0		69.6		
184(d)	2/3	1/3	clear	-14,61	30.2	37.6
184(e)	1/2	1/2	clear	-16.6,50.3	13.7	21.6
1849f)	1/3	2/3	opaque	-22.1,30.3	-1.1	5.5
	0	1		-26.5		

B20H-84

Blend	wt fraction PVB	wt fraction PEI	Film Appearance	DMTA Tg/°C	Fox Eqn Tg/°C	Rule of Mixtures Tg/°C
	1	0		64.4		
184(g)	2/3	1/3	clear	-6.9,66.9	27.5	34.1
184(h)	1/2	1/2	clear	-18.5,55.9	11.9	19
184(i)	1/3	2/3	opaque	-15.8,46.7	-2.2	3.8
	0	1		-26.5		

Table 4.21

Blends of Trifluoroacetylated B20H with Diorex

B20H-84

Blend	wt fraction PVB	wt fraction Diorex	Film Appearance	DMTA Tg/°C	Fox Eqn Tg/°C	Rule of Mixtures Tg/°C
	1	0		64.4		
167(a)	2/3	1/3	clear	32.6	23.0	31.27
167(b)	1/2	1/2	clear	-35.3,24.3	6.12	14.7
167(c)	1/3	2/3	clear	3.1	-9.1	-1.87
	0	1		-35		

Table 4.22

Blends of Trifluoroacetylated B20H with TMXDI/NPG

B20H-84

Blend	wt fraction PVB	wt fraction TMXDI/NPG	Film Appearance	DMTA Tg/°C	Fox Eqn Tg/°C	Rule of Mixtures Tg/°C
	1	0		64.4		
176(a)	2/3	1/3	opaque	67.5,97.3	75	75.8
176(b)	1/2	1/2	opaque	77.7,96	80.6	81.5
176(c)	1/3	2/3	opaque	102	86.4	87.1
	0	1		98.5		

Figure 4.42

DMTA
Head: Standard 300°C

TITLE : 183 (a)
SUBTITLE: B20H-74/PEI
FILENAME: Pressed Film
OPERATOR: D.Cunliffe

DATE RUN: May/12/1992
FREQ : 1
STRAIN : 1
DIM: 1.00, 11.840, .287

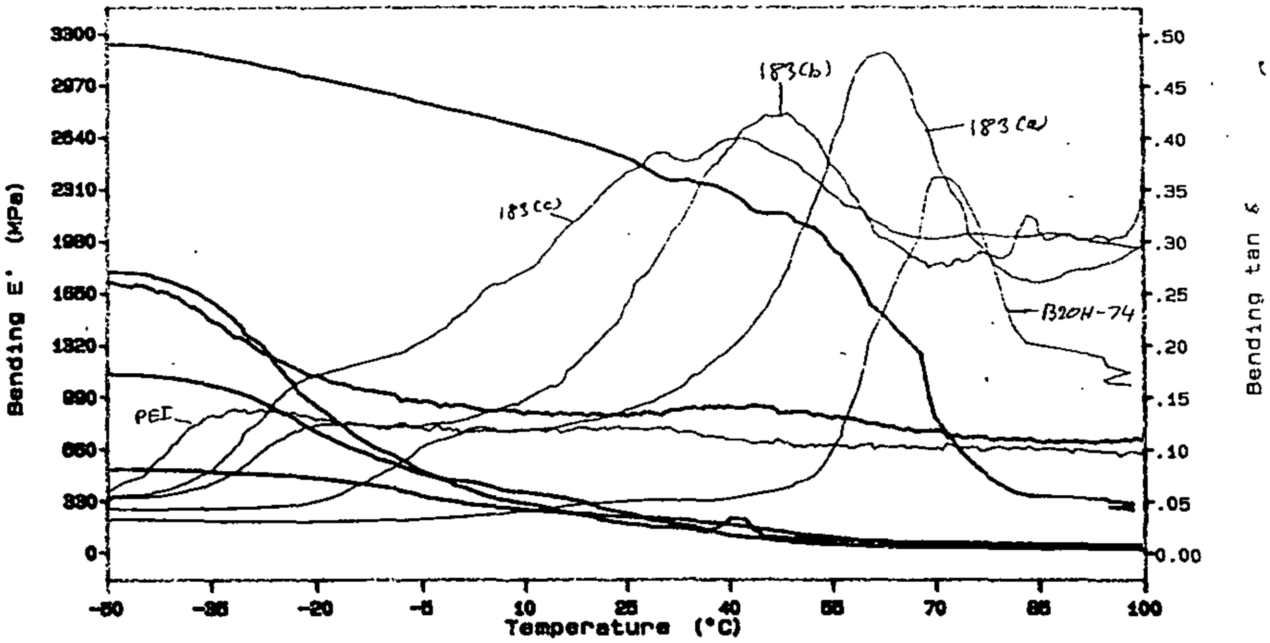

Blends of B20H-74 with PEI in air

VERSION: V5.20

Figure 4.43

DMTA
Head: Standard 300°C

TITLE : 183 (d)
SUBTITLE: B20H-76/PEI
FILENAME: Pressed Film
OPERATOR: D.Cunliffe

DATE RUN: May/13/1992
FREQ : 1
STRAIN : 1
DIM: 1.00, 10.207, .303

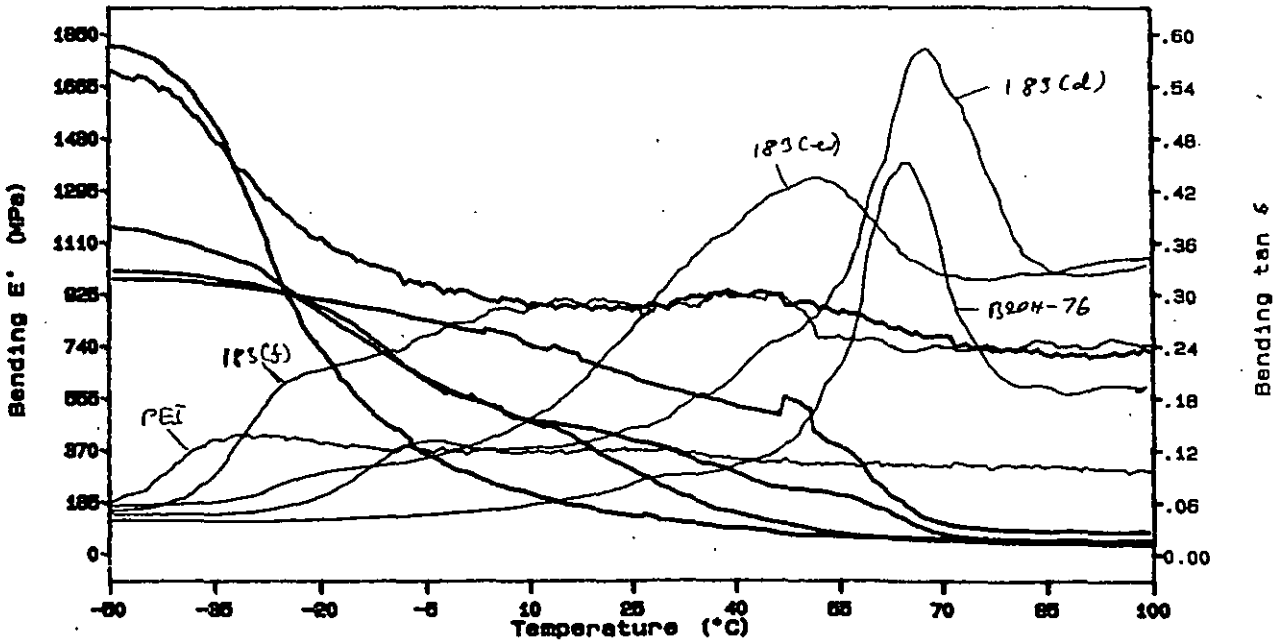

Blends of B20H-76 with PEI in air

VERSION: V5.20

Figure 4.44

DMTA
Head: Standard 300°C

TITLE : 184 (a)
SUBTITLE: B20H-78/PEI
FILENAME: Pressed Film
OPERATOR: D.Cunliffe

DATE RUN: May/24/1992
FREQ : 1
STRAIN : 1
DIM: 1.00, 10.661, .385

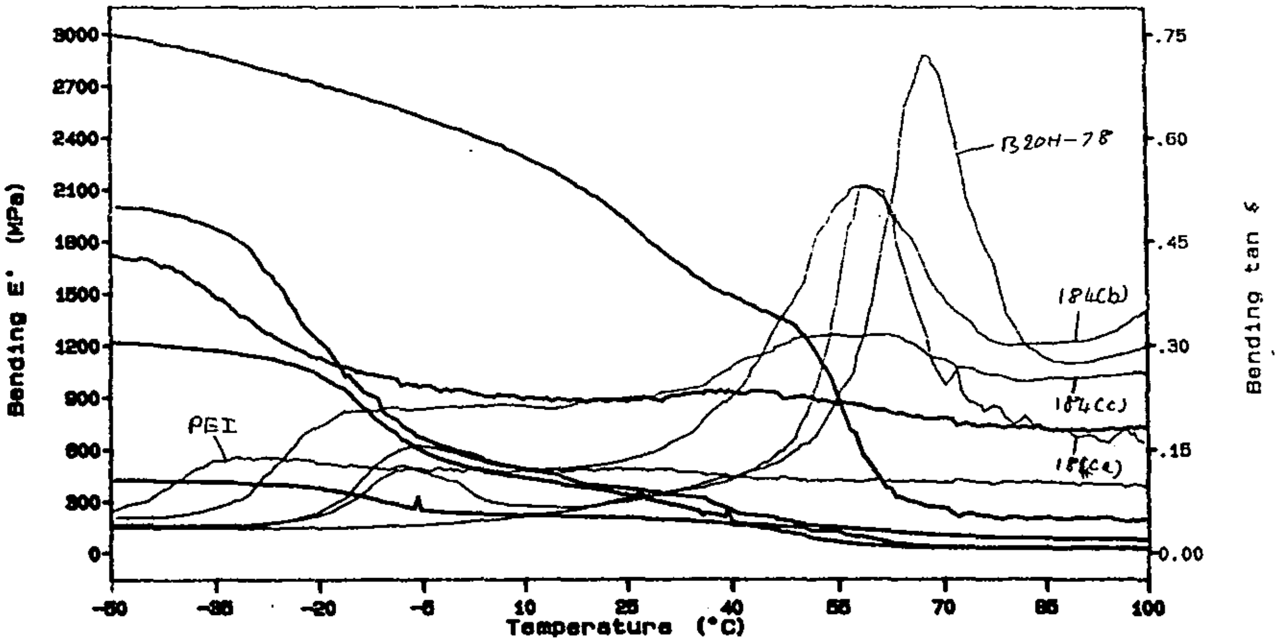

Blends of B20H-78 with PEI in air

VERSION: V5.20

Figure 4.45

DMTA
Head: Standard 300°C

TITLE : 184 (d)
SUBTITLE: B20H-78/PEI
FILENAME: Pressed Film
OPERATOR: D.Cunliffe

DATE RUN: May/26/1992
FREQ : 1
STRAIN : 1
DIM: 1.00, 11.709, .292

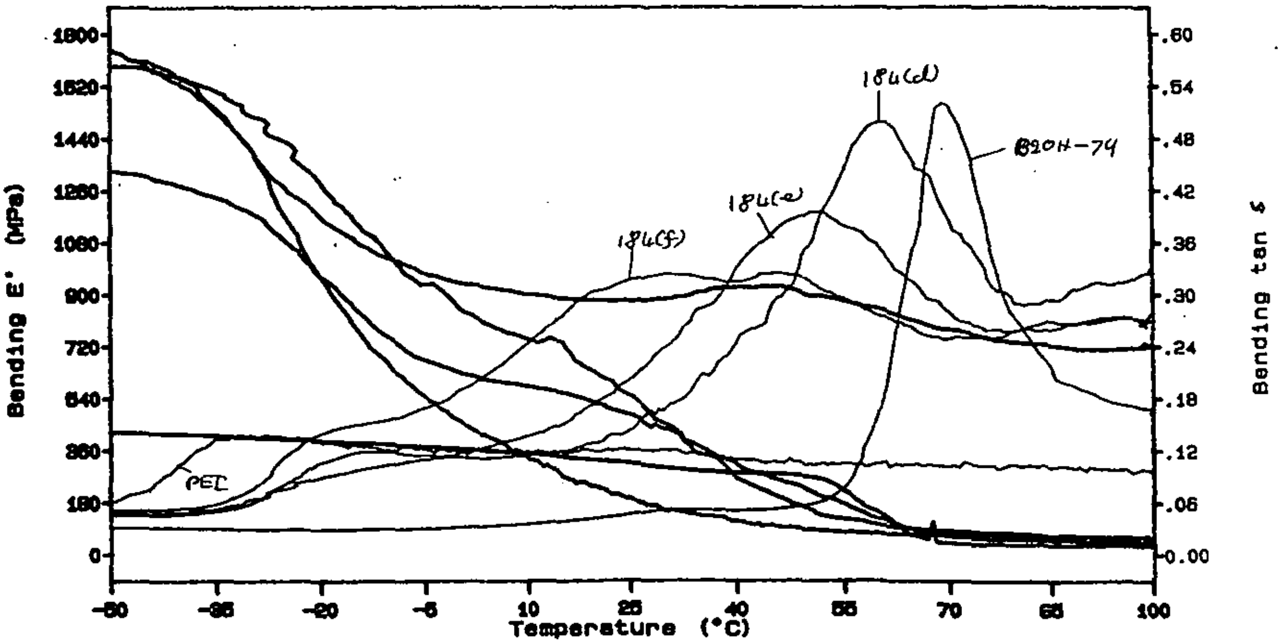

Blends of B20H-78 with PEI in air

VERSION: V5.20

Figure 4.46

DMTA
Head: Standard 300°C

TITLE : 184 (g)
SUBTITLE: B20H-84/PEI
FILENAME: Pressed Film
OPERATOR: D.Cunliffe

DATE RUN: May/25/1992
FREQ : 1
STRAIN : 1
DIM: 1.00, 9.915, .308

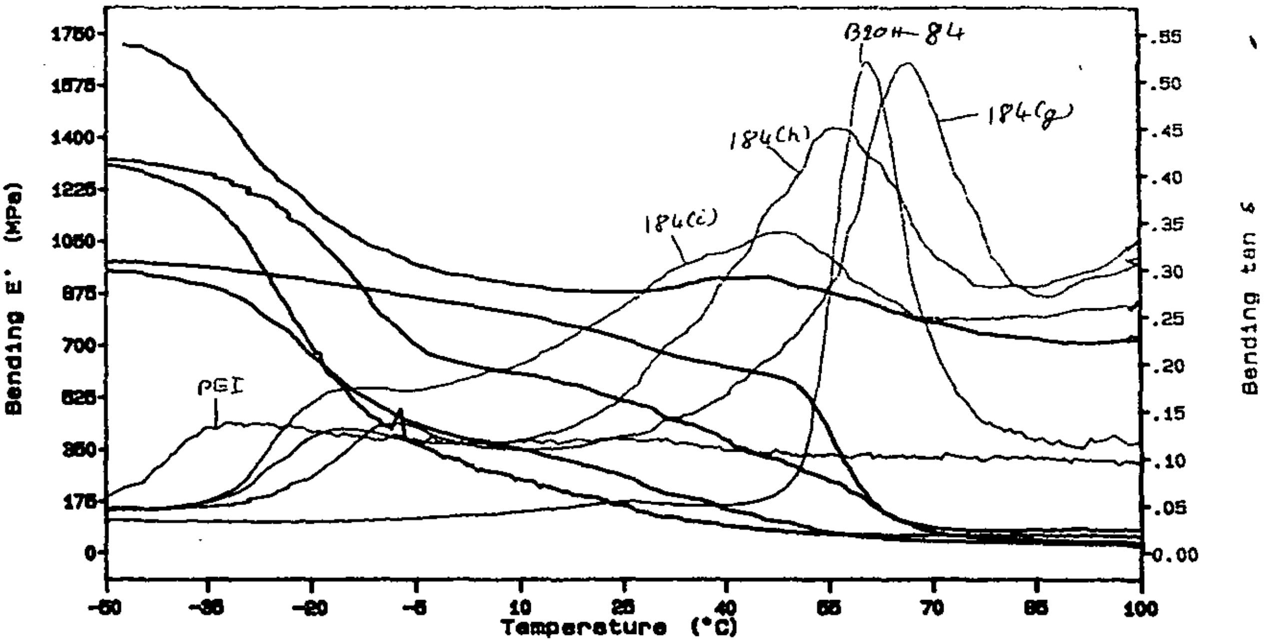

Blends of B20H-84 with PEI in air

VERSION: V5.20

Figure 4.47

DMTA
Head: Standard 300°C

TITLE : PVB
SUBTITLE: B20H-84
FILENAME: B20H-84
OPERATOR: D.Cunliffe

DATE RUN: Jun/11/1991
FREQ : 1
STRAIN : 4
DIM: 2.00, 13.215, .275

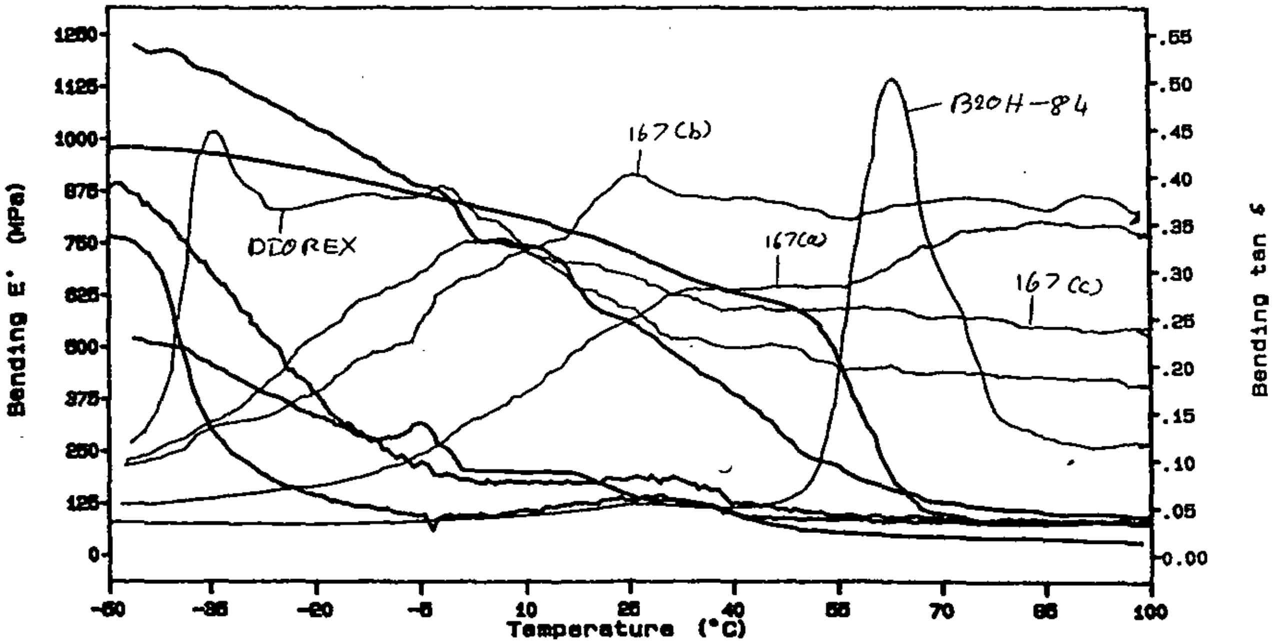

Blends of B20H-84 with Diorex in air

VERSION: V5.20

Figure 4.48

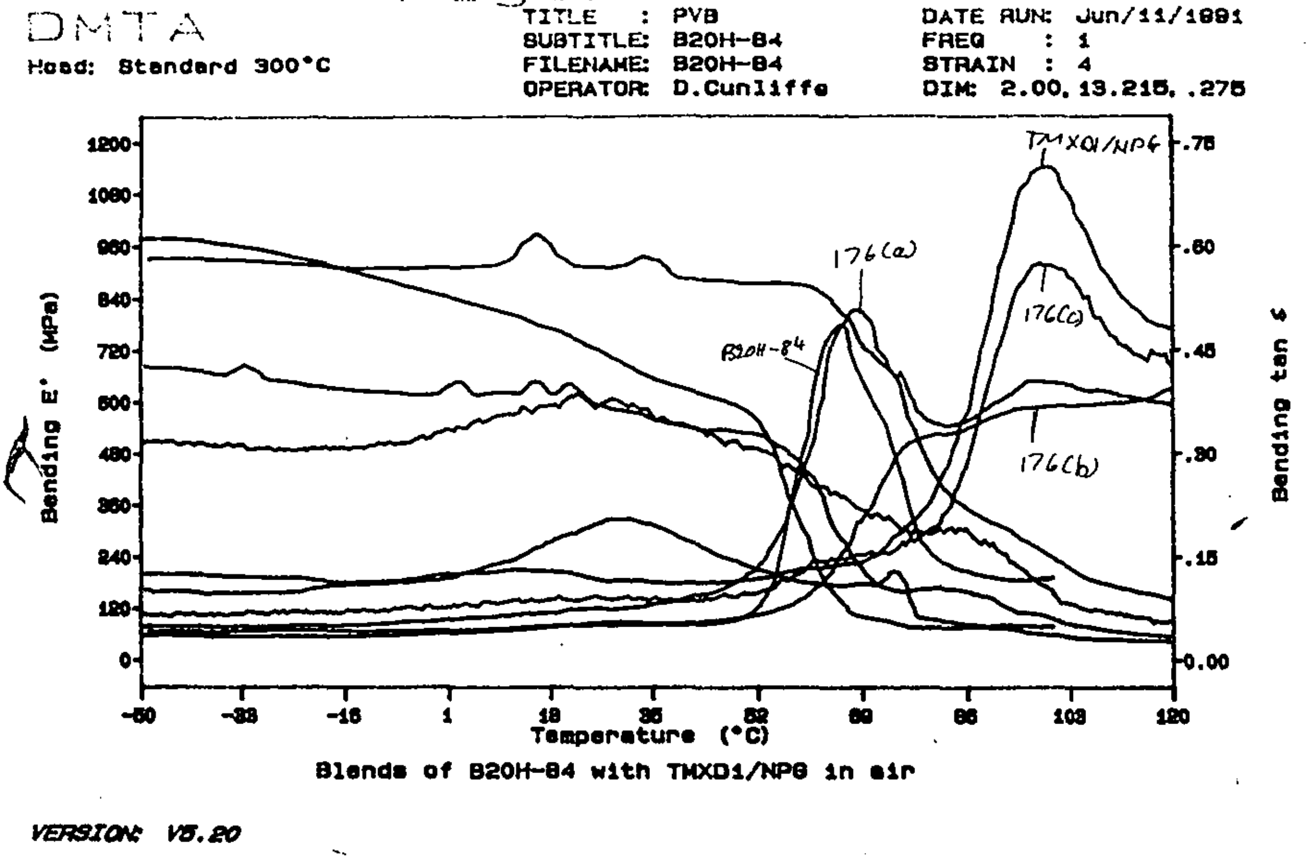

DMTA

Head: Standard 300°C

TITLE : PVB
SUBTITLE: B20H-84
FILENAME: B20H-84
OPERATOR: D.Cunliffe

DATE RUN: Jun/11/1991
FREQ : 1
STRAIN : 4
DIM: 2.00, 13.215, .275

Blends of B20H-84 with TMXD1/NPG in air

VERSION: V5.20

The results of blending with diorex are given in table 4.21. Blends of B20H-84 with a PVB/diorex ratio of 2:1 a single broad glass transition which is about 10 °C higher than that predicted by the Fox equation and correlates with that predicted by the rule of mixtures. With a PVB/diorex ratio of 1:1 two broad Tg values are observed. The low temperature transition corresponds to that of diorex, the high temperature transition is 20°C lower than that of PVB. With a PVB/diorex ratio of 1:2 a single broad transition is observed, as illustrated in figure 4.47. This indicates partial miscibility of the polymers with microphaseheterogeneity.

The results of blending with TMXDI/NPG are given in table 4.22. Blends of B20H-84 with a PVB/TMXDI/NPG ratio of 2:1 two broad Tg values are observed correlating with those of the unmixed polymers. With a PVB/TMXDI/NPG ratio of 1:1 two broad transition are observed one in between those of the unmixed polymer and one corresponding to unmixed TMXDI/NPG. This indicates partial miscibility with some microphaseheterogeneity. With a PVB/TMXDI/NPG ratio 1:2,a single Tg is observed which is 5°C above that unmixed polyurethane, here as with some of the the blends of benzoated samples of PVB crosslinking may have occurred by reaction between free hydroxyl groups of PVB and isocyanate groups of the polyurethane. This is illustrated in figure 4.48.

The solubility characteristics of trifluroacetylated samples of B20H were investigated in a number of solvents. The results are given in table 4.23. As can be seen trifluoroacetylation increases the solubility of PVB in aromatic hydrocarbon possibly due to charge transfer interactions between trifluoroacetate groups and the aromatic nucleus.

Table 4.23

Solubility Characteristics of Trifluoroacetylated samples of B20H

Polymer	Methanol	Acetone	Ethyl Acetate	Ethyl Acetate/ Methanol 1:1	THF	Benzene	Toluene	Hexane	Cyclohexane	Chloroform
B20H	✔	✔	✔	✔	✔	swell	swell	X	X	✔
B20H-94	✔	✔	✔	✔	✔	✔	✔	X	X	✔
B20H-95	✔	✔	✔	✔	✔	✔	✔	X	X	✔
B20H-99	✔	✔	✔	✔	✔	✔	✔	X	X	✔
B20H-106	✔	✔	✔	✔	✔	✔	✔	X	X	✔
B20H-109	✔	✔	✔	✔	✔	✔	✔	X	X	✔

Poly (vinyl butyral) is known to form inter- and intra-molecular hydrogen bonds, which lead to aggregate formation in many solvents[94-101]. At low concentrations the polymer coils do not interpenetrate to any great extent hence intramolecular hydrogen bonding causes the polymer coils to contract which lowers the solution viscosity. As the concentration is increased the polymer coils increasingly interpenetrate[166] and intermolecular hydrogen bonding predominates leading to aggregation, increasing the volume of the coils and the viscosity increases. Modification of PVB by esterification producing non-polar pendent groups, which reduces the number of proton donating species to take part in hydrogen bonding. At low concentrations, the coils are more expanded and the solution viscosity is higher than the unmodified PVB. As the concentration is increased the polymer coils interpenetrate but aggregates are not formed and hence the solution viscosities are lower than those of unmodified PVB. This is illustrated in figure 4.49. Therefore, modification of PVB removing species capable of proton donation reduces aggregate formation in THF, but this can only be prevented by complete modification.

The thermodynamic driving force for promoting the miscibility of PVB with the polymers studied is by hydrogen bonding with the functionality of the other polymers, the hydroxyl groups of PVB acting on the proton donors. This behaviour has been reported by several authors. Painter[167] et al have studied hydrogen bond formaton in blends of poluyrethanes. It has been found that copolymerisation of para-hydroxystyrenes with styrene improves the miscibility of polystyrene with poly(methyl methacrylate), poly (butylacrylate) and poly (vinyl ketones)[168-174]. Complexation behaviour has also been observed between poly(styrene-co-hydroxystyrene) and poly (vinyl pyrrolidone). The glass transitions of the complexes prepared by precipitation are found to vary with the solvent used as precipitant and are higher than those obtained by solution casting[175].

The domain sizes of the complexes have been estmated to be of the order of 2.5nm[176]. Intermacromolecular complexes have been extensively reviewed by Tsuchida and Abe[177].

Figure 4.49

Variation of relative viscosity with concentration for *PVB* in *THF*

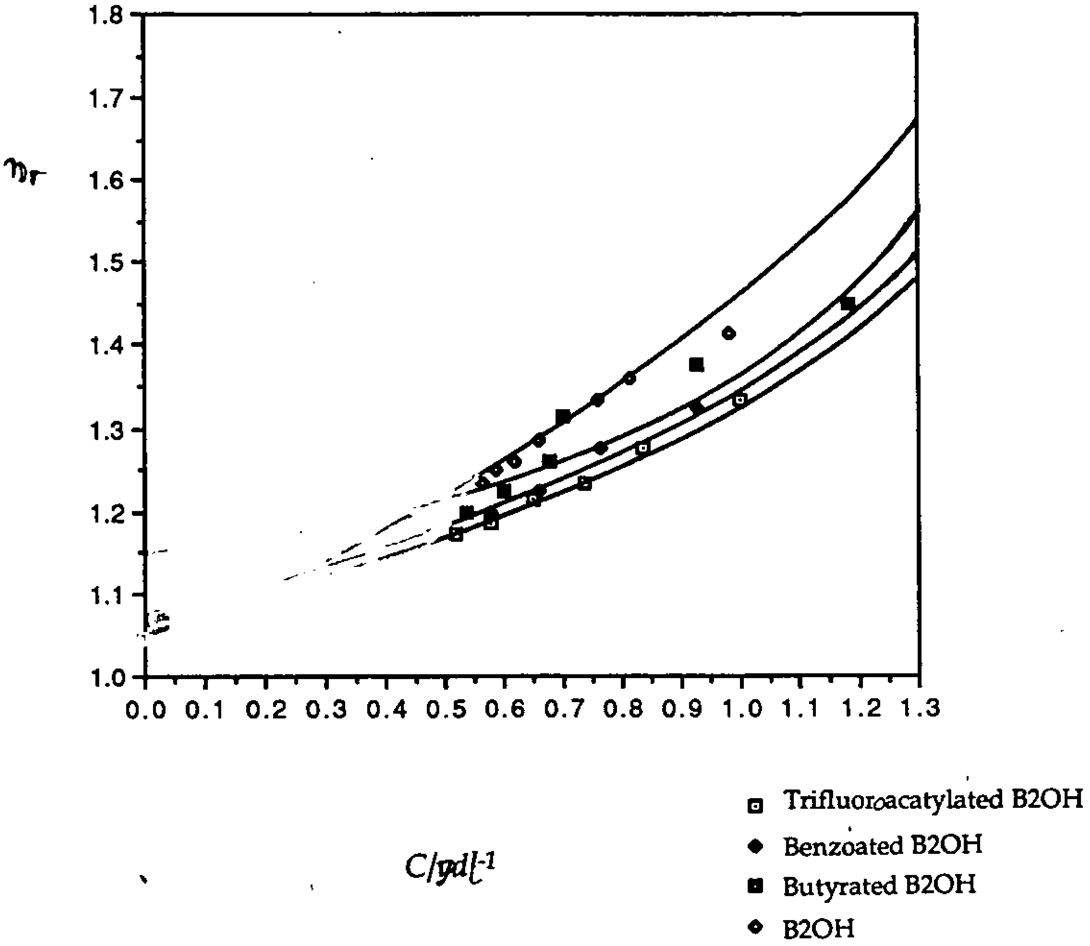

4.5 Phthalated PVB

A number of phthalated samples of B20H were prepared. Their intrinsic viscosities were determined in THF and methanol and the results given in tables 4.24 and 4.25. Samples B20H-130 and B20H-174 exhibit polyelectrolyte behaviour in methanol shown by the upward curvature of Huggins plots as shown in figure 4.50, but give linear Fuoss and Strauss plots (equation 2.15). The ratio of phthalate groups to butyral groups was determined by NMR spectroscopy; a spectrum is given in figure 4.51. The molecular masses, acid content, transition data and ratio of phthalate groups to butyral groups are given in table 4.26. The variation of intrinsic viscosity of phthalated B20H with acid content and molar ratio of phthalate groups to butyral groups are given in figures 4.52 and 4.53. These show a small decrease in intrinsic viscosity in THF with increasing degree of modification. The variation of k_{SB} with acid content and ratio of phthalate groups to butyral groups in THF are given in figures 4.54 and 4.55.

Figure 4.50

Huggins plots for *B2OH - 130* and *B2OH -174* is methanol

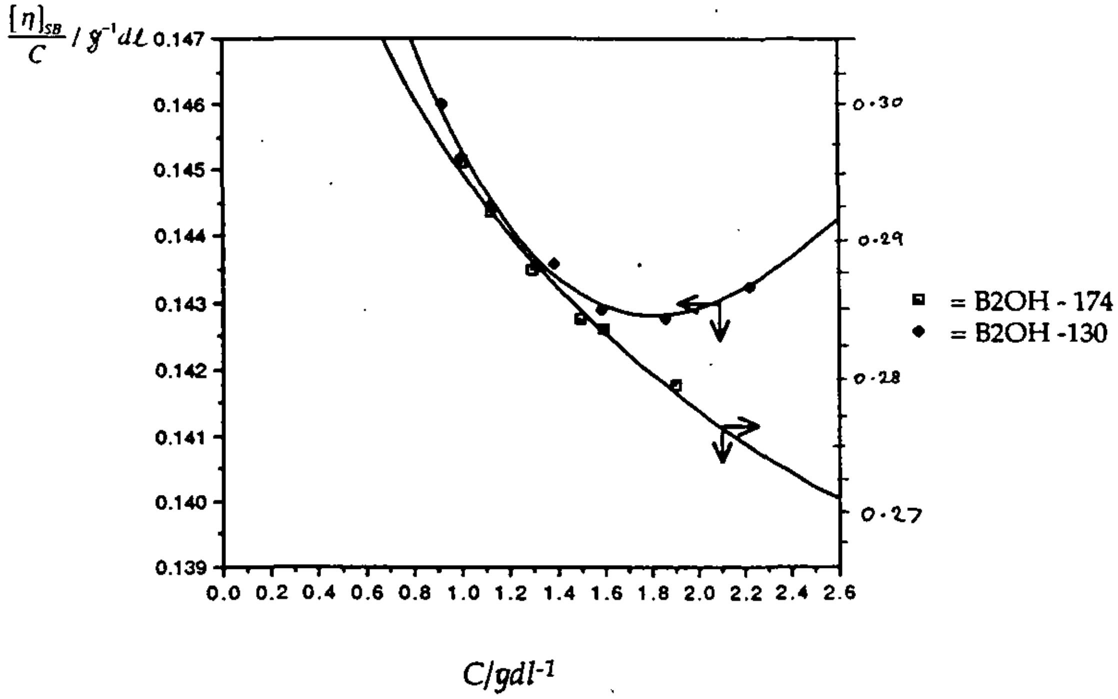

Figure 4.51

Figure 4.51
N.M.R. Spectrum of Phthalated B2OH

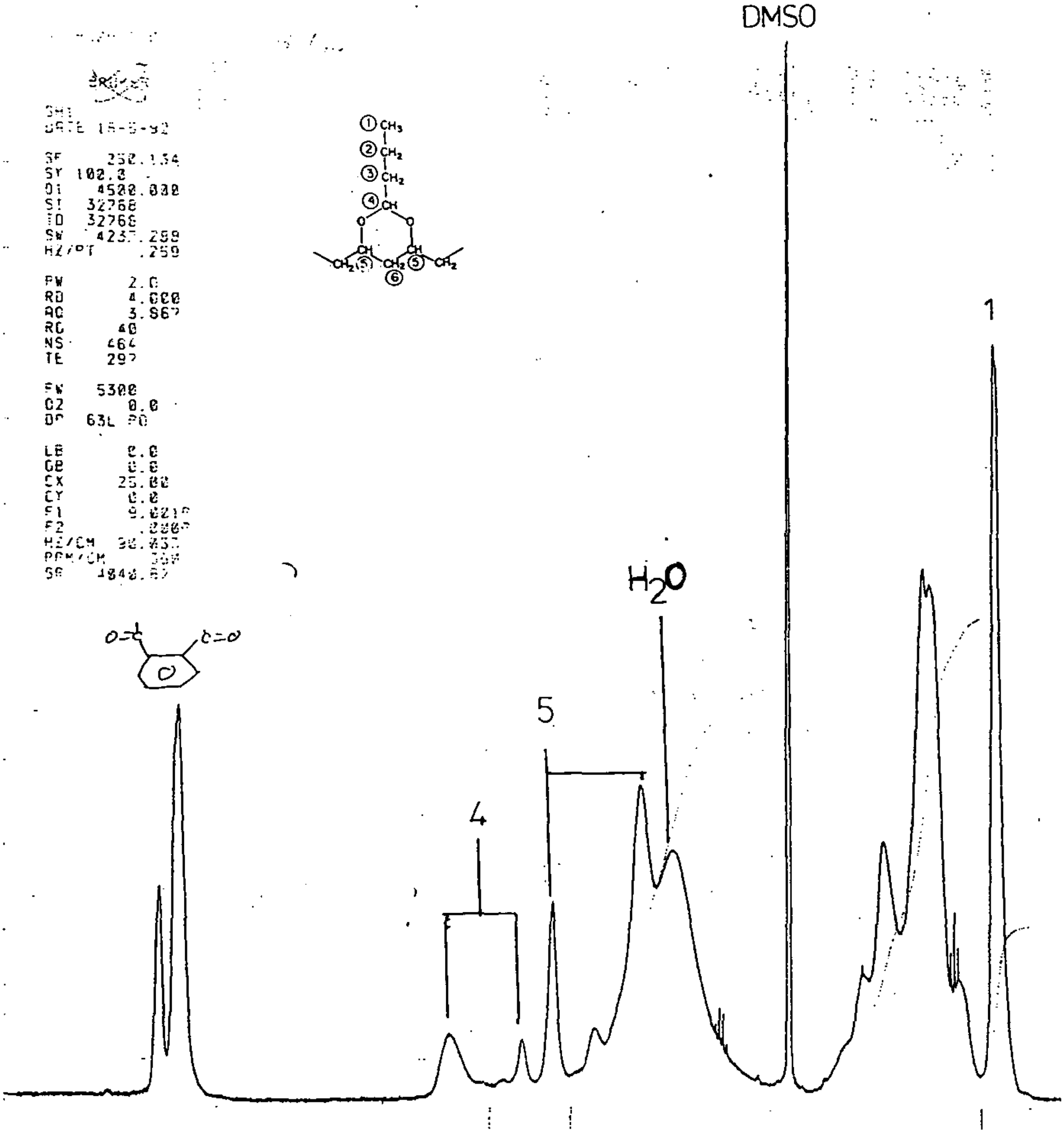
```
BRUKER
SH1
DATE 15-5-92

SF      250.134
SY 100.0
O1     4500.000
SI   32768
TD   32768
SW    4237.288
HZ/PT      .259

PW         2.0
RD         4.000
AQ         3.867
RG      40
NS     464
TE     297

FW    5300
O2         0.0
DP    63L PO

LB         0.0
GB         0.0
CX        25.00
CY         0.0
F1         9.021P
F2          .280P
HZ/CM    98.837
PPM/CM      .395
SR    1848.67
```

Table 4.24

Intrinsic Viscosity Data of Phthalated Samples of B20H in THF

polymer	$[\eta]_H$ / $g^{-1}dl$	$[\eta]_k$ / $g^{-1}dl$	$[\eta]_{SB}$ / $g^{-1}dl$	$[\eta]_M$ / $g^{-1}dl$	k_H	k_k	k_{SB}	k_M
B20H	0.3382	0.3464	0.3436	0.3411	0.474	0.0816	0.359	0.410
B20H-110	0.2059	0.2115	0.2110	0.2098	1.26	-0.42	0.885	1.00
B20H-124	0.2344	0.2365	0.2371	0.2376	0.71	-0.091	0.557	0.578
B20H-130	0.1045	0.1076	0.1086	0.1059	1.93	-0.93	1.25	1.62
B20H-174	-	-	-	-	-	-	-	-

Table 4.25

Intrinsic Viscosity Data of Phthalated Samples of B20H in Methanol

polymer	$[\eta]_H / g^{-1}dl$	$[\eta]_k / g^{-1}dl$	$[\eta]_{SB} / g^{-1}dl$	$[\eta]_M / g^{-1}dl$	k_H	k_k	k_{SB}	k_M
B20H	0.1828	0.2025	0.2107	0.1995	2.63	-0.883	1.03	1.51
B20H-110	0.2013	0.2008	0.2015	0.2014	0.205	0.261	0.20	0.21
B20H-124	-	-	-	-	-	-	-	-

Polymer	$[\eta]_{FS} / g^{-1dl}$	$\gamma_{FS} / g^{-\frac{1}{2}} dl^{\frac{1}{2}}$
B20H-130	0.1506	0.26
B20H-174	0.3511	0.54

Table 4.26

Molecular Mass, Acid Content and Transition Data for Phthalated Samples of B20H

Polymer	$\bar{M}n$	$\bar{M}w$	Mp	M*wd*	[CO$_2$H]/mmol g^{-1}	T*g*/°C	Phthalate/Butyral
B20H	9000	23000	14000	2.56	0.0	71	0
B20H-110	5000	17000	9000	3.55	39.76	113	0.642
B20H-124	5000	1000	7000	1.96	32.88	107	0.730
B20H-130	5000	12000	8000	2.25	26.6	66.8	0.734
B20H-174	2000	9000	17000	3.58	15.54	111.0	-

B20H-174 by SEC in DMF relative to PEO/PEG standards[178]

Figure 4.52

$[\eta]_{SB}$ against $[CO_2H]$ for phthalated *B2OH* in *THF*

[illegible] 10^{-2} [illegible] $r = -0.65$

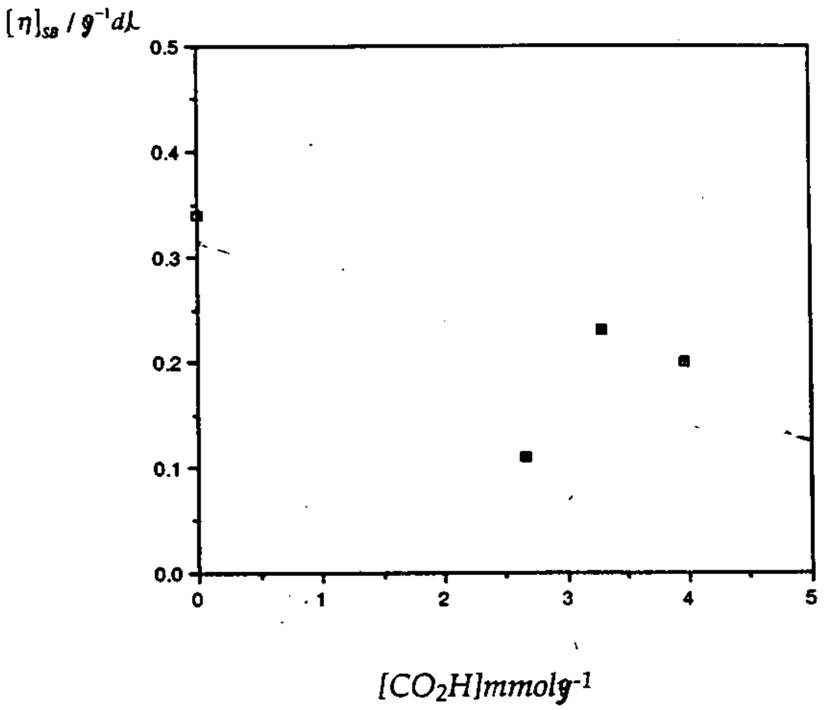

Figure 4.53

$[\eta]_{SB}$ against ratio of Phthalate groups to Butyral groups for Phthalated *B2OH* in *THF*

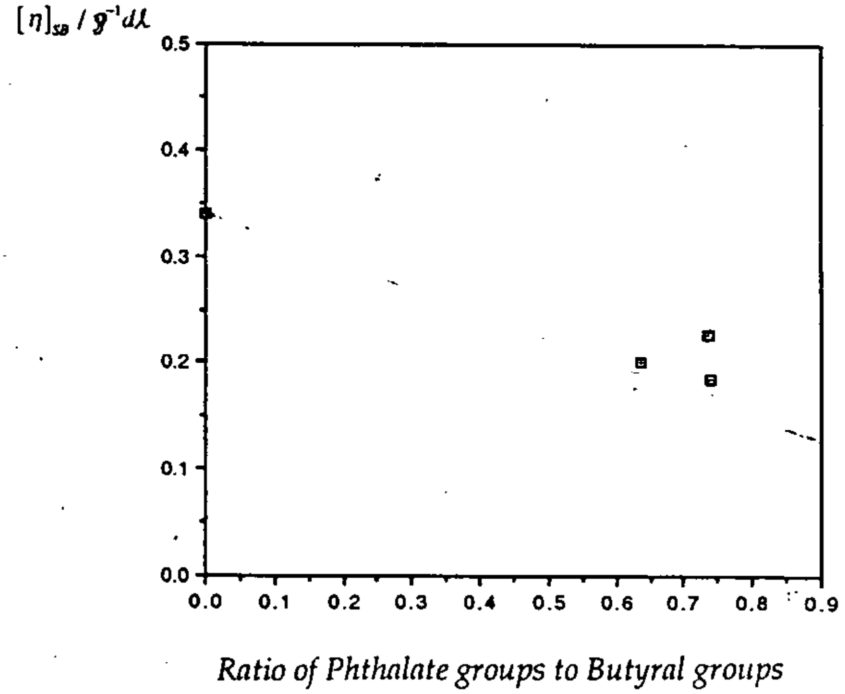

Figure 4.54

k_{SB} against $[CO_2H]$ for Phthalated *B2OH* in *THF*

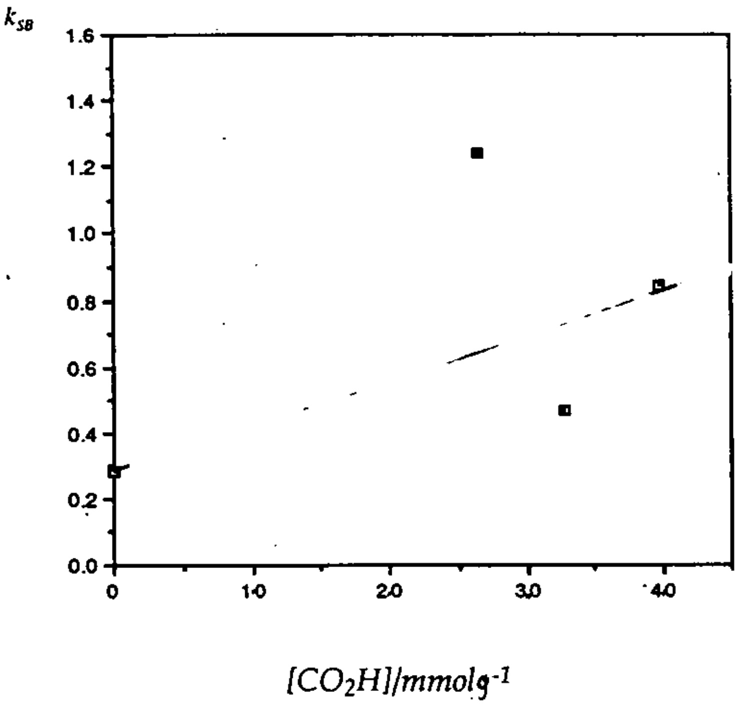

Figure 4.55

k_{SB} against ratio of Phthalate groups to Butyral groups for

Phthalated *B2OH* in *THF*

[illegible] = 0.70 [illegible] = 0.69

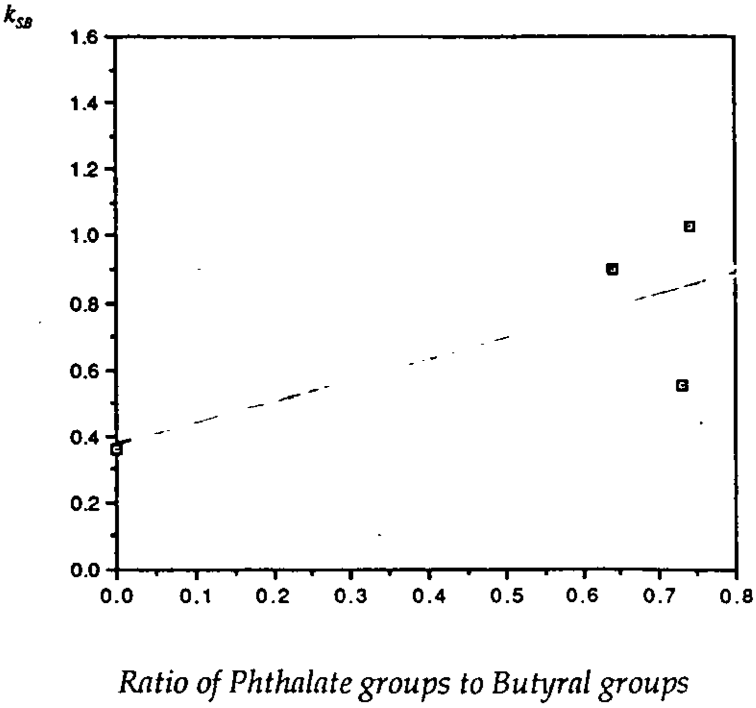

The phthalate groups increase the extent of inter- and intramolecular hydrogen bonding in THF. Hence, at low concentrations the polymer chains are more tightly coiled which decreases the solution viscosity as illustrated in figure 4.56. At higher concentrations the greater extent of intermolecular hydrogen bonding causes the slope constant to increase. The greater polarity of methanol is able to disrupt aggregate formation by forming hydrogen bonds with the polymer in solution. Hence B20H-110 has a k_{SB} value of 0.2 (table 4.25) in methanol whereas B20H has a k_{SB} value of 1.03 ((table 4.25) in methanol. In dilute solution in methanol the polymer chains are less tightly coiled so the solution viscosity is not decreased to the extent as in THF, this is illustrated in figure 4.57.

Blends of phthalated samples of B20H with diorex, TMXDI/NPG, PEI and PVP wre prepared by solution casting and examined by DMTA. The results of blending with diorex are given in table 4.27. For blends of B20H-124 with PVB/diorex ratios of 2:1, 1:1 and 1:2, two broad Tg peaks are observed. As the diorex content is increased the low temperature transition shifts from -26.7 to -30.6^{0}C while the high temperature transition shifts from 40.8^{0}C to 12.3^{0}C and the tan δ peak broadens as the diorex content is increased as illustrated in figure 4.58. This indicates the presence of two phases, one which is rich in diorex and the other a mixture of PVB with diorex with some microphasheterogeneity present. For blends of B20H-130 with PVB/diorex ratios of 2:1, 1:1 and 1:2, two glass transitions are observed. The low temperature transition corresponds to that of diorex, while the high temperature transition shifts from 39.5^{o}C to 29.6^{o}C as the diorex content is increased with a broadening of the tan δ peak. This indicates the presence of two phases, one unmixed diorex the other a mixture of PVB with diorex with some microphaseheterogeneity as illustrated is figure 4.59. For blends of B20H-174 with PVB/diorex ratios of 2:1, 1:1 and 1:2 two glass transitions are observed. The low temperature transition corresponds to that of unmixed diorex. The high temperature transition shifts from 77.8^{O}C to 71.2^{O}C and the tan δ peak broadens as the diorex content is increased; this is illustrated in figure 4.60. This indicates the presence of two phases, one consists of unmixed diorex while the other is a mixture of PVB with diorex with some microphaseheterogeneity.

Figure 4.56
Variation of relative viscosity with concentration
for phthalated B20H in THF

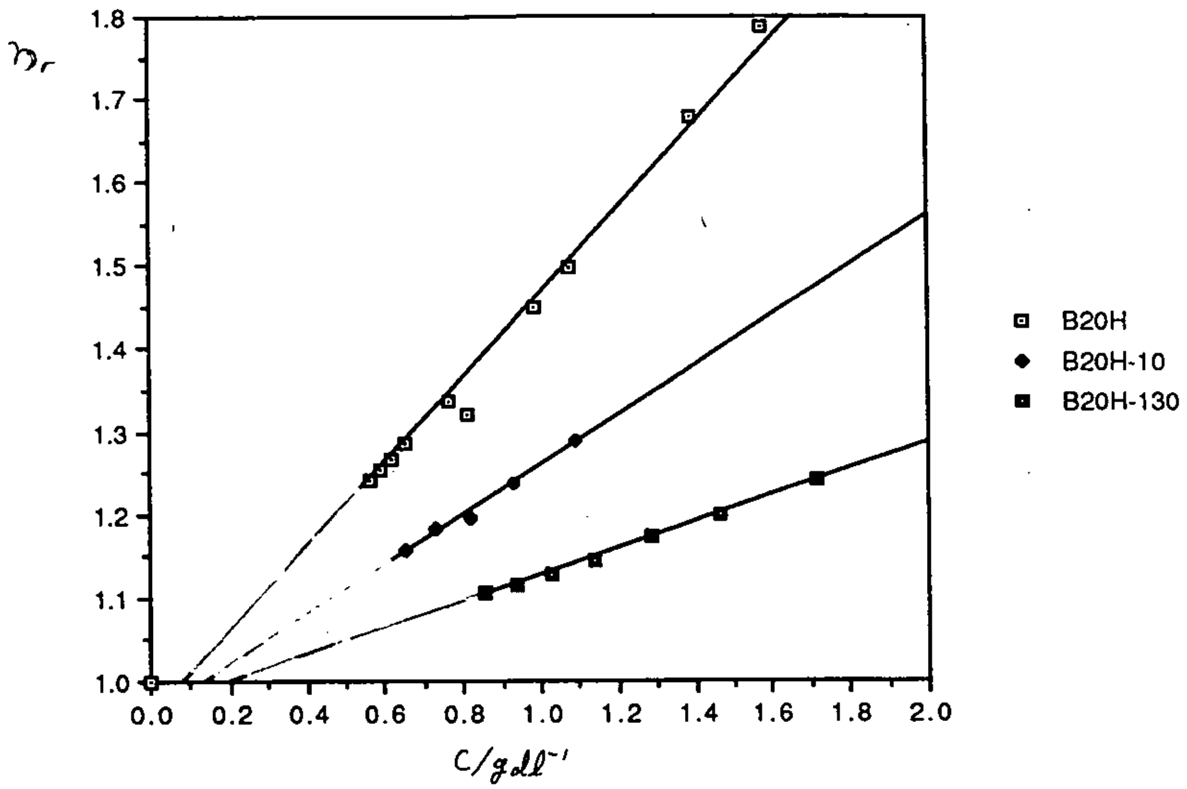

Figure 4.57
Variation of relative viscosity against concentration
for phthalated B20H in Methanol

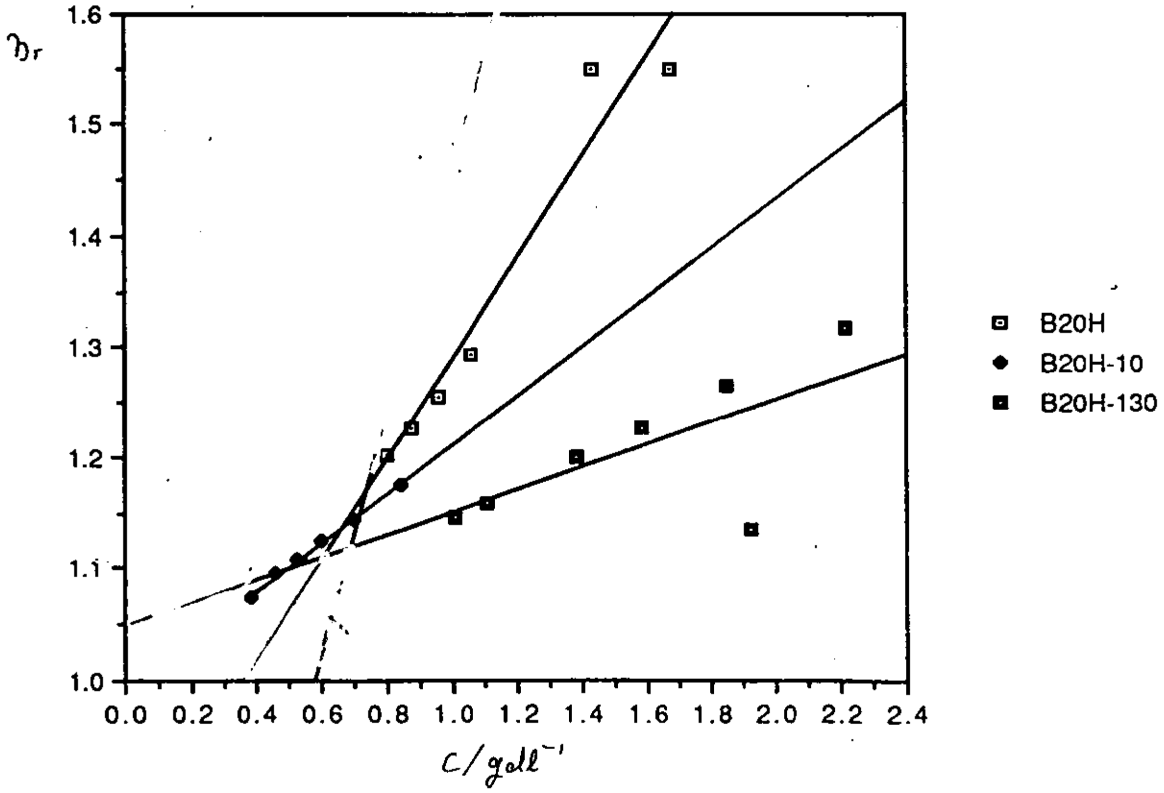

Table 4.27

Blends of Phthalated B20H with Diorex

B2OH-124

Blend	wt fraction PVB	wt fraction Diorex	Film Appearance	DMTA Tg/° C	Fox Eqn Tg/° C	Rule of Mixtures Tg/° C
	1	0		107		
181(a)	2/3	1/3	clear	-26.7,40.8	44.0	59.7
181(b)	1/2	1/2	clear	-27.8,28.5	19.7	36
181(c)	1/3	2/3	clear	-30.6,12.3	-1.13	12.3
	0	1		-35		

B20H-130

Blend	wt fraction PVB	wt fraction Diorex	Film Appearance	DMTA Tg/° C	Fox Eqn Tg/° C	Rule of Mixtures Tg/° C
	1	0		66.8		
187(a)	2/3	1/3	opaque	-30.5,39.5	24.2	32.67
187(b)	1/2	1/2	opaque	-31.9,34.5	6.8	15.75
187(c)	1/3	2/3	opaque	-31.7,29.6	-8.7	-1.2
	0	1		-35		

B20H-174

Blend	wt fraction PVB	wt fraction Diorex	Film Appearance	DMTA Tg/° C	Fox Eqn Tg/° C	Rule of Mixtures Tg/° C
	1	0		111		
178(a)	2/3	1/3	opaque	-35.7,77.8	45.8	62.3
178(b)	1/2	1/2	opaque	-31.0,77.1	20.9	38
178(c)	1/3	2/3	opaque	-32.9, 71.2	-0.5	13.7
	0	1		-35		

Figure 4.58

DMTA
Head: Standard 300°C

TITLE : 181 (a)
SUBTITLE: B20H-124/Diorex
FILENAME: Pressed Film
OPERATOR: D.Cunliffe

DATE RUN: May/12/1992
FREQ : 1
STRAIN : 1
DIM: 1.00, 16.880, .407

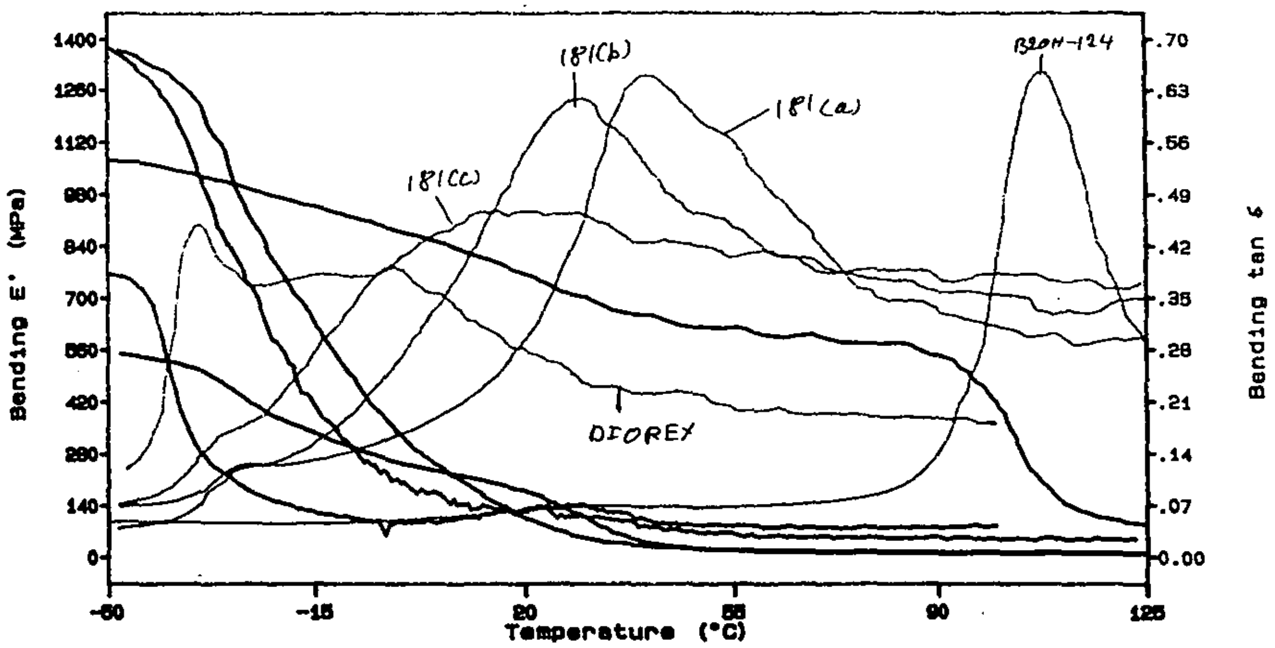

Blends of B20H-124 with Diorex in air

VERSION: V5.20

Figure 4.59

DMTA
Head: Standard 300°C

TITLE : 187 (a)
SUBTITLE: B20H-130/Diorex
FILENAME: Pressed Film
OPERATOR: D.Cunliffe

DATE RUN: Jun/01/1992
FREQ : 1
STRAIN : 1
DIM: 1.00, 11.365, .345

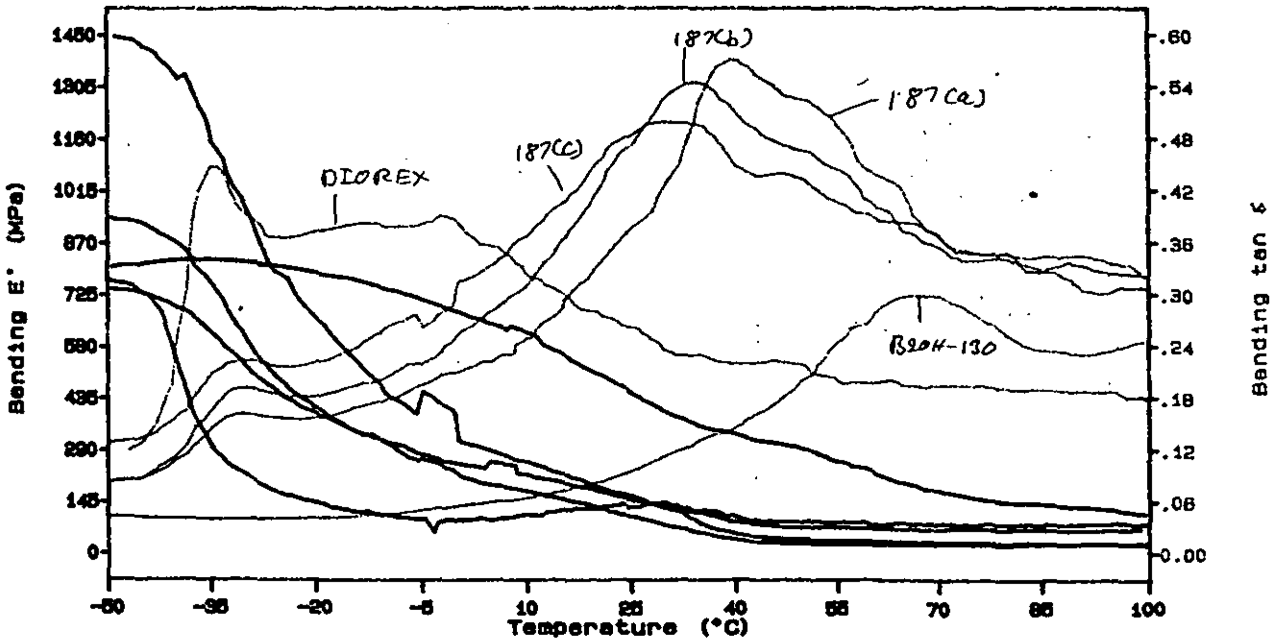

Blends of B20H-130 with Diorex in air

VERSION: V5.20

Figure 4.60

DMTA
Head: Standard 300°C

TITLE : Diorex
SUBTITLE: Pressed Film
FILENAME: Cotton
OPERATOR: D.Cunliffe

DATE RUN: Feb/25/1992
FREQ : 1
STRAIN : -1
DIM: 1.00, 12.967, .214

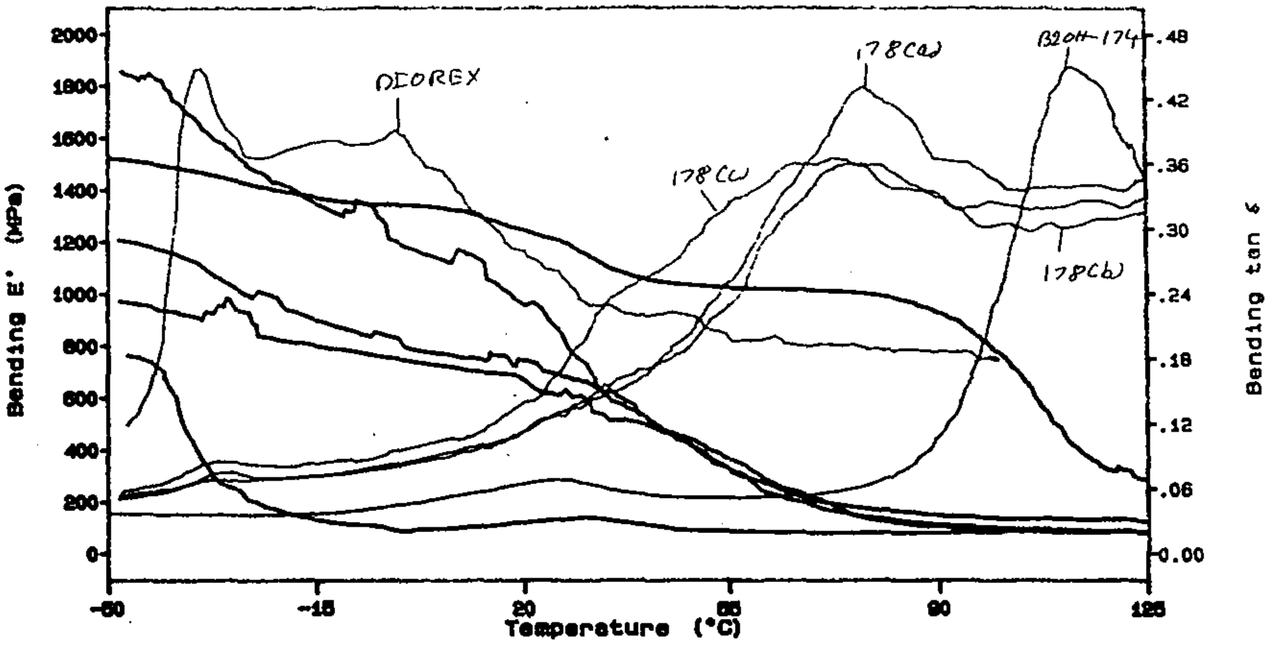

Blends of 820H-174 with Diorex in air

VERSION: V5.20

The phthalate groups in the modified PVB have improved the miscibility of B20H with diorex by hydrogen bonding. The carbonyl groups of the polyester acts as the proton accepting species and the phthalate groups as the proton donor. This sort of behaviour has been observed by Coleman[179] who observed hydrogen bonding between polymers containing methacrylic acid and ether groups. The ability of the phthalate groups to hydrogen bond with the carbonyl of the polyester will depend upon the nature of the solvent used to prepare the blends or the presence of other polymers. This has been reported by Tsuchida[180]

The results of blending with TMXDI/NPG are given in table 4.28: Blends of B20H-124 with PVB/TMXDI/NPG ratios of 2:1, 1:1 and 1:2 single glass transitions are observed which correlate with those predicted by the Fox equation and rule of mixtures; the breadth of the tan δ peaks at the glass transition for the homopolymers and blends is about 75°C. As illustrated in figure 4.61. Although a single Tg is observed the blend films are opaque in appearance and there is the possibility of crosslinking with free isocynate groups and unreacted hydroxyl groups on the PVB. Miscibility may be improved by hydrogen bonding between the acid groups and the urethane units of TMXDI/NPG. The variation of glass transition with blend composition is given in figure 4.63, illustrating little difference between observed and predicted values. Blends of B20H-174 with PVB/TMDI/NPG ratios of 2:1, 1:1 and 1:2 give single Tg values which are about 5-6 °C below the values predicted by the Fox equation or rule of mixtures with the tan δ peaks for the blends and homopolymers having a width of 39°C at the glass transition, as illustrated in figure 4.62. Again, although a single glass transition is observed in the blends, the films are opaque indicating the possibility of crosslinking. The variation of glass transition with blend composition is given in figure 4.64, showing negative deviation from predicted values.

The results of blending with PVP are given in table 4.29. Blends of B20H-110 with PVP in air show two broad glass transitions at all compositions showing that atmospheric moisture greatly influences the miscibility of these polymers. This is illustrated in figure 4.65. Under an atmosphere of dry nitrogen, single narrow glass transitions are observed at 10-20°C above those predicted by the Fox equation and rule of

Table 4.28

Blends of Phthalated B20H with TMXDI/NPG

B20H-124

Blend	wt fraction PVB	wt fraction TMXDI/ NPG	Film Appearance	DMTA Tg/°C	Fox Eqn Tg/°C	Rule of Mixtures Tg/°C
	1	0		107		
185(a)	2/3	1/3	opaque	103	104.1	104.2
185(b)	1/2	1/2	opaque	101	102.7	102.8
185(c)	1/3	2/3	opaque	101	101.3	101.3
	0	1		98.5		

B20H-174

Blend	wt fraction PVB	wt fraction TMXDI/ NPG	Film Appearance	DMTA Tg/°C	Fox Eqn Tg/°C	Rule of Mixtures Tg/°C
	1	0		111		
179(a)	2/3	1/3	opaque	101	106.7	106.8
179(b)	1/2	1/2	opaque	98.2	104.6	104.8
179(c)	1/3	2/3	opaque	99	102.6	102.7
	0	1		98.8		

Figure 4.61

DMTA
Head: Standard 300°C

TITLE : 185 (a)
SUBTITLE: B20H-124/TMXD1
FILENAME: Pressed Film
OPERATOR: D.Cunliffe

DATE RUN: May/26/1992
FREQ : 1
STRAIN : 1
DIM: 1.00, 12.910, .410

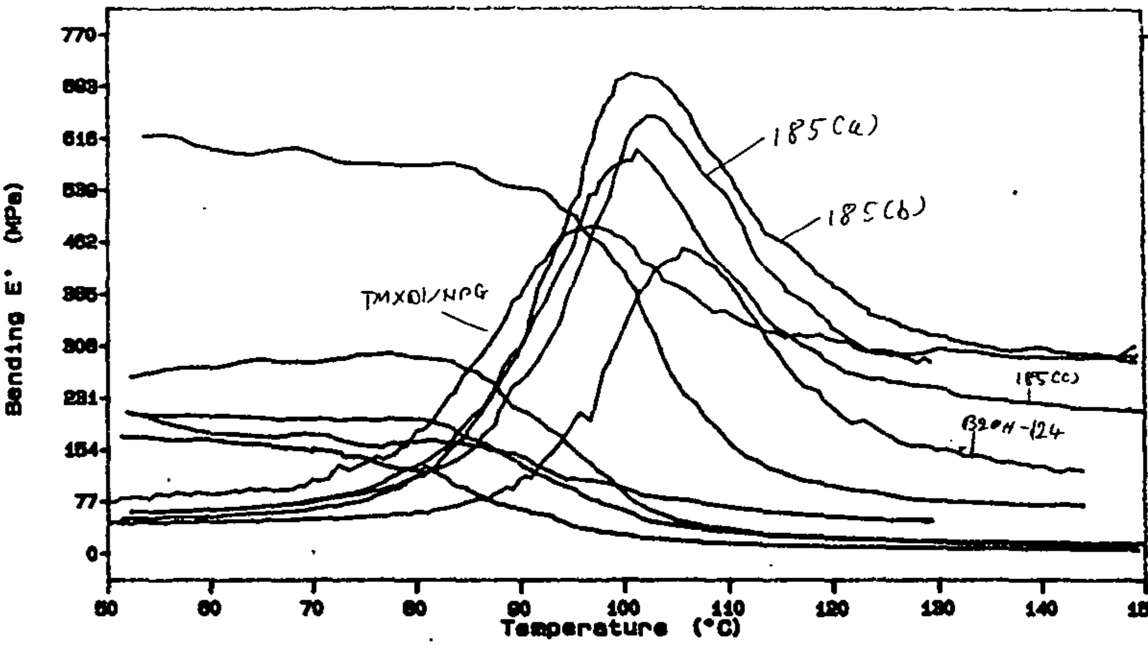

Blends of B20H-124 with TMXD1/NPG in air

VERSION: V5.20

Figure 4.62

DMTA
Head: Standard 300°C

TITLE : TMXD1/NPG
SUBTITLE:
FILENAME: Pressed Film
OPERATOR: D.Cunliffe

DATE RUN: Mar/17/1992
FREQ : 1
STRAIN : 0
DIM: 1.00, 9.930, .271

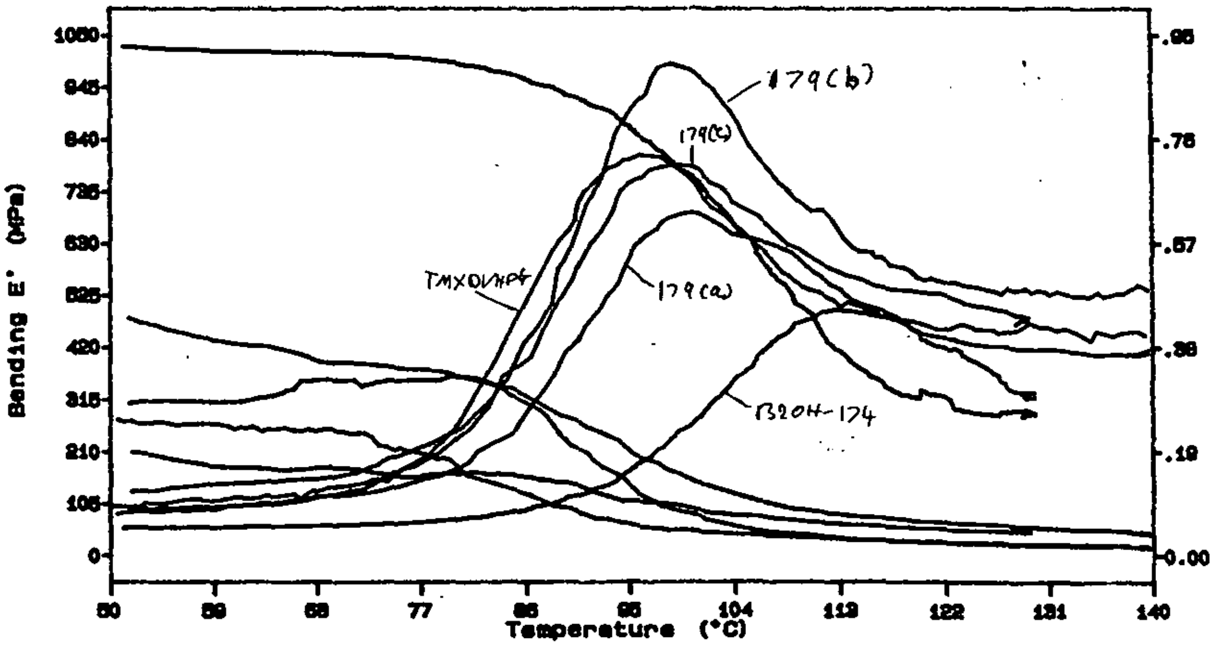

Blends of B20H-174 with TMXD1/NPG in air

VERSION: V5.20

Figure 4.63

Tg versus wt% TMXPl/NPG for blends with B20H-124

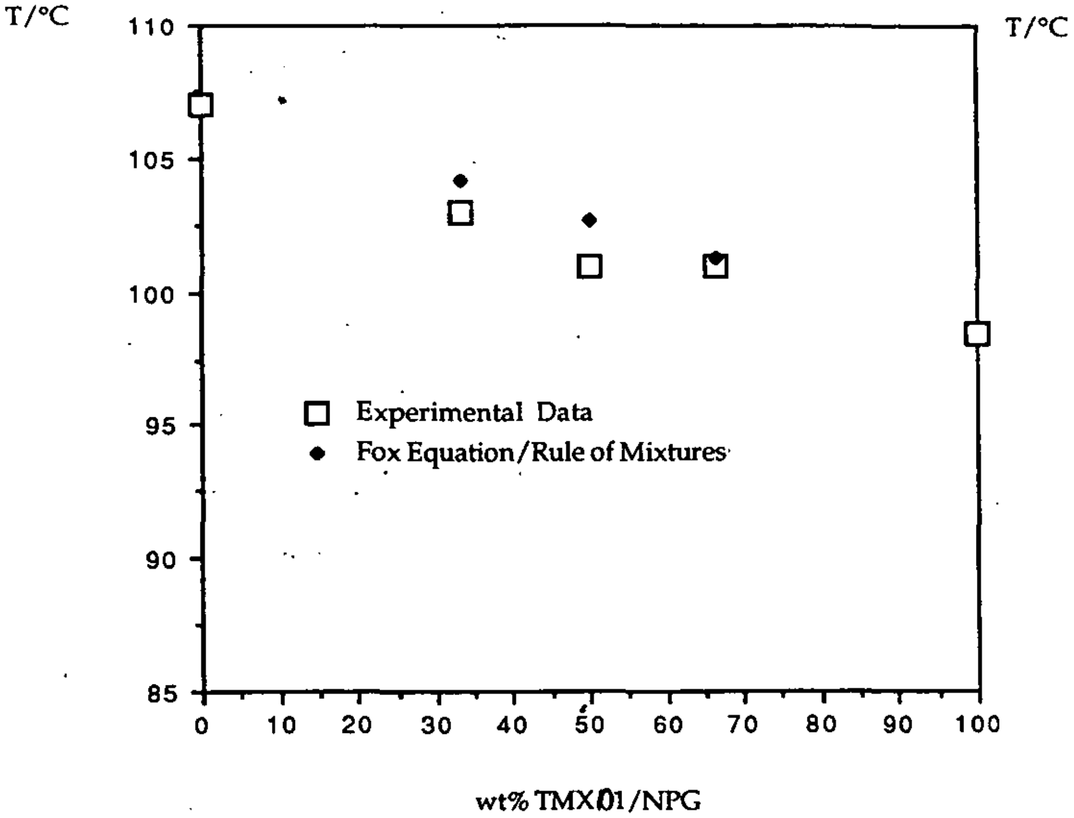

Figure 4.64

Tg verus wt% TMXDL/NPG for blends with B20H-174

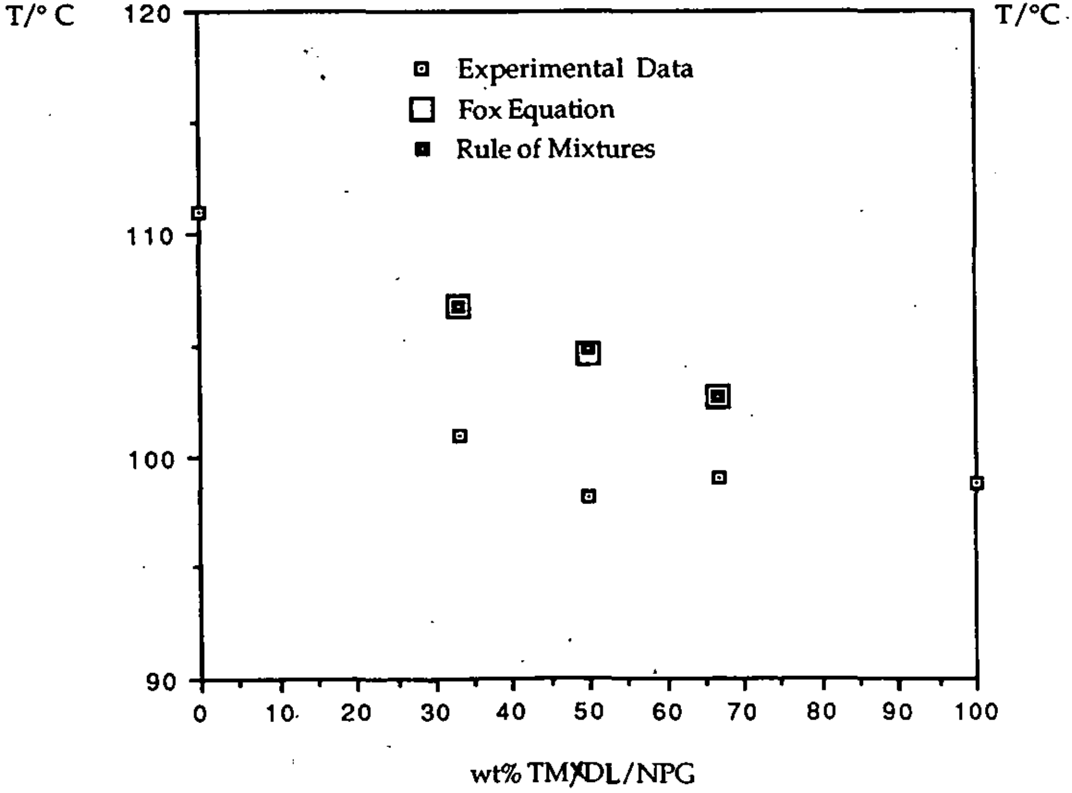

Table 4.29

Blends of Phthalated B20H with PVP

B20H-110 In Air

Blend	wt fraction PVB	wt fraction PVP	Film Appearance	DMTA T_g/°C	Fox Eqn T_g/°C	Rule of Mixtures T_g/°C
	1	0		113		
165(a)	2/3	1/3	clear	132,175	130.6	132.3
165(b)	1/2	1/2	clear	137	140.0	142.0
165(c)	1/3	2/3	clear	154	150.0	151.7
	0	1		171		

B20H-110 Under Dry Nitrogen

Blend	wt fraction PVB	wt fraction PVP	Film Appearance	DMTA T_g/°C	Fox Eqn T_g/°C	Rule of Mixtures T_g/°C
	1	0		113		
165(a)	2/3	1/3	clear	149	130.6	132.30
165(b)	1/2	1/2	clear	161	140.0	142.0
165(c)	1/3	2/3	clear	164	150.0	151.7
	0	1		171		

B20H-130 Under Dry Nitrogen

Blend	wt fraction PVB	wt fraction PVP	Film Appearance	DMTA T_g/°C	Fox Eqn T_g/°C	Rule of Mixtures T_g/°C
	1	0		66.8		
188(a)	2/3	1/3	clear	152	.95	101
188(b)	1/2	1/2	clear	155	111.5	118.5
188(c)	1/3	2/3	clear	153	129.5	135.99
	0	1		171		

Figure 4.65

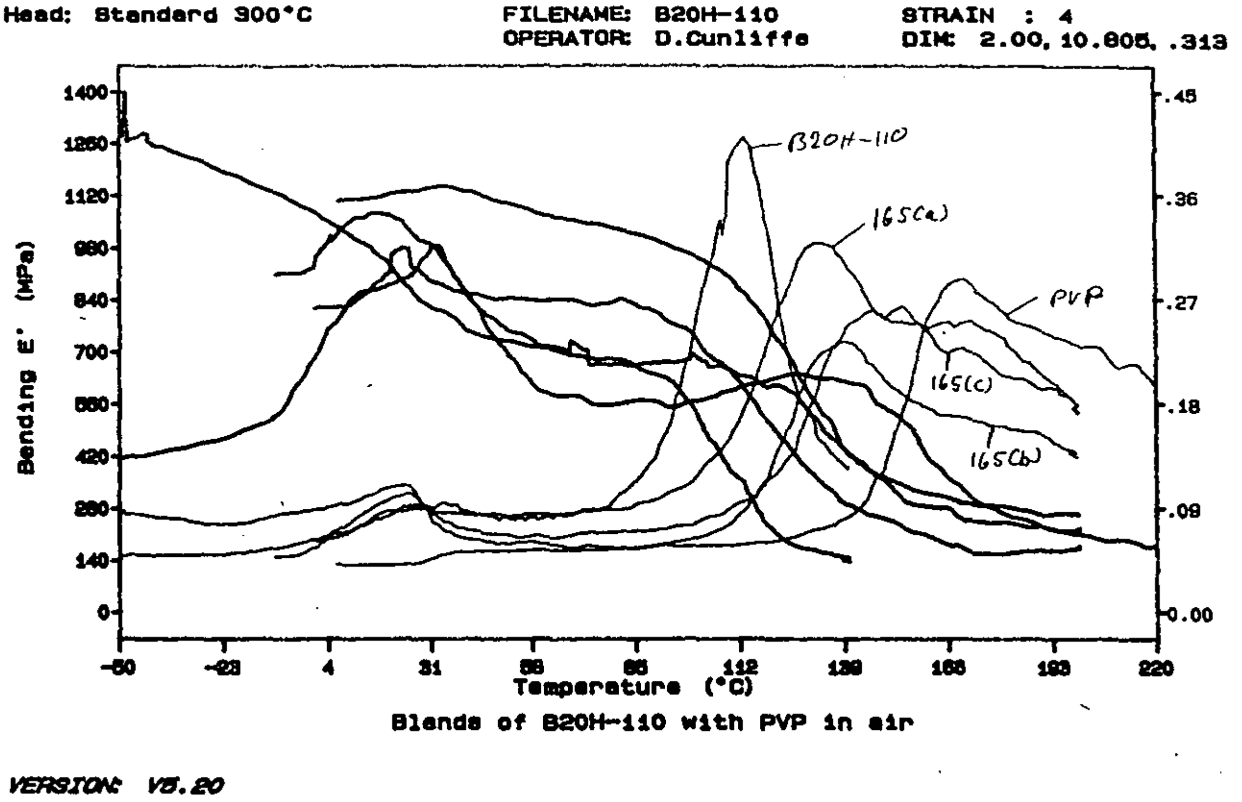

DMTA

Head: Standard 300°C

TITLE : PVB
SUBTITLE: B20H-110
FILENAME: B20H-110
OPERATOR: D.Cunliffe

DATE RUN: Aug/24/1991
FREQ : 1
STRAIN : 4
DIM: 2.00, 10.805, .313

Blends of B20H-110 with PVP in air

VERSION: V5.20

Figure 4.66

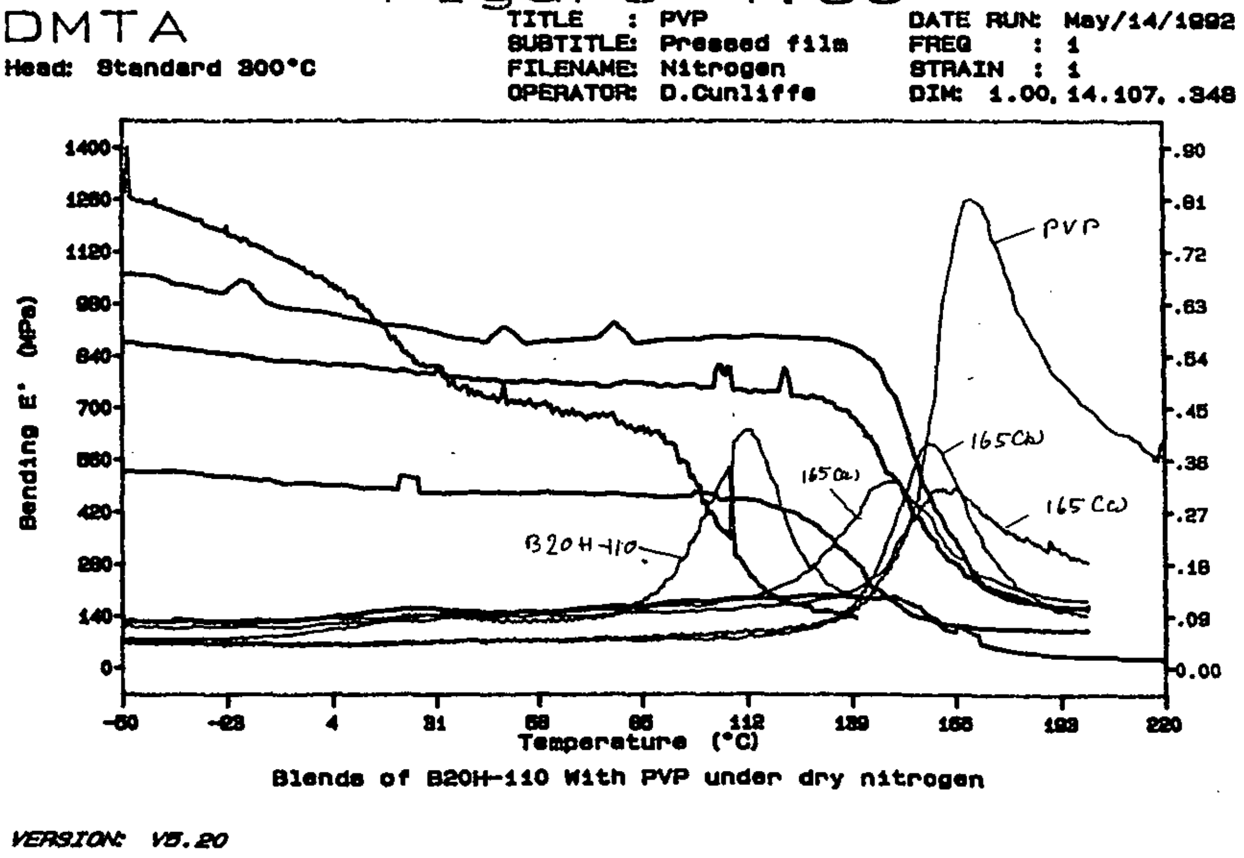

DMTA

Head: Standard 300°C

TITLE : PVP
SUBTITLE: Pressed film
FILENAME: Nitrogen
OPERATOR: D.Cunliffe

DATE RUN: May/14/1992
FREQ : 1
STRAIN : 1
DIM: 1.00, 14.107, .348

Blends of B20H-110 With PVP under dry nitrogen

VERSION: V5.20

Figure 4.68

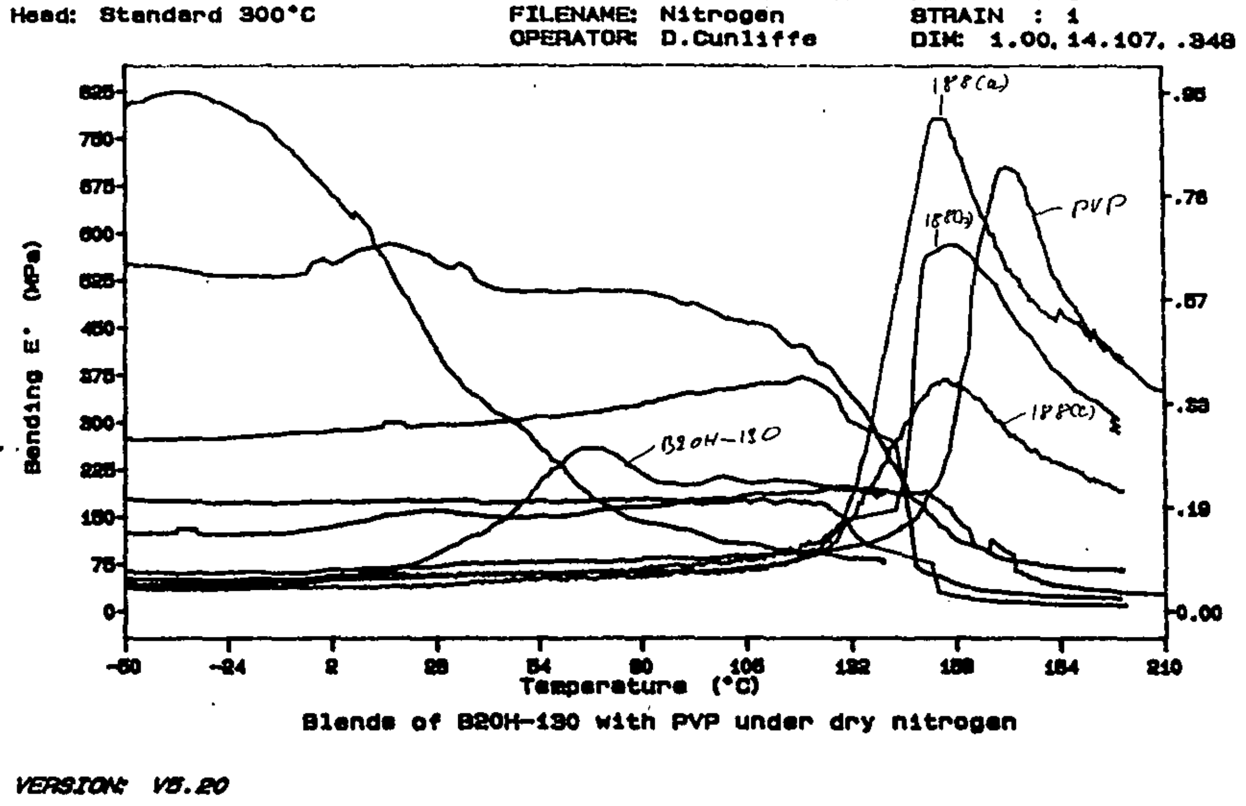
DMTA
Head: Standard 300°C
TITLE : PVP
SUBTITLE: Pressed film
FILENAME: Nitrogen
OPERATOR: D.Cunliffe
DATE RUN: May/14/1992
FREQ : 1
STRAIN : 1
DIM: 1.00, 14.107, .348
Bending E' (MPa)
825
750
675
600
525
450
375
300
225
150
75
0
Bending tan δ
.95
.76
.57
.38
.19
0.00
-50
-24
2
28
54
80
106
132
158
184
210
Temperature (°C)
188(a)
188(b)
188(c)
PVP
B20H-130
Blends of B20H-130 with PVP under dry nitrogen
VERSION: V5.20

Figure 4.67

Tg versus wt% in blends with B20H-110 under dry nitrogen

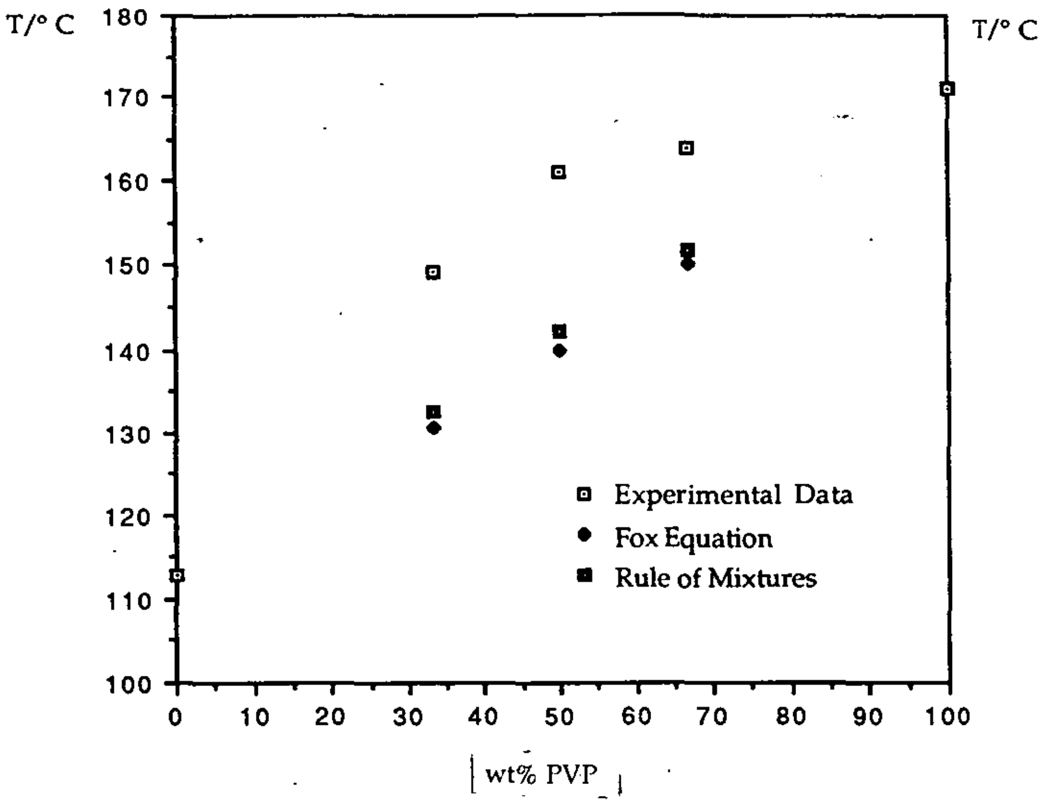

Figure 4.69

Tg versus wt% PVP in blends with B20H-130 under dry nitrogen

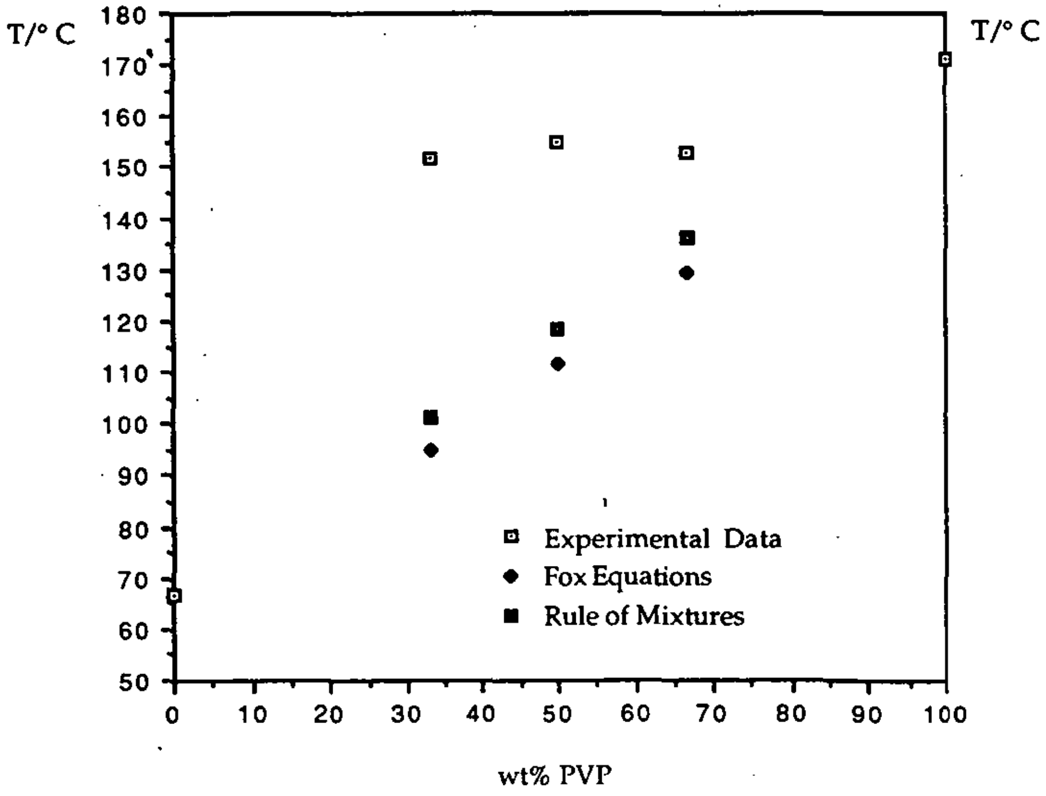

mixtures, as illustrated in figure 4.66. The variation of glass transition with blend composition is given in figure 4.67 which shows the positive deviation of experimental data from predicted values. Blends of B20H-130 with PVB/PVP ratios of 2:1, 1:1 and 1:2 give single narrow transitions under an atmosphere of dry nitrogen as shown in figure 4.68. The glass transitions are 30-60°C above those predicted by the Fox equation or rule of mixtures. The variation of glass transition with blend composition is given in figure 4.69, showing the positive deviation of experimental data from predicted values. This indicates the presence of strong specific interactions between the blend components.

It is well known that PVP is able to form intermacromolecular complexes with polymers containing carboxylic acids[181-186] and that the stability of the complex depends upon the proton accepting ability of the solvent[187,188] Upon mixing the solutions of phthalated PVB with PVP an initial precipitate in formed which dissolves on standing, indicating strong interaction between the polymers giving a complex which later dissociates. It has been reported[189] that the dynamic mechanical properties of these blends is greatly affected by the polarity of the solvent. Initial solid state NMR studies of blends of phthalated PVB with PVP indicates that in sample 188(a) the blend is homogeneous on a scale of 30nm[190] but inhomogeneous at a scale of 5nm which is in approximate agreement with DMTA results. The intimacy of mixing will depend upon the solvent used for preparing the blends.

The results of blending with PEI are given in table 4.30. Mixing solutions of B20H-110, B20H-124 and B20H-130 with a solution of PEI produces a precipitate at all compositions. In each of these cases, the ratio of acid groups to free amine groups is greater than 1.5, mixing a solution of B20H-174 with a solution of PEI gives a precipitate when the PVB/PEI is 2:1 and 1:1, when the ratio of PVB/PEI is 1:2 the blend remains in solution as illustrated by sample 180(*i*) where the ratio of acid groups to free amine groups is less than 1.5. This is an example of the effect of solution conditions upon complex formation. If the pH of the solution is high enough and the number of amino groups very much larger than the acid groups, then there will be insufficient Coulombic interaction to cause precipitation. The DMTA behaviours of these

Table 30
Blends of Phthalated B20H with PEI

B20H-110

Blend	wt fraction PVB	wt fraction PEI	Film Appearance	DMTA Tg/°C	Fox Eqn Tg/°C	Rule of Mixtures Tg/°C
	1	0		113		
169(a)	2/3	1/3	Yellow Precipitate	110.4	51.7	66.5
169(b)	1/2	1/2	Yellow Precipitate	80.4	22.9	43.3
169(c)	1/3	2/3	yellow precipitate	52.7	7.3	20
	0	1		-26.5		

B20H-124

Blend	wt fraction PVB	wt fraction PEI	Film Appearance	DMTA Tg/°C	Fox Eqn Tg/°C	Rule of Mixtures Tg/°C
	1	0		107		
180(a)	2/3	1/3	precipitate	97.5	48.9	62.5
180(b)	1/2	1/2	precipitate	75.1	26.0	40.3
180(c)	1/3	2/3	precipitate	64.9	6.2	18.0
	0	1		-26.5		

B20H-130

Blend	wt fraction PVB	wt fraction PEI	Film Appearance	DMTA Tg/°C	Fox Eqn Tg/°C	Rule of Mixtures Tg/°C
	1	0		66.8		
180(d)	2/3	1/3	precipitate	113	28.74	35.7
180(e)	1/2	1/2	precipitate	71.8	12.73	20.15
180(f)	1/3	2/3	precipitate	-7,65.3	-1.67	4.6
	0	1		-26.5		

Table 4.30 continued

B20H-174

Blend	wt fraction PVB	wt fraction PEI	Film Appearance	DMTA Tg/°C	Fox Eqn Tg/°C	Rule of Mixtures Tg/°C
	1	0		111		
180(g)	2/3	1/3	precipitate	87.7	50.8	65.2
180(h)	1/2	1/2	precipitate	31,64.3	27.3	42.3
180(i)	1/3	2/3	clear	49	6.9	19.3
	0	1		-26.5		

Figure 4.70

DMTA
Head: Standard 300°C

TITLE : PVB
SUBTITLE: B20H-110
FILENAME: B20H-110
OPERATOR: D.Cunliffe

DATE RUN: Aug/24/1991
FREQ : 1
STRAIN : 4
DIM: 2.00, 10.805, .313

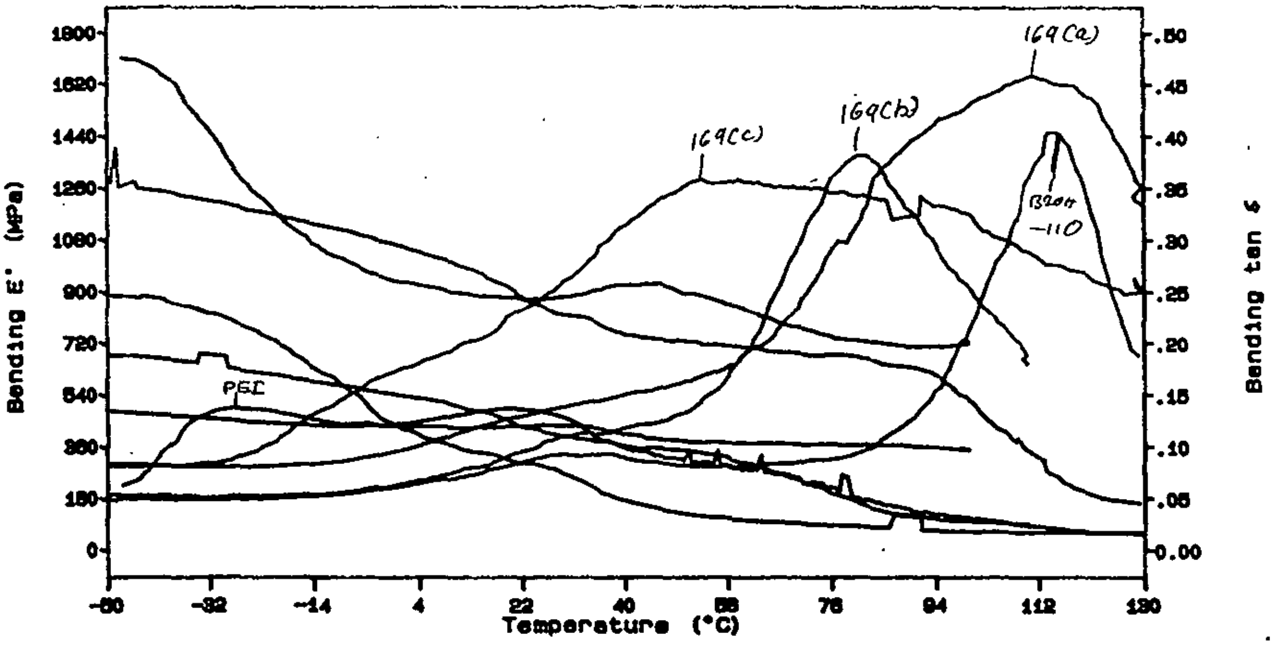

Blends of B20H-110 with PEI in air

VERSION: V5.20

Figure 4.71

DMTA
Head: Standard 300°C

TITLE : PVB
SUBTITLE: B20H-124
FILENAME: B20H-124
OPERATOR: D.Cunliffe

DATE RUN: Oct/18/1991
FREQ : 1
STRAIN : 4
DIM: 2.00, 12.118, .327

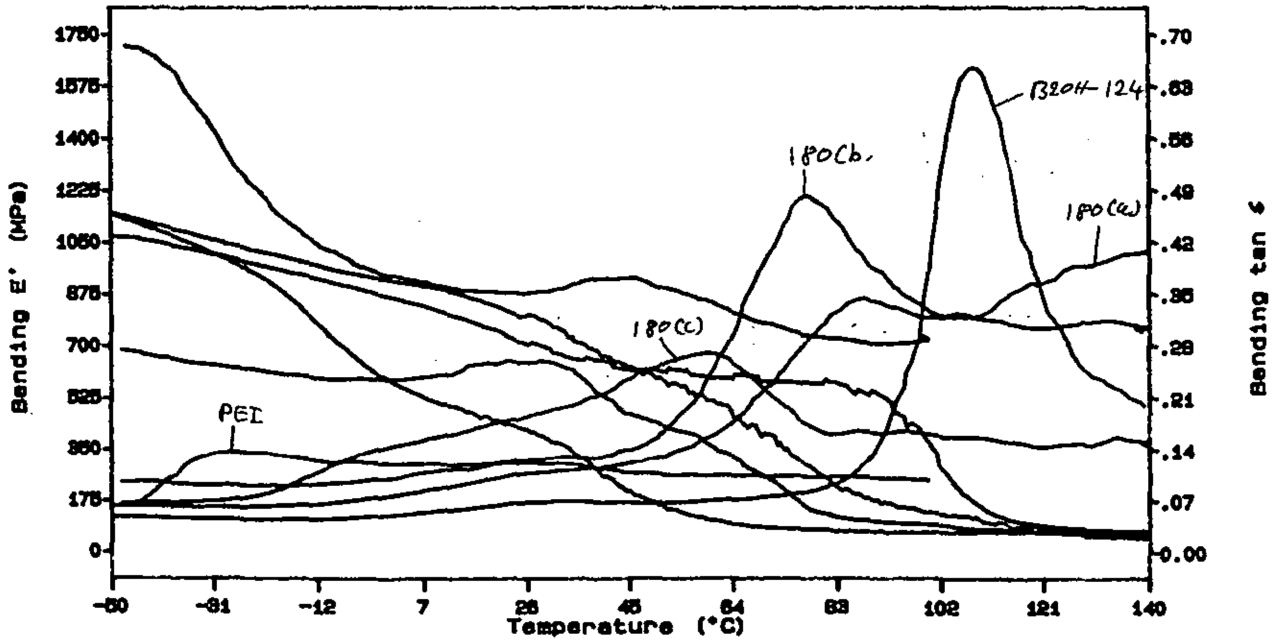

Blends of B20H-124 with PEI in air

VERSION: V5.20

Figure 4.72

DMTA
Head: Standard 300°C

TITLE : 180 (e)
SUBTITLE: B20H-130/PEI
FILENAME: Pressed Film
OPERATOR: D.Cunliffe

DATE RUN: May/04/1992
FREQ : 1
STRAIN : 1
DIM: 1.00, 7.358, .320

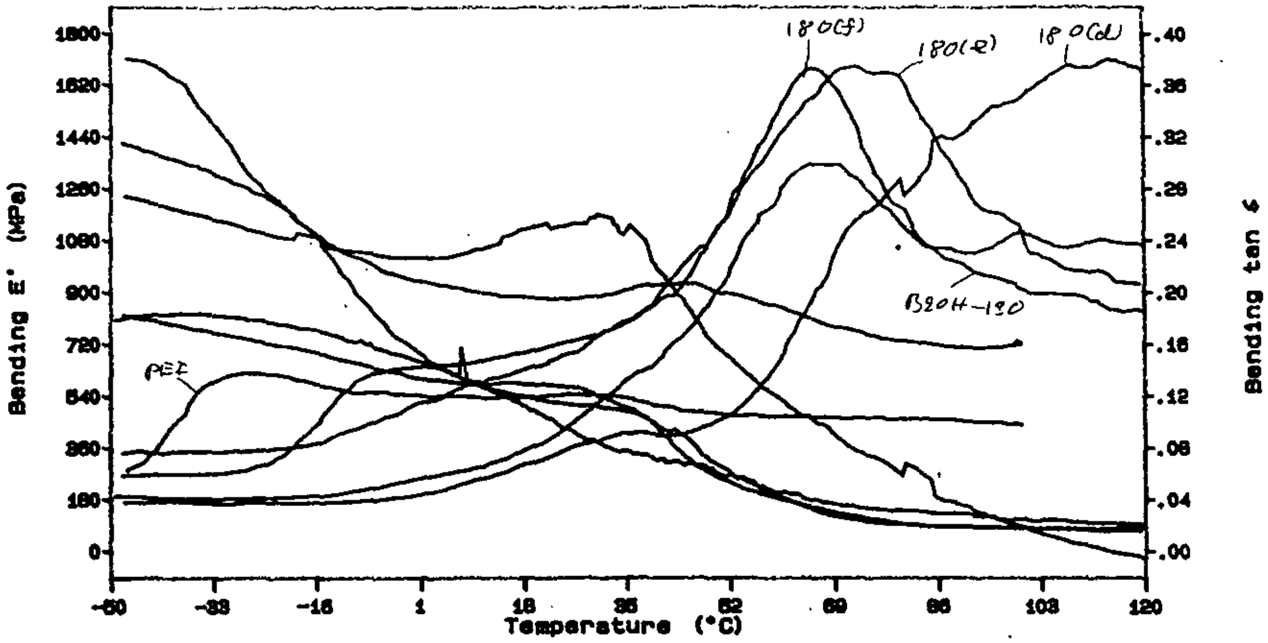

Blends of B20H-130 with PEI in air

VERSION: V5.20

Figure 4.73

DMTA
Head: Standard 300°C

TITLE : 180 (g)
SUBTITLE: B20H-174/PEI
FILENAME: Pressed Film
OPERATOR: D.Cunliffe

DATE RUN: May/11/1992
FREQ : 1
STRAIN : 1
DIM: 1.00, 13.720, .382

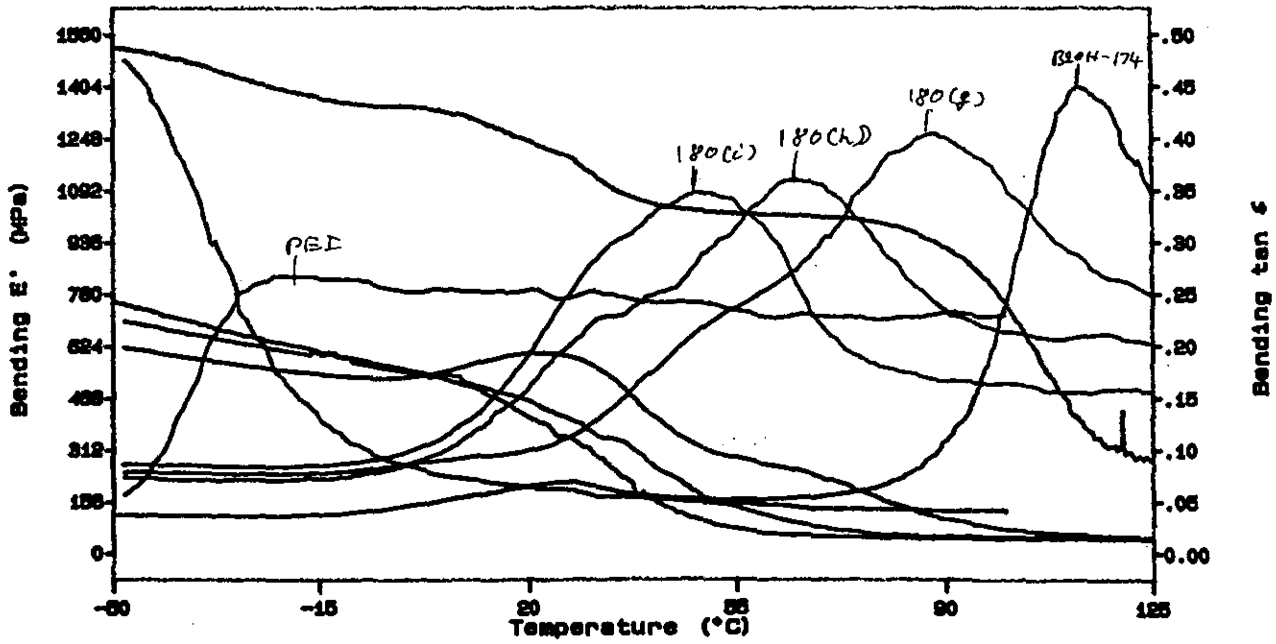

Blends of B20H-174 with PEI in air

VERSION: V5.20

blends are given in figures 4.70-4.73. The variations of Tg with blend composition are given in figures 4.74-4.77. As in the case of blends with PVP, the blends show positive deviation from values predicted by the rule of mixtures or the Fox equation. Again, this indicates strong intermacromolecular interactions.

The influence of pH upon complexation of poly (methacrylic acid) with PEI has been studied by Abe and Tsuchida[191]. Acid base interactions in blends of methacrylic acid copolymers with poly (vinyl pyridine) have also been studied[192]. Interactions between strong acids and weak bases or strong bases and weak acids are influenced less by the solvent used. Blends prepared with polysulphonic acids and poly (vinyl pyridine) have been studied by Huglin[193] and MacKnight[194], and Eisenberg has studied blends of polyamides with lithium or sodium sulphonated polystyrene ionomers[195]. It has been suggested[196] that the enhancement of miscibility of weakly charged polyelectrolytes is due to the translational entropy of counter ions and the requirements that the domains are electrically neutral.

The solubility of phthalated samples of PVB was investigated in a number of solvents, the results are given in table 4.31. This shows that the presence of carboxylic acid groups greatly change the solubility of PVB. The polymers are only soluble in polar solvents and solubility can be influenced by pH.

Figure 4.74

Tg versus wt% PEI in blends with B20H-110

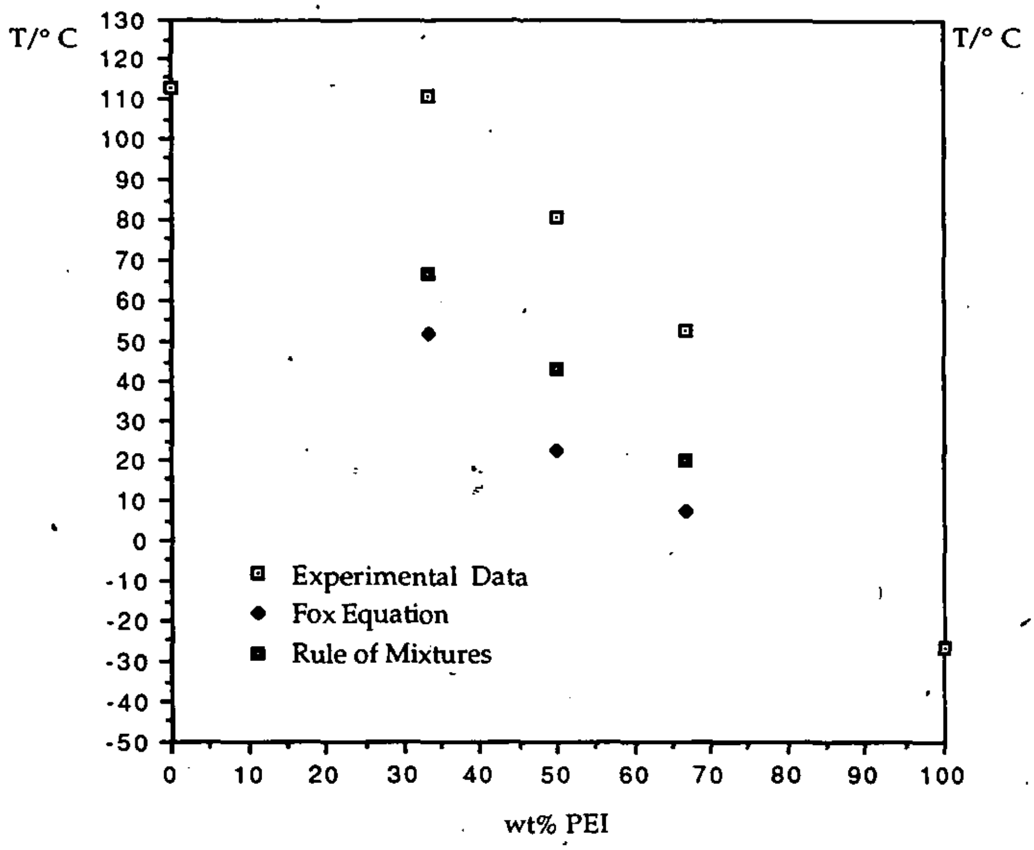

Figure 4.75

Tg versus wt% PEI in blends with B20H-124

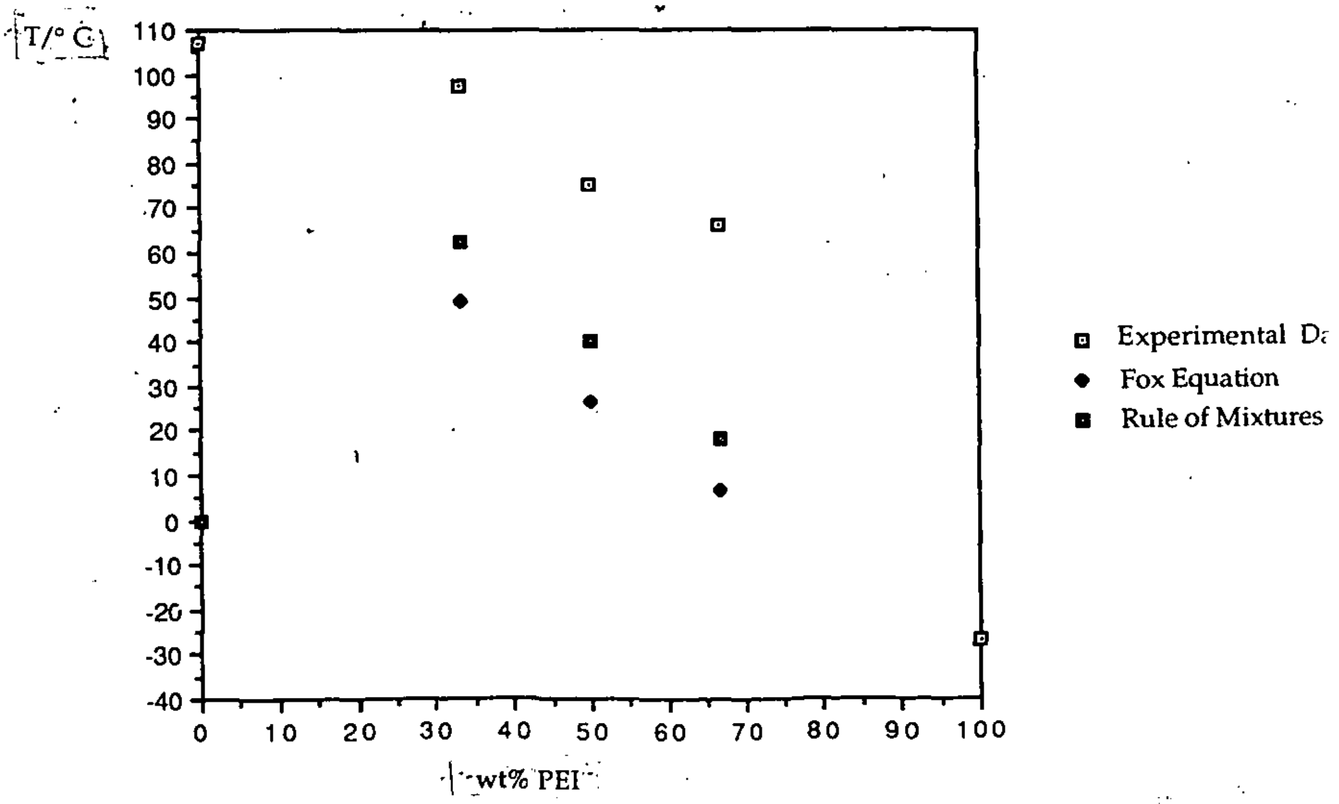

Figure 4.76
Tgversus wt% PEI in blends with B20H-130

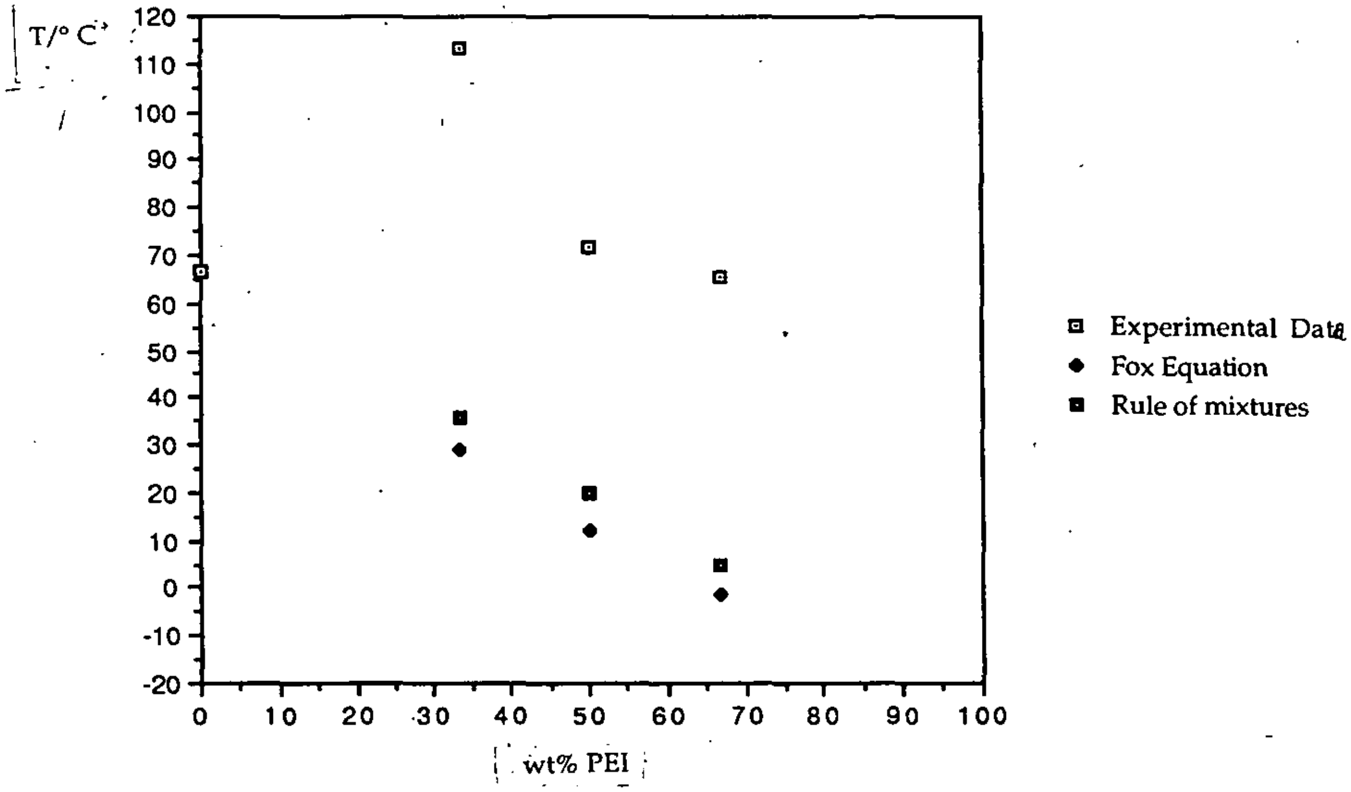

Figure 4.77
Tg versus wt% PEI in blends with B20H -174

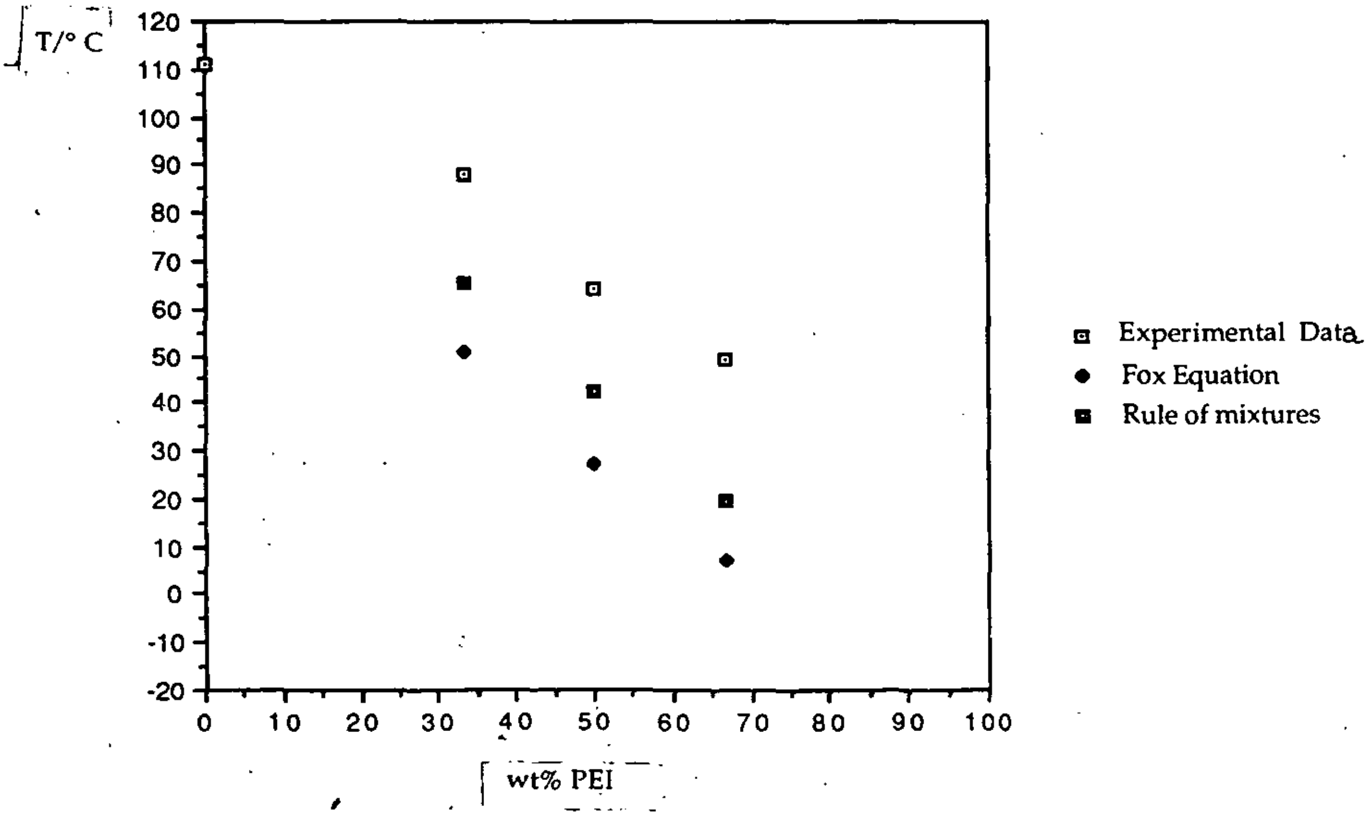

Table 4.31

Solubility Characteristics of phthalated samples of B20H

Polymer	Methanol	Acetone	Ethyl Acetate	Ethyl Acetate/ Methanol 1:1	THF	Water
B20H	✔	✔	✔	✔	✔	x
B20H-110	✔	✔	✔	✔	✔	✔ (b)
B20H-124	X(a)	✔	✔	✔	✔	✔(b)
B20H-130	✔	X	X	✔	✔	✔(b)
B20H-174	✔	X	X	✔	X	✔(b)

(a) only at > 50^{o}c
(b) only at pH ≥ 8

4.6 Succinated PVB

A number of succinated samples of B20H were prepared. The intrinsic viscosities were determined for solutions with THF, methanol and water as solvents. Sample B20H-107 showed polyelectrolyte behaviour in methanol and water as shown by the curvature of the Huggins plots as illustrated in figure 4.78 and 4.79, but gave linear Fuoss and Strauss plots for solutions in these solvents. The results are given in tables 4.32 - 4.34. The molecular masses, acid content and transition data were given in table 4.35. Determination of the ratio of succinate groups to butyral groups by NMR could only be accomplished for B20H-104 and B20H-107 as the signal from the methylene protons of the succinate group are masked by the signal from the residual protons in d6-DMSO. An NMR spectrum of B20H-107 is given in figure 4.80.

The variation of intrinsic viscosity and k_{SB} with acid content are given in figures 4.81 and 4.82.

The variation of intrinsic viscosity and k_{SB} with acid content in methanol are given in figures 4.83 and 4.84.

Due to the greater polarity of methanol it is more efficient at disrupting intra- and intermolecular hydrogen bonding than THF.

Table 4.32

Intrinsic Viscosity Data for Succinated Samples of B20H in THF

polymer	$[\eta]_H / g -^{-1}\, d$	$[\eta]_k / g^{-1}\, d\ell$	$[\eta]_{SB} / g^{-1}\, d\ell$	$[\eta]_M / g^{-1}\, d\ell$	k_H	k_k	k_{SB}	k_M
B20H	0.3382	0.3464	0.3436	0.3411	0.474	0.0816	0.359	0.410
B20H-104	0.3218	0.3219	0.3240	0.3230	0.353	0.152	0.296	0.321
B20H-107	-	-	-	-	-	-	-	-
B20H-129	0.2636	0.2633	0.2696	0.2657	0.552	-0.022	0.398	0.482
B20H-134	0.2931	0.2977	0.3006	0.2970	0.579	-0.035	0.404	0.479
B20H-136	.2195	.2203	0.2228	0.2225	0.405	0.127	0.287	0.306

Figure 4.78
Hugg. ins Plot for B20H-107 is methanol

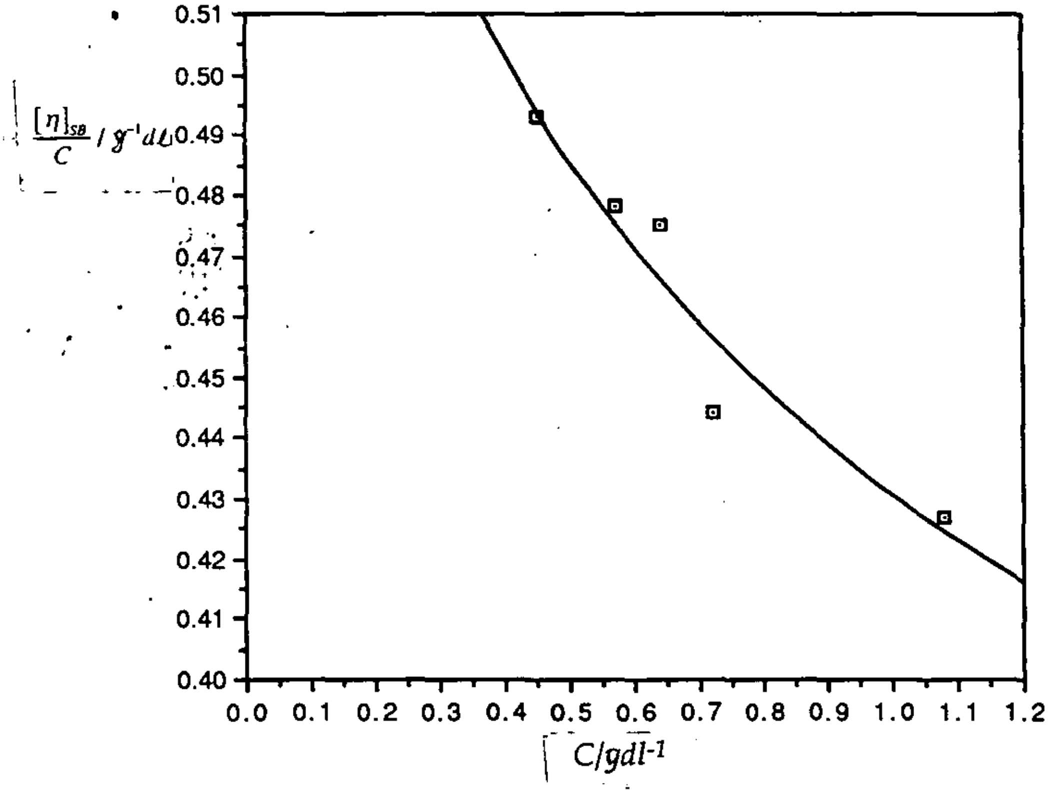

Figure 4.79
Hugg. ins Plot for B20H-107 in water

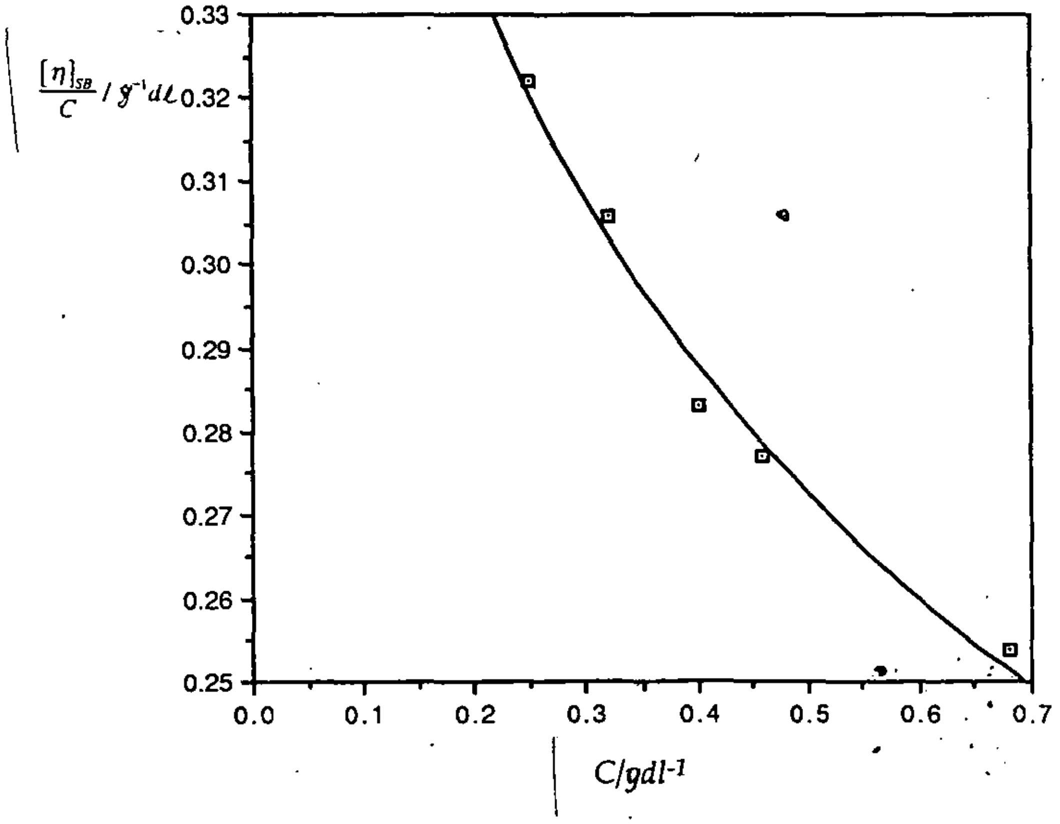

Table 4.33

Viscosity Data for Succinated B20H in Methanol

polymer	$[\eta]_H / g^{-1} dl$	$[\eta]_k / g^{-1} dl$	$[\eta]_{SB} / g^{-1} dl$	$[\eta]_M / g^{-1}$	k_H	k_k	k_{SB}	k_M
B20H	0.1828	0.2025	0.2107	0.1995	2.63	-0.88	1.03	1.51
B20H-104	-	-	-	-	-	-	-	-
B20H-107	-	-	-	-	-	-	-	-
B20H-129	0.2419	0.2390	0.2421	0.2420	0.154	0.270	0.143	0.147
B20H-134	0.2365	0.2498	0.2437	0.2403	0.955	-0.205	0.67	0.78
B20H-136	0.1273	0.1304	0.1315	0.1270	1.026	0.262	0.69	0.952

Table 4.34
Intrinsic Viscosity Data for Succinated B20H in Methanol and Water

polymer	$[\eta]^{FS} / g^{-1} dl / MeOH$	$\gamma_{FS} / g^{-\frac{1}{2}} dl^{\frac{1}{2}} / MeOH$	$[\eta]_{FS} / g^{-1} dl / H_2O$	$\gamma_{FS} / g^{-\frac{1}{2}} dl^{\frac{1}{2}} H_2 0$
B20H-107	0.6983	0.542	0.618	2.57

Table 4.35

Molecular Mass, Acid Content and Transition Data for Succinated B20H

Polymer	$\bar{M}n$	$\bar{M}w$	M*p*	M*wd*	$[CO_2H]$/*mmol g*$^{-1}$	Tg/°C	Succinate/ butyrate
B20H	9000	23000	14000	3.17	-	70.7	-
B20H-104	7000	14000	10000	1.91	1.93	60.5	0.28
B20H-107	-	-	-	-	15.69	68.7	0.62
B20H-129	12000	32000	20000	2.64	3.28	64.4	-
B20H-134	7000	25000	13000	3.83	4.80	71.4	-
B20H-136	14000	34000	22000	2.4	3.62	67.5	-

Figure 4.80
N.M.R. Spectrum of succinated B20H

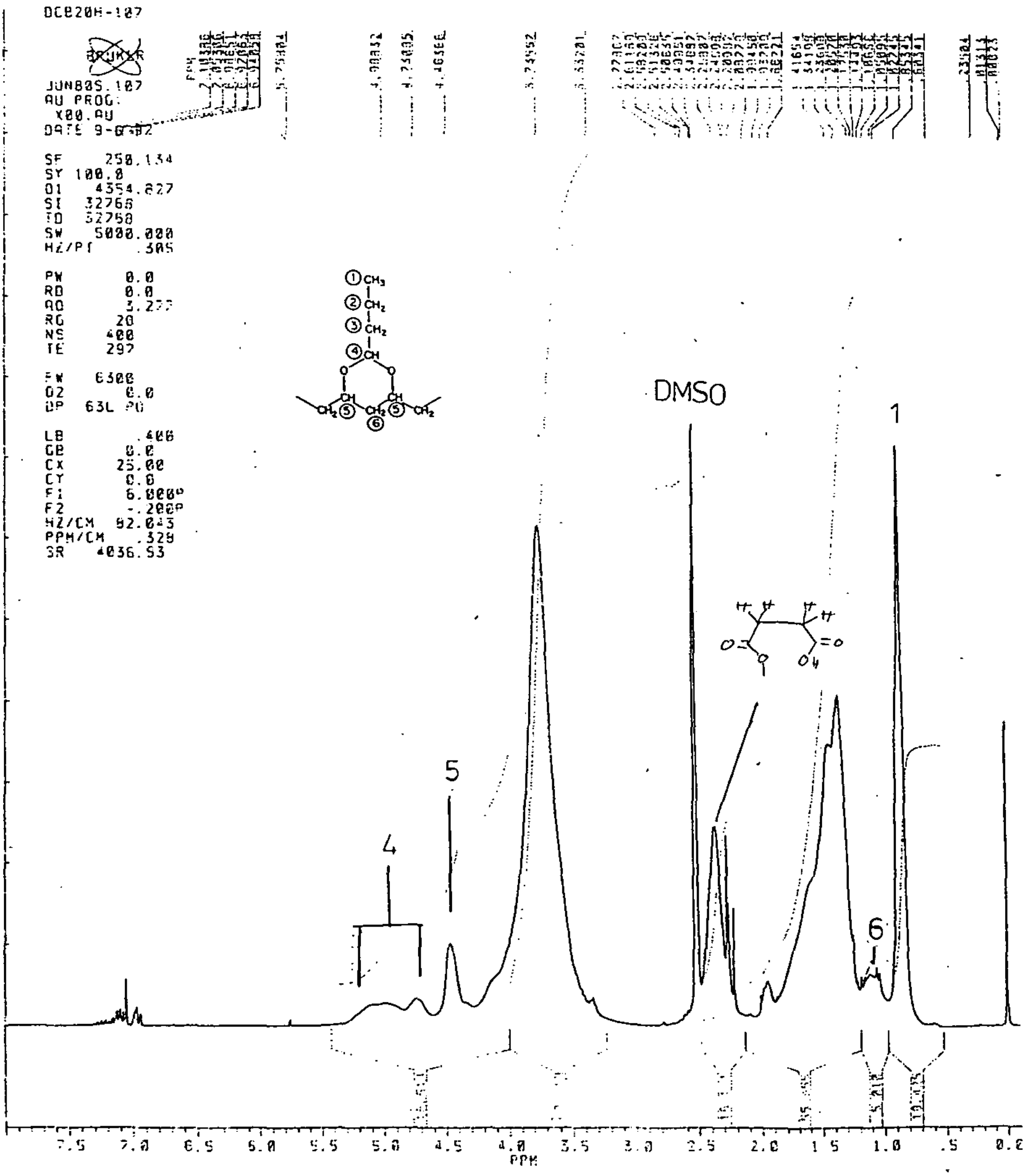

Figure 4.81
[η] against [CO2H] for succinated B20H in THF

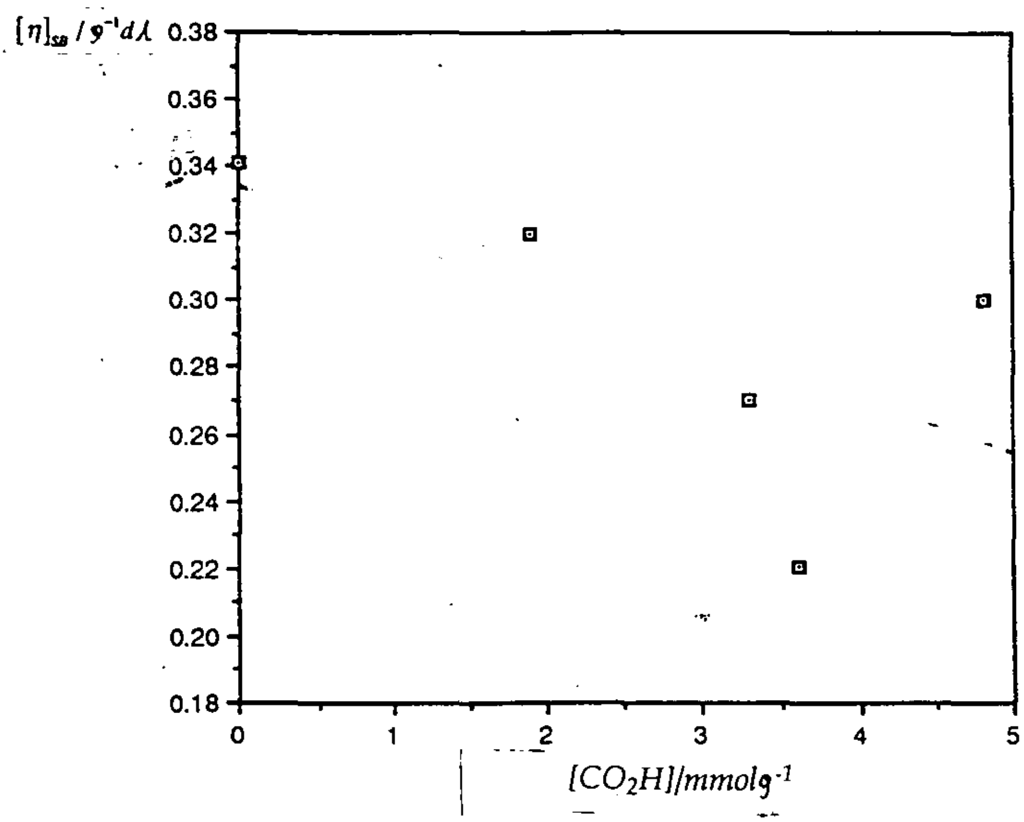

Figure 4.82
kSB [CO2H] for succinated B20H in THF

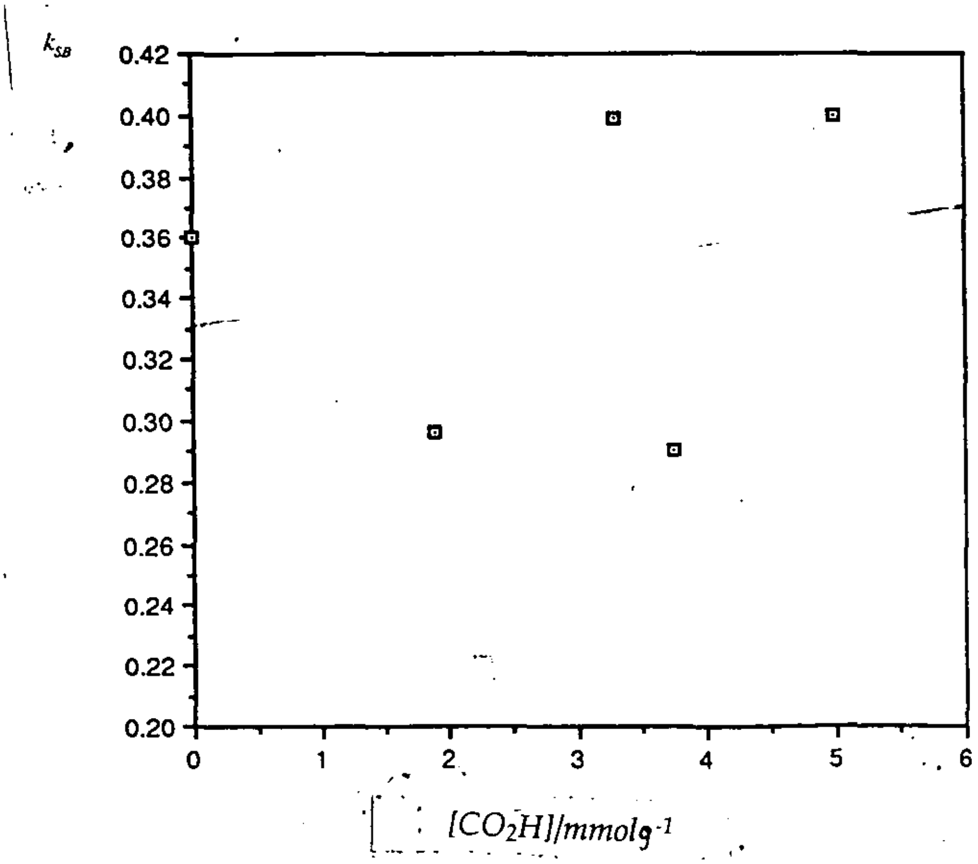

The solubilities of succinated samples of B20H were investigated in a number of solvents and the results given in table 4.36. This shows that the presence of pendant acid groups require solvents of a high polarity to dissolve the polymers and that solubility is pH dependent.

Figure 4.83
[η]SB against [CO2H] for succinated B^{20H} in Methanol

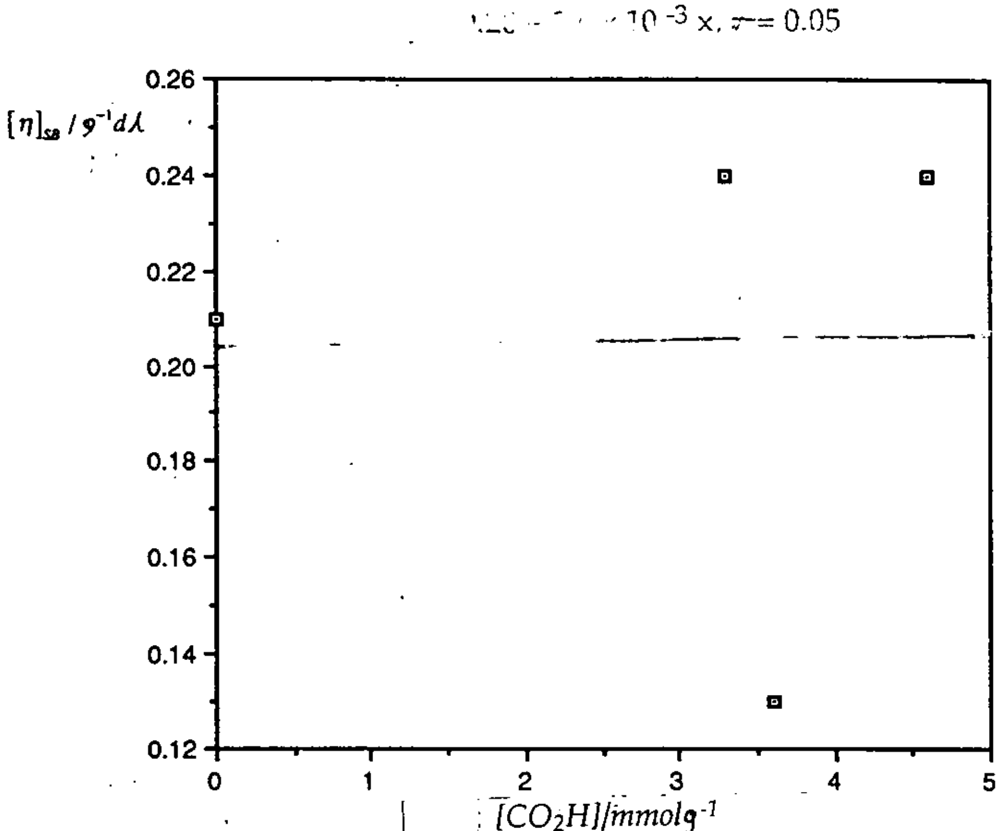

Figure 4.8.4
k_{SB} against [CO$_2$H] for succinated B20H in Methanol

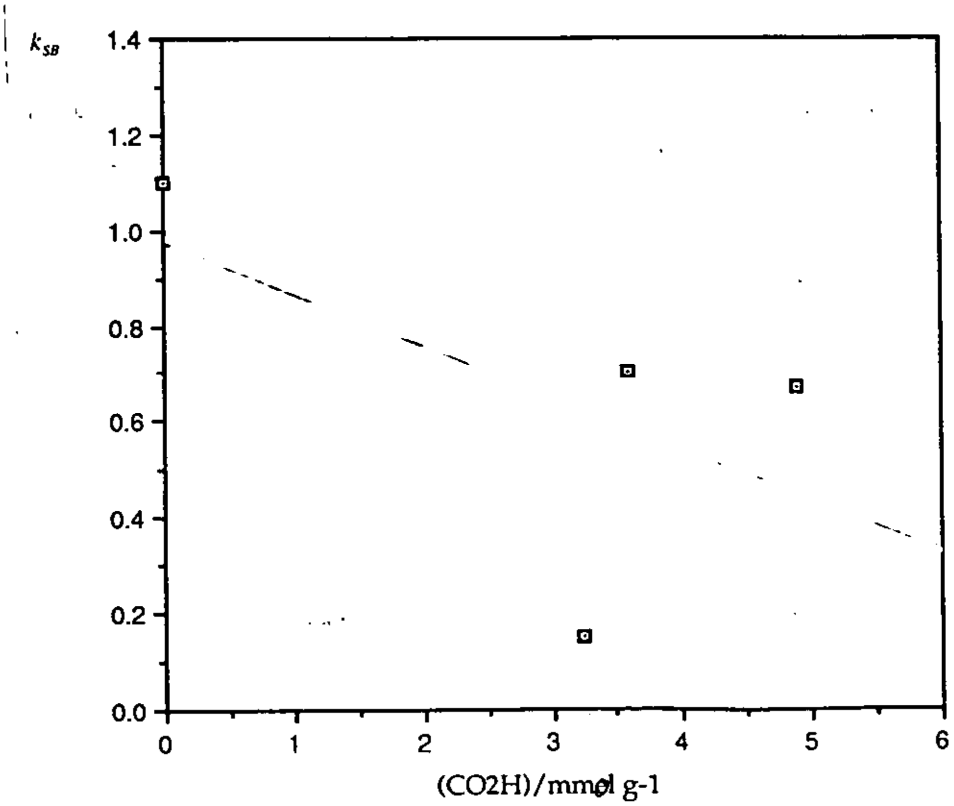

Table 4.36

Solubility Characteristics of Succinated samples of B20H

Polymer	Methanol	Acetone	Ethyl Acetate	Ethyl Acetate/ Methanol 1:1	THF	Water
B20H	✓	✓	✓	✓	✓	X
B20H-104	X	✓	✓	✓	✓	X
B20H-107	✓	X	X	X	X	✓
B20H-129	✓	X	X	✓	✓	✓(a)
B20H-134	✓	X	X	✓	✓	✓(a)
B20H-136	✓	X	X	✓	✓	✓(a)

(a) only at $\mathrm{pH} \geq 8$

5 Conclusions and Recommendations

The hydroxyl groups of poly (vinyl butyral) are known to greatly influence its solution viscosity in many solvents due to intermolecular hydrogen bonding. They are also responsible for promoting miscibility with other polymers. The aim of this work was to study the effect of chemical modification of hydroxyl groups upon solution viscosity and miscibility with other functional polymers. It was found that:

1. The chemistry used for modification can be that used in carbohydrate chemistry involving esterification or etherification of the hydroxyl groups, esterification being the simplest procedure
2. Modified poly (vinyl butyral) with non-polar pendant groups show reduced tendency toward aggregation in THF as observed by dilate solution viscometry. With pendant acid groups, poly (vinyl butyral) shows a greater tendency toward aggregation in THF, due to possible dimerisation of the acid groups. In methanol these aggregates are broken up due to the greater polarity of the solvent.
3. Modified poly (vinyl butyral) with non-polar pendant groups show reduced miscibility with the polyurethane (TMXDI/NPG), the polyester (diorex) polyethylenimine and poly (vinyl pyrrolidone). This indicates that hydrogen bonding is the thermodynamic driving force for miscibility with other polymers and removal of the hydroxyl groups removes the chances of hydrogen bonding. The influence of hydroxyl groups in poly (vinyl butyral) upon the miscibility withpolyurethanes has recently been reported by David and Sincock[197,198]. Poly (vinyl butyral) with pendent carboxyl groups shows improved miscibility with polyurethane, polyester and showed evidence of complex formation with polyethylenimine and poly (vinyl pyrrolidone)

Recommendation for further work.

1. To prepare modified poly (vinyl butyral) with pendant basic groups and study the effect of having proton accepting species attached to the chain upon solution viscosity and miscibility
2. Study the effect of solvent upon complexation behaviour of the acid derivatised samples of poly (vinyl butyral) with polyethylenimine

and poly (vinyl pyrrolidone)

3 Study intermolecular interactions by infrared spectroscopy and NMR

4 Study the intimacy of mixing by microscopy and NMR.

APPENDIX

Figure A.1

DMTA

Head: Standard 300°C

TITLE : Polystyrene
SUBTITLE: Pressed film
FILENAME: BDH 100000
OPERATOR: D.Cunliffe

DATE RUN: Jul/22/1991
FREQ : 1
STRAIN : 4
DIM: 2.00, 12.583, .620

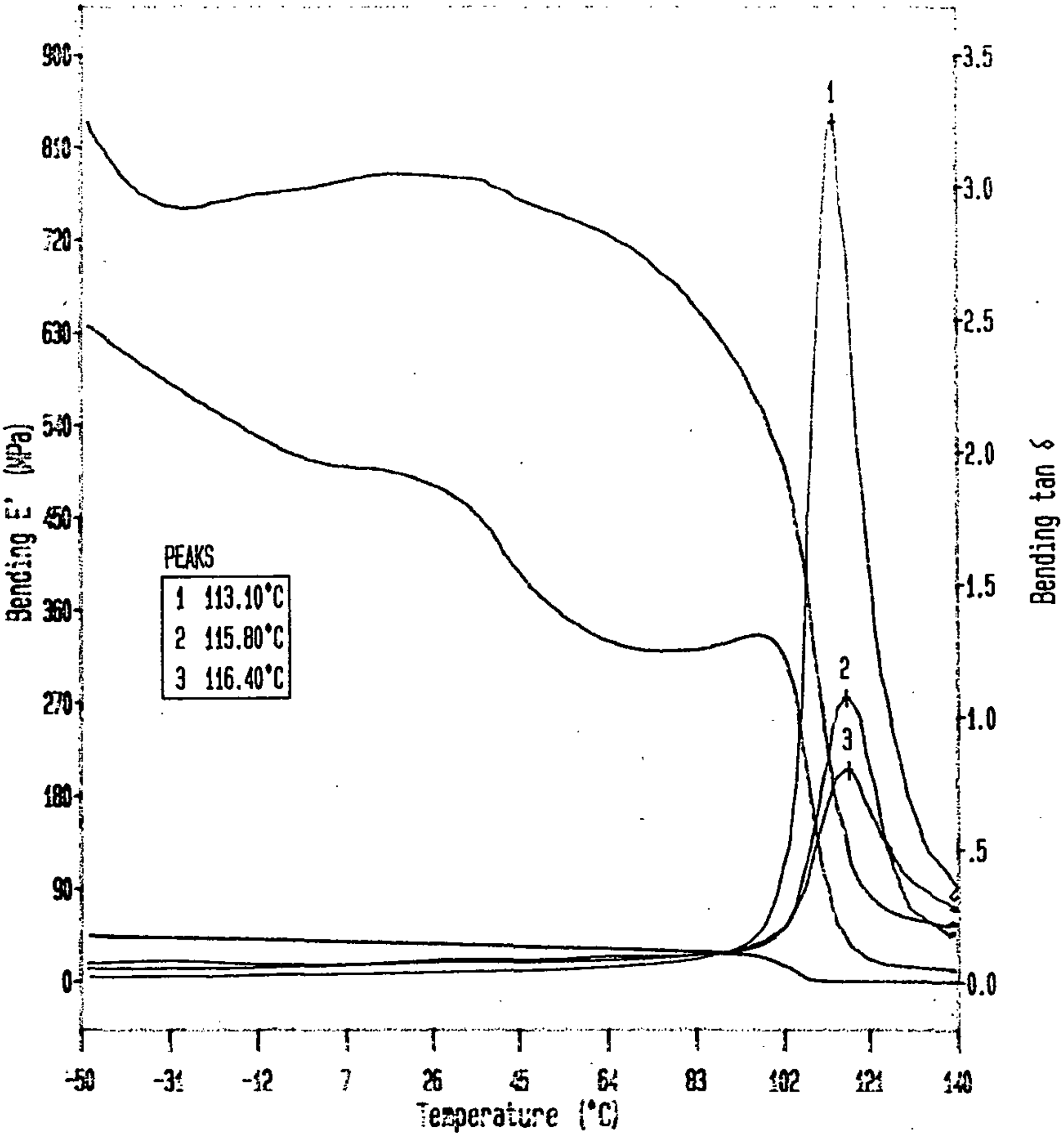

Comparison of cast bar and pressed films of polystyrene
1= Cast Bar, 2= Filter Paper, 3= Bleached Cotton

VERSION: V5.20

REFERENCES

1. P Hodge and D C Sherrington (eds) *'Polymer - Supported Reactions in Organic Synthesis'* Wiley - Interscience. New York 1980

2. D C Sherrington and P Hodge (eds) *'Synthesis and Seperations Using Functional Polymers'*. Wiley Chichester 1988

3. N K Mathur, C K Narang and R E Williams *'Polymers asAids in Organic Chemistry'*. Academic Press, New York. 1980

4. W T Ford, A C S Symp. Ser. 308, 1986

5. A Akelah and D C Sherrington Chem. Rev. 1981, 81, 557

6. A Akelah and D C Sherrington Polymer, 1983, 24, 1369

7. Y Chauvin, D Commereuc and F Dawans Prop. Polym. Sci. 1977, 5, 95

8. E C Blossey and W T Ford *'Comprehensive Polymer Sceince'* (Eds G Allen and J C Bevington), Pergamon Press, Oxford Vol. 6 p 81 (1989)

9. A F Kydonieus (ed) Controlled Release Technologies Theory and Application. C R C Press Brea Raton (1980)

10. F Gavina, A M Coster and S V Luis, J Org. Chem. 1984, 49, 4617

11. E Leonhardi *'ChemischesWortebach der Allgemene Begriffe der Chemice* Leipzeig 1781,27

12. H Braconnet Annali Chem. Phys. 1833, 52, 290

13. U S Patent 3, 633

14. J Blyth and A W Hofman, Liebigs, Ann. Chem. 1845, 53, 316

15. H Staudinger and J Fritchi. Helv. Chem. Acta. 1922, 5, 785

16. H Staudinger, E Geiger and E Huber, Ber. Dtsch. Chem. Gen. 1929, 62, 263

17. Chemical Reactions of Polymers. Ed. by E M Fettes. Interscience, New York 1964

18. Reactions on Polymers, Ed. by J A Moore, D Reidal, Dordricht Holland 1973

19. H Morawetz, Accounts Chem. Res. 1970, 3, 354

20. H Morawetz *'Macromolecules in Solution'* 2nd Edition. Wiley New York 1975

21. H G Elias *'Macromolecules'* Vol. 2, Chap. 23. Wiley new York 1973

22. N A Plate, Pure and Appl. Chem. 1976, 46, 49

23. P Remp. Pure and Appl. Chem. 1976, 46, 9

24. N A Plate and O V Noah, Adv. Polym. Sci. 1979, 31, 133

25. A G Brydon and G G Cameron, Prog. Polym. Sci. 1975, 4, 209

26. E A Boucher. Prog. Polym. Sci. 1978, 6, 63

27. *'Modification of Polymers'* Ed. C E Carraher Jr. and M Tsuda A C S Symp. Ser. 121, 1980

28. N A Platé, IUPAC 27th Int. Symp. Macromol. Chem. Main. Lect. 1981

29. A D Jenkins and J F Kennedy (Eds) *'Macromolecular Chemistry'*, Royal Society of Chemistry. London.
    - a G G Cameron, 1980, 1, 350
    - b G G Cameron, 1982, 2, 271
    - c D C Sherrington, 1984, 3, 303

30. E Marachel in *'Initiation a la Chimie et a la Physiochemie Macromoleculaires, Groupe. Francais etEtudes et d'Application de Polymers, Grenoble 1980, vol. 3*

31. G Odian *'Principles of Polymerisation'* Wiley New York 1981

32. P Remp and E W Merrill *'Polymer Synthesis'* Huthig Wepf New York 1986.

33. V V Korchack, Russ. Chem. Rev. (Engl. Tram) 1980, 49, 1135

34. H Morawetz. J. Polym. Sci. Polym. Symp. 1985, 72, 9

35. Polym. Eng. Rev. 1983, 2, 31

36. D C Sherrington *'Encyclopaedia of Polymer Science and Engineering'* 1988, 14, 101

37. C E Carraher and J A Moore *'Modification of Polymers'* Plenum. Press New York, 1983

38. J L Benham and J F Kinstle *'Chemical Reactions on Polymers'* ACS Symp. Ser. 364, 1988

39. F G Thorpe in *'New Methods of Polymer Synthesis'* Ed. by J R Ebdon Blackie 1991

40. J C Soutif and J C Bross, React. Polym. 1990, 12, 3

41. J C Soutif and J C Bross, React. Polym. 1990, 12, 133

42. J C Soutif and J C Bross. React-Polym. 1990,13,1

43. J C Soutif and J C Bross. React. Polym. 1991, 14, 1

44. H Morawetz *'Macromolecules in Solution'* 2nd Ed. Wiley New York 1975

45. H Lodenheim and H Morawetz, J AM Chem. Soc. 1959, 81, 4860

46. Y Imanichi. J Polym. Sci. Rev. Macromol. Chem. 1979, 14,1

47. C G Overberger and A C Guterl Jr. J Polym. Sci. Polym. Symp. 1978, 62, 13

48. C G Overberger and A C Guterl Jr. J Polym. Sci. Polym. Chem. Ed. 1979, 17, 1887

49. J Millan, G Martinez and Y C Mijangon, Rev. Plast. Mod. 1985, 351, 317

50. Galin in ref 27

51. Kiyoshi Fujii, Junji Ukida and Masakazu Matsumota. Makromol Chem. 1963, 65, 86

52. Kiyoshi Fujii, Junji Ukida and Masakazu Malsumoto, J Polym. Sci. 1963, B-1, 693

53. Kyoichiro Shibatane, Kiyoshi Fujii, Junfi Ukidu and Masokazu Masumoto 'IUPAC Symposium on Macromolecular Chemistry No. 5-5-03, Tokyo Japan 1966

54. E Klesper et al. Makromol. Chem. 1974, 175, 523

55. M. Camps and F Benroika, Polym. Communications, 1991, 32, 433

56. E A Boucher. J Chem. Soc. Faraday Trans. 1, 1973, 69, 1839

57. B D Coleman and R M Fuoss, J Am. Chem. Soc. 1955, 77, 5472

58. R M Fuoss, M. Watanabe and B D Coleman. J Polym. Sci. 1960, 48, 5

59. J J Bourquignon. These. Strasbourg 1978

60. Y Frere and P Gramain Macromolecules, 1992, 25,3184

61. P J Flory. J Am. Chem. Soc. 1939, 61, 1518

62. F T Wall. J Am. Chem. Soc. 1941, 62, 803

63. F T Wall. J. Am. Chem. Soc. 1941, 63, 821

64. R Simha. J. Am. Chem. Soc. 1941, 61, 1479

65. E Merz, T Alfrey and G Goldfinger, J Polym. Sci. 1946, 1, 75

66. T Alfrey, C Lewis and B Mogal. J. Am. Chem. Soc. 1949, 71, 3793

67. G O Morrison and A F Price U S Patent 2179051 (1939). J G McNally and R H Van Dyke, U S Patent 2269216 and 2269217 (1945)

68. P J Flory J. Am. Chem. Soc. 1950, 72, 5052

69. Y Ogata, M Okana and T Ganker. J. Am. Chem. Soc. 1956, 78, 2962

70. P Raghavendrachar and M Chanda. Eur. Polym. J. 1983, 19, 391

71. P G de Gennes, J. Chem. Phys. 1982, 76, 3316

72. P G de Gennes, J. Chem. Phys. 1982, 76, 3222

73. M L Huggins. J. Phys. Chem. 1938, 42, 91

74. M L Huggins, J. Phys. Chem. 1939, 43, 439

75. M L Huggins, J. Am. Chem. Soc. 1942, 64, 2716

76. W R Moore, Prog. Polym. Sci. 1967, 1, 1

77. E O Kraemer. Ind. Eng. Chem. 1938, 30, 1200

78. G V Schulz and F Blaschke. J. Prakt. Chem. 1941, 158, 130

79. A F Martin. American Chemical Society Meeting Memphis. April 1942

80. T Sakai. J. Polym. Sci. Polym. Phys. Ed. 1968, 6, 1659

81. H G Elias and O Etter. Makromol. Chem. 1963, 66, 56

82. E W Ibrahim J Polym. Sci. Part A, 1965, 3, 469

83. M Engiegbalam and D J Hourston. Polymer, 1979, 20, 818

84. C I Simionescu, B C Simionescu, I Neamtu and S Ioan Polymer, 1987, 28, 165

85. B C Simionescu, I Ioan, A Flander and CI Simionescu Angew Makromol, Chem. 1987, 152, 121

86. P A Lovell, Comprehensive Polymer Science Vol. 1, page 173, 1989

87. R M Fuoss and U P Strauss. J. Polym. Sci. 1948, 3, 602

88. R M Fuoss. J Polym. Sci. 1948, 3, 603

89. I Noda, T Tsuge and M Nagasowa. J. Phys. Chem. 1970, 4, 710

90. D T F Pals and J J Hermans. J. Polym. Sci. 1950, 5, 733

91. H G Elias Macromolecules. Wiley New York, Vol. 1 1977

92. A Dondos, C Tsitulianis and G Staikoss. Polymer, 1989, 30, 1690

93. A M Pedley, J S Higgins, D G Peiffer and A R Rennie. Macromolecules, 1990, 23, 2494

94. H Matsuda, K Yamono and H Inaguki, Kagyo Kagaku Zasshi (J. Ind. Chem. Japan) 1970, 73, 390

95. J Danhelka and L Mrkvickova, V Stepan and I Kossler, Angew Makromol Chem. 1984, 122, 77

96. C W Paul and P M Cotts. A C S Symp. Ser. 350, 1987

97. C W Paul and P M Cotts. Polym. Preps. (Am. Chem. Soc. Div. Polym. Chem.) 1986, 27, 215

98. P M Cotts and A C Ouano in Microdomains in Polymer Solutions (Ed. P Dubin) Plenum Press New York 1985

99. P M Cotts and C W Paul. Macromolecules, 1986, 19, 692

100. C W Paul and P M Cotts. Macromolecules, 1987, 20, 1986

101. E E Remson, J. Appl. Polym. Sci. 1991, 42, 503

102. A Viallet, R Pedro Bom J P Cohen Addad. and S Perez, Polymer, 1992, 33, 4379

103. Solid State NMR of Polymers. Ed. L J Mathias, Penum Press New York, 1991

104. C H Klein Douwel, W E J R Maas, W S Veeman G H Werumeus Buning and J M J Vankan. Macromolecules 1990, 23, 406

105. J B Miller, K J McGrath, C M Roland, C A Trask and A N Garroway. Macromolecules, 1990, 23, 4543

106. L Jong, E M Pearce and T K Kwei, Macromolecules 1990, 23, 5071

107. A Simmons, A Natansohn. Macromolecules, 1991, 24, 3651

108. X Zhang, K Takagoshi and K Hikichi, Macromolecules, 1991, 24, 5756

109. J H Watton, J B Miller and C M Roland. J Polym. Sci. Part B. Polym. Phys. 1992, 30, 527

110. J Grabilny. D M Price, F E Karasz and W J Macknight Polym. Commun. 1990, 31, 86

111. D S Kaplan. J Appl. Polym. Sci. 1976, 20, 2615

112. D R Paul and S Newman *'Polymer Blends'* Volumes 1 and 2 Academic Press. New York 1979

113. O Olabisi, L M Robeson and M T Shaw, *'Polymer - Polymer Miscibility'* Academic Press. New York, 1979

114. J A Manson and L J Sperling. *'Polymer Blends and Composites'* Heyden New York, 1982

115. K Sole. *'Polymer Compatibility and Incompatibility'* Harvard New York, 1982

116. P W Williams, PhD Thesis, Loughborough University of Technology 1985

117. D J Walsh *'Comprehensive Polymer Science'* Volume 2 page 135. Pergamon Oxford, 1989

118. D W Fox and R D Allen *'Encyclopaedia of Polymer Science and Engineering'* Volume 3, page 758, 1985

119. D R Paul, J W Barlow and H Keskhula *'Encyclopaedia of Polymer Science and Engineering'* Volume 12, page 399, 1985

120. M E Fowler, J W Barlow and D R Paul. Polymer, 1987, 28, 1177

121. R E Bernstein, C A Cruz and D R Paul. Macromolecules, 1977, 10, 681

122. A C Fernandez, J W Barlow and D R Paul. J Appl. Polym. Sci. 1986, 32, 548

123. H W Kammer, T Inoue and T Ougizawa. Polymer 1989, 30, 888

124. He Manjum, Lui Yangming, Feng Yi, Jiang Ming, and C C Han. Macromolecules. 1991, 24, 464

125. P J Flory *'Principles of Polym er Chemistry'* Cornell. New York, 1953

126. M L Huggins Physical Chemistry of High Polymers. Wiley 1953

127. S Krause Pure and Appl. Chem. 1986, 58, 1553

128. M M Coleman, C J Serman, D E Bhagivagar and P C Painter. Polymer 1990, 31, 1187

129. P C Painter, Yung Park and M M Coleman Macromolecules, 1989, 22, 570

130. P C Painter, Yung Park and M M Coleman. Macromolecules, 1989, 22, 80

131. P C Painter, J F Graf and M M Coleman. Macromolecules, 1991, 24, 5630

132. M M Coleman, A M Lichkus and P C Painter Macromolecules, 1989, 22, 586

133. T G Fox and P J Flory. J Am. Chem. Soc. 1948, 70, 2384

134. T G Fox and P J Flory J Appl. Phys. 1950, 21, 581

135. A K Doolittle, J. Appl. Phys. 1951, 22, 1471

136. A K Doolittle. J. Appl. Phys. 1952, 23, 236

137. M L Williams. R F Landel and J D Ferry, J Am. Chem. Soc. 1955, 77, 3701

138. J H Gibbs and E A DiMarzio. J. Chem. Phys. 1958, 28, 373

139. J H Gibbs and G Adams. J. Chem. Phys. 1965, 43, 139

140. M Gordon and J S Taylor. J Appl. Chem. 1952, 2, 493

141. T G Fox. Bull. Am. Phys. Soc. 1956, 1, 123

142. P R Couchman. Polym. Eng. Sci. 1984, 24, 135

143. H A Schneider and E A Di Marzio, Polymer 1992, 33, 3453

144. N G McCrum, B E Read and G Williams *'Anelastic and Dielectric Effects in Polymeric Solids'* Wiley New York, 1967

145. T Murayama *'Dynamic Mechanical Analysis of Polymeric Materials'* Elsevier Scientific. 1978

146. N M Hodgkinson, Private Communication

147. G M Kline *'Analytical Chemistry of Polymers III'* Interscience 1962

148. T P Gladstone Shaw. Ind. Eng. Chem. Anal. Ed. 1944, 16, 541

149. T A Coleman, Loughborough University of Technology PhD Thesis 1983

150. Toshiko Yoshitake. Japanese Patent 54-28390, 1977

151. S H Merrill and D A Smith U S Patent, 286157, 1958

152. S H Merrill and C C Unruh. US Patent 3002003, 1961

153. Chemical Abstracts 170940 Volume 88, 1978

154. Chemical Abstracts 194045 Volume 91, 1979

155. Chemical Abstracts 797110 Volume 105, 1986

156. J Huang and Q Guo. Makromol Chem. Rapid Commum 1990, 11, 613

157. J I Eguiaz bal, J J Iruin, M Carptazar and G M Guzman. Makromol.Chem. 1984, 185, 1761

158. M Aubin and R E Prud homme. Polym. Eng. Sci. 1988, 28, 1355

159. S Harris, Eur. Pat. 0311381, 1989

160. B J R Scholtens and B H Bijsterbosch. J. Polym. Sci. Polym. Phys. Ed. 1979, 17, 1771

162. R Hippe. Bull. Acad. Polon Sci. Ser. Sci Chim 1975, 23, 77

163. R Hippe. Bull. Acad. Polon. Sci. Ser. Sci Chim 1975, 23, 355

164. V D Tonchera, S D Ivanova and R S Velichkova. Eur. Polym. J. 1992, 28, 191

165. Steve O'Donohue, Polymer Laboratories Essex Road, Church Stretton, Shropshire.

166. A Dondos and C Tsitsilianis, Polymer International, 1992, 28, 151

167. M M Coleman, D J Skrovanek, J Hu, and P C Painter. Macromolecules. 1988, 21, 59

168. C J Sermon, Y Xu, P C Painter and M M Coleman Macromeolecules. 1989, 22, 2015

169. M M Coleman, A M Lichkus and P C Painter. Macromolecules, 1989, 22, 586

170. C Qin. A T N Pires and L Belfoire, Macromolecules, 1991, 24, 666

171. X Zhang, K Takegochi and K Hikiche, Macromolecules, 1992, 25, 4871

172. X Yang, P C Painter and M C Coleman, Macromolecules, 1992, 25, 2156

173. G C Campbell, D L Vand Hart, Y Feng and C C Han. Macromolecules 1992, 25, 2107

174. J M G Cowie and A A N Reilly, Polymer, 1992, 33, 4814

175. L F Wang, E M Pearce and T K Kwei, J Polym. Sci. Part B. Polym Phys 1991, 29, 619

176. T Suzuki, E M Pearce and T K Kwei, Polymer, 1992, 33, 198

177. E Tsuchida and K Abe. Adv. Polym. Sci. 1982, 45, 1

178. Determined by Dr E Meehan, Polymer Laboratories, Essex Road Church Stretton, Shropshire, United Kingdom

179. J Y Lee, P C Painter and M M Coleman, Macromolecules 1988, 21, 346

180. K Abe, M Koide and E Tsuchida, Macromeolecules, 1977, 10, 1259

181. H Ohno and E Tsuchida, Makromol. Chem. Rapid. Commun, 1980, 1, 159

182. L A Bimendina, E A Bekturoo, G S Tleubaeva and V A Frolova, J Polym. Sci. Polym. Symp. 1977, 66, 9

183. R Subramanian and P Natarajam. Makromol Chem. Rapid. Common. 1980, 1, 47

184. H Ohno, K Abe, and E Tsachida. Makromol Chem. 1978, 179, 755

185. A Perez-Dorado, I F Pierola, J Baselga, L Gargallo and D Radic. Makromol Chem. 1989, 190, 2975

186. A Perez-Dorado and I F Pierola. Makromol Chem. 1990, 191, 2905

187. H Ohno, A Nii and E Tsuchida. Makromol Chem. 1980, 181, 1227

188. K Abe, H Ohno, A Nii and E Tsuchida. Makromol. Chem. 1978, 179, 2043.

189. T Tsutsui, H Nakano, R Tanaka and T Tanaka. Konbunshi Ronbunshi, 1978, 35, 512

190. With thanks to Dr D K Thomas, University of Durham Industrial Laboratories, for recording the NMR spectra.

191. K Abe and E Tscuhida. Makromol Chem. 1975, 176, 803

192. J Y Lee, P C Painter and M M Coleman. Macromolecules, 1988, 21, 954

193. M B Huglin and J M Rego. Polymer, 1990, 31, 1269

194. K Sakurai, E P Douglas and W J MacKnight. Macromolecules, 1992, 25, 4506

195. A Molnar and A Eisenberg, Macromolecules, 1992, 25, 5774

196. A R Khokhlov and I A Ngrkova. Macromolecules, 1992, 25, 1493

197. D J David and T F Sincock, Polymer, 1992, 33, 4505

198. D J David and T F Sincock, Polymer, 1992, 33, 4515